Technische Universität München
Fakultät für Elektrotechnik und Informationstechnik
Lehrstuhl für Energiewirtschaft und Anwendungstechnik

Economic and Environmental Assessment of Electric Vehicle Charging Strategies

Steffen Fattler

Vollständiger Abdruck der von der Fakultät für Elektrotechnik und Informationstechnik der Technischen Universität München zur Erlangung des akademischen Grades eines

Doktor-Ingenieurs

genehmigten Dissertation.

Vorsitzende:	Prof. Dr. Myriam Koch
Prüfer der Dissertation:	1. Prof. Dr.-Ing. Ulrich Wagner
	2. apl. Prof. Dr. Martin Wietschel

Die Dissertation wurde am 14.04.2021 bei der Technischen Universität München eingereicht und durch die Fakultät für Elektrotechnik und Informationstechnik am 16.07.2021 angenommen

Danksagung

An erster Stelle möchte ich mich herzlich bei meinem Doktorvater Prof. Ulrich Wagner für die Betreuung meiner Arbeit und die jahrelange Begleitung auf meinem wissenschaftlichen Weg durch die Energiewirtschaft bedanken. Durch Ihre kompetente, ruhige Art und Ihr mir entgegengebrachtes Vertrauen haben Sie mich in meiner Arbeit sehr unterstützt und darin bestätigt, auf dem richtigen Weg zu sein.

Zudem gilt mein Dank unserem Geschäftsführer Prof. Wolfgang Mauch. Sie haben die Forschungsstelle zu dem gemacht, was sie heute ist und mir in den letzten Jahren dort das Arbeiten in einem Umfeld ermöglicht, wie es angenehmer und spannender nicht sein könnte.

Besondere Unterstützung habe ich auch durch meinen Mentor Dr. Marcus Bollig erfahren. Die vielen spannenden Diskussionen und Ihr wertvoller Input aus der Praxis der Automobilwirtschaft waren ein wichtiger Beitrag zu meiner Promotion. Vielen Dank dafür!

Bei Prof. Martin Wietschel möchte ich mich für die Bereitschaft bedanken, meine Arbeit als Zweitprüfer zu begutachten. Sie haben es bereits in der Zeit meines Studiums geschafft, mich für die Themen der Energiewirtschaft zu begeistern und damit gewissermaßen den Grundstein für diese Arbeit gelegt.

Mein besonderer Dank gilt der Hans und Klementia Langmatz Stiftung, die dieses Promotionsprojekt ermöglicht und mir damit die Freiheit verschafft hat, mich mit diesem spannenden Thema so intensiv und vollumfassend auseinanderzusetzen.

Die FfE lebt in ganz besonderem Maße von dem unschlagbaren Team, das durch seinen unermüdlichen Einsatz, die angeregten Diskussionen, die gegenseitige Unterstützung und nicht zuletzt die vielen Freizeitaktivitäten das Arbeiten auch in den intensiven Phasen so angenehm macht. Namentlich möchte ich mich insbesondere bei meinen Bürokollegen Jochen Conrad und Simon Greif sowie Adrian Ostermann, Anika Neitz-Regett, Christoph Pellinger, Simon Pichlmaier, Tapio Schmidt-Achert und Timo Kern für die gute und produktive Zusammenarbeit bedanken.

Mein besonderer Dank gilt außerdem den vielen Studierenden, die mich auf diesem Weg unterstützt haben. Mit eurem unermüdlichen Einsatz, den wichtigen Diskussionen und dem konstruktiven Austausch habt ihr einen wichtigen Beitrag zu meiner Arbeit geleistet.

Auch außerhalb meines Arbeitsumfelds haben viele Menschen dazu beigetragen, mir diese herausfordernde Phase zu erleichtern. Mein Dank geht dabei an meine Freunde, die immer für mich da waren und mich auch in diesem Lebensabschnitt begleitet haben. Ebenso möchte ich an dieser Stelle meinen Eltern für ihre Unterstützung auf meinem bisherigen Weg danken. Ihr standet von Anfang an uneingeschränkt an meiner Seite, habt mich gefördert und mir das alles erst ermöglicht. Abschließend geht mein besonderer Dank an dich, Martina. Du hast mich durch alle Berge und Täler dieses langen Weges begleitet, mir den Rücken freigehalten und warst immer für mich da. Danke.

Kurzfassung

Im Jahr 2019 verursachte der Verkehrssektor rund 20 Prozent der gesamten deutschen Treibhausgasemissionen, wovon ein Großteil auf den Straßenverkehr entfiel. Um die nationalen Klimaschutzziele zu erreichen, werden neben dem Ausbau des ÖPNV und der Förderung des Bahnverkehrs Elektrofahrzeuge eine zentrale Rolle in der notwendigen Verkehrswende spielen. Deren Emissionsreduktionspotenzial hängt eng mit den Entwicklungen im Stromsektor zusammen. Nur durch einen konsequenten Ausbau Erneuerbarer Energien und der damit einhergehenden Dekarbonisierung der Strombereitstellung können Elektrofahrzeuge ihr volles Potenzial entfalten und einen maßgeblichen Beitrag zum Klimaschutz leisten. Gleichzeitig können sie durch die gezielte Steuerung der Ladevorgänge als flexible Speicher genutzt werden und so zur besseren Integration dieser Erzeuger beitragen. Ziel dieser Arbeit ist die ökonomische und ökologische Bewertung von vier Ladestrategien, die ein besonders hohes Potenzial zur Emissionsreduktion oder zur verbesserten Integration von Erneuerbaren Energien haben. Dabei liegt der Fokus auf der Reduktion der betrieblichen Emissionen und Kosten der Fahrzeuge, der Glättung der Residuallast sowie der Vermeidung von Engpassmanagementmaßnahmen. Letztere beinhalten das Einspeisemanagement Erneuerbarer Energien sowie den Redispatch von konventionellen Kraftwerken.

Um das Potenzial dieser Ladesteuerungen zur bewerten, werden zunächst die historischen und zukünftigen Entwicklungen im Stromsektor vorgestellt. Auf dieser Basis wird eine konsistente Methodik zur Berechnung historischer und zukünftiger, stündlich aufgelöster Emissionsfaktoren sowie zeitlich und räumlich hochaufgelöster Zeitreihen von Einspeisemangement- und Redispatch-maßnahmen vorgestellt. Empirische Daten der beiden größten, deutschen Mobilitätserhebungen „Mobilität in Deutschland" und „Mobilitätspanel" werden zur Erstellung von repräsentativen Jahresfahrprofilen von Elektrofahrzeugen kombiniert und mit Hilfe eines Verbrauchsmodells in elektrische Bedarfsgänge übersetzt. Das lineare Optimierungsmodell eFLAME wird zur Bewertung der beschriebenen Ladesteuerungen weiterentwickelt und um ein Modul zur Emissionsbewertung erweitert. Das Modell ermöglicht den Vergleich von ungesteuertem Laden mit unidirektional und bidirektional optimierten Ladevorgängen. Im Rahmen einer umfangreichen Sensitivitätsanalyse werden die wichtigsten Einflussparameter auf das Potenzial der Ladesteuerungen identifiziert und mögliche Systemrückwirkungen analysiert.

Die Analysen zeigen das große Potenzial, insbesondere der bidirektionalen Ladesteuerungen. So können die betrieblichen Emissionen der Fahrzeuge im Falle des emissionsoptimierten Ladens in zukünftigen Jahren sogar negative Werte erreichen. Das Erlöspotenzial der Ladesteuerungen hingegen ist aufgrund der aktuellen Abgabe und Umlagestruktur eher als gering einzuschätzen. Als zentraler Einflussfaktor kann das Verhalten der Fahrzeugnutzer identifiziert werden. Durch ihr Ladeverhalten, das Vorgeben von Mindestbatteriefüllständen während des Ladens sowie zu erzielenden Mindestladezuständen zum Zeitpunkt der Abfahrt haben diese einen maßgeblichen Einfluss auf das verfügbare Flexibilitätspotenzial. Dieses wird zusätzlich durch die aus Netzsicht notwendigen Restriktionen der aus der optimierten Ladesteuerung folgenden Lastspitzen beschränkt. Die Analyse der Systemrückwirkungen der residuallastoptimierten Ladesteuerung zeigt den Rückgang konventioneller und die bessere Integration erneuerbarer Stromerzeugung. Aufgrund der kleinen Zahl aktuell zugelassener Fahrzeuge ist das Reduktionspotential von Engpassmanagementmaßnahmen gering. Das Laden von anderweitig abgeregeltem Strom in Kombination mit einer Emissionsoptimierung führt auf Fahrzeugebene jedoch zu den geringstmöglichen, betrieblichen Emissionen. Die erzielten Emissionseinsparungen führen im Kontext der Lebenszyklusanalyse zu einer deutlichen Reduktion der ökologischen Amortisationszeit von Elektrofahrzeugen gegenüber konventionellen Fahrzeugen.

Abstract

In 2019, the transport sector accounted for approximately 20 % of Germany's total greenhouse gas (GHG) emissions, with road transport constituting a large proportion of this. To achieve the national climate protection targets, electric vehicles (EVs) will play a central role in the necessary transformation of the transport sector. Their emission reduction potential is closely linked to developments in the electricity sector. Only by consistently expanding renewable energies EVs can realize their full potential and make a significant contribution to climate protection. At the same time, they can be used as flexible electricity storage devices through the targeted control of charging processes and thus contribute to the better integration of volatile renewable energies (vRES) such as wind and solar.

The objective of this work is the economic and environmental evaluation of four different charging strategies that have a particularly high potential for reducing emissions or improving the integration of renewable energies. The charging strategies aim at reducing operational emissions and costs of the EVs, smoothing the residual load, and avoiding congestion management (CM) measures in the context of the curtailment of renewable energies' feed-in and the redispatch of conventional power plants.

To evaluate the potential of these charging strategies, the historical and future developments in the power sector are presented first. On this basis, a consistent methodology for calculating historical and future hourly resolved emission factors (EMFs) as well as temporally and spatially highly resolved time series of feed-in management and redispatch measures is presented. Empirical data from the two largest German mobility surveys, "Mobility in Germany" and "Mobility Panel," are combined to create representative annual mobility profiles of EVs, which are translated into electric demand profiles using a consumption model. The linear optimization model eFLAME is further developed for the evaluation of the described charging strategies and extended by a module for the assessment of operational emissions. The model enables the comparison of uncontrolled charging with unidirectionally and bidirectionally optimized charging processes. Within the scope of an extensive sensitivity analysis, the most important influencing parameters on the potential of the charging controls are identified.

The analyses show the great potential especially of bidirectional charging strategies. Thus, in the case of emission-optimized charging, the operational emissions of the vehicles can even reach negative values in future years. The revenue potential, on the other hand, is estimated to be rather low due to the current levy and apportionment structure. Moreover, the behavior of the vehicle users can be identified as a central influencing factor. They have a significant impact on the available flexibility potential through their charging behavior, as well as the specification of minimum state of charge (SOC) values during charging and departure to be achieved. The restriction of the load peaks resulting from the optimization, which is necessary from the grid point of view, further limits the possible potential of an intelligent charging strategy. Nonetheless, the analysis of the system feedback effects of the residual load-optimized charging strategy shows the decrease of conventional and the better integration of renewable power generation. Due to the small number of registered vehicles, the reduction potential of CM measures in 2019 was small. However, charging of otherwise curtailed electricity in combination with emission optimization leads to the lowest possible operational emissions at the vehicle level. In the context of lifecycle analysis, the emission savings achieved lead to a significant reduction in the ecological payback period compared to conventional vehicles.

Index

Abbreviations

AC	Alternating Current
BASt	Bundesanstalt für Straßenwesen
BNetzA	Bundesnetzagentur
CAPEX	Capital Expenditure
CATI	Computer-assisted telephone interview
CAWI	Computer-assisted web interview
CBPF	Cross-Border Physical Flows
CHP	Combined Heat and Power
CM	Congestion Management
DC	Direct Current
DLR	German Aerospace Center
EEG	Erneuerbare Energien Gesetz
EFC	Equivalent Full Cycle
eFLAME	electric Flexibility Assessment Modelling Environment
EMF	Emission Factor
ENTSO-E	European Network of Transmission System Operators for Electricity
EnWG	Energiewirtschaftsgesetz
EV	Electric Vehicle
FREM	FfE Regionalized Energy System Model
GHG	Greenhouse Gas
GUI	Graphical User Interface
GWP	Global Warming Potential
ICEV	Internal Combustion Engine Vehicle
ISAaR	Integrated Simulation Model for unit Dispatch and Expansion with Regionalization
KBA	Kraftfahrzeugbundesamt
LCA	Lifecycle Assessment
LCOE	Levelized Cost of Electricity
LSTM	Long-/Short-Term Memory
MiD2008	Mobility in Germany 2008
MiD2017	Mobility in Germany 2017
MONA 2030	Merit Order Grid Expansion 2030

MOP	Mobility Panel
MSE	Mean Square Error
NABEG	Netzausbaubeschleunigungsgesetz
NEDC	New European driving cycle
OEM	Original Equipment Manufacturer
OFAT	One Factor at a Time
OPEX	Operational Expenditure
OSM	OpenStreetMap
PAPI	Paper and Pencil Interview
PES	Primary Energy Savings
RES	Renewable Energy Source
ResOpt	Residential Optimizer
RMSE	Root Mean Square Error
SOC	State of Charge
UBA	Umweltbundesamt
V2G	Vehicle to Grid
V2H	Vehicle to Home
vRES	Variable Renewable Energy Source

List of Figures

List of Tables

1 Introduction

In this thesis, an assessment of electric vehicles (EVs) charging strategies is conducted with respect to resulting costs and emissions and their potential impact on the power system. This introduction provides the motivation in section 1.1 and an overview of the current state of research in regard to the topic in section 1.2. Based on that overview the research objective and specific research questions are presented in section 1.3.

1.1 Motivation

In the course of energy transition, Germany's energy supply is being reorganized with the aim of reducing greenhouse gas (GHG) emissions by 80 to 95 % by 2050 (compared with the base year 1990) [1]. This goal can only be achieved if emission reductions are consistently implemented in all four final energy sectors and the supply sector. In the transport sector the historical increase in CO_2 emissions has been halted and even slightly reduced despite a tripling of energy consumption since 1960. They are however stagnating at a consistently high level compared with the other sectors private households, industry, and commerce and services [2], [3]. In 2019, these emissions amounted to a total of 164 million tons and thus account for around a fifth of the total GHG emissions of 810 million tons of CO_2-equivalents in Germany [4]. To achieve the national climate protection targets, it is necessary to decarbonize the transport sector almost completely by 2050 [5]. In addition to hydrogen and Power2Liquid fuels, the political and public debate mainly focuses on electrification with simultaneous use of renewable electricity. This is manifested in the German government's target of seven to 10 million EVs on Germany's roads by 2030 [6].

EVs initially represent an additional electrical load, which must be covered at least in part by fossil, emissions-intensive power plants. When assessing emissions in the operating phase of those vehicles, a large number of influencing factors must be taken into account. On the one hand, the driving and charging behavior of the vehicle users must be mapped correctly, which determines how much energy the vehicles draw from the system at what point in time. Depending on which generators are used for the electricity production at the time of charging, the specific emissions of the electricity mix vary significantly. This must be considered when accounting operational emissions in the vehicle's utilization phase. In course of the German energy transition, the fundamental composition of the electricity generation is undergoing a fundamental change. In this context, the German government is focusing primarily on the expansion variable renewable energies (vRES) like wind and solar generators while simultaneously phasing out nuclear and coal-fired power plants.

The increasing share of these volatile power generators poses fundamentally new challenges for the electricity system, which has thus far been based mainly on fossil and controllable generators. Wind and solar infeed on the other hand is of a volatile nature and does not necessarily coincide with electricity demand. In addition to this temporal variance, the spatial distribution of those mostly decentralized generators also poses a challenge. Wind turbines are currently mostly installed in northern Germany whereas load centers are located in the south. This uneven distribution repeatedly leads to grid congestion on the transmission grid level, which is currently being compensated by short-term measures such as the redispatch of conventional power plants or the targeted curtailment of vRES [7]. With the decision to phase out nuclear power and coal, conventional and flexibly controllable power plant capacities are increasingly being ousted from the German generation

portfolio. At this point, the charge control of EVs may represent a possibility to provide the flexibility required in terms of time and space.

1.2 Current state of research

Especially in recent years the general topic of EVs and their interactions with the energy system has received considerable interest with a growing body of literature investigating individual aspects. In order to present the current state of research on the topic, this section describes studies, dissertations, and models relevant to the topic. Due to the fast number of studies, the following selection of research is limited to the most relevant topic-related project reports and peer-reviewed studies published within the last five years. Studies prior to 2015 are available, but since the fundamental composition of the energy system has already changed significantly during this time and they do not provide additional insights, they are not presented here. The section is sorted by year of publication and follows the scheme:

1. Name of the institution and the authors
2. Explanation of the subject of the study and the methodology used
3. Summary of the central findings

Based on this overview, a conclusion is drawn in section 1.3 and the research questions of this thesis are derived.

2021, Sabrina Ried, Karlsruhe Institut für Technologie (KIT). Dissertation. „Gesteuertes Laden von Elektrofahrzeugen in Verteilnetzen mit hoher Einspeisung erneuerbarer Energien" [8]

In the dissertation of Sabrina Ried, the impact of bidirectionally charged vehicles on curtailment measures in Schleswig-Holstein is assessed. For that purpose a branch-flow optimizing curtailment model is coupled with the temporally dissolved electricity demand of EVs based on the survey "Mobility Panel" and extended by a peak-shaving algorithm. A mixed integer optimization model is used to assess the influence of a cost- and curtailment-optimized charging of EV in four scenarios with increasing flexibility for the years 2015 for 2030. The author concludes that a maximum of 19 % of the overall curtailed energy can be used by bidirectionally charged vehicles. She furthermore states, that the impact on the vehicle level can be significant with individual vehicles covering up to 95 % of the charged electricity by otherwise curtailed energy and reductions of operational emissions of EVs to a minimum of 7 g CO_2/km are possible.

2020, Kern et al., Forschungsgesellschaft für Energiewirtschaft mbH (FfE). „Integrating Bidirectionally Chargeable Electric Vehicles into the Electricity Markets" [9]

In this peer-reviewed "energies" publication, the authors assess the potential revenues of bidirectionally charged vehicles on the German day-ahead and intraday electricity market. They use a mixed integer linear, rolling horizon optimization model considering real trading information based on historical data of both markets and assess potential revenues for various user groups considering technical and behavioral sensitivities and the regulatory framework. They find, that in the best-case scenario revenues of up to 1,300 €/EV/a are possible but emphasize the significant influence of the regulatory framework in terms of taxes and levies.

2020, Wulff et al., German Aerospace Center (DLR). "Comparing Power-System and User-Oriented Battery Electric Vehicle Charging Representation and Its Implications on Energy System Modeling" [10]

The authors of this peer-reviewed energies paper assess the impact of a power system-oriented charging behavior and a user user-oriented charging behavior of EV on energy system optimization results. For that purpose they couple the utility-based stock and flow model VECTRO21, the utility-based microsimulation of charging decisions VencoPy, and the energy system model REMix and use the framework for a scenario study for nine million EV in Germany in 2030. They come to the conclusion that a user-oriented charging and users' plug-in behavior significantly decreases the load shifting potential of the fleet. They also found that the load shifting patterns relate to the weather-dependent infeed of vRES, due to high wind infeed towards the night hours in northern Germany and due to high solar infeed towards midday hours in the south of Germany. They furthermore found a significant impact of the underlying charging behavior on the curtailment of wind power. They conclude that curtailment can be reduced by 10 % when energy system-oriented charging is considered, whereas it is increased by 17 % when user-oriented charging is assumed.

2020, Gaete-Morales et al., German Institute for Economic Research (DIW Berlin). "An open tool for creating battery-electric vehicle time series from empirical data: emobpy" [11]

The publication by Gaete-Morales et al. doesn't provide an assessment of EVs charging strategies but gives a detailed description of the Python-based open-source tool *emobpy*, that allows users to generate individual EV mobility profiles from the empirical dataset of the survey "Mobility in Germany 2017". Based on customizable assumptions, the model creates meaningful and empirically founded EV profiles with the option of differentiating the user group of the driver. As an output, three types of time series are created that constitute a EV profile, the motor electricity consumption, grid availability and the grid electricity demand to charge the battery for different charging strategies. These time series can be used for the integration into energy system models or for independent, vehicle-specific evaluations. The model itself uses probability distributions of the number of trips per day, durations at locations and trips distances from the empirical dataset of the survey to create contiguous mobility profiles.

2020, Lei et al., Karlsruhe Institut für Technologie (KIT). „ Greenhouse gas emissions of electric vehicles in Europe considering different charging strategies" [12]

The authors of this paper, published in the journal "Transportation Research", assess the effect of unidirectional and bidirectional charging strategies on GHG emissions in Europe in 2050 and consider the life cycle perspective of EV with regard to emissions from battery production and disposal. They integrate an EV module and a LCA model in the European energy system model PERSEUS-EU and evaluate four distinct EV scenarios within the context of a highly decarbonized European energy system in 2050 (no EV, direct charging, unidirectionally as well as bidirectionally optimized charging). Similarly to the results presented in section 8.4.2 they conclude that the consideration of an optimized charging considerably reduces the amount of electricity production of gas-fired generators and leads to an increase in vRES-use. This effect is even more pronounced, when bidirectionally charged vehicles are used. They conclude that the resulting decrease in GHG emissions associated with electricity generation more than overcompensate the additional emissions from the battery and vehicle production in that case.

2019, Wietschel et al., Fraunhofer-Institut für System- und Innovationsforschung (ISI). "Die aktuelle Treibhausgasemissionsbilanz von Elektrofahrzeugen in Deutschland" [13]

This paper by Wietschel et al. discusses the impact of various electricity supply scenarios on the LCA of three configurations of EVs and compares them to equivalent conventional diesel and gasoline ICEVs. The authors present and compare different approaches of accounting hourly EMFs (EMF) and also come to the conclusion that the attributional approach is the most adequate for the task at hand. They use an integrative energy system model approach to map a residual load-optimized charging behavior of EVs and describe a similar resulting charging behavior to the one discussed in section 8.4. They conclude their analysis by comparing the total emissions from the production and operation phase of EVs with equivalent conventional ICEVs. The environmental payback periods differ slightly to the ones discussed in section 8.7 in this thesis which can mainly be explained by different assumptions on battery capacities, consumption values of ICEV and annual mileages. The authors discuss various sensitivities and finally emphasize the importance of underlying energy system assumed for both battery production and charging during the operating phase.

2019, International Renewable Energy Agency (IRENA). "Innovation Outlook: Smart charging for electric vehicles" [14]

The authors of this report carried out an extensive literature review of recent international studies on the impact of direct and smart charging on the energy systems of individual countries. They present various pilot projects and discuss business models and the current regulatory framework of smart charging and necessary adaptations. Based on an exemplary isolated energy system, the short-term and long-term effects of a fleet of uncontrolled charging, as well as unidirectionally and bidirectionally optimized EVs are assessed. Simulation results show that smart charging provides "significant benefits in the short-term operation of isolated systems in terms of curtailment mitigation, reduction of peak demand and electricity costs". The assessment of long-term effects shows that unidirectional and bidirectional charging increases the dispatch and potential expansion of vRES and reduce their curtailment and, in case of bidirectional charging, significantly increases the integration of cheap solar generators, facilitating overall cheaper system costs. They conclude the study with 13 concrete action points for policy makers.

2019, Navigant, Kompetenzzentrum Elektromobilität und RE-xpertise, Agora Verkehrswende. "Verteilnetzausbau für die Energiewende - Elektromobilität im Fokus" [15]

At the core of the project carried out by the Navigant Consulting Inc. on behalf of Agora Verkehrswende, various grid simulations were conducted on the low-voltage and medium-voltage level, assessing the impact of EVs under parameter variations and different charging strategies. They considered typical network infrastructures of three spatial categories, urban, semi-urban, and rural, and evaluated the resulting infrastructure expansion costs for the years 2030 and 2050, taking into account a variation of available charging capacity and the total number of EVs. Based on those scenarios they evaluated a direct charging and two strategies aiming at the smoothing of local residual load and the reduction of load peaks relevant for the dimensioning of the distribution grid. The authors conclude that grid-friendly charging strategies lead to a significant reduction in necessary grid infrastructure investment but emphasize the lack of a corresponding regulatory framework or incentive mechanisms.

2019, ifeu GmbH, Agora Verkehrswende. "Klimabilanz von Elektroautos. Einflussfaktoren und Verbesserungspotenzial" [16]

In this study carried out by the ifeu GmbH on behalf of the Agora Verkehrswende, the total climate impact of EVs is discussed with a focus on the production of batteries and the use phase of the

vehicles. Furthermore, different approaches are shown that can lead to an improvement of the climate impact. First, a comprehensive literature review of the emissions generated during battery production is provided, illustrating the wide range of these values. Various sensitivity analyses show the importance of the production phase of EVs and highlight the impact of the electricity used for the production of batteries. For the use phase of the vehicles, the impact of the charged electricity, the mobility behavior and lifetime mileage are discussed. The authors show, that in all cases even under conservative assumption the overall climate impact of EVs is smaller than the one of ICEV. They see significant potential for improving those advantages when more efficient production processes are considered but conclude, that the most important influencing factor is the decarbonization of the electricity sector resulting in lower operational emissions of the EVs.

2018, Schill & Gerbaulet, German Institute for Economic Research (DIW Berlin). "Power System Impacts of Electric Vehicles in Germany: Charging with Coal or Renewables?" [17]

In the discussion paper Schill & Gerbaulet compare the effect of a user-driven (direct) charging with a cost-optimized unidirectional optimization of charging processes with regard to the impact on the electricity generation. For that they use of a mixed-integer linear optimization model that optimizes power plant dispatch and simultaneously the charging processes of EVs. They evaluate different scenarios for the years 2020 and 2030 with different numbers of EVs and different charging scenarios, ranging from user-controlled direct charging to system-optimal unidirectional shifting of charging processes, considering different gradations in between. They come to the conclusion, that all charging strategies lead to an additional dispatch of fossil generators and that the cost driven optimization reduces the use of pumped hydro power plants. The cost driven operation of EVs does therefore increase overall system emissions since charging processes are shifted mostly to times in which lignite power plants are under-utilized. It should be noted, however, that the model only considers the dispatch of power plants and does not include their expansion. To account for this, they exogenously increase the installed capacity of vRES and reevaluate the scenarios. That way optimized charging does reduce charging costs and emissions and leads to a better integration of vRES generation.

2017, Zhao et al., University of Central Florida, "Boosting the adoption and the reliability of renewable energy sources: Mitigating the large-scale wind power intermittency through vehicle to grid technology" [18]

The peer-reviewed "Energy" paper by Zhao et al. aims at the evaluation of GHG emission savings of mitigating intermittency resulting from the introduction of wind generation by bidirectionally charged vehicles. They assess potential savings in seven independent system operator regions in the US with various wind integration levels. The authors consider different additional wind penetration rates as well as degrees of willingness on the part of EV owners to use bidirectional charging. The bidirectionally charged vehicles are used to mitigate ancillary services, resulting from the volatile infeed of those wind generators, and currently mostly provided by combustion generators . They compare the potential savings to the additional emissions from marginal electricity generation caused by the additional electricity demand from EVs. They conclude, that in most cases the emission savings from bidirectionally charged EVs would exceed the additional emissions for marginal electricity generation due to the additional load of the fleet. This is true for all but the lowest degrees of willingness of EV owners to use bidirectional charging.

2015, Jochem et al., Karlsruhe Institut für Technologie. „Assessing CO_2 emissions of electric vehicles in Germany in 2030" [19]

The authors of this paper published in the "Transportation Research" journal in 2015 assess operational emissions of EVs in Germany in 2030 under consideration of four emissions assessment methods (average annual electricity mix, average time-dependent electricity mix, marginal electricity mix, and balancing zero emissions). They assume a market penetration of six million EVs in 2030 and base the mobility behavior of those vehicles on the survey "Mobility in Germany 2008". To assess the influence of a fleet of direct charging EVs they considering its electricity demand as an additional load for the energy system model PERSEUS-NET-TS. For controlled charging the fleet is integrated unit into the equation system of the model. In the uncontrolled case the consideration of a time-dependent average mix yields the same results as the annual average approach. When charging processes are optimized, they are reduced by 14 % from 58 to 50 g CO_2/km. For the assessment of marginal emissions, the authors subtract the resulting electricity generation from a scenario without EVs from a scenario with EVs. That way the marginal dispatch as well as the expansion of power plants can be evaluated. Results show an increase in generation output from conventional power plants leading to the highest value of EVs operational emissions of 110 g CO_2/km in the case of direct charging. However this value can be reduced by 31 % to 76 g CO_2/km when optimized charging is considered. They conclude by recommending political measures to support the decarbonization of the electricity generation and incentivize controlled charging.

1.3 Research questions

There has been extensive research on the topic of EVs and their dynamic interactions with the current and future energy system. Most studies however only focus either on an evaluation of those relationships in the past or in the future energy system. To the authors knowledge, a consistent methodology for comparing the effect of charging strategies under the current state of the system, based on real historical market data, and future state, based on simulated scenario data has not yet been described. Besides the lag of comparable results of charging strategies for past and future years, most studies only consider one or two optimization targets (such as price or a smoothing of (local) residual load). However, a comparison of these results across different studies is hardly possible due to the sometimes very different assumptions and modeling approaches. This dissertation focuses on modeling four individual charging strategies for past and future years and comparing them from an economic and environmental perspective.

Furthermore, most studies view charging strategies from the perspective of the overall optimized energy system. However they mostly neglect the influence of the individual charging behavior of EV owners with regard to their plug-in or mobility behavior and further user-specific parameters that can reduce the effect of such an optimized charging strategy. Ried [8] and Kern et al. [9] do consider some of these sensitivities, but neglect others and have a different focus with respect to the optimization objective of the considered charging strategies. In the context of this work, the evaluations are deliberately made from the perspective of the EV user or the aggregator responsible for the implementation of such charging strategies and shed light on the sensitivities in this regard. EV users do not always behave rationally, and aggregators have limited information and do not necessarily target the optimal solution to the system as energy system models do. It is assumed that electric vehicle owners are interested in reducing operating costs and also attach greater importance to the environmental impact of their vehicles. For this reason, all of the charging controls examined relate to these goals and, where possible, are also evaluated in terms of potential revenue and emissions reductions.

Since with higher numbers of EVs the feedback effects they and especially the charging strategies discussed here have on the energy system, those are considered accordingly. The questions to be answered include the contribution that vehicles can make to decarbonizing the transport sector and the extent to the assessed charging strategies can contribute to improved integration of vRES. Furthermore potential negative feedback effects with regard to resulting additional load on the grid as well as the vehicles themselves have to be addressed.

From this general topic, the following research questions are derived:

- How can the specific emissions in the electricity mix be estimated on a consistent methodological basis now and in the future and what is the influence of taking into account the upstream chain of fuels and the plants involved in the electricity supply in this context?

- Which type of emission accounting (mix or marginal) should be used for the accounting of consumers and which should be used as a target of charging strategies?

- What charging strategies make sense to meet the requirements of an energy system increasingly characterized by volatile energy sources?

- What revenue potential can be expected from these charging strategies?

- What are the most important influencing factors that define the potential of such charging strategies?

- Can the charge control of EV contribute to the balancing of regional imbalances between renewable energy feed-in and electricity demand to reduce grid congestion (Redispatch/Curtailment)?

- What contribution can the charge control of EVs make to reducing the operational emissions of the vehicles and thus the environmental "payback period" of the vehicles after the energy-intensive battery production?

- What impact does the optimized charging of EVs have on the energy system?

2 Methodology

This dissertation focuses on emissions during the operating phase of electric vehicles and their relationship with the changing energy system. It investigates the extent to which charge control strategies (use cases) affect costs and emissions during operation and how the vehicles can play an active role in an increasingly integrated energy system. The methodology for mapping these relationships is shown in Figure 2-1.

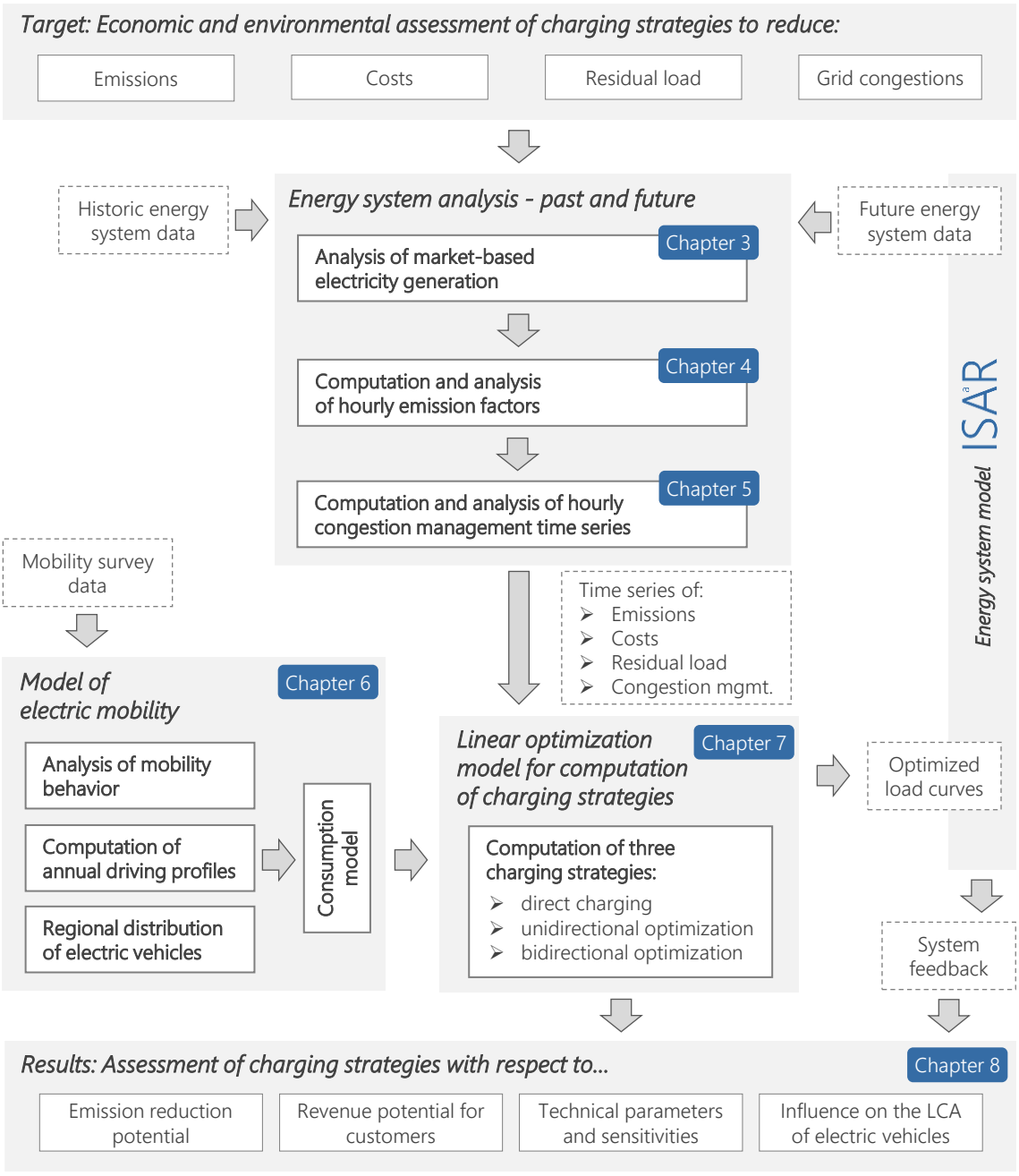

Figure 2-1: Structure of the underlying methodology

The approaches applied in this work, shown in the diagram, are briefly introduced in the following section, and the methodological challenges are explained.

Energy system analysis

Increasing shares of vRES accompanied by a phaseout of both nuclear and coal-fired power plants have fundamentally changed the structure of the German energy system. Since EVs operational emission directly depend on the electricity mix they use in the charging process, this has to be considered when those emissions are assessed. Taking that information into account, the historical and future development of installed capacities and electricity generation is described in detail in chapter 3. Furthermore, the resulting values of the residual load as well as the day-ahead prices are presented, and their correlation is discussed. At this point, the impact on grid infrastructure and resulting congestion are not yet addressed. The focus lies on the market-based power generation and the associated wholesale prices.

The emissions of electrical consumers such as EVs are directly linked to the emissions resulting from the generation of electricity. Since these emissions change with the deployment of generators over time, hourly EMFs are calculated and assessed based on three methodical approaches in chapter 4. In the first approach, generation-based EMFs are calculated with respect to the electric output of generators in Germany. The second approach considers the existence of an integrated European electricity market and the resulting exchange of electricity across national borders. In this consumption-based approach, emissions are allocated in accordance with the electricity consumption in Germany, considering the exchange of electricity across borders and the emissions of all generators in the integrated European energy system. In the third approach, marginal EMFs are assessed based on the hourly emissions of the marginal power plant according to the German merit order curve. The merit order curve is defined as the power plant capacities sorted in ascending order according to their marginal costs. According to this order, power plants are selected in the electricity market until the demand for electricity is met. In such a market, based on marginal pricing, the marginal cost of the last power plant to be selected determines the market price. All three EMFs are calculated for historical and future years and assessed with regard to their correlation with other variables in the energy system. Based on that, their suitability as an optimization target for charge controls, as well as the right measure for the accounting of operational emissions, is discussed.

Increasing shares of wind and solar-electric generators in Germany repeatedly lead to grid congestion, which is currently compensated for by short-term measures such as the redispatch of conventional power plants or the curtailment of those vRES. These congestion management (CM) measures and the usage of otherwise diminished and, at least in the case of curtailment, emission-free electricity comprise another focus of this thesis. To assess the potential reduction of CM-measures in the past, a methodology is described in chapter 5 for transforming plant-based data on individual measures into spatially and temporally high-resolution time series of CM measures. Furthermore, redispatch measures are evaluated with regard to their net emission effect.

Model of electric mobility

The mobility behavior of vehicle users plays a decisive role in the assessment of the operational emissions of EVs as well as the potential of charge control strategies. In that context, it is not sufficient to use previously collected first-user profiles of EV owners as a basis for the evaluations as these do not necessarily reflect the behavior of users in the broad population. Since no data is yet available that meets these requirements, a methodology is developed (in chapter 6) to synthesize coherent and statistically correct annual driving profiles based on the two major mobility surveys in Germany. The empirical data presented in the surveys “Mobility in Germany 2017” and “Mobility panel” is first analyzed regarding the suitability of the modeling approach and key indicators for the assessment of charging strategies. For the evaluation of the potential of an electric fleet for the reduction of CM

measures, the number of vehicles, and their regional distribution for past and future years are derived.

Model for computation of charging strategies

As mentioned, the goal of this dissertation is the assessment of the economic and environmental impact of charging strategies for EVs. In this context the effect of a unidirectional optimization of charging processes by shifting charging processes to time periods corresponding to the optimization goal is to be assessed. In addition, the potential effect of a vehicle-to-grid charge control is also investigated, where vehicles can be charged and discharged while they are connected to the grid and are therefore used similar to an electric storage unit. The focus here is on those use cases that have a particularly high potential for reducing emissions or improving the integration of vRES. Along with the evaluation of the resulting emissions, an estimation of the revenue potential from the point of view of the vehicle users, is also conducted. Figure 2-2 provides an overview of the use cases analyzed.

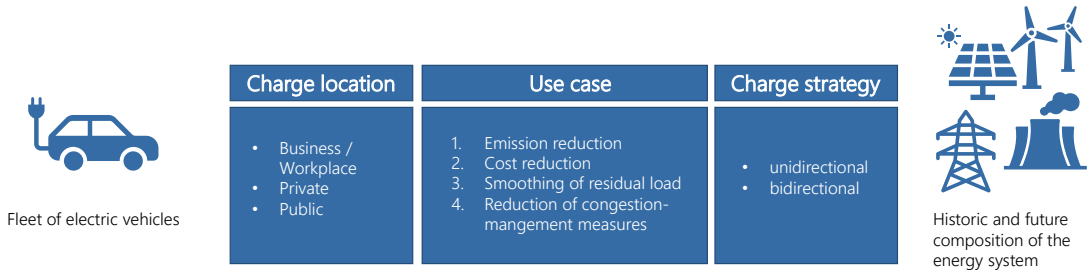

Figure 2-2: Use cases investigated in this thesis

All assessments are performed on historical data from 2019 and in most cases with regard to scenario data for 2030 and 2040. Since no reliable information on future CM-measures was available, these evaluations are only carried out for the historical year 2019. In particular, the potential for improved integration of vRES in the future energy system and the possible emission savings are evaluated. Finally, these results are classified in the LCA along with their influence on the ecological payback period of the vehicles.

To assess the revenue and emission reduction potential, a linear optimization model is developed and described in chapter 7. The model is designed in MATLAB and integrated into the framework of the PostgreSQL database FREM[1] [20]. Due to that structure, dynamic adaptation of input parameters, easy usability, and comprehensible results for all use cases can be achieved. In a first step, the mobility profiles, synthesized as described in chapter 6, are transformed into time series of electric load by means of a consumption model addressing traveled distance, speed, and outdoor temperature. The resulting profiles are then merged with the technical parameters of vehicles, charging infrastructure, user behavior, and market data, and translated into a linear optimization problem. Solving that optimization problem regarding the minimization of costs/emissions and/or the reduction of CM measures results in the charging and discharging behavior for every vehicle under consideration.

The modeling approach described in those two chapters works well for large numbers of simulated vehicles and only then meets the statistical validity for a sufficient representation of German mobility behavior. Computational limitations and practicability, however, restrict the number of profiles that can be simulated. The aspired integration of these mobility profiles into the larger modeling

[1] The FfE Regionalized Energy System Model (FREM) [20], www.ffe.de/frem

framework of the FfE's energy system model ISAaR[2] [21] restricts the number of usable profiles even further. Hence, various clustering algorithms and an approach of stochastic drawing are used to identify the number of representative profiles needed to meet the requirements of each of those applications.

Assessment of charging strategies

In chapter 8, the findings and results from the previous chapters are merged in the assessment of four different use cases aimed at the reduction of operational emissions, costs, and CM measures. In all cases, the potential emission reduction is the focus, but possible revenues for vehicle owners are discussed as well. Various sensitivities are then analyzed to understand the most influential parameters and their impact on possible emission reductions and repercussions on the vehicle, as well as on the energy system. Finally, the resulting annual emissions of vehicles are used in an LCA, and their influence on the ecological payback period of EVs is discussed.

[2] Integrated Simulation Model for Planning the Operation and Expansion of Power Plants with Regionalisation [21], www.ffe.de/isaar

3 Electricity Generation in Germany – Past, Present and Future

As the underlying energy system plays an important role in the evaluation of charging strategies, past and future energy-related developments are presented in this section. In contrast to the grid-side effects of these developments discussed in chapter 5, the focus in this chapter is purely on market-based power generation and resulting electricity prices. First, a short introduction of the data used for the current and historical electricity production in Germany is provided in section 3.1. Numerous gas- and coal-fired power plants in Germany have a combined production of heat and power (CHP). In those cases, emissions as well as costs must be allocated according to the heat and power output for every hour. Since no data on the operation of these plants is available, a methodology is presented in section 3.2. testing various machine learning (ML) algorithms to predict their operation based on outdoor temperature and electricity prices. Since charge operations are not only assessed for recent years, section 3.3 summarizes the scenario quEU, developed in the project eXtremOS [22], which shows a possible development path until 2040. Sections 3.4 and 3.5 then focus on the historical and (scenario-based) future developments of electricity generation, residual load, and wholesale prices of electricity.

3.1 Data basis—historical market data

For the evaluation of charging strategies, both hourly and annual data on German electricity production is needed. Data on the annual gross electricity production in Germany is derived from the Federal Ministry for Economic Affairs and Energy (BMWi) [23]. Further information on the annual electricity generation from CHP power plants is provided by the Working Group on Energy Balances (AGEB) [24]. Figure 3-1 shows the German gross electricity production in 2019 subdivided by the respective energy sources.

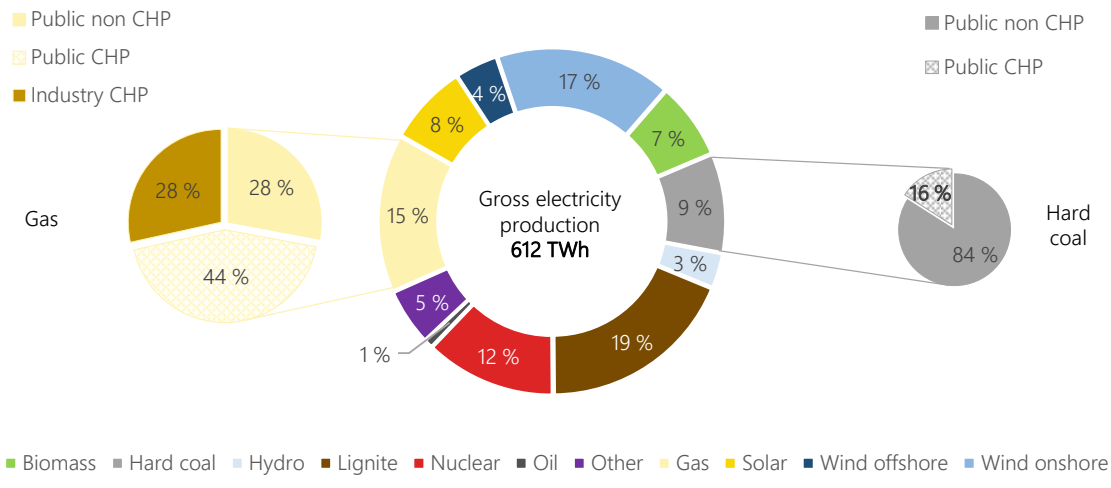

Figure 3-1: Gross electricity production in Germany 2019

Increasing the installed capacities of renewable wind and solar generators, as well as the beginning phaseout of nuclear power plants, has substantially altered the generation portfolio. In 2019, a total of 39 % of the generated electricity was produced by renewable generators. The remaining fossil production mainly consists of nuclear (12 %), lignite (19 %), hard coal (9 %), and gas (15 %). As the data show, the last two have a high proportion of CHP plants, which must be considered accordingly when assessing operating emissions and costs. CHP plants can be subdivided into two categories: public power plants connected to district heating networks and industrial power plants used to cover base load process heat. Since no hourly generation data of those power plants exists, a methodological approach must be applied here, as described in the following section.

3.2 Prediction of CHP production with a machine learning approach

Since no data on the operation of CHP plants is publicly available, a modeling approach was developed in [25] and revised in [26]. In both studies, a bottom-up approach is described using publicly available data on district heating systems in Germany provided by the AGFW [27] as well as hourly data on outdoor temperature and wholesale electricity prices to derive hourly heat and electricity production profiles. In a first step, the heating demand for the 33 largest district heating networks in Germany is determined from information on outdoor temperature. Then CHP types (defined by fuel, generator technology, and efficiency) are allocated to the corresponding district heating network, and the hourly wholesale price of electricity is used to attain individual time series of heat and power generation for each plant from 2011 to 2015. Figure 3-2 shows the resulting electricity generation from CHP plants in Germany as a function of outdoor temperature and day-ahead prices.

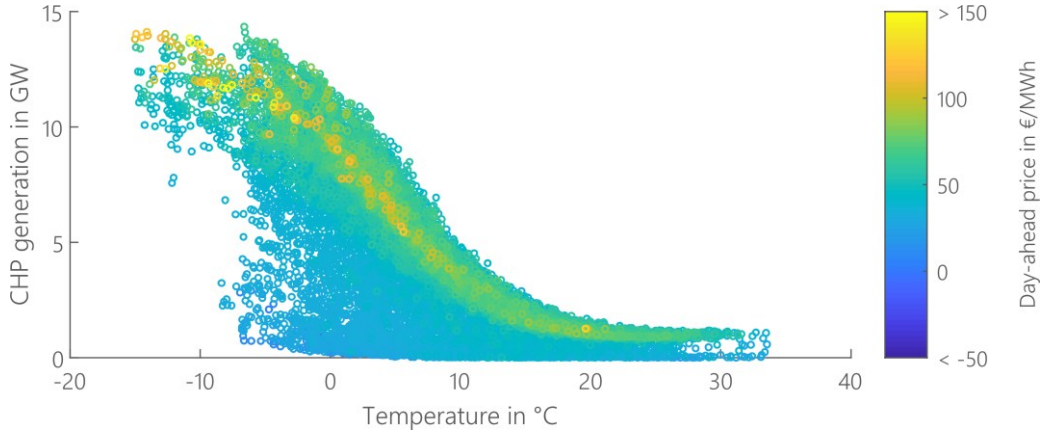

Figure 3-2: Electricity generation from CHP plants in Germany as a function of outdoor temperature and day-ahead prices, 2011–2015 (derived from [25])

As expected from the model description, a clear correlation between both outdoor temperature as well as day-ahead prices and the resulting electricity generation from CHP plants can be observed. Lower temperatures lead to higher heating demand in district heating networks, resulting in a higher generation from CHP plants. Since at least some share of those plants also considers possible revenues on the day-ahead market as an incentive, high prices also increase CHP production.

However, no simulated data was available for 2019, which is the historical base year for all the simulations conducted in the context of this thesis. Furthermore, missing up-to-date input data required for the modeling resulted in the need for a different approach. Due to the large dataset of simulation results for the years 2011–2015 and the knowledge of the modeling approach depending solely on existing power generators, outdoor temperature, and wholesale market prices, supervised

ML algorithms are tested to predict hourly time series of Germany's power generation from CHP plants. For the task at hand, four algorithms of supervised ML were tested, decision tree, random forest, supper vector regressor and long term/short term memory neural network (LSTM). Supervised ML algorithms are used to identify correlations in datasets when inputs and output are known. Generally, the dataset is subdivided into separate training and test datasets. The algorithms are trained on the training dataset and then used to predict the output for the test dataset. Deviations (represented by, e.g., the root mean square error [RMSE] or the coefficient of determination R^2) from the predicted and original data in the test dataset are then used to quantify the validity of the prediction.

For the prediction, the Python-based module Scikit-learn was used [28]. Scikit-learn provides a wide range of ML algorithms, both for supervised and unsupervised problems. For a detailed description of the algorithms considered, refer to the documentation in https://scikit-learn.org. For the problem at hand, we proceed as follows:

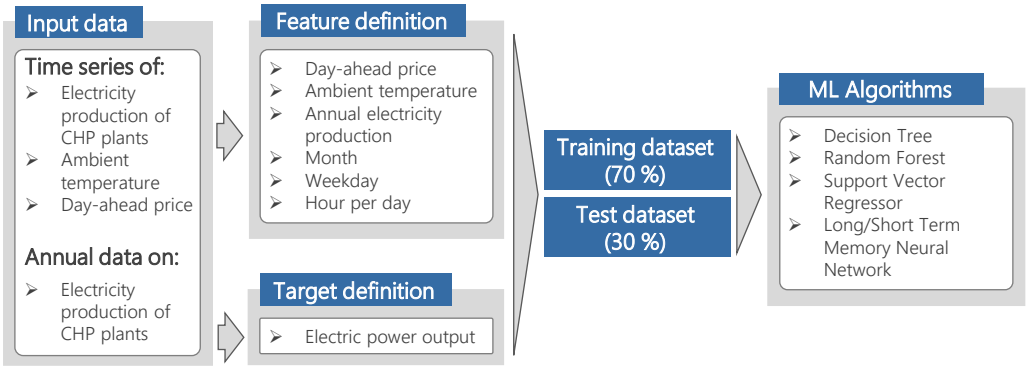

Figure 3-3: Process of ML-based prediction of CHP electricity production

First, the available output data of the model for the years 2011-2015 are categorized and processed into features and outputs (targets). Electricity price, outdoor temperature, and annual electrical power produced from CHP were scaled to a standard normal distribution using Scikit-learn StandardScaler. The resulting dataset is then subdivided into a training (70 % of all data points) and a test dataset (30 % of all data points), and the ML algorithms are tested. Various configurations of the algorithms with respect to mode of operation and hyperparameters were tested to identify the subset showing the best prediction performance. The following configurations were finally used, resulting in the RMSE and R^2-values presented in Table 3-1:

Table 3-1: Configuration and results of the ML algorithms used

	Decision Tree	Random Forest	Support Vector Regressor	LSTM Neural Network	
Configuration	• Max depth: 11 • Split criterion: Mean Square Error (MSE) • Rest: Default	• N estimators: 1000 • Criterion: MSE • Out of bag score: True • Rest: Default	• Kernel: Poly • Epsilon: 0.65 • Degree: 4	• 1 LSTM Layer • 1 fully connected layer • Lookback: 24 h • Loss: MSE	• Epochs: 32 • Batch size: 8 • Optimizer: Adam • Hidden units: 12
RMSE train	233	81	1984	701	
R^2 train	0.995	0.999	0.651	0.951	
RMSE test	323	214	2044	779	
R^2 test	0.99	0.995	0.598	0.94	

Based on those results, Random Forest was identified as the best-performing algorithm and was used to predict the electricity generation from CHP plants for 2014–2019, which is later used as an input time series for the calculation of hourly EMFs.

3.3 Scenario description quEU

Scenario data for the future development in the electricity sector are derived from the scenario quEU, designed in the project eXtremOS [22]. The main objective of the project is the establishment and application of methods that allow for the investigation of the value of flexibility under extreme technological, regulatory, and social developments. The modeling and scenario approach not only focuses on changes in Germany but recognizes the existence of an interconnected European energy system and therefore considers an integrated scenario process for 16 European countries.

The scenario quEU is described in detail by Fiedler et al. in [29] and is explained as follows: "In the quEU scenario, the socio-political context in Europe worsens compared to today and society perceives that the costs of containing climate change outweigh the benefits. The lack of incentives to promote fuel switch measures beyond today's trends results in only a moderate phase-in of EVs and heat pumps in the household, tertiary and transport sector. The energy transition in the industrial sector is slowed significantly and solely efficiency improvements are realized, while industry structure and process technologies remain similar to today." (p. 1) This situation is to be considered rather conservative, but due to the assumed cost degradation, renewable generators such as wind and solar are strongly expanded despite the lack of incentives. While the demand sectors do not undergo fundamental changes, and the energy transition especially in the industrial sector is even slowed significantly, the trends in electricity production, especially in 2030 and 2040, can still be considered as ambitious. Overall, these are the developments that are relevant for the evaluations in the context of this thesis. The following section describes the changes in the power sector in Germany "from past to the future", based both on historical data and the scenario data derived from quEU. A more detailed description of quEU and the underlying assumptions can be found in [29].

3.4 Installed capacities and electricity production by type

Figure 3-4 shows the installed capacities of renewable as well as fossil generators in Germany from 2010 to 2040. Here, historical data is derived from [23], whereas future values are based on the scenario quEU.

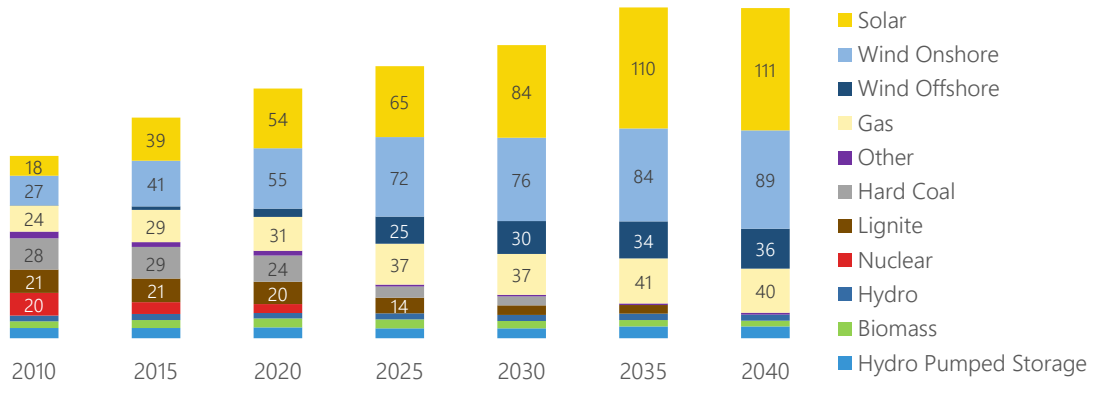

Figure 3-4: Installed generation capacities in Germany in GW

Even though the situation cannot be considered a climate mitigation scenario, the generation portfolio changes significantly. The phaseout of nuclear and coal leads to a strong decrease of those capacities. The scenario assumes a strictly market-based approach without additional subsidies. Due to the cost degradation of vRES, installed capacities are heavily expanded, dominating overall electricity production in future years, as presented in Figure 3-5.

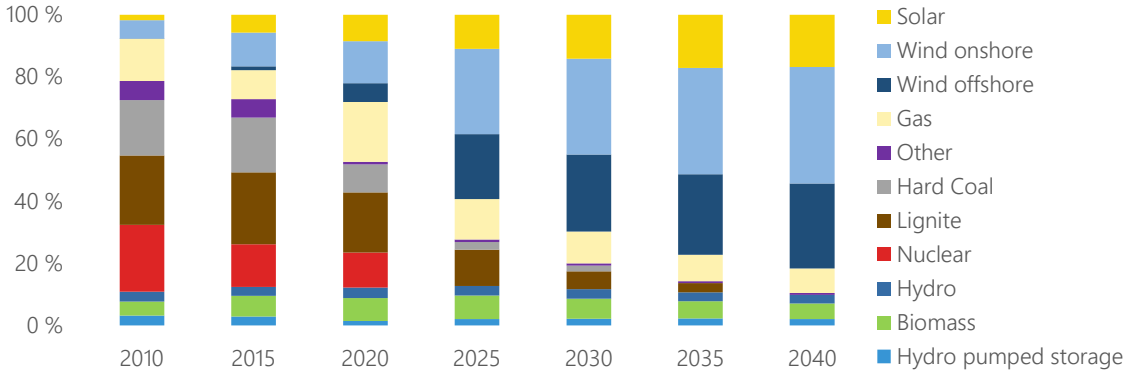

Figure 3-5: Share of energy carriers in gross electricity production in Germany

The consideration of the generated electricity quantities shows the same picture. Even without subsidies, renewable generation from wind and solar accounts for 70 % in 2030 and 82 % in 2040. The only remaining emitting generators are gas-fired turbines, but they account for only 10 % in 2030 and 8 % in 2040 due to high total renewable generation.

3.5 Residual load and day-ahead prices

The term residual load refers to the electrical power demand in an electricity system minus the share of fluctuating feed-in from volatile generators such as wind or solar generators (vRES). It represents the residual demand for electrical power that must be covered by controllable power plants, such as pumped hydro storage and fossil-fuel power plants like gas or coal. It is therefore an important indicator of how "green" the electricity generation in each hour is and how much surplus renewable energy could potentially be used by charge controlled EVs. Figure 3-6 shows the annual duration curve of the residual load in 2019 and 2030.

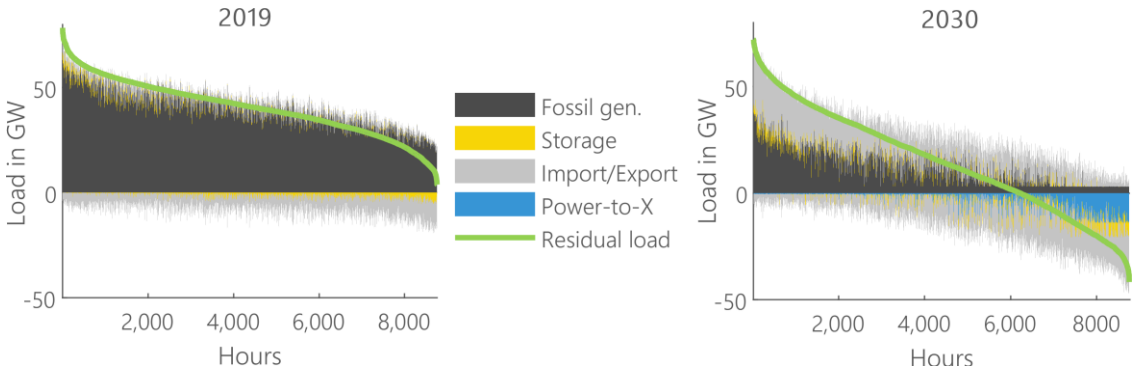

Figure 3-6: Annual duration curve of residual load in 2019 and 2030

In addition to the residual load, the plot also shows the hourly values of the remaining fossil generation, charging and discharging of storages (in 2019, mainly hydro pumped storage; in 2030, battery storage as well), imported and exported electricity, and in 2030, the amount of electricity used for applications such as power to heat and power to hydrogen. In 2019 fossil generators

dominate the overall electricity production at all times. Residual load values are positive the entire year, indicating that there is no excess production of vRES that could be used by EVs. In 2030, the circumstances change significantly. Residual load is negative in 2,538 hours of the year, mainly used by storage facilities, power-to-x applications, or the export to neighboring countries. Besides hydroelectric storage plants, battery storages are increasingly used to store excess electricity. Electricity production from fossil generators is drastically reduced, becoming more of a backup solution than the general means of production.

Since renewables enter the market with zero marginal cost, their increasing share also has a strong impact on the wholesale electricity price as shown in Figure 3-7.

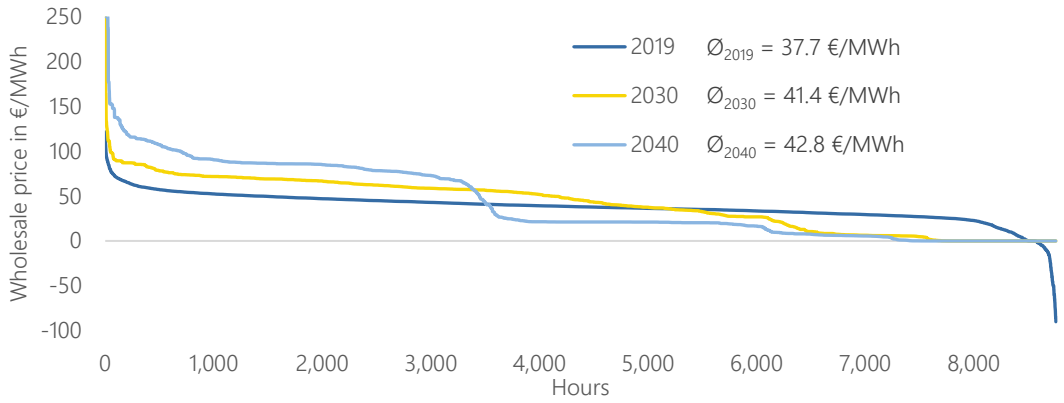

Figure 3-7: Annual duration curve of wholesale prices in 2019, 2030, and 2040

Hours on the right with a wholesale price of zero or below are times when renewables constitute the marginal power plant. In 2019, that was the case in 212 hours; in 2030, in 761; and in 2040, in 1,006. Note that linear optimization models such as ISAaR are not able to map negative price values. Besides an increasing number of hours with a wholesale price of zero €/MWh, times with higher prices increase as well, leading to overall higher average prices over the course of the year. In 2019 a heterogenous portfolio of power plants and underlying marginal costs lead to a very smooth progression of the annual duration curve. Nuclear plants are still operational, CHP and non-CHP lignite and especially hard coal, as well as gas-fired power plants, all with very distinct marginal costs, still make up a large share of the overall installed generation capacity. Future years, on the other hand, do show an increasingly stepped progression, since the number of distinct generator-types regresses. In 2040 mainly high-cost CHP and non-CHP gas-fired power plants with similar marginal costs and vRES with zero marginal costs remain. The range of prices in between is defined by storage and power-to-x technologies as well as the import of electricity from neighboring countries. This future market situation, characterized by periods of low wholesale prices and periods of higher prices, indicates an increasing revenue potential of price-based optimization of EVs. A further discussion of pricing mechanisms in such a future energy system is presented in Böing and Regett (2019) [30] as well as the project report of the project Dynamis in [31].

The same smooth progression of the duration curve in 2019, as well as the stepwise progression in 2040, can be observed when the day-ahead prices are compared to the values of the residual load in Figure 3-8.

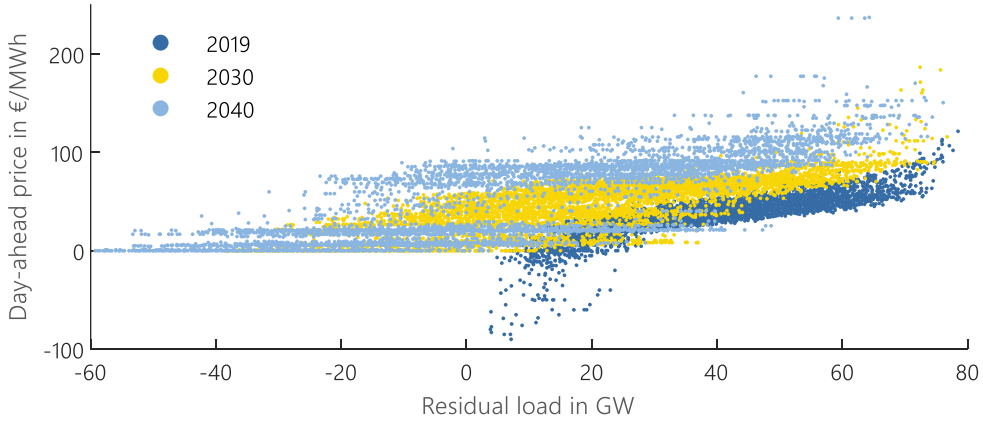

Figure 3-8: Correlation between day-ahead prices and residual load values

In 2019 the electricity generation is still dominated by fossil power plants leading to positive residual load values over the entire year. However, high vRES feed-in already leads to low values of residual load accompanied by negative day-ahead prices in 212 hours of the year. In both future years, the increased capacity of the vRES generators results in an overproduction of electricity accompanied by negative values of the residual load in many hours of the year. However, these times are not always characterized by wholesale electricity prices of zero (negative prices cannot be mapped by the energy system model ISAaR). The additional demand of power-to-x applications and storage capacities, as well as international electricity trading, result in prices sometimes well into double digits, even in times of negative residual load. Therefore, price-optimized charging of EVs does not necessarily coincide with the goal of targeting periods of high vRES feed-in.

3.6 Conclusion

As stated in the beginning of this chapter, the underlying energy system plays an important role in the evaluation of both operational emissions of EVs as well as their charging strategies. In this chapter the historical and assumed future developments (based in the scenario quEU, section 3.3) in the power sector were described. Since a significant share of Germanys power plants are CHP plants and no corresponding generation time series of those plants is publicly available, a ML approach was described in section 3.2 to predict those time series based on the outdoor temperature and the day-ahead price. The generation time series of those and all other power plants in Germany are used in the following chapter 4 to derive hourly EMFs. The presentation and discussion of historical day-ahead prices and residual load values forms the basis for the respective charging strategies discussed in sections 8.3 and 8.4.

4 Emission Assessment of Electricity Generation

When assessing the operational emissions of EVs, the most important influencing factor is the electricity generation and the resulting specific emissions per kWh electricity (EMF) in the underlying energy system. According to Wietschel et al. [13], Johnson et al. [32], and Regett [33], various dimensions such as

- temporal resolution (annual, daily, hourly)
- geographical resolution (local, regional, national, transnational)
- accounting method (mix method, marginal method)
- time horizon (historical, future)
- considered emissions (CO_2 emissions/all GHG emissions, only direct/with upstream)
- data basis (historical data, power system model results)

can be considered when assessing EMFs. In praxis, when accounting emissions of electric consumers, such as EVs, often historical annual average values of EMFs in g CO_2/kWh_{el} are considered. Due to the high temporal variability of the charging processes as well as increasingly volatile feed-in of renewable generators in the course of energy transition, these are not deemed sufficient for the evaluation of the actual ecological footprint of EVs during operation. Hence, hourly EMFs of the underlying electricity mix must be considered. In principle, a distinction can be made among three types of accounting methods for hourly EMFs.

The most used method is to calculate average generation-based EMFs based on the shares of different generators and energy sources in each country for each hour with distinct efficiencies and underlying stoichiometric EMFs of the respective primary energy carriers (see section 4.3). However, as stated in Tranberg et al. [34], this generation-based approach only reflects national production and neglects the existence of an integrated European electricity market and the resulting exchange of electricity across national borders. Hence, a more detailed approach is needed that has the actual electrical load in each country as a reference, taking into account the production by type in the market area and the import and export of electricity resulting from cross-border electricity trade. The resulting consumption-based EMFs reflect these coherences well and can be used to assess the actual emissions of electric consumers as part of this integrated energy system. In section 4.4 the methodology for the assessment of historical consumption-based EMFs as described in [34] is applied and extended to consider electricity generation from CHP plants in Germany.

When accounting for emissions of EVs, studies can generally be subdivided into two groups according to the way EMFs are considered [35]. The attributional approach uses the mix EMF, whereas in the consequential approach, marginal EMFs are calculated. After an extensive discussion of the mix method, section 4.5 focuses on the calculation of marginal EMFs and the related merit order dilemma of emissions. Section 4.6 presents results for past and future years and analyzes correlations with other values in the energy system. Furthermore, it discusses the application of each of the accounting methods for the assessment of operational emissions and the impact of charging strategies.

In the context of this thesis, a uniform methodology is developed for all three accounting methods (generation-based, consumption-based, and marginal), allowing the consistent calculation of EMFs

based on both historical market data as well as model-derived future electricity generation data. Figure 4-1 provides a brief overview of the input data used for the calculation of the EMFs for historical data and that derived from the energy system model for evaluations of future EMFs.

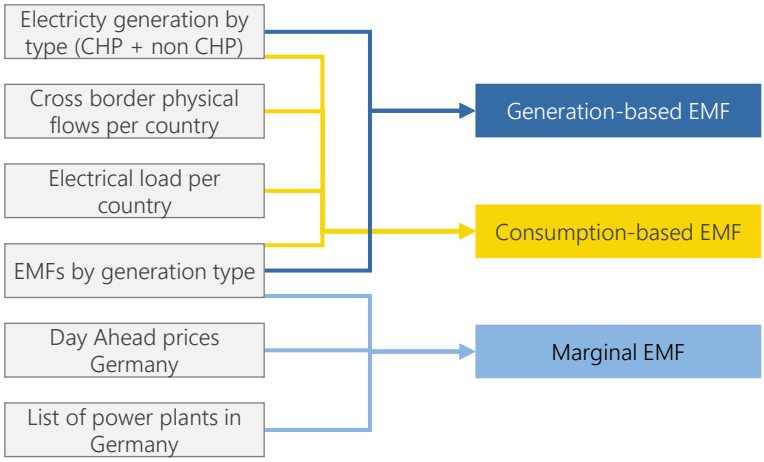

Figure 4-1: Overview of input data for the calculation of the three types of EMFs

The developed methodology forms the basis for the consistent and comparable ecological assessment of EVs and charging strategies in the past and in the future energy system and is described in detail in the following sections.

4.1 Data basis for the assessment of historical emission factors

Regardless of the time horizon and the accounting method, the specific emissions of the energy sources involved in electricity generation are needed to drive hourly EMFs. In principle, a distinction can be made here between system boundaries, both in terms of the GHG accounted for and the considered upstream emissions that result from fuel extraction and refining as well as the construction of the fossil or renewable generator/power plant itself. Since the overall climate impact of both the assessment of uncontrolled charged vehicles and charging strategies is the scope of the evaluations, GHG EMFs with consideration of upstream emissions are considered. Those factors with respect to the produced electricity are derived from the ecoinvent database version 3.6 [36], wherein the IPCC 2013 LCIA accounting approach is used. Figure 4-2 shows the resulting CO_2 and GHG EMFs per generation type considered in the calculation of the hourly EMFs.

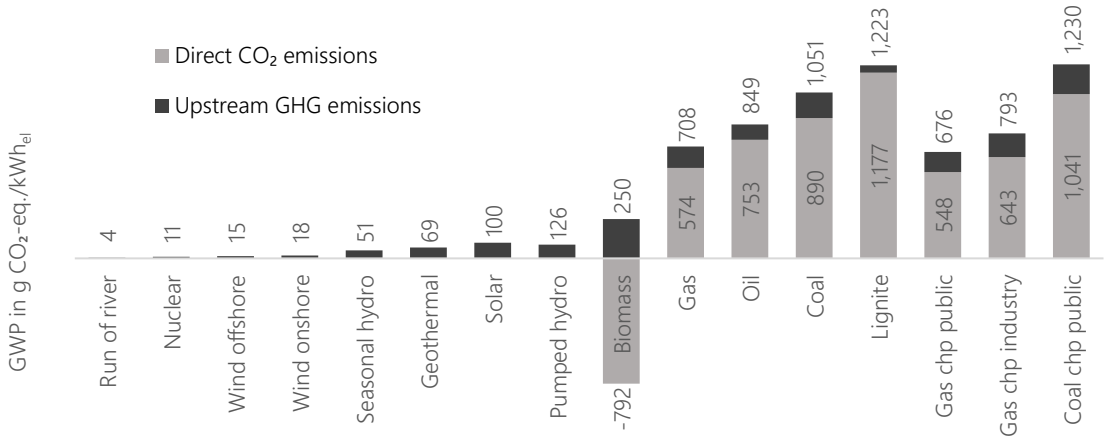

Figure 4-2: Global warming potential (GWP) of electricity production per energy carrier based on [36]

The CO_2 EMFs given in Figure 4-2 are used for validation purposes in section 4.3, where the resulting average annual EMFs are compared with the ones published by the German Environment Agency (Umweltbundesamt [UBA]) [37]. Furthermore, current national and international climate legislation and regulation, as well as public debate of this topic, still mostly considers CO_2 emissions. Therefore, some of the results are also given with direct CO_2 emissions as a reference. The negative value of -0.792 kg CO_2/kWh_{el} for biomass results from the use of different accounting methods. Since biomass is considered renewable, the direct CO_2 emissions in the LCIA approach are neglected, leading to overall emissions of 0.25 kg CO_2-eq/$kWh_{el.}$ They are, however, considered in the accounting method for direct CO_2 emissions, leading to emissions of 0.792 kg CO_2/kWh_{el}.

Strong political support and subsidies have led to a significant share of electricity production from gas- and coal-fired CHP plants in Germany, as shown in section 3.4. Since those power plants have a combined production of heat and power, EMFs must be accounted for accordingly. As outlined in section 4.2, the Carnot method is used in the context of this work, leading to the values presented on the right of Figure 4-2.

4.1.1 Data basis for calculation of historical electricity generation

Table 4-1 presents an overview of the data used for the calculation of the three types of historical EMFs. For future years all the data is derived from simulation results of the energy system model ISAaR.

Table 4-1: Input data for the calculation of historical hourly EMFs

Data type	Temporal resolution	Geographical scope	Provider
Net generation of CHP plants	Hourly	D	Based on [25] and [26], predicted for 2019 (see section 3.2)
Net electricity generation by production type	Hourly	EU	European Network of Transmission System Operators for Electricity (ENTSO-E) Transparency Platform [38]
Load values	Hourly	EU	ENTSO-E Transparency Platform [38]
Cross-border physical flows (CBPF)	Hourly	EU	ENTSO-E Transparency Platform [38]
Day-ahead prices	Hourly	DE	EEX data portal [39]
List of power plants	Annual	DE	Federal Network Agency [40]
Gross electricity generation by production type	Annual	DE	Federal Ministry for Economic Affairs and Energy (BMWi) [23]
Net electricity generation of CHP plants by production type	Annual	DE	Working Group on Energy Balances (AGEB) [24]

The average EMFs are calculated with reference to the gross electricity production including grid losses. Hence, the hourly data on net electricity generation provided by [38] and net electricity generation from CHP plants derived from [25] and predicted to the base year 2019 (as described in section 3.2) are scaled to the annual data on gross electricity production provided by the Federal Ministry for Economic Affairs and Energy (BMWi) [23] and the Working Group on Energy Balances (AGEB) [24]. Since the data from the European Network of Transmission System Operators for Electricity (ENTSO-E) on hourly electricity generation by type, load, and cross-border physical flows (CBPF) are the main source for the calculations, a critical appraisal of the data quality is presented in the following section.

4.1.2 Critical assessment of the ENTSO-E Transparency Platform data quality

The most comprehensive data source on power system data in Europe is the Transparency Platform [41] operated by ENTSO-E. The platform was initiated by ENTSO-E to fulfill the EU Regulation No. 543/2013 defining the necessity for transparent and open-source access to data on electricity production, transportation, consumption, and market prices. The platform offers access to the data via a website graphical user interface (GUI) and RESTful API, as well as direct access through an SFTP server. Data is provided by several national institutions such as transmission system operators (TSO) and distribution grid operators (DSO) as well as power exchanges.

Hirth et al. [42] have conducted extensive research on data quality, identifying several shortcomings. For the evaluations conducted in this study, data completeness and consistency are of utmost importance. Hence, a quick review of the data quality is presented in this section with respect to completeness of the datasets used for the calculation of historical hourly EMFs, namely actual total load [6.1.A], aggregated generation per type [16.1.B&C], and physical flows [12.1.G].

Figure 12-1 in the appendix displays an overview of the completeness of the date in those types. Values for generation by type and individual imports and exports have been aggregated on a country level for better presentability. Although the overall completeness of the data in most countries amounts to 100 %, there are significant gaps for some countries, making the calculation of EMFs impossible. For countries with smaller gaps in load and generation by type, a methodology was developed to fill those gaps. Smaller gaps were interpolated, and larger gaps were filled based on the development of these values in neighboring countries. Since there is no way to validate or

interpret the values of CBPF, no further processing was considered here. After further validation of the overall dataset, the number of countries was reduced from 36 to 26 of the neighboring countries of Germany. For the calculation of Germany's consumption-based EMFs, this is deemed adequate since their influence on Germany's consumption-based EMF (including imports and exports) is highest. Furthermore, due to missing data points, especially in the past years, for the calculation of consumption-based EMFs relying on a complete representation of electricity production and trade for all considered countries, only 2019 was included.

4.2 CHP allocation and its influence on specific emissions

As shown in Figure 3-1, in 2019, 20 % of German fossil electricity production was generated by CHP plants, mostly gas- and coal-fired. Since those power plants have a combined production of heat and power, emissions as well as costs must be allocated accordingly. There are many methods for the allocation, and various studies have compared those methods in the past decade. Beginning with Beer and Wagner [43] in 2007, Wiesemeyer et al. [44] in 2010, and Tereshchenko et al. [45] or Hertle et al. [46] in 2014, extensive work has been done on the topic, leading up to the formulation in VDI guideline 4661 (2014), stating that there is "no method that would be equally compelling to apply overall, i.e. according to thermodynamic, economic and ecological criteria." Since the chosen method has a significant influence on the resulting costs and emissions, a brief overview is presented here with the example of a gas-fired CHP plant.

The methodology for the calculations of the respective allocation factors $\alpha_{th/el}$ is described in detail in [46], p. 120 et seq and [44]. Since in the scope of this work, the Carnot method is used in the calculation of EMFs in general, and the Finnish method is used for the validation of results with the annual EMFs published by the German Environment Agency [37], both are described herein. The Finnish method considers the primary energy savings (PES) of a CHP plant compared to individual and uncoupled generation of electricity and heat in a reference system with reference values for efficiency $\eta_{el,ref}$ and $\eta_{th,ref}$. These values are set by [47] to $\eta_{el,ref}$ = 40 % and $\eta_{th,ref}$ = 80 %. The allocation factors for electricity and heat $\alpha_{el/th}$ are defined as

$$\alpha_{el} = (1 - PES) \cdot \frac{\eta_{el}}{\eta_{el,ref}} \qquad \alpha_{th} = (1 - PES) \cdot \frac{\eta_{th}}{\eta_{th,ref}}$$
$$\text{with } PES = 1 - \left(\frac{\eta_{th}}{\eta_{th,ref}} + \frac{\eta_{el}}{\eta_{el,ref}}\right)^{-1} \tag{4-1}$$

resulting in allocated absolute emissions $Em_{el/th}$ and specific EMFs $emf_{el/th}$ for the energy carrier ec as

$$Em_{el}(f) = emf_{ec} \cdot \alpha_{el} \cdot W_{ec} \qquad emf_{el}(ec) = \frac{Em_{el}(ec)}{W_{el}}$$
$$Em_{th}(f) = emf_{ec} \cdot \alpha_{th} \cdot W_{ec} \qquad emf_{th}(ec) = \frac{Em_{th}(ec)}{W_{th}} \tag{4-2}$$

with W_{ec} in *kWh* amount of energy carrier used

W_{el} in *kWh* amount of electricity produced

W_{th} in *kWh* amount of heat produced

emf_{ec} in *kg CO_2-eq./kWh_{fuel}* specific EMF of the energy carrier

The Carnot method, on the other hand, reflects the exegetic potential of the products electricity and heat as the basis for the allocation. In contrast to the Finish method, the allocation does not depend on the external definition of reference processes but only uses endogenous parameters. It does,

however, consider the temperature level of the produced heat T_{out} as well as the reference outdoor temperature T_a as a calculation basis for the exegetic Carnot factor η_c, which is defined as

$$\eta_c = \frac{T_a}{T_{out}} \tag{4-3}$$

Both temperature levels are defined in [48], resulting in η_c = *26.36 %*. The allocation factors for heat and electricity are defined as

$$\alpha_{el} = \frac{\eta_{el}}{\eta_{el} + \eta_c \eta_{th}} \qquad \alpha_{th} = \frac{\eta_c \eta_{th}}{\eta_{el} + \eta_c \eta_{th}} \tag{4-4}$$

The resulting allocated absolute emissions $Em_{el/th}$ and specific EMFs $emf_{el/th}$ are then calculated according to equation (4-2). Figure 4-3 summarizes the resulting allocations of total emissions as well as the specific EMF when allocated by the four most discussed allocation methods for an average German gas-fired industrial CHP plant with η_{el} = 24 % and η_{th} = 56 %.

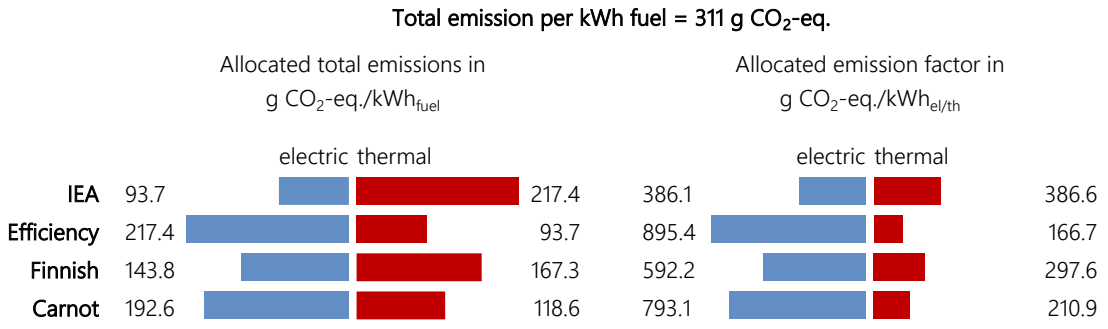

Figure 4-3: Influence of CHP accounting methods on resulting EMFs and total emissions

As stated in VDI guideline 4661, there is no single allocation method that perfectly represents all the thermodynamic, economic, and ecological criteria of a CHP plant. Nevertheless, the exegetic representation of outputs in the Carnot method factors in their thermodynamic qualities and is furthermore unbiased by externally set reference processes. For those reasons, it is chosen as the CHP allocation method in this thesis.

4.3 Calculation of generation-based emission factors

As shown in Figure 4-1, generation-based EMFs only consider the national gross electricity generation by energy carrier W_{ec} as well as the respective EMF emf_{ec}. For each point in time t, the share of each production type on the total electricity generation $q_{gen,ec}$ is calculated as:

$$q_{gen,ec}(t) = W_{ec}(t) / \sum_{ec=1}^{m} W_{ec}(t) \tag{4-5}$$

With consideration of the fuel-specific EMFs emf_{ec}, the average generation-based EMFs for m energy carriers results in:

$$emf_{el,gen,avg}(t) = \sum_{ec=1}^{m} q_{gen,ec}(t) \cdot emf_{ec} \tag{4-6}$$

According to these equations, the average consumption-based EMFs can be calculated for both the hourly historical data (described in section 4.1.1) and scenario-based generation data derived from the energy system model ISAaR for the scenario quEU described in section 3.3.

4.4 Calculation of consumption-based emission factors

In contrast to generation-based EMFs, consumption-based EMFs are calculated with reference to the actual demand for electricity. In an integrated energy market such as the European one, large amounts of electricity are transported across national borders. Hence, not only must the national generation of electricity be considered but also those electricity flows as well as the generation in the neighboring countries. Only such an approach reflects the reality of an integrated energy market well and is suitable for accounting for the emissions of consumers, such as EVs, according to their cause. Scott [49] has proposed a set of linear equations to evaluate emissions due to consumption of electricity in each US state. Li et al. [50] and Zengkai at al. [51] have adopted that method, calling it carbon-flow tracing, and applied it to the Chinese energy system. Tranberg et al. used the same methodology on the dataset of electricitymap.org and discussed its implications in detail in [34].

Not only does this approach allow for the allocation of emissions to the consumer of electricity, but it also characterizes the hourly imports and exports by share of production types, allowing conclusions to be drawn about which energy sources are exported or imported. The underlying mathematical formulation was extended to account for the electricity production from German CHP plants (as described in section 3.2) and can be summarized as follows. The basic assumption is that, as mentioned above, in an interconnected energy system such as the ENTSO-E area, the calculation of national generation-based EMFs is not sufficient because it ignores imported emissions from and exported emissions to neighboring countries resulting from cross-border electricity trade. Therefore, not only must the national generation of a country be considered but also that of its electrical neighbors. All these coherences can be represented by a linear system of equations: For any given point in time and all r, countries $n_1 \dots n_r$ have an electricity production by m different energy carriers $W_{n_i,ec}$ for energy carrier $ec = 1, \dots, m$ and electric load L_{n_i} and the storage charge and discharge of pumped hydro storage plants as $S^+_{n_i,php}$ and $S^-_{n_i,php}$. Furthermore, the amount of energy exported from country n_i to country n_j is defined as F_{n_i,n_j}. The energy balance for each point in time t and each country n_i can therefore be described as:

$$L_{n_i} + S^-_{n_i,php} + \sum_j F_{n_i,n_j} = \sum_{ec} W_{n_i,ec} + \sum_j F_{n_j,n_i} + S^+_{n_i,php} \tag{4-7}$$

Rearranging equation (4-7) and applying it to all countries $n_1, \dots, n_r$ leads to the following set of linear equations (4-8). Solving that system of linear equations, we can now calculate the share $q_{cons,n_i,ec}$ of each production type ec on the total generation, including the imports and exports of energy due to CBPF between the r European countries.

$$\begin{bmatrix} z_{n_1} & -F_{n_2,n_1} & \dots & -F_{n_r,n_1} \\ -F_{n_1,n_2} & z_{n_2} & \dots & -F_{n_r,n_2} \\ \vdots & \vdots & \ddots & \vdots \\ -F_{n_1,n_r} & -F_{n_2,n_r} & \dots & z_{n_r} \end{bmatrix} \begin{bmatrix} q_{cons,n_1,ec} \\ q_{cons,n_2,ec} \\ \vdots \\ q_{cons,n_r,ec} \end{bmatrix} = \begin{bmatrix} W_{n_1,ec} + S^+_{n_1,php} \\ W_{n_2,ec} + S^+_{n_2,php} \\ \vdots \\ W_{n_r,ec} + S^+_{n_r,php} \end{bmatrix} \tag{4-8}$$

Here, $q_{cons,n_i,ec}$ is the share of production type ec on the total produced electricity in the country n_i with reference to the electrical load and $z_{n_i} = L_{n_i} + S^-_{n_i,php} + \sum_{j=1}^{r} F_{n_i,n_j}$. Based on these shares, we can then calculate the average consumption-based EMF for each point in time t and each country n_i as:

$$emf_{el,cons,avg,n_i}(t) = \sum_{ec=1}^{m} q_{cons,n_i,ec}(t) \cdot emf_{ec} \tag{4-9}$$

where $emf_1, \dots, emf_m$ are the m-different EMFs for each production type ec. Solving this system of linear equations for all hours of the year results in the desired hourly timeline of consumption-based EMFs. This method is applied on the historical data presented in Table 4-1 as well as the simulations results of the energy system model ISAaR based on the scenario described in section 3.3.

4.5 Calculation of marginal emission factors

The last method for allocating emissions is the marginal method. Marginal EMFs follow the consequential approach. According to [52], a consequential approach is a "system modelling approach in which activities in a product system are linked so that activities are included in the product system to the extent that they are expected to change as a consequence of a change in demand for the functional unit." In the context of EV emission accounting, that approach focuses on the impact that the additional load of the vehicles has on the energy system.

According to Marmiroli et al. [35], a distinction must be made between short-term and long-term effects. When assessing the impact of EVs on the electricity generations, short term and long term are usually identified with the dispatch of power plants versus the long-term expansion of production capacities [53]. While the long-term impacts of major load changes must be simulated with expansion models such as ISAaR, the short-term impacts can be estimated with marginal EMFs associated with the marginal power plant in each hour according to the merit order of the power plants.

There are two main approaches for the calculation of marginal EMFs. The first, as applied and described in Böing & Regett [30], can be used for energy system models by marginally increasing the electrical load in each time step and comparing the resulting power plant dispatch with a reference scenario. The second approach uses the pricing mechanism of the day-ahead market. Since day-ahead prices are set by the marginal power plant with respect to the merit order curve, the time series of those prices can be employed as an indicator for marginal EMFs, as described and published in [54]. In contrast to the first approach, this allows a consistent calculation applicable to both historical and future scenario data from energy system models. The methodology has been revised, adapted, and applied to the year 2019 as well as the scenario data for 2030 and 2040.

For clarity, the methodology is briefly presented here again. In addition to the time series of day-ahead prices, data on all available power plants, with their technical specifications and economic parameters such as fuel and CO_2 certificate prices, are needed. This data is derived from the power plant database of the Research Center for Energy Economics (FfE). The database consists of three parts, namely the lists of existing plants and planned additions or deconstructions ([55], [56], and [57]), and manually researched data on plant-specific parameters, and techno-economic parameters of different plant types ([58] and [59]). Data for fuel and CO_2 costs is derived from the scenario data used in quEU [29] as presented in Table 4-2.

Table 4-2: Assumed prices for energy carriers and CO_2 certificates

	2019	2030	2040	Unit
CO_2 certificates	22.9	27	75	€/t
Lignite	4.3	4.3	-	€/MWh
Gas	16.7	27.4	29	€/MWh
Hard coal	11.1	16		€/MWh
Nuclear	1.7	-		€/MWh
Oil	38.6	61.3	66	€/MWh

Based on this data, the merit order curve of power plants in Germany can be derived. In a merit order curve, all generators are sorted by their marginal costs in ascending order. Based on this order, all power plants that provide electricity in each hour are determined in the day-ahead market. Figure 4-4 shows that curve for the data assumed for 2019. Power plants are colored according to the underlying energy carrier.

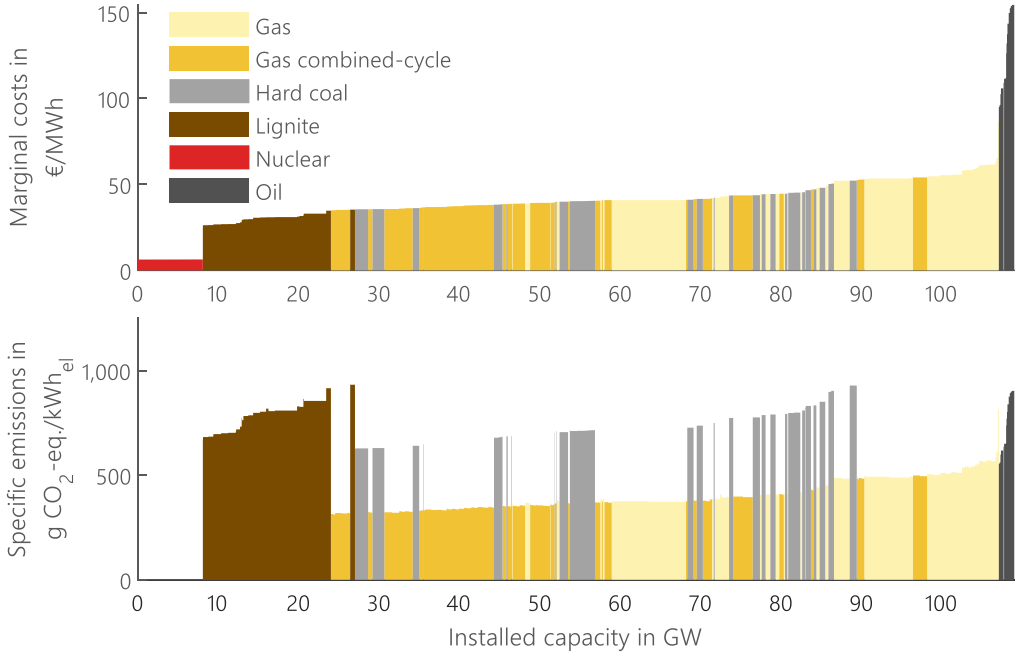

Figure 4-4: Merit order curve (2019) for marginal costs and emissions (CHP allocation according to Carnot method)

In contrast to the original publication in [54], emissions and marginal costs of CHP power plants are allocated according to the Carnot method. Furthermore, instead of using direct CO_2 EMFs, the GHG EMFs, including upstream emissions, are used as described in section 4.1. As shown in Figure 4-4, 2019 is the first year in history when increasing CO_2 prices in combination with low gas prices, lead to a so-called fuel switch. In prior years, overall low CO_2 prices have led to the merit order dilemma of emissions, as described in [60], meaning that emission-intensive lignite and hard coal power plants were preferred over gas-fired power plants due to lower marginal costs. Since the reform of the ETS market in 2018 [61], prices for CO_2 certificates have risen sharply, as described in [62], leading to the new dispatch order of power plants beginning to resolve the merit order dilemma, as shown in Figure 4-4. Figure 4-5 depicts the same evaluation for 2030.

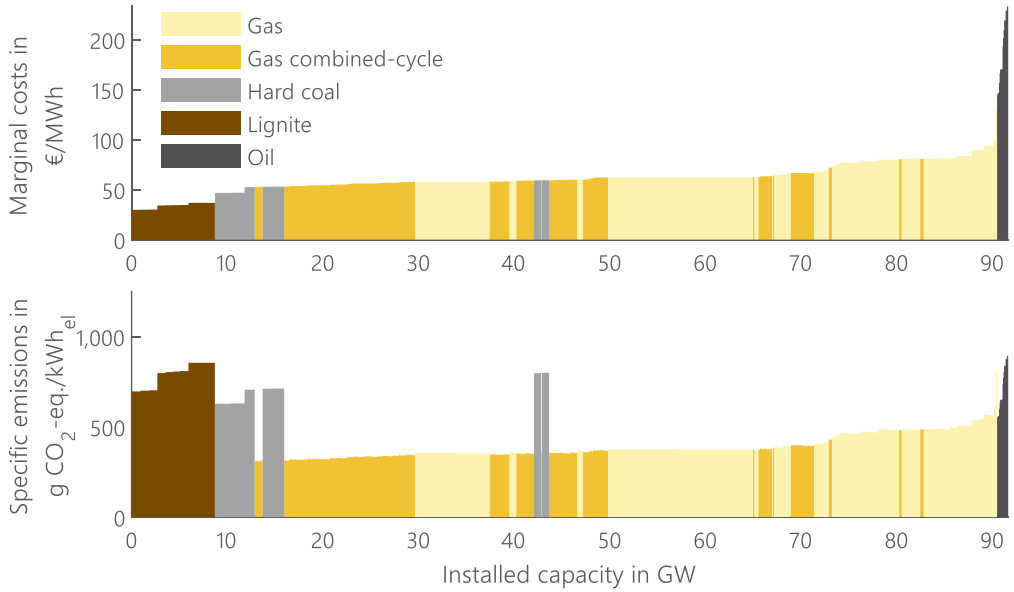

Figure 4-5: Merit order curve (2030) for marginal costs and emissions (CHP allocation according to Carnot method)

Due to the assumption of a steep increase in gas prices from 16.7 to 27.4 €/MWh$_{th}$ with only a moderate increase in CO_2 prices from 22.9 to 27 €/t CO_2, as shown in Table 4-2, the fuel switch has been reversed in 2030. Efficient lignite and hard coal plants now have lower marginal costs and are therefore still prioritized over most gas-fired power plants.

For every hour, the day-ahead price is matched with the marginal prices of all German power plants, identifying the marginal power plant. The resulting marginal EMF $emf_{el,cons,marge}$ for each hour t is then calculated by

$$emf_{el,cons,marge}(t) = \frac{emf_{ec,pp_{marge}}(t)}{\eta_{pp_{marge}}(t)} \quad (4\text{-}10)$$

where $emf_{ec,pp_{marge}}$ is the stoichiometric EMF of the used energy carrier and $\eta_{pp_{marge}}$ the electric efficiency of the marginal power plant pp_{marge}. To address inaccuracies and reduce excessive fluctuations in the resulting time series, a power range of +/- 1 MW is defined around the identified marginal power plant, and the resulting average marginal emissions are derived from all power plants in this range. The described method is applied on the historical data presented in Table 4-1 as well as the simulations results of the energy system model ISAaR based on the scenario described in section 3.3 for the year 2030 to derive hourly time series of marginal EMFs.

4.6 Results

In this section, the methodology described in sections 4.3 to 4.5 is applied to the historical data presented in section 4.1.1 as well as the model results for the scenario described in section 3.3.

4.6.1 Validation of results

As a first step, the methodology is validated by comparing the resulting average annual generation-based EMFs to the data on annual specific CO_2 emissions of the German electricity mix published by the UBA [37]. The report calculates specific CO_2 emissions without consideration of upstream

production stages (upstream chains) such as fuel extraction and transport, as well as other GHG, based on the fuel input used for electricity generation in Germany as published annually by the AGEB [63]. Furthermore, the Finnish method is used for allocation of CHP emission instead of the Carnot method used here (as described in section 4.2). The UBA also considers imports and exports of electricity to derive a consumption-based EMF but uses a different approach, not including electricity generation in neighboring countries. Hence, only the generation-based EMFs are considered for the validation. Furthermore, the direct CO_2 EMFs (as shown in Figure 4-2) and the Finnish method for CHP allocation are applied for the validation. Table 4-3 illustrates the comparison of both values for the available years 2015 to 2019.

Table 4-3: Comparison of calculated CO_2 EMFs in Germany with data from [37]

	2015	2016	2017	2018	2019	Unit
Own calculations	510	503	476	463	399	g CO_2/kWh$_{el}$
Values by UBA	527	523	485	468	401	g CO_2/kWh$_{el}$
Deviation	**+ 3.3 %**	**+ 4.1 %**	**+ 1.9 %**	**+ 1.0 %**	**+ 0.5 %**	

Deviations in resulting EMFs can be considered small. Further investigation of the raw data on electricity generation by type in [37] already shows minor deviations to the one used in the calculations described in this work, explaining some of the overall deviations depicted in Table 4-3. Furthermore, the different approach of UBA, using the fuel input as a basis for the calculation of total emissions instead of the actual electricity output, leads to expectations of smaller deviations. Overall, the differences are insignificant enough to validate the general methodology applied here.

4.6.2 Development of generation-based emission factors over time

In a next step, the methodology was applied to historical data from 2015 to 2019 as well as to the model results for the scenario for 2030 and 2040, now with respect to GHG EMFs with consideration of upstream emissions. Calculations are only conducted for Germany. The resulting values are shown as a boxplot in Figure 4-6.

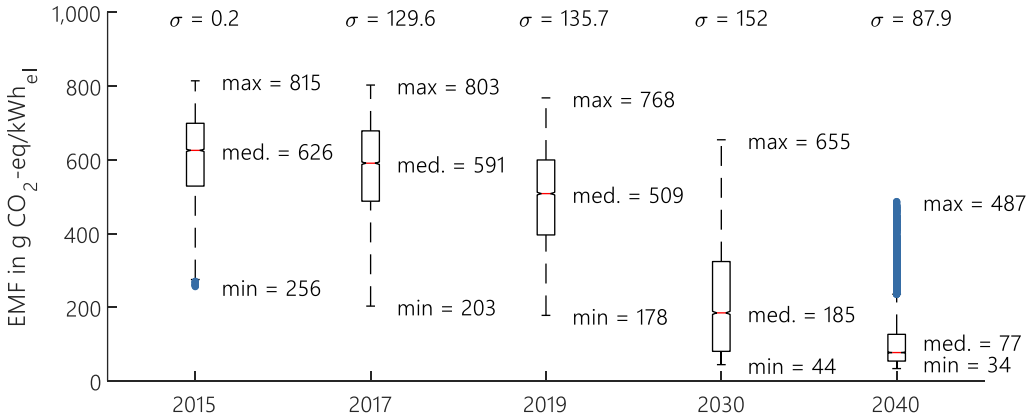

Figure 4-6: Generation-based EMFs for 2015 to 2040

Since electricity production from vRES has increased significantly over the considered time horizon (as described in section 3.4), the median EMF decreases. Especially in the two scenario years 2030 and 2040, the coal phaseout accompanied by a strong expansion of vRES results in very low median values. The still quite high maximum value of 655 g CO_2-eq./kWh in 2030 indicates times of low vRES feed-in in which the remaining coal-fired power plants provide a large part of the electricity

generation. The growing shares of volatile renewable generators also lead to an increase in volatility of the resulting EMFs, represented by an overall higher standard deviation σ. The standard deviation then decreases in 2040 since all high-emission coal plants are decommissioned, and electricity is mostly generated by vRES and low-emission gas-fired power plants. This can be interpreted as a good indicator of the increasing potential of especially bidirectionally emission-optimized charge controls of EVs in 2030 since a high volatility in EMFs yields higher potential revenues.

4.6.3 The difference between generation-based and consumption-based emission factors

Next, the historical data is used for the calculation of consumption-based EMFs according to the methodology described in section 4.4. For that purpose, not only is data on Germany's electricity generation by type needed but also generation data from its electrical neighbors as well as on CBPF and electrical demand. Since the data quality varies significantly in the countries under consideration but improves over time (as described in section 4.1.2), the calculation is only performed for 2019. Figure 4-7 shows the resulting generation-based EMFs according to the methodology described above for all 26 considered European countries, their imported and exported emissions due to CBPF, and the sum of those values, which is defined as the consumption-based EMF.

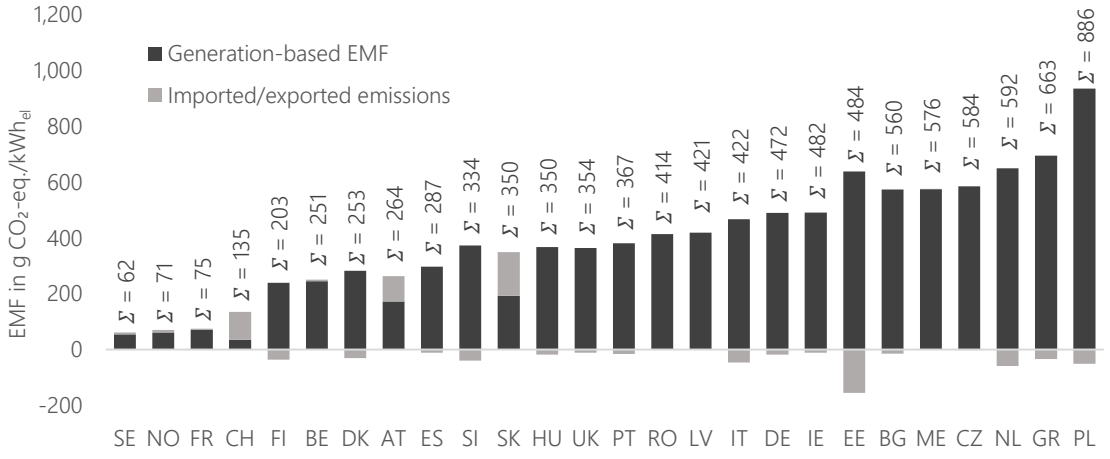

Figure 4-7: Generation-based EMFs of 26 countries in 2019 and imported/exported emissions due to electricity trade

Some countries show significant differences between generation-based and consumption-based EMFs. Several countries can be described as net exporters of emissions such as Spain, the Netherlands, Estonia, Greece, and Poland; others (e.g., Switzerland, Austria, Slovakia, and Latvia) import a large part of their emissions while having a relatively low national generation-based EMF themselves. Reasons for that are manifold and can be found in the individual structure of each country's energy market and the ones of their neighboring countries, individual market-coupling mechanisms as well as available transmission capacities in-between countries. Austria for example has a relatively low average generation-based EMF due to high shares of hydro power plants and wind generators but imports large shares of its electricity from its emission-intensive neighbors Germany and the Czech Republic. Slovakia is a similar case with a low "local", generation-based EMFs resulting from high shares of nuclear energy and large amounts of high-emission electricity from its neighbors Poland and the Czech Republic. Estonia (EE) is a good example of contrasting relations. An overcapacity of emission-intensive and cheap shale oil generators and a good integration with its neighboring countries results in a significant overproduction and large exports to its neighbor

Latvia (12.3 TWh of which 1.9 TWh were exported in 2018, [64]), leading to 24 % lower consumption-based EMF.

In addition to these high-level evaluations, the carbon-flow tracing method also allows a more precise interpretation of country-specific conditions. Since all the following evaluations are only conducted for Germany the country index n_i is omitted in the description. First, the hourly shares $q_{cons,ec}(t)$ are multiplied with the respective EMF emf_{ec} resulting in the share of the energy carrier-specific EMF $emf_{el,cons,ec}(t)$ on the total average EMF. The same calculations are applied for national electrical generation resulting in $emf_{el,gen,ec}(t)$. Based on that, the difference between the average consumption-based EMF and the average generation-based EMF can be calculated for each energy carrier as:

$$\Delta emf_{ec}(t) = emf_{el,cons,ec}(t) - emf_{el,gen,ec}(t) \quad (4\text{-}11)$$

It must be noted though, that just as with consumer emissions accounting, there are two views of accounting emissions for electricity trade - the marginal and the mix approach. One could argue that from a market perspective exports and imports of electricity from the country under consideration must be considered as marginal and thus also assessed with marginal EMFs according to the merit order curve. On the other hand side just as electric consumers are to be considered as a part of the energy system, all countries in an integrated European electricity market must be considered as equal parts of the overall European energy system. Based on that assumption, emissions of imports and exports must be assessed with the mix-method. Therefore, in case of an exemplary export of 1 MWh in a specific hour the exported emissions and shares by generation type are based on the generation mix occurring in that hour in the exporting country. Under those assumption the difference of generation-based and consumption-based EMFs can be explained in detail for each country in every hour. Figure 4-8 shows this annual evaluation for Germany in 2019.

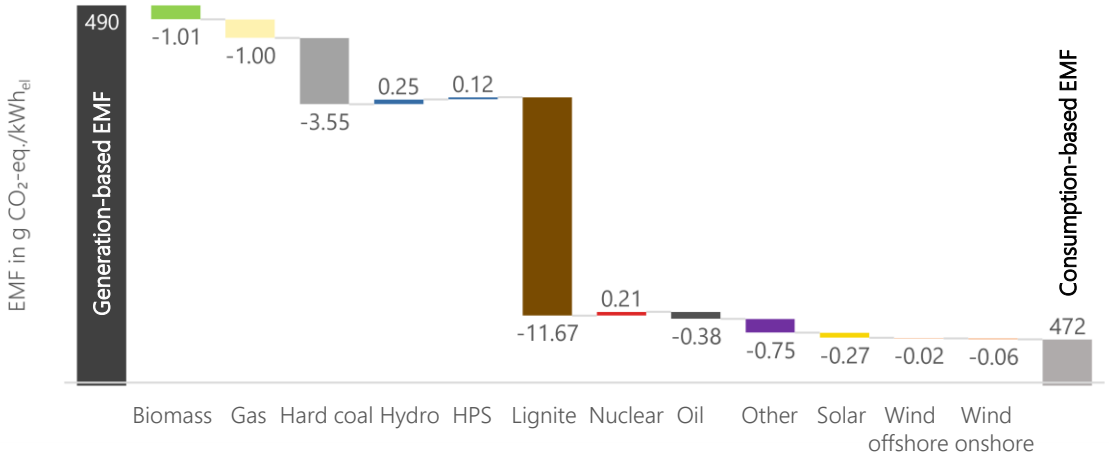

Figure 4-8: Difference between generation-based and consumption-based EMF in Germany 2019

The figure illustrates the average annual generation-based EMF on the left and the average annual consumption-based EMF on the right side with the delta broken down by generation types Δemf_{ec} in a waterfall diagram. The evaluation shows, that the main driver for overall lower consumption-based EMFs in 2019 is the export of electricity from lignite power plants. Exports primarily happen when the national electricity prices are lower than the ones in neighboring countries. This mainly occurs in times of low loads and heigh shares of renewables in the system. Due to the dispatch of power plants according to their position on the merit order curve the residual load is mostly covered

by nuclear and lignite power plants in those times. The same is true for cheaper hard coal fired power plants leading to a net export of emissions from those generators.

Table 4-4 presents the evolution of average generation-based and consumption-based EMFs for Germany in the considered timeframe from 2019 to 2040.

Table 4-4: Evolution of generation-based and consumption-based EMFs in Germany from 2019 to 2050

	2019	2020	2025	2030	2035	2040	Unit
Generation-based EMF	490	515	329	234	176	118	g CO_2/kWh_{el}
Consumption-based EMF	472	515	308	205	151	102	g CO_2/kWh_{el}
Deviation	**- 4 %**	**- 2 %**	**- 7 %**	**- 12 %**	**- 14 %**	**- 13 %**	

Under the current market scheme, increasing vRES shares with marginal costs of 0 €/MWh lead to lower prices in hours with high vRES infeed. As discussed in section 3.5, in 2019, prices were at or below 0 in 212 hours; in 2030, in 761; and in 2040, in 1,006 hours, respectively. Due to the interconnected electricity market, electricity is exported when prices in Germany are lower than in the neighboring countries and imported when prices are higher. Under the historical and assumed future development of the European energy system, this leads to Germany being a net exporter.

Regarding exported and imported emissions, it is assumed that in an integrated system, it is not possible to distinguish which type of electricity is imported or exported. Every time an export happens, emissions are exported according to the mix method. The same is true for imported electricity. Overall, with Germany being and remaining a net exporter, this results in more electricity produced than needed and therefore generation-based EMFs being higher than consumption-based EMFs.

Since consumption-based EMFs best represent the reality of an integrated European energy system, all the following evaluations are based on these.

4.6.4 Statistical analysis and correlations

As mentioned at the beginning of this chapter, EMFs of electric consumers can be accounted for in two ways [35]. The attributional approach uses the mix EMF, and the consequential approach calculates marginal EMFs. The questions to be answered here are which approach to consider both for the accounting of operational emissions and for use as an optimization target for the vehicles and the influence that decision has on both assessments. Since the approach has a significant influence on results, the characteristics, and correlations of each of the EMFs with relevant values in the energy system are evaluated in the following section.

4.6.4.1 Temporal distribution of consumption-based emission factors

First, the consumption-based EMFs for 2019 and 2030 are illustrated as a histogram in Figure 4-9 to provide a rough sense of the density of the underlying distribution.

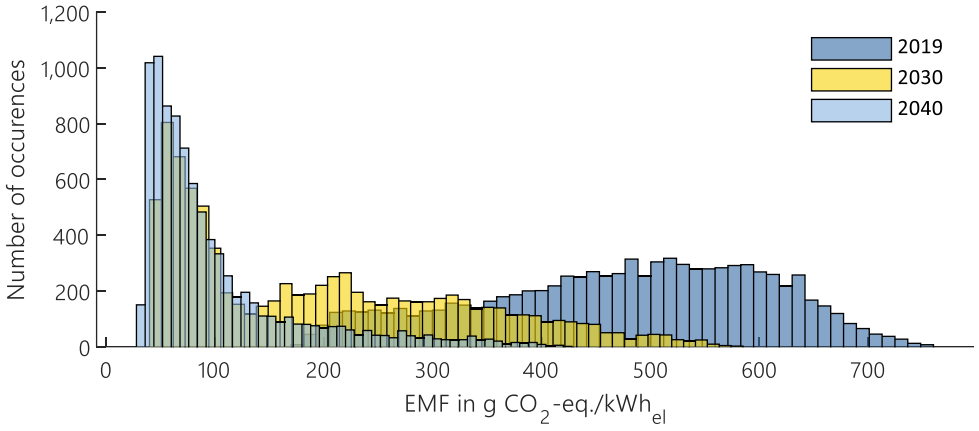

Figure 4-9: Histogram of consumption-based EMFs in 2019 and 2030

Increasing shares of RES, as well as a nearing phaseout of coal-fired power plants in 2030, lead to a significant shift toward lower emissions, which is even more pronounced in 2040. Not only are the median values much lower in the future years but also the number of hours in which EMFs are low. Whereas EMFs are below 100 g/kWh in 37 % of all hours in 2030 and 69 % in 2040, respectively, due to still high shares of coal-fired power plants, they are distributed more broadly in 2019.

This can also be observed when considering the daily and annual distribution of these values as presented in the form of heat maps for 2019, 2030, and 2040 in Figure 12-3 in the appendix. Two patterns can be observed in all years. First, solar infeed during the day leads to low emission values. Due to higher installed capacities, this pattern is much more pronounced in the future, not only far reaching into the early and late months of the year but also beginning earlier and ending later during the days. The second pattern can be explained by the increased expansion of wind energy. In 2019, a period of strong winds in early March led to low EMFs over the course of consecutive days. This phenomenon occurs with increasing frequency in 2030 and 2040, where many periods can be observed with low EMFs throughout several consecutive days. During those days, a unidirectional and even bidirectionally optimized charging of EVs will not have a strong effect since EMFs are low all the time.

For the emission reduction potential of optimized charging strategies, the variation of the targeted time series is the deciding factor. This variation can best be described by the standard deviation σ. Since the emission reduction potential depends on the variation of EMFs while the EV is connected, and these periods are usually in the range of eight to 20 hours, the daily standard deviation is assessed. The annual duration curve, as well as the histogram of those values for the years under consideration, is presented in Figure 4-10. The data for 2040 are not shown in the histogram for better readability.

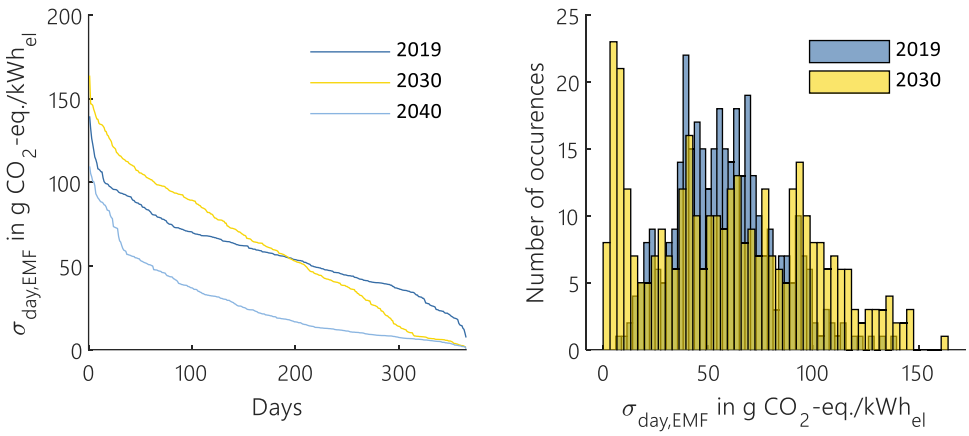

Figure 4-10: Daily standard deviation $\sigma_{day,EMF}$ of consumption-based EMFs in 2019, 2030, and 2040

The analysis confirms the previously formulated thesis. Comparing the annual duration curve of $\sigma_{day,EMF}$ for the years 2019 and 2030 shows an increase of entire days with a low standard deviation of EMFs. This phenomenon is even more pronounced in 2040. Increased capacities of vRES generators in 2030 compared to 2019 in combination with still existing coal-fired power plants also leads to more days when the daily standard deviation is higher than in 2019. Here, solar generators dominate electricity production during the day, leading to low EMFs, but coal-fired power plants are still widely used during the night, leading to higher EMFs and therefore higher values of daily standard deviations. In 2040, those coal-fired power plants are decommissioned and replaced mostly by lower-emission gas-fired power plants, hence decreasing the daily standard deviation.

4.6.4.2 Temporal distribution of consumption-based and marginal emission factors

In a subsequent step, the statistical distribution of the consumption-based EMFs is compared to that of the marginal EMFs. Since marginal EMFs were only assessed for 2019 and 2030, only these years are considered for the comparison. Figure 4-11 shows the distribution of marginal and consumption-based EMFs on the left and their daily standard deviation on the right for 2019. The same evaluation is presented for both years in the appendix in Figure 12-2.

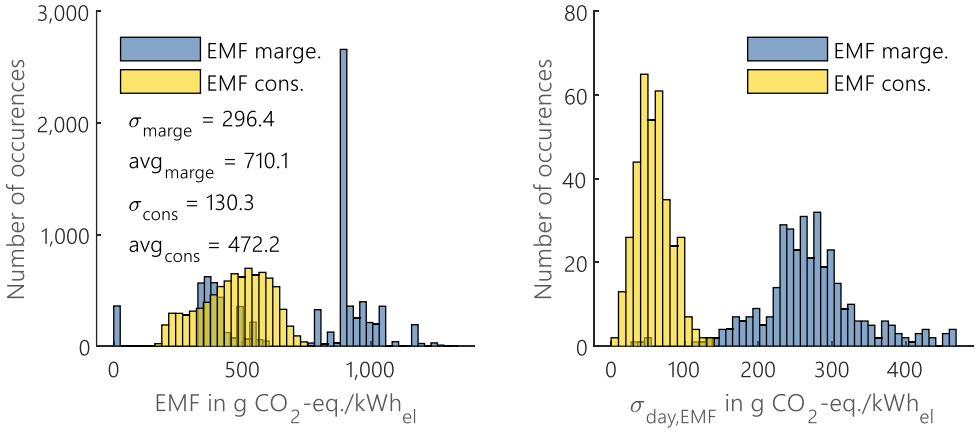

Figure 4-11: Histogram of marginal and consumption-based EMFs of 2019 (left) and their daily standard deviation (right)

Starting with the total number of occurrences on the left, we can see the clear dominance of coal-fired power plants still operational as marginal power plants in 2019. They are to be considered as

marginal in 2,660 hours of the year. This dominance of coal-fired power plants also leads to a much higher annual average in marginal EMFs. The histogram of marginal EMFs shows three accumulations, defined by hours when RES (marginal EMF = 0), gas-fired power plants (marginal EMF between 400 and 600), and coal-fired power plants (EMF between 900 and 1,200) are considered marginal. The dispersion around these peaks can be explained by the consideration of CHP plants as well as different efficiency values. Consumption-based mix EMFs, on the other hand, show a smoother distribution of values. This coherence is also reflected by high values of standard deviation in the case of marginal EMFs and lower ones in the case of consumption-based EMFs.

This smoothness in value distribution can also be seen in the assessment of daily standard deviation on the right of Figure 4-11. Daily standard deviations of consumption-based EMFs range from zero to 120 g CO_2-eq./kWh_{el}. Marginal EMFs show a much higher scattering of values during the day, resulting in standard deviation values in the range of 100 to 450 g CO_2-eq./$kWh_{el.}$ As presented in Figure 4-4, increasing price levels of CO_2 certificates in combination with decreasing gas prices in 2019 resulted in a partial fuel switch. Several of the gas-fired power plants now show lower marginal costs than coal-fired power plants, leading to a fuel mix in the course of the merit order curve. Under these circumstances, even small load increases can lead to a jump in marginal EMFs, resulting in those high daily standard deviation values. This scattering of values will lead to high potential emission reductions when considered as an optimization target for charging strategies. On the other hand, due to this "fuel-mix" in the merit order curve, marginal EMFs are much more sensitive with regard to load changes. In addition, the calculation of marginal EMFs depends on a variety of parameters, such as fuel prices, CO_2-certificates, or the accounting method of CHP-plants, that determine the order of power plants in the merit order curve. Even smaller changes of those parameters can have substantial impacts on this order and therefore the resulting EMFs. In contrast to the mix method, the marginal method is therefore to be regarded as less resilient, both with regard to load changes and to the calculation method itself.

4.6.4.3 Consumption-based emission factors versus day-ahead prices

With regard to potential revenues, the economic optimization of charging strategies based on electricity prices might perhaps be the most obvious charging strategy from the customer's perspective. To assess the potential impact on emissions, the correlation between the hourly consumption-based EMFs and the day-ahead price is examined over the course of 2019 to 2040, as shown in Figure 4-12.

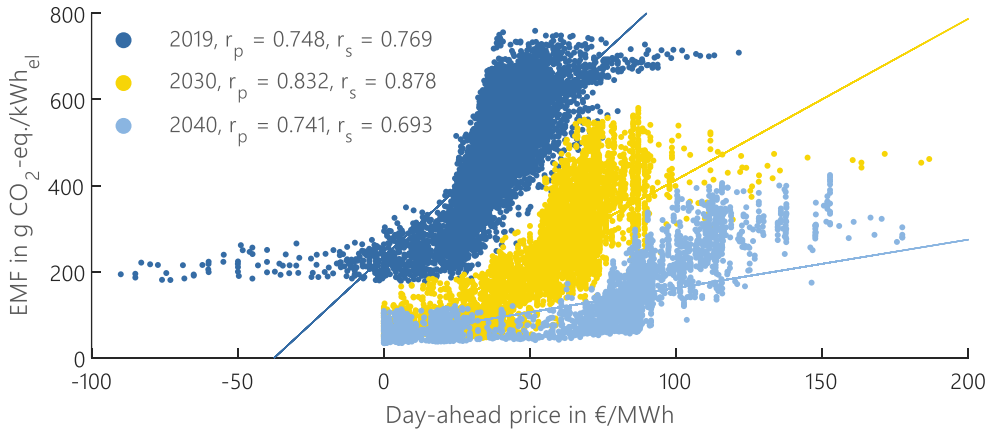

Figure 4-12: Correlation between generation-based EMFs and day-ahead prices

Both the Pearson product-moment correlation coefficient r_p and the Spearman rank-order correlation coefficient r_s are calculated. Where the Pearson correlation evaluates linear relationships, the Spearman coefficient is better suited for the evaluation of monotonic relationships between two variables [65]. Whereas in the years 2019 and 2030, the correlation of both values can be slightly better described as monotonic ($r_s > r_p$), the opposite is true for 2040. Generally speaking, the graph shows the substitution of low-cost/high-emission generators such as lignite and hard coal in the early years with high-cost/low-emission gas-fired power plants in the later years. This is represented by a strong decrease in the slope of values, meaning that in 2019, periods with low day-ahead prices often coincide with high EMFs, whereas in 2040 (the other extreme case), they increasingly do not. EMFs in 2040 only rise significantly at price levels beyond €70/MWh, already indicating that a price-optimized operation of EVs will result in a reduction of emissions as well. Increasing CO_2 prices and the removal of coal-fired power plants resolve the so-called merit order dilemma of emissions. Correlation between EMFs and prices can overall be considered high but with a decreasing slope in future years. The scenario data do not show negative prices due to the model construction as a linear optimization model. It must be noted, though, that negative prices only exist in the current system because inflexible conventional power plants have high shutdown and startup costs and therefore are willing to except negative prices for as long as this is economical from their perspective.

On the other hand, §51 (1) of the Renewable Energy Sources Act 2017 (EEG2017) only reduces the feed-in remuneration of renewable generators when "the value of the hourly contracts for the price zone for Germany on the spot market of the power exchange is negative in the previous day's auction for at least six consecutive hours" [66]. In the current version of the Renewable Energy Sources Act 2021 (EEG2021) [67], this period has been reduced to four hours. Since a growing number of inflexible conventional power plants are being replaced by flexible gas-fired power plants, it can be assumed that longer periods of negative prices are becoming less likely.

4.6.4.4 Generation-based emission factors versus residual load

The residual load in an energy system is defined as the load less the infeed of wind and solar generation for every hour (vRES). It gives a good indication of how green the electricity mix is at any given point in time. Here, the correlation between the generation-based EMFs and the residual load is analyzed as illustrated in Figure 4-13.

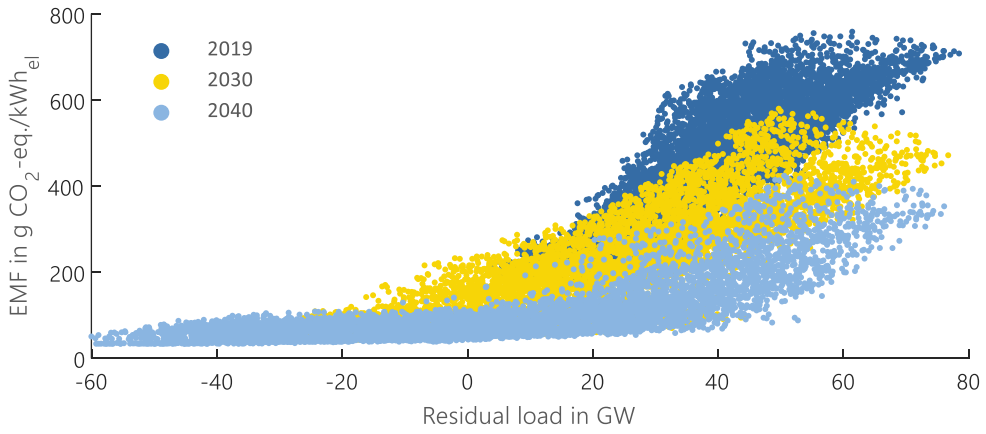

Figure 4-13: Correlation between consumption-based EMFs and residual load

Whereas historical data does not show negative values for residual load, increasing shares of vRES in future years lead to negative values in 27 % of all hours in 2030 and 48 % in 2040. These negative values in residual load are not necessarily represented well by the EMFs. Especially in the later years

of 2030 and 2040, the EMFs alone do not allow statements about how negative the residual load actually is and therefore, how much excess vRES infeed is available. If the reduction of operational emissions of EVs is the only target, using EMFs as an optimization target will serve its purpose well. However, if the goal is the best possible integration of vehicles into the energy system and the resulting optimal use of resources, then residual load as an optimization objective better meets this requirement. Therefore, the smoothing of residual load is considered one of the optimization targets in the context of this thesis (see section 8.4). Furthermore, the resulting system feedback is evaluated as well by considering the resulting load curves of such an optimized charging for an iteratively run simulation with the energy system model ISAaR. Results of this simulation and the resulting changes in the dispatch of power plants and storages are discussed in section 8.4.2.

4.6.4.5 Marginal emission factors versus residual load

In Figure 4-14, the same coherences are analyzed for marginal EMFs in the main years of observation, 2019 and 2030.

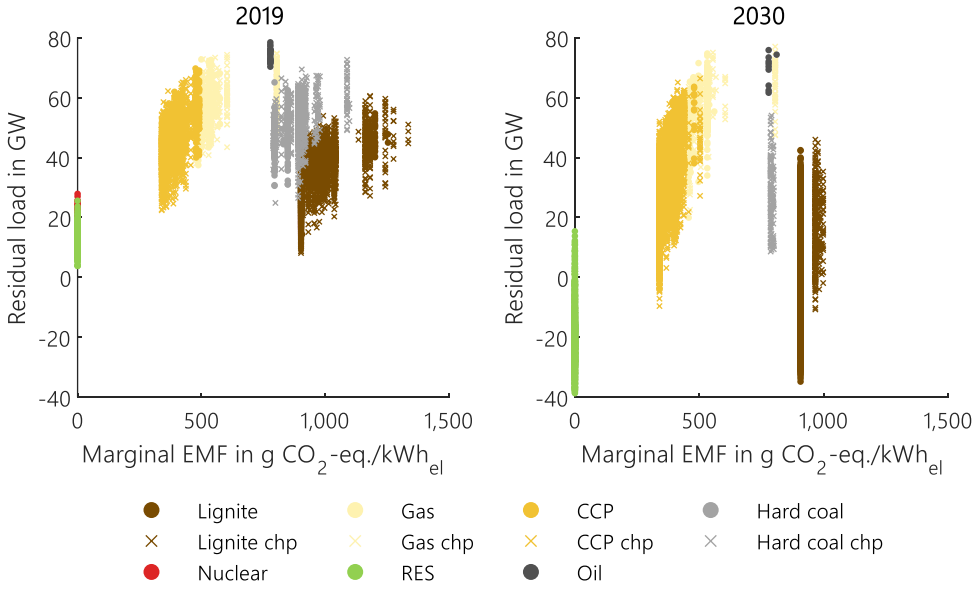

Figure 4-14: Correlation between marginal EMFs and residual load

Each point in the figure is color-coded according to the underlying marginal power plant. Furthermore, dots represent normal power plants without CHP, whereas crosses represent marginal plants with CHP. The comparison of both years shows the strong increase of negative residual load values, where vRES are considered marginal. In those times, the marginal EMF equals zero. Residual load values in those times range from four to 25 GW in 2019 and from -40 to 18 GW in 2030. This wide range can be explained by transborder electricity trades as well as must-run and CHP power plants that are still active despite negative electricity prices (see section 3.5).

In direct contrast to generation-based EMFs presented in Figure 4-13, marginal EMFs constitute a better indicator for surplus renewable electricity and serve well as an optimization target in those cases. Considering the positive values of marginal EMFs, however, that correlation does not exist. Due to the merit order of power plants and the underlying price structure, in times with high residual load values, low-emission gas-fired power plants constitute the marginal plants. Low-cost but high-emission lignite power plants, on the other hand, are often marginal in times of high shares of vRES and low corresponding residual loads. Using marginal EMFs as an optimization target would therefore result in an increase in peak residual loads and are not a good indicator to reflect the share of vRES in the system.

4.6.4.6 Consumption-based emission factors versus marginal emission factors

As a final correlation assessment, consumption-based EMFs are compared to marginal EMFs. Figure 4-15 presents these correlations for the years 2019 and 2030. Again, each point in the figure is color-coded according to the underlying marginal power plant.

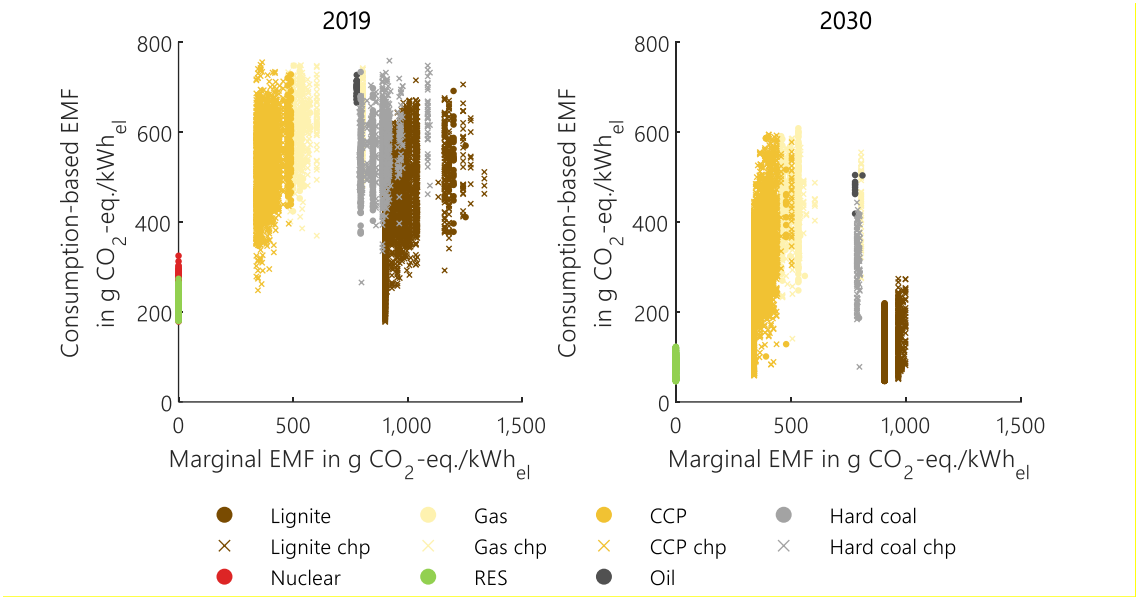

Figure 4-15: Correlation between marginal and consumption-based EMFs

Since consumption-based EMFs show high correlation values with the residual load, the overall picture is very similar to the comparison of marginal EMFs and residual load. The comparison of both EMFs demonstrates that the methods can lead to opposing EMFs. This is especially true in hours when lignite or hard coal-fired power plants are marginal. In 2019, the consumption-based EMFs span almost the entire range of values from 200 to almost 800 g CO_2-eq./kWh_{el}. In 2030, most of these power plants are decommissioned, but the same is still true for times when gas-fired plants are marginal, with simultaneously occurring consumption-based EMFs spanning the entire range of values.

4.7 Conclusion

This chapter presented three different ways of accounting for hourly EMFs. The generation-based and consumption-based EMFs follow the attributional approach, whereas marginal EMFs are calculated in alignment with the consequential approach. In the attributional approach, average mix EMFs are derived and used for the assessment of operational emissions. The assumption is that all consumers in the system are equally responsible for the dispatch of power plants and are therefore attributed the same average emissions in each hour. In the consequential approach, on the contrary, the focus is on "the cause-and-effect relationship between possible decisions and their environmental impacts" [35] p. 9. The choice of the type of EMF considered both as an optimization target for the charging strategies investigated and the actual accounting of operational emissions has a significant influence on results. To adequately address this, a summary of the findings is provided, and implications are discussed in this section.

In section 4.6.4, the resulting temporal characteristics and correlations with residual load and wholesale prices were evaluated to assess the use of these EMFs as optimization targets for charging strategies. Compared to generation-based EMFs, consumption-based EMFs better represent the

existence of an interconnected European electricity market, and general statements with respect to correlations and temporal characteristics are similar. For this reason, the consumption-based EMFs are used for all further analyses and simulations, leaving the comparison of consumption-based mix with marginal EMFs. Table 4-5 presents an overview of the discussed strengths and weaknesses of those EMFs as well as key indicators for the years 2019 and 2030. The upper part of the comparison originates from evaluations presented in [54], © 2018 IEEE.

Table 4-5: Strengths, weaknesses, and key indicators of consumption-based and marginal EMFs for the evaluation of charging strategies in this thesis © 2018 IEEE

Representation of:	Consumption-based mix EMF	Marginal EMF
Share of renewables	+ high correlation (R^2=0.95)	- low correlation due to merit order dilemma (costs versus emissions)
Excess renewable electricity	- no information about surplus electricity	o times with surpluses are shown but not amount of surplus
Carbon intensity of electricity sector	+ quantification of average emissions of total electricity generation	- only emissions on the margin are quantified
System effects of electrification measures	- average values of existing system do not reflect effects of load changes	(+) quantification of short-term marginal emission effects due to load changes
Statistical indicators (2019/2030):		
Annual average value	472.2/194.5 g CO_2-eq./kWh_{el}	710.1/559.2 g CO_2-eq./kWh_{el}
Standard deviation	130.3/130.7 g CO_2-eq./kWh_{el}	296.4/318.4 g CO_2-eq./kWh_{el}
Sensitivity against load change	low	high

First, the consideration of both EMFs as an optimization target is discussed. The analysis of correlations shows that mix EMFs better represent the share of vRES within the total electricity generation as well as the resulting carbon intensity of the electricity generation. Due to the aforementioned merit order dilemma, however, marginal EMFs do not. In addition, neither approach quantifies surplus renewable generation. Figure 4-13 shows that the residual load becomes increasingly negative in subsequent years, but this coherence is not reflected well by consumption-based EMFs. The marginal EMFs are at least zero during these periods but do not contain any information about the amount of surplus renewable energy. Those surpluses are only reflected well by the actual residual load value. Especially the potential of bidirectional charging mainly depends on the variance of the targeted time series. The higher the variance, the more spreads the optimization can use to reduce emissions (or costs). Marginal EMFs' standard deviation in both of the considered years is about 2.3 times higher than that of consumption-based EMFs, presumably leading to a significantly higher reduction potential. However, the overall goal of the charging controls studied is to optimize the overall system utility as well as to better integrate vRES. These requirements are fulfilled much better by the mix approach since they correlate better with the share of vRES and represent the total carbon intensity of the electricity generation.

Another aspect that must be discussed here is the fact that load changes generally lead to dynamic feedback effects in the energy system. If more electricity is required, more power plants are dispatched according to their position in the merit order curve to cover that additional load. The only way to fully address these effects is to iteratively run energy system model simulations based on those new load curves or even integrate the flexible consumers (e.g., EVs) in the system of

equations of the model. Due to high computational efforts, however, this is not deemed practical for the number of simulations evaluated in the context of this thesis. Furthermore, such simulations by the aggregator responsible for the implementation of such charging strategies in praxis are unlikely. Such an iterative approach is, however, applied as a sensitivity to assess the actual system feedback of charging strategies aimed at the smoothing of residual loads discussed in section 8.4.2. For all other analyses, this leaves the application of static EMFs for the assessment.

Regarding the retroactive effect of (minor) load changes, the mix method is considered less sensitive due to its calculation method. Even though resulting changes in power plant dispatch cannot be accounted for here, the overall effect on the average emissions of all power plants deployed can be considered negligible. However, due to the structure of the merit order curve, especially in 2019 (see Figure 4-4), even small changes in electric load would lead to significant jumps in marginal EMFs. Overall, mix EMFs better represent the vRES share, although they are not a good indicator of excess vRES feed-in. They also have lower statistical dispersion and are considered less sensitive to load changes and therefore more suitable for the task at hand. The implications of using mix or marginal EMFs for the emission accounting of EVs, as well as the influence of optimized charging, are discussed below.

In the past, many studies have addressed the emission assessment of EVs in the context of LCAs, yielding very different and even contradicting results. For instance, Marmiroli et al. [35] conducted a comprehensive meta study in 2018, analyzing 44 such articles published from 2008 to 2018. Using statistical regression, they explained 70 % of the variability in these results due to the carbon intensity of the electricity mix and the underlying accounting approach. Twenty-five of those studies used the mix approach, 17 the marginal, and seven considered both for means of comparable analysis. One of the main reasons mentioned for using marginal EMFs when accounting for emissions is that electric consumers, such as EVs, are considered marginal. That definition poses the questions why other electric consumers are not considered marginal and at what point a marginal consumer becomes an integrated part of the overall system and is treated as such. Even in a future energy system, marginal power plants will often be constituted by fossil generators, yielding much higher corresponding EMFs (see Table 4-5). Consequently, consumers considered marginal will not benefit from the ongoing decarbonization of the energy system and will therefore always be disadvantaged compared to all other consumers. From the author's perspective, this differentiation is infeasible and or at least not appropriate in the context of an integrated and intersectoral energy transformation. If the actual impact of a specific consumer on the ecologic footprint in the short term is to be assessed, that approach is deemed adequate. If operational emissions of consumers as an integral component of the energy system transformation should be evaluated, it is the author's opinion that the mix method should be used as an accounting method.

A similar argument can be made when assessing the emissions resulting from EV charging strategies. Since smart charging of EVs is not yet the norm, the responsibilities and regulatory framework for such charging must still be discussed and defined. However, in an energy system based on flexible and decentralized consumers, prosumers, and generators, charging operations will need to be planned and optimized by a market participant (e.g., an operator of a virtual power plant or a general marketer who has balancing group responsibilities). That means that for every shift in charging processes, electricity will have to be sold (in case of discharging) or purchased (in case of charging) on the day-ahead, intraday, or equivalent (local) flexibility market, and the balancing group will still always have to be closed. When the respective market is closed, the electricity generation from the remaining flexible generators is considered a result of all those components that are equal parts of that system. When comparing two charge modes, one basically compares two system states, one with direct charging and another with optimized charging. Resulting load curves from each charge

mode are an integral part of the respective system state. From the author's point of view, it does not therefore make sense to consider the flexible charging operation of EVs as marginal. They, as well as all other flexible or inflexible consumers, are to be considered as constituent parts of such a system and must thus be accounted for with mix EMFs in alignment with the attributional approach.

Overall, the decision of which approach to follow depends on the specific research question to be answered with the evaluations. If the cause-and-effect relationship between marginal load changes and their environmental impacts are to be assessed, marginal EMFs or consecutive energy system model simulations must be considered. Short-term effects can be assessed by marginal EMFs but are based on the current state of the energy system and neglect its dynamic and integrated development in combination with all its parts. If long-term effects such as the expansion of additional generators should be assessed, complex energy system model simulations must be conducted for every evaluation, which is not deemed adequate for the goal of this thesis.

The main research question here is how charging operations of EVs should be optimized to reduce operational emissions and maximize system benefits. Therefore, maximizing the utilization of vRES' volatile infeed is one of the main objectives, and this can be achieved by using the mix EMF as an optimization target. Regarding the balancing of operational emissions as well as the evaluated charging strategies, EVs and their charging strategies are considered as part of the overall energy system state. The use of mix EMFs as a basis for emissions accounting is therefore considered plausible.

5 Congestion Management in Germany

The increasing share of vRES power generators poses fundamentally new challenges to the electricity system. Their feed-in has a highly volatile character and shows a high temporal variance. For example, wind and solar forecast errors must be compensated for in the short term, and long periods of low feed-in due to calm and cloudy weather must also be compensated for in the long term by additional generation capacities to maintain the balance between generation and consumption. In addition to this temporal variance, the spatial distribution of decentralized generators is also a challenge. The uneven distribution of wind and solar-electric generators, as in Germany, repeatedly leads to grid congestion, which is currently balanced by short-term measures such as the redispatch of conventional power plants (targeted adjustment of the feed-in of power plants to avoid grid congestions, §13 EnWG) [68] or the limitation of vRES in the course of curtailment (§14 EEG) [69]. One target of this thesis is to analyze the extent to which targeted charging control of EVs can be used to prevent the restriction of renewable plants in the course of curtailment or the redispatch of conventional power plants and how, in the first case, this emission-free electricity can reduce operational emissions of the vehicles. Both analyses are only conducted based on historical data for 2019, since no scenario-based data for future CM-measures was available. However, it can be assumed that the basic relationships will also apply to future years.

Section 5.1 provides a brief overview of the history of German congestion management with a focus on redispatch and curtailment. Furthermore, it presents a summary of the recent regulatory reform of German congestion management described as Redispatch 2.0. For the assessment of the described charging strategies, spatially high-resolution time series of redispatch and curtailment measures are needed. Since no such data is published for historical years, section 5.2 describes the methodology for deriving these time series based on the discrete data published by German TSO and DSO. Since a forecast of the future development of congestion management measures is fraught with uncertainty, these evaluations are only conducted for 2019. In the final section, 5.3, the resulting spatially high-resolution time series for 2019 are presented, and further analysis describes the correlations and the impacts on overall system emissions.

5.1 Historical development of congestion management

Since the introduction of the Renewable Energy Law (EEG) in 2000 [70] and the priority feed-in and fixed remuneration of vRES formulated therein, the share of these generators on total electricity production has increased significantly. In 2019, 54 GW onshore wind turbines, 7.5 GW offshore wind turbines, and 47.5 GW PV-solar generators provided renewable electricity of 173.5 TWh and thus a share of 28.3 % [23]. An increasing amount of grid congestion has accompanied that rise. Grid congestion describes a situation in which the amount of electricity fed into the grid exceeds its capacity or that of the affected grid resource for transporting the electrical power. In Germany, §13 para. 1 of the German Energy Industry Act (EnWG [68]) states that TSO are obliged and entitled to eliminate this congestion and provides a serial order of different congestion management measures (CM):

1. Network- or market-related instruments such as countertrading and redispatch (§13 para. 1 EnWG)
2. Regulation of conventional power plants, particularly using balancing energy and contractually agreed interruptible loads (§13 para. 1 EnWG)
3. Curtailment of renewable generators in the course of curtailment according to §13 para. 2 EnWG and §14 EEG

According to §13 para. 1 no. 2, power plant operators and owners of curtailed vRES plants must be compensated appropriately. Hence, grid congestion is therefore not only a challenge for system security but also a financial burden for electricity customers, who indirectly contribute to the compensation payments via the grid fees. Figure 5-1 shows the development of both the development of these measures in TWh per year as well as the associated compensation costs.

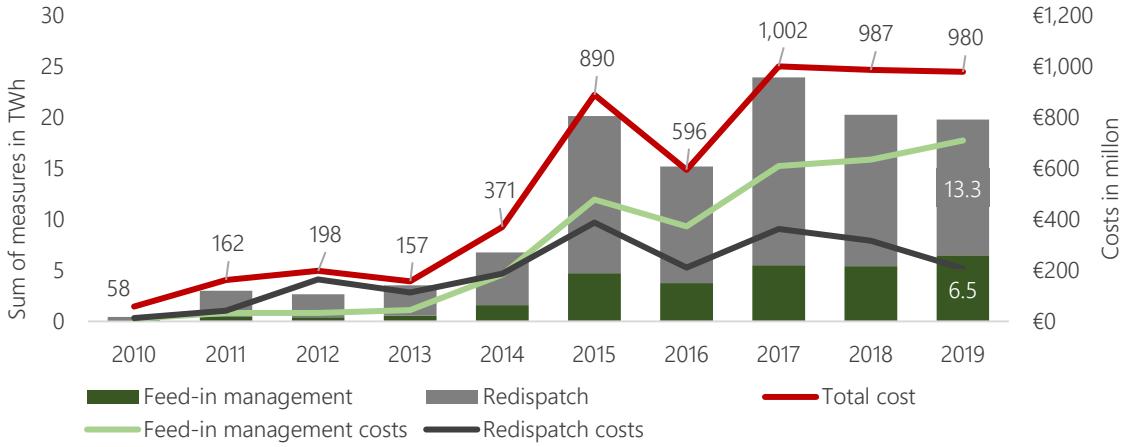

Figure 5-1: Overview of the history of German congestion management

The data presented in Figure 5-1 is published annually in the "Monitoring Report" of the federal network agency (Bundesnetzagentur/BNetzA), pursuant to §63 para. 3 EnWG [71], as well as in the quarterly published "Quarterly Report Network and System Security" [72]. Even though overall costs and measures seem to have stagnated in the past years, compensation payments in 2019 amounted to €207 million for redispatch and €709 million for curtailment measures. The current regulatory state of CM prioritizes the redispatch of conventional power plants over the curtailment of vRES due to the feed-in priority of the latter as defined in §11 para 1 EEG. With increasing shares of vRES in the system, total costs of CM have risen steadily, consequentially leading to higher grid fees. Hence, a public discussion of the future of congestion management and system responsibility arose, leading to the reform of the regulatory framework in the form of the Grid Expansion Acceleration Act (Netzausbaubeschleunigungsgesetz/NABEG, [73]).

The Grid Expansion Acceleration Act, which came into force on May 17, 2019, revised the grid expansion instruments and, in particular, redefined the term "redispatch" as Redispatch 2.0. Starting on October 1, 2021, not only are conventional power plants considered for redispatch measures, but renewable generators of 100 kW or more will also be included. The further developed Redispatch 2.0 process is intended to optimize the total costs from conventional redispatch and curtailment and thus reduce network fees. Even with the integration of renewable generation into Redispatch 2.0, the feed-in priority is to be maintained in principle. [74] states that "if redispatch of conventional generation is suitable for relieving a congestion situation, grid operators may only resort to curtailment of vRES or CHP electricity if this is many times more effective. This 'multiple' is given by the so called 'minimum factor'".

5.2 Methodology for temporally and spatially high-resolution CM-deployment

One of the thesis objectives is to analyze the extent to which targeted charging control of EVs can be used to prevent the curtailment of renewable plants or the redispatch of conventional power plants. Especially when EVs can be used to charge otherwise curtailed infeed of renewable and therefore emission-free electricity, the benefits on the system- as well as the vehicle-level can be considered particularly high. When considering a bidirectional charge control, it is even possible to reduce the redispatch of conventional power plants. This type of charging control could allow vehicles to make an important contribution to a sustainable energy system while possibly reducing their charged emissions. For the evaluation of such a charge strategy, temporally and especially spatially high-resolution curtailment and redispatch time series are derived from the historical deployment data published by German TSO and DSO. The following sections describe the underlying methodology for redispatch (section 5.2.1) and curtailment data (section 5.2.2).

5.2.1 Redispatch

Redispatch data for Germany is published by the four TSO on a central register called netztransparenz.de [75]. For each redispatch measure, detailed information on the duration, direction, maximum power, overall energy, and affected power plant is given. The information on power plants is matched to the power plant list of the federal network agency [40]. The latter also contains the addresses of each power plant, allowing a geographic assignment of the deployment time series. Based on that, a time series of negative and positive redispatch for each power plant, with the exact location, can be derived and later used as an optimization target for the vehicles in that region.

5.2.2 Curtailment

In contrast to redispatch, there is no central register for curtailment where all individual measures are published. However, annual aggregated values are published in the "Monitoring Report" of the federal network agency (Bundesnetzagentur/BNetzA) [71]. Figure 5-2 shows the development of these values over the past nine years subdivided by the types of renewable generators concerned.

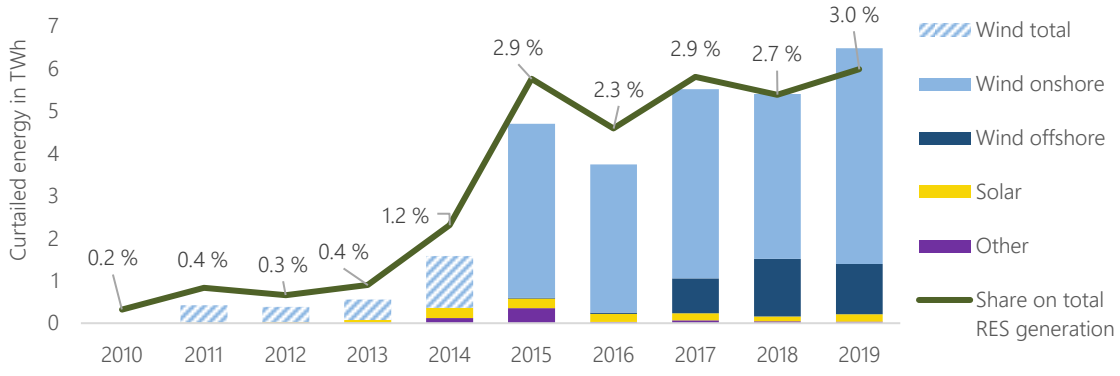

Figure 5-2: Annual data on curtailment measures in Germany as published in [71]

The data published by BNetzA shows that the majority of curtailment measures affect wind generators and that 3 % of the total vRES generation is curtailed due to grid congestion.

To compute temporally and spatially high-resolution time series of curtailed energy, more detailed data on individual measures is needed. The methodology described here has originally been

developed in [76] and revised in [77]. The following passages provide a summary of these publications.

To begin, §11 para. 3 of the Renewable Energy Sources Act (EEG) obliges the network operator to inform the operators of the affected plants "without delay about the actual times, the respective scope, the duration and the reasons for the regulation" [69]. The responsible DSO fulfill this obligation in different ways and provide data with vastly different information content. In the course of this work, a minimum requirement was defined, including the following criteria: location information, time boundedness, stated or computable curtailed energy, and a statement of cause of the measure. In total, eight DSO were identified whose publications meet the above criteria. The curtailment data is then subdivided into two groups according to the structure of the published data:

I. Curtailment levels provided in percentage and time period for each individual renewable generator

II. Curtailed energy and time period provided for an individual transformer station

Only eight out of the 800 German DSO met the criteria allowing the computation of the targeted time series. Their distribution grid areas as well as the annual sum of curtailment measures according to [71] are presented in Figure 5-3.

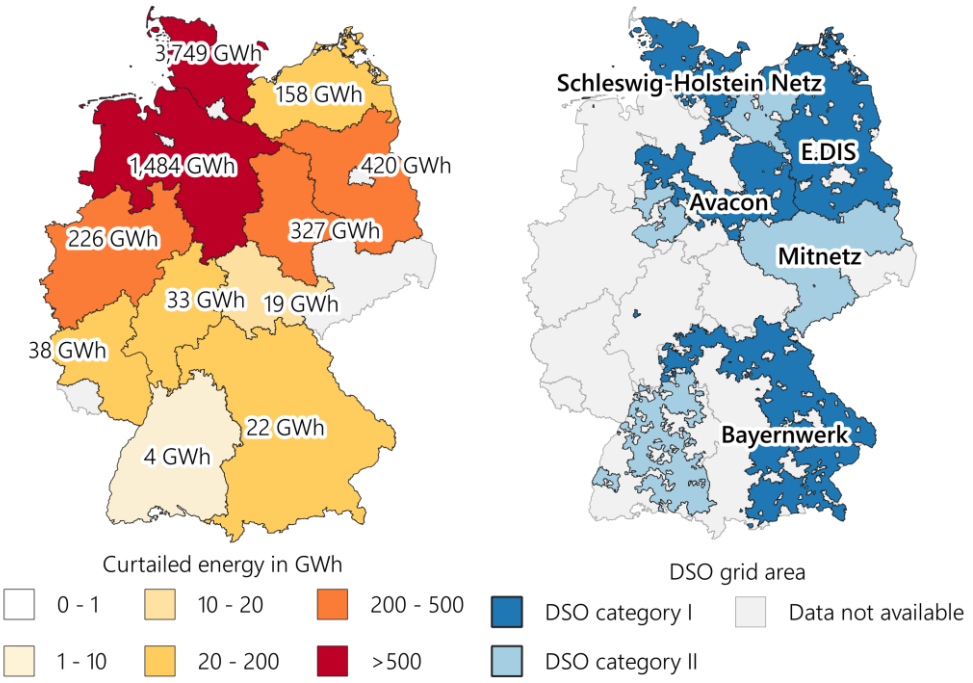

Figure 5-3: Curtailment measures (2019) by federal state according to [71] (left), grid areas of the eight considered DSO (right)

As illustrated in the figure, the network areas of the DSO from which data can be acquired predominantly cover the north, east, and south of Germany. A look at the annual number of curtailment measures by state, as published in [71], makes it clear that the northern federal states also have the largest values. According to [78], the states of Schleswig-Holstein, Niedersachsen, Brandenburg, and Sachsen-Anhalt already accounted for 92 % of all curtailment measures in Germany in 2019. It can therefore be assumed that the data basis is representative and adequate for the planned evaluations.

The fundamental methodological challenge for the creation of curtailment time series lies in the fact that only a curtailment level CL in percentage (0 %, 30 %, 60 %) is published for each curtailed

generation unit. Information on the actual power output of the affected generator after curtailment or the hypothetical power output without curtailment, however, is unknown. Therefore, assumptions must be made regarding these values. As described in [76] and [77], the following three approaches were implemented, each with increasing level of detail, where the curtailed energy is calculated with respect to:

1. Installed capacity of the vRES plant
2. Installed capacity + capacity factor derived from vRES-infeed-in respective control area
3. Installed capacity + capacity factor derived from NASA's MERRA-2 meteorological data

In the first case, the curtailed energy $W_{curt,I}$ for each generator with an installed capacity of P_{inst} is calculated for each time step t as:

$$W_{curt,I} = P_{inst} \cdot (1 - CL) \cdot t \tag{5-1}$$

The approach overestimates the curtailed energy since the actual power output of the generator is usually smaller than the installed capacity. Therefore, in the second approach, the actual generation $P_{g,ca,ec,t}$ per control area ca and energy carrier ec for each time step t, as published by the four German TSO, are taken into account. The control-area-specific capacity factor $CF_{ca,ec,t}$ is then calculated in respect to the installed capacity in that control area $P_{inst,ca,ec,t}$ as:

$$CF_{ca,ec,t} = P_{g,ca,ec,t} / P_{inst,ca,ec,t} \tag{5-2}$$

The resulting curtailed energy from that approach is then calculated for each unit as:

$$W_{curt,II} = P_{inst} \cdot CF_{ca,ec,t} \cdot (1 - CL) \cdot t \tag{5-3}$$

Due to regionally varying wind speeds in the control areas, this calculation, based on the total generation per control area, leads to an underestimation of the curtailed energy. To address the regional distribution of wind speeds and solar radiation, meteorological data from NASA's MERRA-2 was considered in the calculation of the capacity factor in the third and most detailed approach. For biomass, a constant value of 0.65 is assumed, which is based on the full load hours of biomass plants in Germany from 2015 to 2017. For wind generators the meteorological data was used to calculate a capacity factor time series for a 75 m-high wind turbine with an installed capacity of 2 MW for each county in Germany. For the calculation of solar capacity factors, a solar panel with south orientation and a tilt angle inclination of 30° and the radiation data from MERRA-2 were considered. Based on its county c and energy type ec, every plant is matched with its corresponding capacity factor $CF_{c,ec,t}$ for each time step t to derive plant-specific curtailed energy time series $W_{curt,III}$ as:

$$W_{curt,III} = P_{inst} \cdot CF_{c,ec,t} \cdot (1 - CL) \cdot t \tag{5-4}$$

Based on the last approach, the curtailed energy for every plant is calculated and aggregated to the desired spatial level. The resulting annual values are then calculated for the years 2015–2019 and compared to the annual values as published in [71], as presented in Figure 5-4 (here, curtailment of wind offshore plants is excluded from the comparison since this information is not available in the data of the eight DSO).

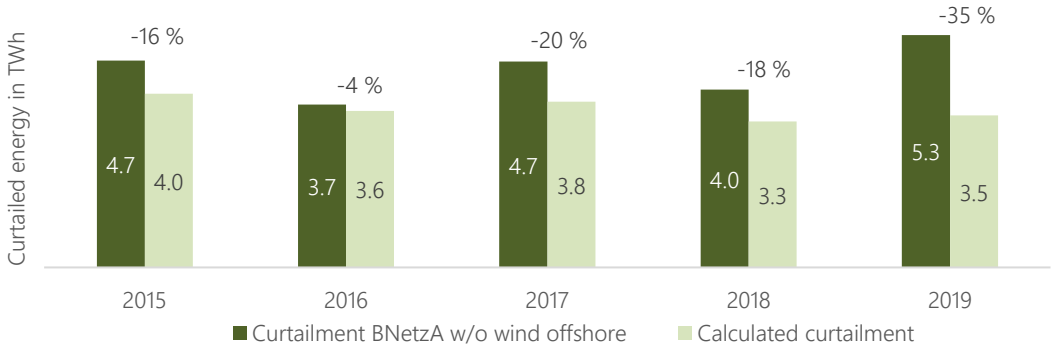

Figure 5-4: Comparison of calculated curtailed energy with values published in [71]

Approach III is deemed the most accurate for calculating time series of curtailed energy based on the information on individual feed-in measures. Nevertheless, significant deviations from the annual values can be observed, reaching up to 35 % in 2019. As discussed in [77], there are several possible explanations for this, starting from delays in publication of data in the annual values of BNetzA to data quality in general or the simplified approach of basing the calculation of capacity factors only on one type of wind turbine and solar power plant. Nonetheless, the described approach is deemed sufficient for the evaluation of general correlations and the application of the obtained time series for the assessment of charging strategies undertaken in this work.

5.3 Statistical analysis of correlations of congestion management measures

Based on the methodology described in sections 5.2.1 and 5.2.2, time series for both redispatch and curtailment measures are calculated for 2019. Based on that data, a variety of analyses are conducted and presented in this section.

5.3.1 Temporal distribution

First, the temporal distribution of measures over the course of 2019 is analyzed. Figure 5-5 and Figure 5-6 show these values over the course of each day.

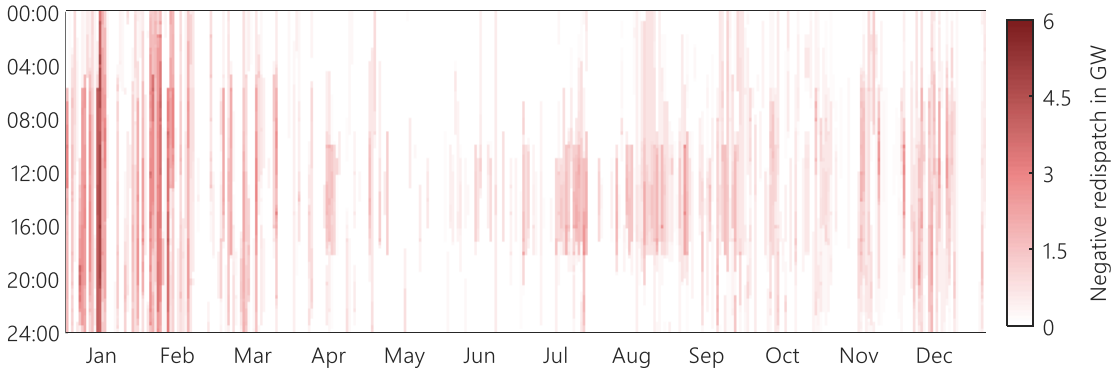

Figure 5-5: Heat map of negative redispatch measures in 2019

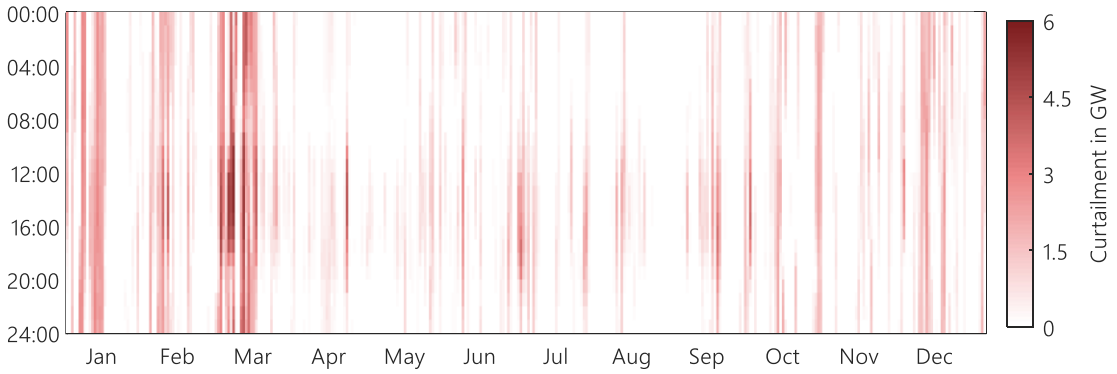

Figure 5-6: Heat map of curtailed energy due to curtailment in 2019

As outlined in Figure 5-1, the total number of congestion management measures has increased significantly over the past several years. Figure 5-5 and Figure 5-6 provide a clear indication that not only has the total annual number of measures increased, but so has the frequency of their dispatch. In 2019, curtailment measures were activated in 80 % of all hours and redispatch measures in 60 %. On average, 3.17 GW of negative redispatch and 0.5 GW of curtailment was activated during those times, with maximum values reaching up to 19.3 GW (negative redispatch) and 5.58 GW (curtailment). Thus, measures initially intended only for emergency situations become a regular process of system management.

5.3.2 Correlation analysis

Both curtailment and redispatch measures seem to occur more often during winter and are more pronounced during the day. To better understand the temporal distribution and correlations with other key variables in the energy system such as prices, vRES production, and EMFs, Spearman's correlation coefficient is calculated and presented in a Spearman correlation matrix as shown in Figure 5-7. The correlation coefficient r_s, varies between -1 and +1. 0, indicating there is no correlation, +/- 0.1 indicates a weak correlation +/- 0.3 indicates a moderate one, values around +/- 0.5 show a strong correlation, and +/- 1 refers to a perfect degree of association between the subject variables [79].

	Curtailment	Cons.-based EMF	Day-ahead price	Residual load	Wind offshore	Wind onshore	Solar
Redispatch down	0.40	-0.09	0.08	-0.04	0.35	0.34	0.12
Curtailment		-0.54	-0.34	-0.46	0.66	0.73	0.04
Cons.-based EMF			0.77	0.84	-0.44	-0.53	-0.23
Day-ahead price				0.88	-0.30	-0.38	0.09
Residual load					-0.41	-0.52	-0.01
Wind offshore						0.71	-0.14
Wind onshore							-0.22

Figure 5-7: Spearman correlation matrix for 2019 values

Besides the obvious and already discussed correlation among EMFs, day-ahead prices, and the residual load, the most pronounced correlation can be observed between curtailment measures and

electricity production from wind on- (r_s = 0.73) and offshore (r_s = 0.66). As described in [76] and [77], curtailment mainly occurs in times of high wind generation in the north due to a delayed grid extension. Negative redispatch measures only show a moderate correlation. Electricity generation from solar power plants, on the other hand, does not correlate with congestion management measures at all. In [77], these coherences are discussed in detail. Furthermore, by means of a k-means++ cluster algorithm, four distinctive systems states were identified, allowing further insights into those coherences and their future development.

5.3.3 Spatial distribution

In the next step, geospatial information on both power plants and renewable generators was used to derive the spatial distribution of redispatch and curtailment measures. Figure 5-8 shows this distribution for 2019.

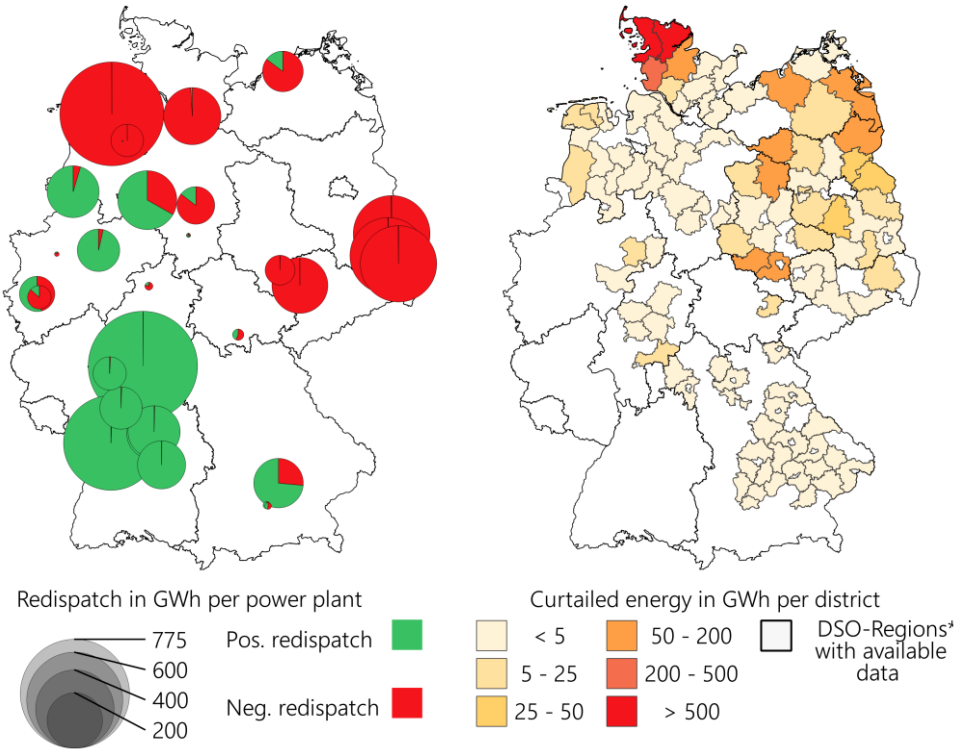

Figure 5-8: Redispatch (left) and curtailment (right) in Germany in 2019

The distribution shows a clear pattern of curtailment and negative redispatch in the northern part of Germany, whereas positive redispatch mainly occurs in southwest Germany. A similar geographic distribution can be observed when assessing installed capacities of wind turbines. The majority of wind turbines is installed in the northern parts of Germany, where wind yields are highest and population density is low. As described in [76] and [77], a strong correlation exists between electricity generation from wind power and curtailment measures in the years under consideration. This is also true for 2019. Furthermore, as stated in [78], 81.5 % of curtailment measures find their cause in grid congestion at the transmission grid level, indicating that missing transport capacities are the main cause for redispatch and curtailment.

5.4 Emission assessment of redispatch measures

Whereas it may be obvious that the curtailment of vRES-plants leads to overall higher emissions, the same does not necessarily apply for the redispatch of power plants. Where some are regulated down, others must increase production; hence, it depends on the types of power plants, and the underlying energy carriers if redispatch in general has a net positive or negative effect on total emissions. To evaluate this effect, an emission assessment of redispatch measures is performed. The plant-specific data on redispatch measures as published in [75] is matched to the power plant database of the Research Center for Energy Economics (FfE). Using the fuel type as well as the efficiency of each affected power plant, the resulting emissions can be derived as presented in Figure 5-9. Since redispatch measures can be considered as short-term interventions in the operational management of the power plants, in contrast to the assessment of the overall climate impact of EVs, only direct CO_2 emissions are considered for the evaluation.

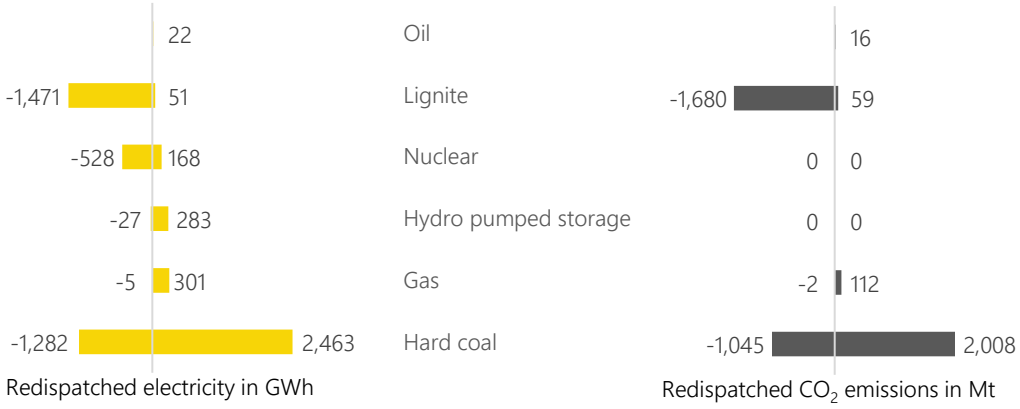

Figure 5-9: Redispatched electricity (left) and resulting CO_2 emissions (right) in 2019 (derived from [75])

The evaluation illustrates that the majority of redispatch measures affects lignite- and hard coal-fired power plants. Where 1,471 GWh of lignite and 1,282 GWh is regulated down, 2,463 GWh of lignite-based electricity production is increased. Overall, this leads to a net reduction of emissions by 531 Mt CO_2. The data not only allows a spatial but also a temporal evaluation of redispatched CO_2 emissions, which is needed for the emission accounting of redispatch-optimized charging strategies in section 8.5.2.3. The sum over all redispatched power plants is presented in Figure 5-10.

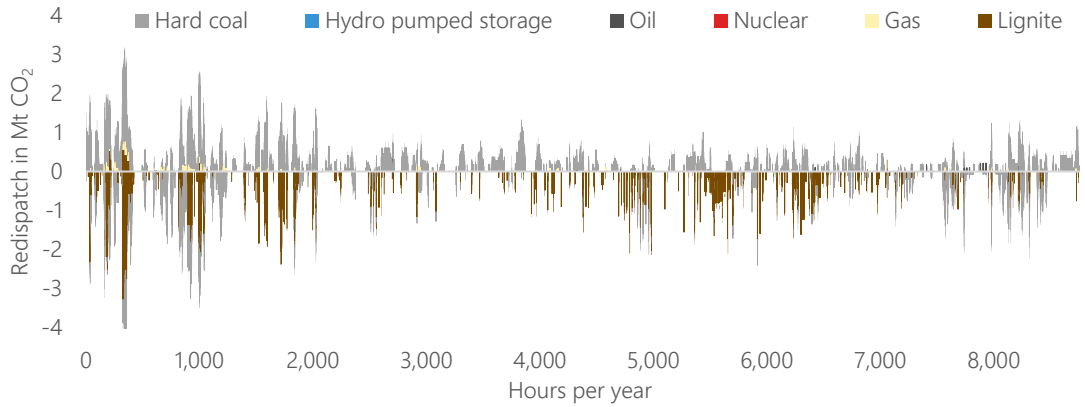

Figure 5-10: Temporal distribution of redispatch emissions in 2019

When discharging operations of EVs can be shifted to times when positive redispatch occurs, the affected power plants in that area would not have to increase their power output. Therefore, the CM measure would be unnecessary, and the "saved" emissions can be counted as negative emissions for the responsible EV. On the other hand, when the shift in charging operations leads to a reduction of negative redispatch measures, the reduction of generated electricity from a conventional power plant is avoided. The emissions of the respective power plant must be completely accounted for from the vehicle. Since, as shown in Figure 5-9 and Figure 5-10, a large part of the power plants performing positive redispatch are currently fired with hard coal, these emissions are higher than those of the electricity mix during this hour. Hence, the goal of reducing costly redispatch measures collides with that of reducing operational emissions of the vehicles.

5.5 Regional approach for evaluation of curtailment and redispatch

To assess the potential of CM-based charging strategies, a regionalization of both EV numbers as well as congestion management measures is needed. Parts of the methodology were published in [80] and are summarized in this chapter.

Since no grid model is available to simulate the actual impact of such charging operations on the distribution and transmission grid, assumptions must be made here. In a previous study, it was shown that the cause of curtailment measures, at least currently, is mainly due to congestion in the transmission grid at the extra-high voltage level [76]. The same applies, at least in large part, to redispatch measures. The working hypothesis here is that for this reason, curtailed or redispatched energy onsite (i.e., in close vicinity of the affected vRES or conventional plants) can be used by a targeted shifting of charging times of EVs, and thus the CM measure would be avoided.

The key questions at this point are which and how many EVs can be considered for mitigating the CM measures without full knowledge of the line-level network topology of the German transmission and distribution grid. To begin answering this question, the locations of the extra-high voltage grid nodes were first investigated. These were geospatially referenced in the Merit Order Grid Expansion 2030 (MONA 2030) project [81] and served as the basis for the German-Austrian grid model created and used in the project. The geospatial referencing of the lines was conducted using data from OpenStreetMap (OSM). For this purpose, the OSM toolkits SciGRID [82], Gridkit [83], and the FLOSM power grid map [84] were used. With the application of these tools, the line data were provided with exact electrical connection points, and, among other factors, the locations of the 490 grid nodes were derived. Figure 5-11 shows on the left the locations of these grid nodes and the Voronoi regions derived from their point coordinates.

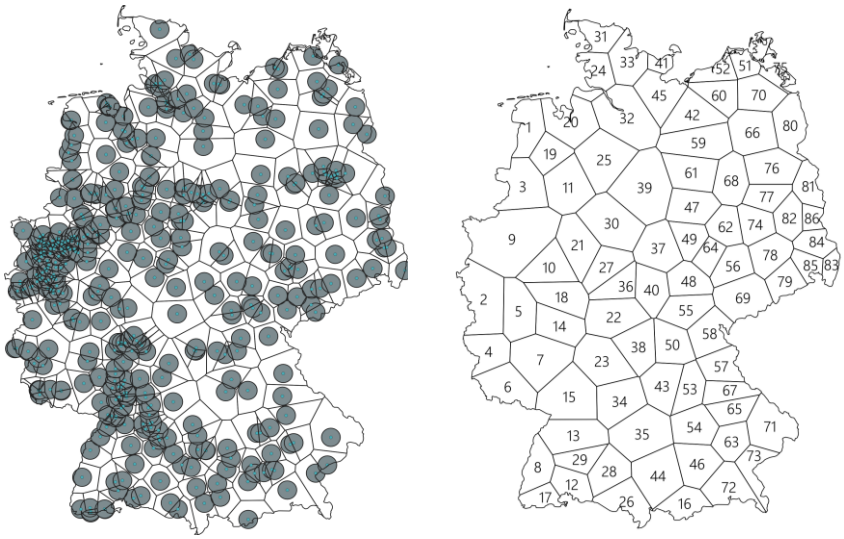

Figure 5-11: Grid nodes of the high-voltage grid with buffer areas and Voronoi regions on the left; newly defined Voronoi regions after merging the overlapping buffer areas on the right

A Voronoi diagram describes a subset of points that have a smaller distance from a given point (network node X) in a point set (all 490 network nodes in Germany) than from all other points in the point set [85]. In this context, it serves as an estimate of the region around each network node where EVs are eligible for the potential assessment of charging controls. Thus, it is assumed that the distribution and medium-voltage grid in this area has sufficient capacity to transport the energy that is curtailed or redispatched due to the congestion in the transmission grid. Figure 5-11 depicts a clear clustering of network nodes in densely populated areas in Germany, which leads to small Voronoi regions at these locations. It is assumed, due to the physical intermeshing of the high-voltage grid regions, that an energy exchange is also possible across the borders of the so-called Voronoi high-voltage grid regions. As a first approximation, a buffer zone of 30 km radius around each grid node is therefore defined (see Figure 5-11, left). All overlapping circular areas are then combined to form an overall area, around the centers of which 86 new Voronoi regions are then formed (see Figure 5-11, right).

In a next step, the data on curtailment and redispatch measures of the years under consideration (2019 and 2030) are aggregated to these areas, as shown in Figure 5-12.

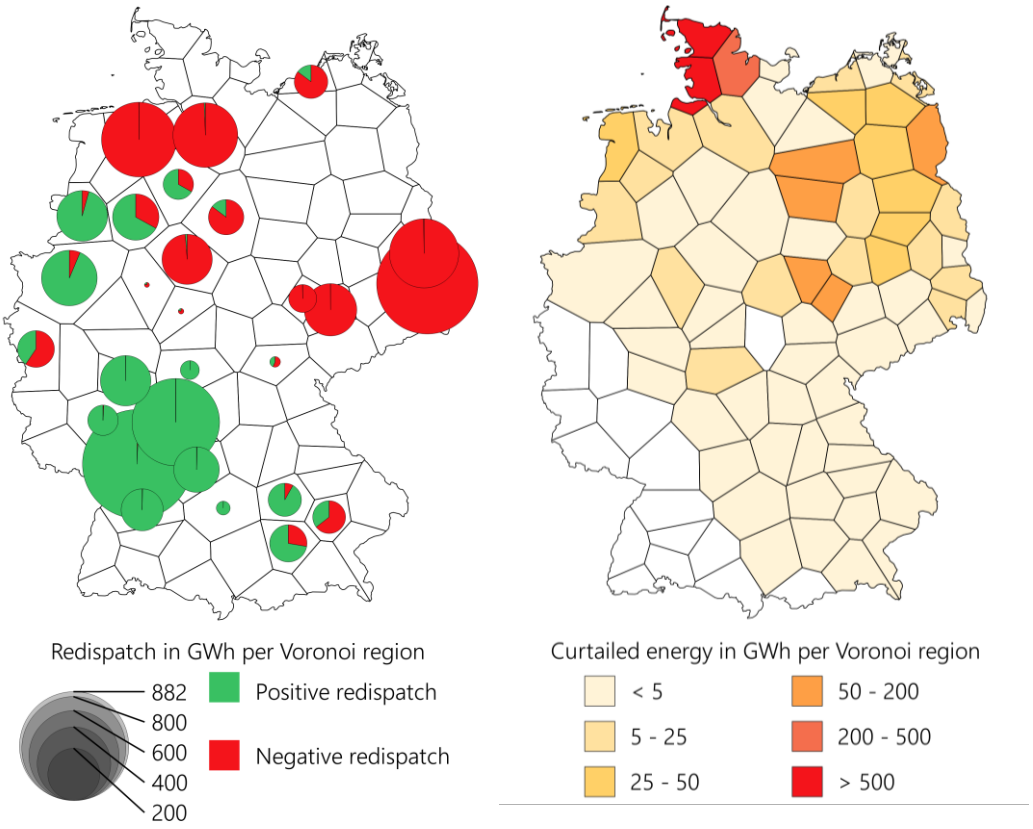

Figure 5-12: Redispatch (left) and curtailed energy (right) in 2019 per Voronoi region

The described methodology yields an aggregated time series of curtailment and redispatch measures for each Voronoi region, which is used as an optimization target for the EVs present in those regions (see description of the scenario in section 3.3 and results in section 8.5).

5.6 Conclusion

In the course of this chapter the historical development of CM-measures in Germany was discussed in detail. Increasing shares of vRES have led to a significant increase of those measures in the past years. Redispatch and curtailment measures have led to annual costs of €916 million in 2019. To assess the reduction potential of related EV charging strategies, a methodological approach was described, deriving temporally and spatially high-resolution curtailment and redispatch time series from the plant/generator-specific data published by the German authorities. Those time series are aggregated to Voronoi areas and used as an optimization target for the associated charging strategies described in section 8.5. It is assumed, that all vehicles in that area can be used for the reduction of those CM-measure. Furthermore redispatch measures were evaluated with regard to the resulting emissions. The time series of those emissions is used for the emission assessment of the related charging strategies (see results in section 8.5.2.3)

6 Electric Mobility in Germany

Besides the boundary conditions set by the underlying energy system, the charged emissions and the potential of charging strategies strongly depend on the mobility behavior of vehicle users. Due to the still limited market shares of EVs, representative data on electric mobility is scarce. Hence, a modeling approach is needed to reflect their mobility behavior. Research on the assessment of charging behavior and the interaction with the energy system can generally be subcategorized into three main groups, whereby the evaluations are based on:

- charging data of existing electric fleets
- measured mobility profiles of conventional or electric vehicles
- empirical mobility survey data of conventional vehicles

The first group of studies is based on measured data of electric fleets. Those studies are relevant because they represent actual EVs and therefore best map their users' charging behavior. However, these kinds of studies have the limitation that they are only based on a small number of vehicles, with users mostly being early adopters, and do not necessarily represent the mobility and charging behavior of users in the broader population. One of the bigger studies in Germany in this category was conducted by Schäuble et. al. [86] in 2017, merging the results of three field trials (Get eReady [87], iZEUS [88], and CHROME [89]) to derive EV load profiles and describe users' charging behavior. It states that the peak simultaneity of charging operations amounts to a value of 0.8 kW/EV, one very similar to the results of the modelling approach developed in this thesis. Another recent example is Gerossier et al. [90], wherein temporal high-resolution charging data of 46 privately owned EVs in Austin, Texas was used to identify charging habit clusters with hierarchical clustering on the Ward linkage method. The identified clusters were then used to estimate the future impact of a larger fleet of EVs on the grid. A good overview of further studies of that type can be found in Schmidt-Achert [91].

The second group of studies uses measured mobility data of conventional or electric vehicles to assess charging operations. An example of this is research conducted by Nobis [92] that used GPS data from a fleet of 130 conventional vehicles collected in the project eFlott [93] and a consumption model for EVs to synthesize time series of electricity demand and then use this in a distribution grid model. Approaches like that again have the limitation that only a small number of vehicles is considered. Nobis compared the results with the German mobility survey "Mobility in Germany 2008" [94], concluding that the mobility characteristics are similar.

Mobility surveys like the aforementioned "Mobility in Germany 2008", with the advantage of being based on a large dataset, are to be considered empirically sound and give a good representation of overall mobility behavior in the focus area. They represent the empirical data basis for the third group of studies. For Germany, three main surveys of that type exist. First is "Mobility in Germany", conducted and published every 10 years and focusing on private mobility, with "Mobility in Germany 2017" (MiD2017) [95] being the latest update. The study "Mobility panel" (MOP) [96], commissioned annually by the Federal Ministry of Transport and Digital Infrastructure, also represents private mobility but is based on a different survey method presenting coherent data for one entire week of mobility behavior. The last survey of that kind is the "Motor Vehicle Traffic in Germany," which is also updated every 10 years and addresses commercial instead of private traffic. The latest updates were published as "Motor Vehicle Traffic in Germany 2010" (KiD2010)" [97] in 2012 by the WVI Prof. Dr. Wermuth Verkehrsforschung and Infrastrukturplanung GmbH. All surveys present a large dataset

with information on trips and locations as well as socioeconomic information on subjects and are therefore well suited as a data basis for the modeling of electric mobility. Hence, many studies researching the assessment of charging behavior or time-dependent energy demand of EVs are based on those surveys. Dallinger [98], for example, has used the data of MiD2008 [94] to assess the potential of smart charging of plug-in EVs to balance the volatile generation of vRES (2012). Heinz [99], on the contrary, used the weekly travel surveys of the MOP to synthesize representative car profiles and assess a similar research objective.

Two more studies must be mentioned here regarding the analysis of the most recent mobility data from MiD2017 [95] and using it as a basis for the modeling of coherent user profiles. Gaete-Morales et al. [11] published an article as well as the open-source code for the tool *emobpy* in 2020. *emobpy* uses the data of MiD2017 to derive coherent annual time series of EV load, grid availability, and grid electricity demand for different charging strategies with customizable technical parameters to be set by the user. They used a probabilistic approach for the selection of the number of trips, destinations, departure times, and trip distances based on the statistics derived from the survey. In contrast to the final study mentioned here (Harbrecht et al. [100]), no interdependencies between trips were considered. However, Harbrecht has provided an extensive statistical analysis on coherences within the MiD2008 dataset and uses that information to build a stochastic bottom-up model to generate load profiles. An inhomogeneous Markov chain has been used to create a sequence of consistent arrival and departure locations with respect to the interdependencies within trips. Although the authors used a Markov chain regarding the weekday and trip index, a more common approach would be inhomogeneity regarding the time of day; however, the authors identified the trip index as having higher informative value. Several assumptions of the modeling approach developed in this thesis are derived from the statistical analysis provided by Harbrecht, as described in section 6.2.3. As shown there, numerous modeling approaches use survey data of conventional vehicles to derive driving or charging profiles of EVs. To prove the validity of that basic assumption, Pareschi et al. [101] have compared the results of such an empirical modeling approach with data derived from EV field tests. They concluded that survey data of conventional vehicles are "an appropriate instrument for generating EV insights" but highlight the importance of accurately modeling input parameters such as EVs' battery size and charging power.

For the potential assessment of charging strategies aiming at the reduction of congestion-management measures (in section 8.5) and the system feedback of residual load-optimized charging (in section 8.4.2) the total number of share of EVs as well as their spatial distribution in Germany is needed and described in section 6.1. Section 6.2 then describes the modeling approach for the mobility behavior of EVs, which integrates the two largest and most recent mobility surveys in Germany, "Mobility in Germany 2017" and "German mobility panel", as a data basis to combine the large amount of data from the first and the information on weekly mobility behavior of the second. Both are presented briefly in sections 6.2.1 and 6.2.2.

Moreover, as shown in the beginning of this chapter, many current models use stochastic approaches such as Markov chains for the synthesis of mobility profiles. Here, the original survey data is first deconstructed and translated to probability distributions of, for example, departure times, traveled distances, and speeds to then reconstruct coherent mobility profiles using further assumptions. Dinkel [102] has reviewed several such Markov chain-based approaches in detail and showed that they tend to lead to very fluctuant and sometimes inconsistent mobility profiles. It is furthermore believed that an intrinsic value lies in the consistent and de facto daily (or weekly in case of the MOP) mobility behavior of individual users provided by the surveys at hand. The methodology described here therefore refrains from the statistical deconstruction of those trip diaries and instead aims at their direct and unaltered utilization in a concatenation process as described in section 6.2.6. This

approach was originally developed by the author in the project "MONA 2030" [103] and published in [104] based on the previous version of the MiD, MiD2008 [105]. It was then applied to the commercial transport survey KID2010 [97] as described in [106]. In the project "Bidirectional Charging Management (BCM)" [107], the latest version of the survey MiD was incorporated, in cooperation with Schmidt-Achert in [91], where the database was expanded to include the weekly mobility behavior provided by the survey MOP [96]. The underlying methodology is described in sections 6.2.3 to 6.2.6. The last section, 6.2.7, summarizes the results of this chapter.

6.1 Development of electric vehicles in Germany

When evaluating the interdependencies between a fleet of EVs and the underlying energy system, the total number of vehicles in the system plays an important role. The reduction potential of congestion management measures using EVs directly depends on the number of vehicles present in the vicinity of the affected power plant or renewable generator.

The market share of EVs in Germany developed slowly over the past few years but has experienced an enormous increase within the last year. This has mainly been due to the funding program of the German government [108] as well as EU regulation limiting the fleetwide average carbon emissions for newly registered cars to 95 g CO_2/km in 2020 [109]. The latter put pressure on Original Equipment Manufacturers (OEM) to increase the share of emission-free (at least under the current regulation) EVs in their fleet since efficiency improvement potential of conventional vehicles is limited. Companies such as VW and others have now officially committed themselves to their own ambitions EV targets, heralding a reversal on their way to largely electrified road transport. Figure 6-1 shows the historical number of registered vehicles per year on the left and the results of a meta study conducted on the future development of vehicles on the right.

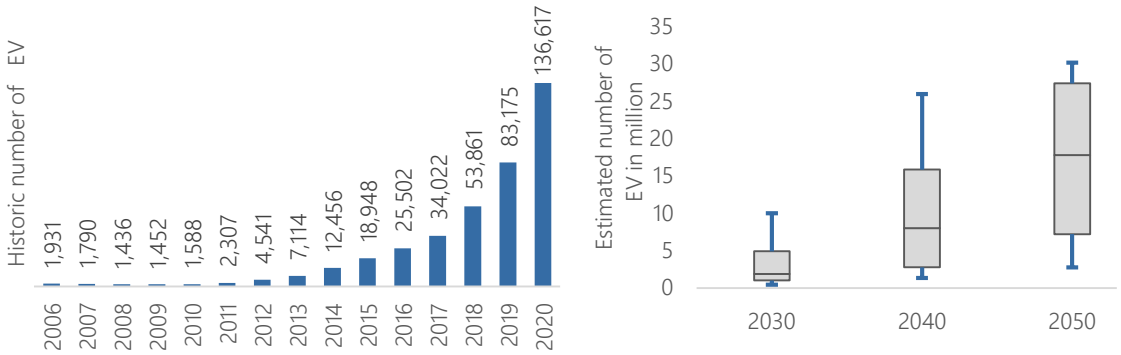

Figure 6-1: Historical development of registered EVs in Germany according to [110] (left), estimated future development of EVs based on meta study (right)

The data presented on the left is derived from the annual balance sheet of the German vehicle fleet published every January by the German Federal Motor Transport Authority (Kraftfahrzeugbundesamt [KBA] [110]). To estimate the future development, a meta study was conducted based on the largest energy system studies of the last several years and other sources on that topic ([111], [112], [17], [113], [114], [5], [115], [31], [116], [117], [118]). Most studies have described climate protection pathways toward a carbon-neutral energy system in 2050 as well as reference paths, where climate targets are not met. The boxplots in Figure 6-1 represent an unweighted collection of all those values. Therefore, the range of values is considerable and even increases when adding the year 2050. In 2030, the estimated numbers span from 0.8 to 10.5 million vehicles.

To put these values into context, the climate protection plan (Klimaschutzprogramm 2030 [119]) set by the German government identifies a number between seven and 10 million EVs in 2030. Since all the evaluations for future years in this study are based on the quEU scenario developed in the project eXtremOS [120], the number of EVs is derived from that scenario as well. For 2030, 2.69 million vehicles are considered and 5.7 million for 2040. Those numbers are based on the latest version of the ENTSO-E's "Ten-Year Network Development Plan" [121]. Considering the momentum of the past years and the commitment of both industry and politics toward an electrified mobility, these values should be considered rather conservative. For the analysis of 2019, the abovementioned 136,617 vehicles are considered.

Spatial distribution of electric vehicles

To assess the reduction potential of congestion management measures using EVs on a local level, the regional distribution of EVs in Germany is needed in addition to the absolute number. In a study for the German TSO as part of the network development plan, a methodology was developed that enables this distribution [107]. In this section, only a brief overview of the underlying methodology is described, and results for the estimated number of vehicles in three phases are presented.

The regionalization approach of EVs is divided into three phases, which are calculated independently of each other. These are the pioneer phase, the mainstream phase, and the standard phase. In each phase, different structural and characteristic parameters are involved, defining the probability of a purchase of an EV, and are calculated per 100x100m cell. The structural parameters include the availability of private and collective garages, commuting distance, and dispersion and describe the extent of mobility in the area. Characteristic parameters are the installed PV capacity per cell, the living space per dwelling, and the mean income. Those factors are assumed to describe users' affinity toward electric mobility. These parameters of different units (distinct numbers, kilowatts, euros, etc.) are transformed into dimensionless points through the application of corresponding weightings and, combined, form the distribution keys per cell for the regionalization approach. Both the aforementioned structural and characteristic parameters are varied in their weighting per phase to quantify the contextual assumptions.

The assumption is made that the pioneer phase is mainly dominated by people with a strong affinity for electromobility who have a high income in a national comparison and own large flats or single-family houses. In addition, the pioneers often already have their own PV system on the roof of their house, which means that an electric car can be at least partially charged by electricity they produce themselves. This phase is capped at three million EVs. After that, the mainstream phase is intended to represent a state of increased penetration of EVs in which they do not yet dominate the market but are no longer a marginal phenomenon. This phase is capped at five million EVs. At the end of the mainstream phase, a maximum of eight million EVs will be distributed in Germany. The final standard phase is applied to all numbers of EVs over eight million. In this phase, characteristic parameters such as income no longer play a role as it is assumed that the purchase of an EV is not dependent on affinity but is only defined by the extent of local mobility. As the three phases are regionalized independently of each other, the resulting numbers of vehicles per cell and phase are added at the end of the calculation to obtain the total number of EVs per cell. The structural and characteristic parameters used for the regionalization approach as well as the corresponding weighting factors for each phase are presented in Table 6-1 and Table 6-2.

Table 6-1: Structural parameters and weighting factors for every phase

Structural parameter	Weighting factor Pioneer phase	Weighting factor Mainstream phase	Weighting factor Standard phase	Source
Private garage	1	0.8	1	[122]
Collective garage	0.1	0.3	1	[122]
Commuting distance, average	$f(\text{commuting dist.})$	$f(\text{commuting dist.})$	$f(\text{commuting dist.})$	Based on [123], see [107]
Commuting distance, dispersion	$f(\text{commuting dist.})$	$f(\text{commuting dist.})$	$f(\text{commuting dist.})$	Based on [123], see [107]

Table 6-2: Characteristic parameters and weighting factors for every phase

Characteristic parameter	Weighting factor Pioneer phase	Weighting factor Mainstream phase	Weighting factor Standard phase	Source
Installed solar capacity	$\min(0{,}5 \times \frac{p_{solar}}{10}, 2)$	$\min(0{,}4 \times \frac{p_{solar}}{10}, 2)$	-	[124]
Living space	1 point for each 50 m² over 70 m²	0.8 points for each 50 m² over 70 m²	-	[125]
Income	1 point per 20,000 € over 20,000 € annual income	0.8 point per 20,000 € over 20,000 € annual income	-	[123]

A more detailed description of the application of these parameters is presented in [107]. Figure 6-2 shows the resulting distribution of EVs for each of the phases.

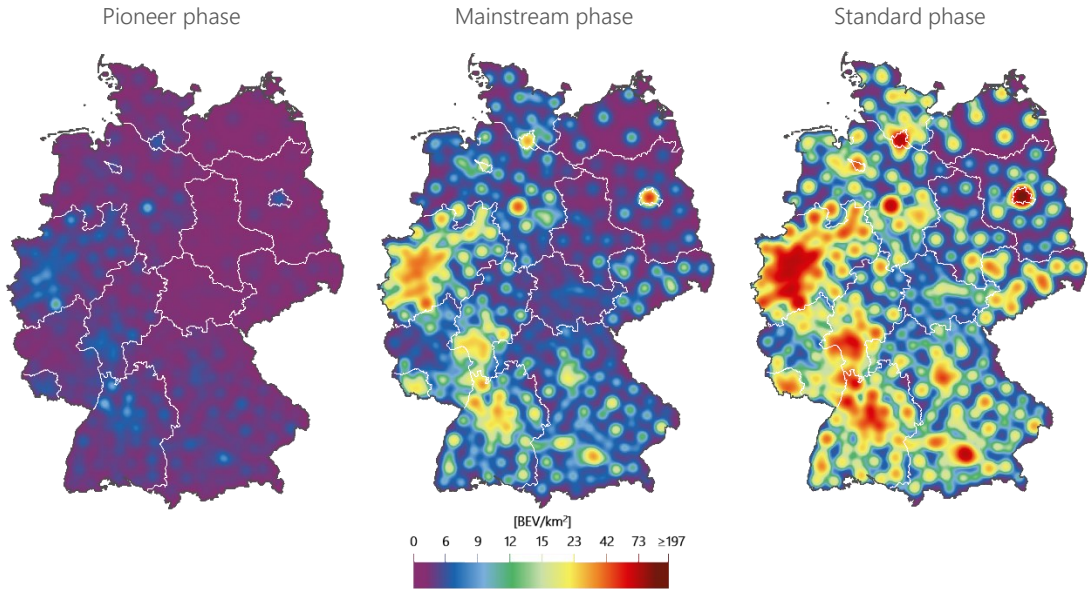

Figure 6-2: Distribution of EVs in each of the three phases

The distribution method is applied to the number of vehicles assumed for 2019 and is used as a basis for the assessment of charging strategies for the reduction of CM measures, as described in section 8.5

6.2 Modeling of electric mobility behavior

As stated in the beginning of this chapter, the modeling of electric mobility in the context of this thesis is based on the survey data provided by both the survey "Mobility in Germany 2017" (MiD2017) [95]) and the "German mobility panel" (MOP) [96]. The following sections present those surveys and describe the underlying methodology for the synthesis of coherent annual mobility profiles.

6.2.1 Survey description: "Mobility in Germany 2017"

The MiD2017 [95] presents the latest version of a series of traffic surveys in Germany that have been conducted since the mid-1970s by the "infas Institute für Angewandte Sozialwissenschaften GmbH" in Bonn and the Institute for Transport Research at the German Aerospace Center (DLR) in Berlin. The goal is to collect representative data to depict everyday mobility behavior of the German resident population. The survey was conducted with a random sample size of more than 150,000 households and was implemented by telephone, in writing, or via the web. The aim of the survey was the detailed recording of the mobility behavior of all residents of each of the households in one day. In total, data on more than 300,000 participants and 960,000 individual trips is provided. In addition, basic data to describe and categorize households and individuals was collected. The survey was performed over the course of an entire year but only contains information on the individual mobility behavior of individual participants over the course of one day. The dataset presents survey information on the following subcategories with the respective number of data points:

- Households (156,420)
- Persons (316,361)
- Trips (960,691)
- Vehicles (216,844)
- Travels (38,905)
- Trip stages (11,000)

In all categories, detailed and comprehensive survey data such as socioeconomic or geographic information and various other categories is provided. In the described approach, the first four categories are used for the synthesis of coherent mobility profiles. The survey was conducted using the following four methods:

- Computer-assisted telephone interview (CATI)
- Computer-assisted web interview (CAWI)
- Paper and pencil interview (PAPI)

That is relevant because the level of detail of the provided data in these categories varies significantly. For example, the information on which car of the household was used for a trip is not provided in PAPI, making it a methodological challenge to generate vehicle-specific mobility profiles from the participants' information.

In some cases, the formation of the sample and the way the survey was conducted lead to a skewed distribution of results. For example, the selection basis for the survey is, on the one hand, the population registers of the municipalities and, on the other hand, the landline and mobile phone register in Germany. A person selected from the population register represents his or her household. Since all persons from the household are surveyed in that case, the household sample results directly from the sample of individuals. This leads to an underrepresentation of smaller households. In cases where representative results are to be calculated for the whole population of Germany, weighting

factors are published compensating for those effects. Further information on the study and the methodology used is available in the related methodological report [95].

In Harbrecht et al. [100], an extensive statistical analysis of the dataset of MiD2008 was conducted, identifying the most significant influencing factors on residential mobility behavior. Various questions and hypotheses regarding socioeconomic and socio-demographical influencing factors were tested with Cliff's method and the $\chi 2$-test of independence. Some of the results are used for the definition of behavior-homogeneous user groups in section 6.2.4. In the context of this thesis, only a brief overview of the most relevant parameters is presented regarding the modeling approach at hand.

6.2.2 Survey description: "Mobility panel"

To assess weekly mobility behavior and increase the statistical database for the synthesis of annual mobility profiles, data provided by the MOP [96] is considered as well. The survey is conducted annually and represents the mobility behavior of around 3,000 participants and 70,000 trips. In contrast to the daily survey of the MiD, the MOP survey spans over a period of one week, providing further information needed to synthesize statistically correct mobility profiles. Participants are selected randomly and encouraged to partake in the survey for three consecutive years. The survey then consists of two stages. First, a trip dairy is filled out over the course of one week, and survey data on households and participants is collected. In the second stage, a fuel log is completed over the course of two months. The data is provided in the following four categories with the respective number of data points for the last available version of the survey published for 2016:

- Households (1,757)
- Persons (2,874)
- Trips (66,109)
- Fuel log (1,553)

In addition, in the case of the MOP, the formation of the sample and the way the survey was conducted lead to a skewed distribution of results, which is why corresponding weighting factors are also published here.

Since mobility behavior did not considerably change over the course of the past several years, according to [96], and to further increase the statistical data basis, the latest survey data from 2010 to 2016 are considered for the evaluations in this thesis.

6.2.3 Data processing of survey data

The data provided by both surveys is first subjected to a screening and validation process to filter out those trips and corresponding vehicle and participant data that are implausible, duplicate, or lack information needed for further analysis. Table 6-3 shows that filtering process and the corresponding number of trips eliminated in the process.

Table 6-3: Filtering and validation process for trip data of MiD and MOP

	MiD 2017	MOP 2010–2016
Total number of trips	960,619	377,120
Trips not driven (as a driver of a car)	561,511	180,656
Removed due to implausible speed values	48,038	14
Removed due to overlap	1,311	304
Removed due to missing information	-	560
Remaining trips	349,759	180,642

The foundation of both studies is a sample of persons, whereas the target of the modeling approach described here is focused on the mobility behavior of individual vehicles. That poses a methodological challenge (addressed later), but as a first step, all trips not driven as the driver of a privately owned car are excluded from the dataset. Furthermore, trips that have implausible speed values, overlap with other trips of the same user, or lack other information needed for the synthesis of vehicles mobility profiles are eliminated. In total, 530,401 remain after that preliminary filtering process.

After that screening process, the remaining dataset is further processed to assign start and end locations for every trip and to identify and assign the main driver and the corresponding behavior-homogenous user group of the vehicle.

Assignment of start and end locations

Since no information is given on the actual start and end location of trips in either survey, assumptions are made as follows. In the MiD data, the start location of the first trip is defined by the variable "W_SO1." According to its value, the start location of that trip is set either to "at home" or to "other." Since no such variable exists in the MOP data, it is assumed that all first trips start at home. All the following start and end locations of trips are then derived from the information on the trip's purpose, given by the variables "w_zweck" (MiD) or "zweck" (MOP). Based on that, three distinct end locations—at home, at work/school, and other—are allocated to each trip, and it is assumed that the next trip starts at the same location. For 683 (MiD) and 650 (MOP) trips, it was not possible to derive a consistent sequence of start and end locations that way, so they are excluded from further use.

Identification of main driver and assignment of corresponding user group

One of the main challenges of the approach at hand is the fact that the survey data provided is a sample of persons, whereas mobility profiles of vehicles are to be generated. At the same time, as stated in the beginning of the chapter, the MiD data only includes information connecting the trip data of participants with the corresponding vehicle for a small subset of the survey, whereas the MOP does not contain that information at all. Hence, a three-step approach with increasing methodological vagueness is applied based on the information available for each vehicle:

1. Corresponding car defined by ID of vehicle (w_wauto, only subset of MiD)
2. Only one car in household → all trips of household members are considered (MiD + MOP)
3. More than one car in household → each person is assigned to a single vehicle according to the number of trips per car, and this vehicle is used exclusively by this person (MiD + MOP)

The third approach must especially be considered a strong assumption but at the same time represents the only way to use the underlying trip information. Since the subset in the MiD, where

information on participants and corresponding vehicles is available, shows that 98 % of vehicles in the survey are used by only one main driver, this approach is deemed admissible.

Socioeconomic information of the assigned main driver of each vehicle is then used to categorize vehicles into twelve behavior-homogeneous user groups derived from the statistical analysis in [100]. The user groups are defined according to occupation type, presence of underage children in the household, and the use frequency of cars and are later used for concatenating individual daily survey data to coherent annual mobility profiles.

The result of this process is data on 234,315 vehicles with the allocated behavior-homogeneous user group and on 518,290 trips with information on start and end locations, time, traveled distance, duration, average speed, and the weekday of the trips. This dataset is then used for the synthesis of annual mobility profiles as described in the next chapter. Figure 6-3 shows the average number of trips per day and the average distance traveled per trip for all mobile vehicles that result from the process described in this section.

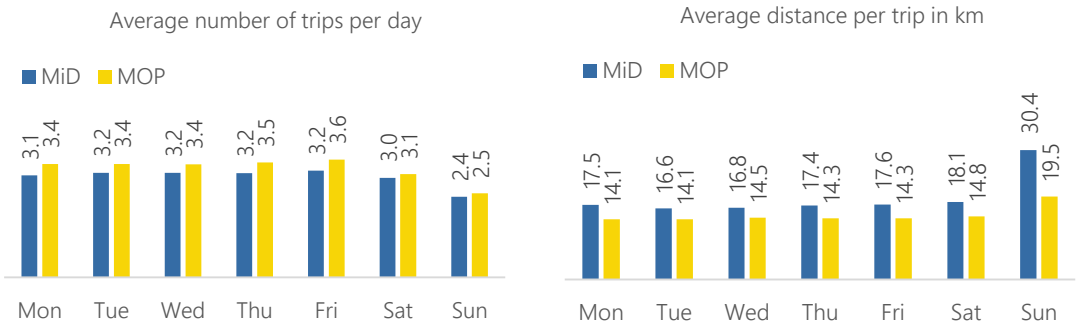

Figure 6-3: Average number of trips per day (left) and average distance per trip (right) of mobile vehicles

It must be noted that vehicles with no mobility on the survey day are considered in the overall process but not in the evaluation above. The number of trips traveled per day during the week, rather than on weekends, have lower average distances. This could be explained by the assumption of commuter traffic during the week, weekend excursions with longer distances, and smaller numbers of individual trips on the weekend. There are significant differences between both surveys concerning these values, especially considering the average distances per trip. Those differences might be explained by the survey design, but no final conclusions can be drawn based on the data provided.

6.2.4 Definition of behavior-homogeneous user groups

The basic approach for the synthesis of coherent annual mobility profiles is the concatenating of daily mobility profiles provided by the survey data under certain assumptions. The key assumption is that vehicle users can be subdivided into behavior-homogeneous user groups. Harbrecht et al. [100] have conducted an extensive statistical analysis of the mobility behavior provided by the MiD2008 [105]. Various questions and hypotheses regarding the influence of socioeconomic and socio-demographical factors on user behavior were tested with Cliff's method and the $\chi 2$ test of independence. When considering a regional distribution of vehicles to assess the potential of charging strategies to reduce congestion management measures (see results in section 8.5), it is important to know if mobility behavior is influenced by the place of residence of the vehicle owner. The results in [100] show that that is not the case, and the place of residence does not have a strong influence on the vehicle's mobility behavior.

Average values for key indicators of mobility behavior for the four distinct area types provided by the current version of the MiD2017 are presented in Table 6-4. Note that in the case in which cars without recorded trips are considered here as well, this leads to a lower number of trips in comparison to the assessment in Figure 6-3.

Table 6-4: Key mobility indicators of vehicles located in four distinct area types based on evaluation of MiD2017 data [95]

Average values for…	Large city without a district	Municipal district	Rural district with densification tendencies	Sparsely populated district
Annual mileage	13,221	14,334	14,805	14,849
Kilometers per day	13.17	17.58	16.96	15.75
Average distance per trip	6.6	8.3	8.34	8.36
Number of trips per day	1.63	1.99	1.87	1.77
Number of cars per household	1.66	1.96	2.02	2.03
Share of private parking spots	55 %	81 %	87 %	87 %

The average values reflect several deviations, especially when considering the mobility behavior in large cities, but overall, these can be considered small enough not to be relevant for the modeling approach of individual vehicles at hand. The most dominant deviations can be found in the number of cars per household and the information on the usual parking spot. The latter has an influence on the charging behavior of EVs due to the varying availability of a charging infrastructure in public spaces but does not necessarily influence the mobility behavior itself. A differentiation according to the place of residence is therefore not considered.

Harbrecht [100], however, has indicated that driving behavior is mainly influenced by the occupation of the main user. Full-time employees park significantly longer at work than part-time employees. Furthermore, members of households with (underage) children tend to take more trips than those without children. These categories are used for the definition of the following 12 behavior-homogeneous user groups.

Table 6-5: Definition of behavior-homogenous user groups

User group ID	Occupation	Children in household	Frequent driver	User group ID	Occupation	Children in household	Frequent driver
1	full-time	no	no	**7**	part-time	yes	no
2	full-time	no	yes	**8**	part-time	yes	yes
3	full-time	yes	no	**9**	unemployed	no	no
4	full-time	yes	yes	**10**	unemployed	no	yes
5	part-time	no	no	**11**	unemployed	yes	no
6	part-time	no	yes	**12**	unemployed	yes	yes

These user groups are later used for the concatenating process.

6.2.5 Discussion of commuting behavior

As stated, the basic approach for the synthesis of coherent annual mobility profiles is the concatenating of daily mobility profiles under certain assumptions. In the case of non-commuting profiles, this is done by only choosing those from a single behavior-homogeneous user group (as

described in section 6.2.4) and respecting additional concatenating criteria. In the case of commuters, a more consistent mobility behavior is to be assumed for trips to the workplace. Therefore, a more detailed approach must be used here.

The original version of the mobility profile generator (developed in 2016 and described in this chapter) was solely based on the survey data on daily mobility provided by the MiD2008 [105]. Since no data on weekly mobility behavior of individual users is provided, assumptions were made to concatenate those profiles. To represent commuter behavior, it was assumed that commuters drive to work every workday. Furthermore, the assumption was made that those commuters have a consistent mobility behavior regarding their arrival times at work and the distance traveled. Based on those two values, profiles identified as commuters by a trip to work were categorized into 12 commuter groups, which were then used to concatenate commuter profiles during workdays (see [104]).

In the context of the revision of that original approach, MOP survey data was considered additionally, providing actual information on weekly mobility behavior of commuters. The data show that in contrast to the assumptions of a consistent commuting behavior (driving to work every single day of the week), a much more inconsistent behavior must be considered.

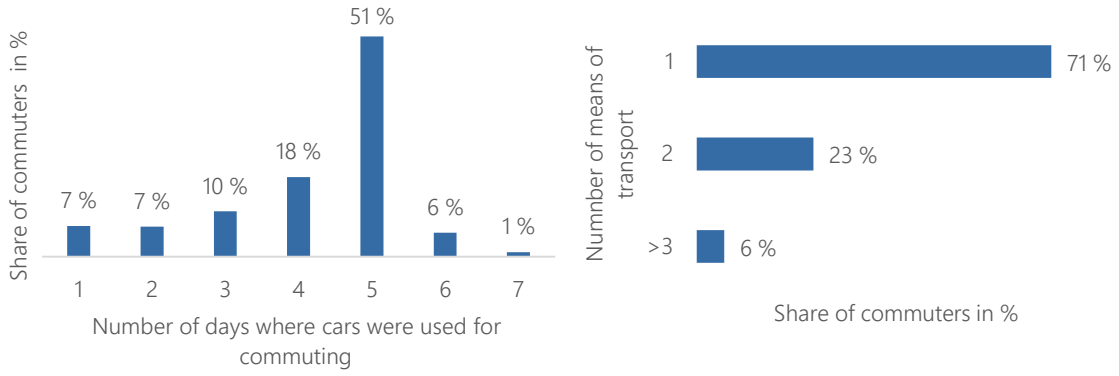

Figure 6-4: Evaluations on commuting behavior based on MOP-data [96]

The evaluation shows that only 51 % of all participants (who are defined as commuters since they drive to work at least once by car) drove to work by car five days of the week, and 71 % used one single means of transport. Hence, the assumption made beforehand of a consistent commuting behavior was revised and updated for the concatenating logic of profiles in those groups (see section 6.2.6).

Furthermore, the assumption was made that commuters arrive at work at roughly the same time each day and drive the same distance there. To verify this assumption, the distribution of arrival times and the standard deviation of those values for every commuter over the course of one week were calculated as illustrated in Figure 6-5. Here, only trips driven by car were considered.

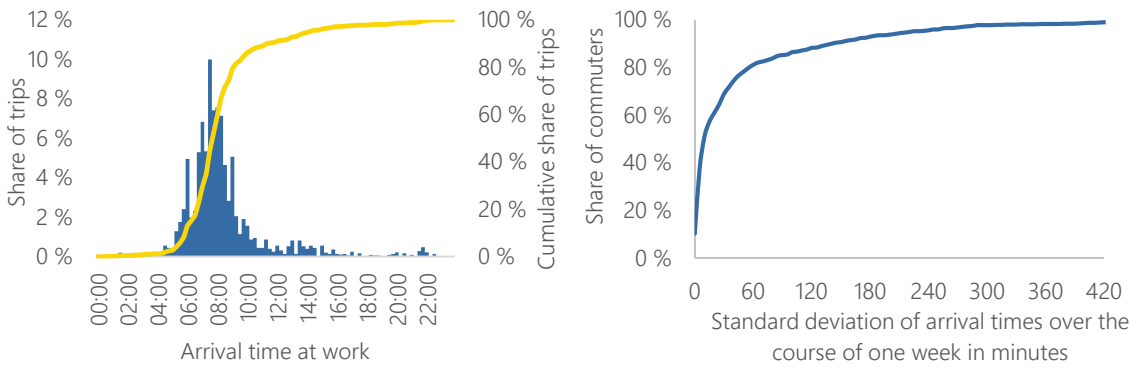

Figure 6-5: Histogram (left) and cumulative standard deviation of arrival times at work

The evaluation depicts that 50 % of all users arrive at work every morning before 8:00 a.m. and the other half after that. The cumulative distribution of weekly standard deviations of arrival times shows that 51 % of all commuters arrive at work within a timeframe of 10 minutes and 81 % within one hour. The assumption of homogeneous behavior in that area can therefore be considered valid. The same evaluation was applied for the distance traveled to work, as shown in Figure 6-6.

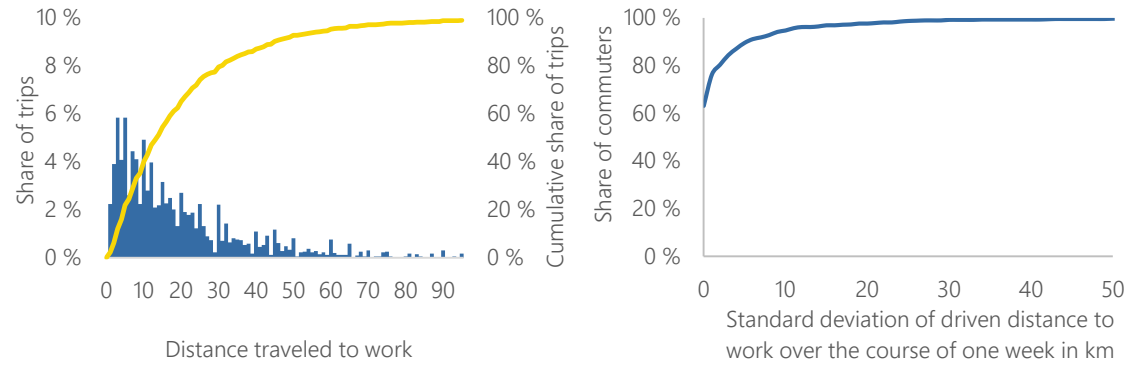

Figure 6-6: Histogram (left) and cumulative standard deviation of distances traveled to work

The distribution of distances traveled to work is much more heterogeneous and reaches values up to 100 km. Forty percent of all commuters travel less than 10 km to work, 25 % between 10 and 20 km, 22 % between 20 and 40 km, and the remaining 13 % travel more than 40 km. The values of the standard deviation of those distances during the week show consistent behavior: 63 % do not deviate at all from their daily travel distance to work over the course of one week, and only 5 % deviate more than 10 km. Overall, the evaluation of the data confirms the assumption of a homogeneous commuting behavior of vehicle users. The following definition of commuter groups is therefore used for the concatenating process:

Table 6-6: Definition of commuter groups

Commuter group ID	Arrival time at work	Distance to work	Commuter group ID	Arrival time at work	Distance to work
1	before 08:00	<10 km	**5**	after 08:00	<10 km
2	before 08:00	10–20 km	**6**	after 08:00	10–20 km
3	before 08:00	20–40 km	**7**	after 08:00	20–40 km
4	before 08:00	>40 km	**8**	after 08:00	>40 km

6.2.6 Concatenation to annual mobility profiles

The uniform daily mobility profiles described in section 6.2.3 are then concatenated to annual mobility profiles regarding the weekly commuting behavior derived from the survey data of the MOP. The algorithm follows the process below:

1. Pick random weekly profile from MOP survey and identify user group and commuter group.
2. For each workday, select three random daily profiles meeting the concatenating criteria.
3. Create annual profile considering holidays.

In the first step, a random weekly profile from the harmonized MOP data is selected. The profile contains the information on the behavior-homogeneous user group (see Table 6-5) and if trips to work exist, on the corresponding commuter group (see Table 6-6). Based on that information, three random profiles for each day of the week are selected from the sample of daily profiles (based on MiD and MOP data) described in section 6.2.3. The profiles must meet the following criteria:

- same behavior-homogeneous user group
- same commuter group (if a commuter-week profile is selected)
- start location of the next day equals the end location of the previous day
- first trip of the next day does not start before the last trip of the previous day ends

For every weekday of the year, a random profile is chosen from the preselected candidates. The preselection of three candidates for every weekday ensures that the vehicle does not repeat the same mobility behavior every day but at the same time does not result in an entirely random mobility behavior over the course of the year. In that process, information on public holidays is considered by selecting a Sunday profile for each holiday and a Saturday profile for each bridging day as described in [126]. The resulting annual mobility profiles are then discretized to 15-minute time steps and saved to the FfE database FREM as arrays containing information on location, speed, and distance for each time step.

6.2.7 Results and conclusion

The methodology described in this chapter was used to derive 2,000 annual driving profiles for each user group. This synthesis was employed for 2019 as well as the calendar year of 2012 since the simulation results for future years are based on the weather for that year. Based on the data derived from both surveys, the shares of the identified user groups in the total fleet are presented in Table 6-7.

Table 6-7: Share of user groups in total fleet

User group	**1**	**2**	**3**	**4**	**5**	**6**	**7**	**8**	**9**	**10**	**11**	**12**
Share	9.8 %	19.3 %	3.8 %	8.7 %	5.8 %	7.6 %	3.9 %	6.0 %	18.7 %	13.9 %	1.3 %	1.2 %

These shares are used for the assembly of a statistically correct representation of the German fleet from the profiles of user groups. Figure 6-8 shows the share of locations over the course of an average week for the complete German fleet for the synthesized annual profiles and the same evaluation for the original daily mobility profiles derived from the MiD2017.

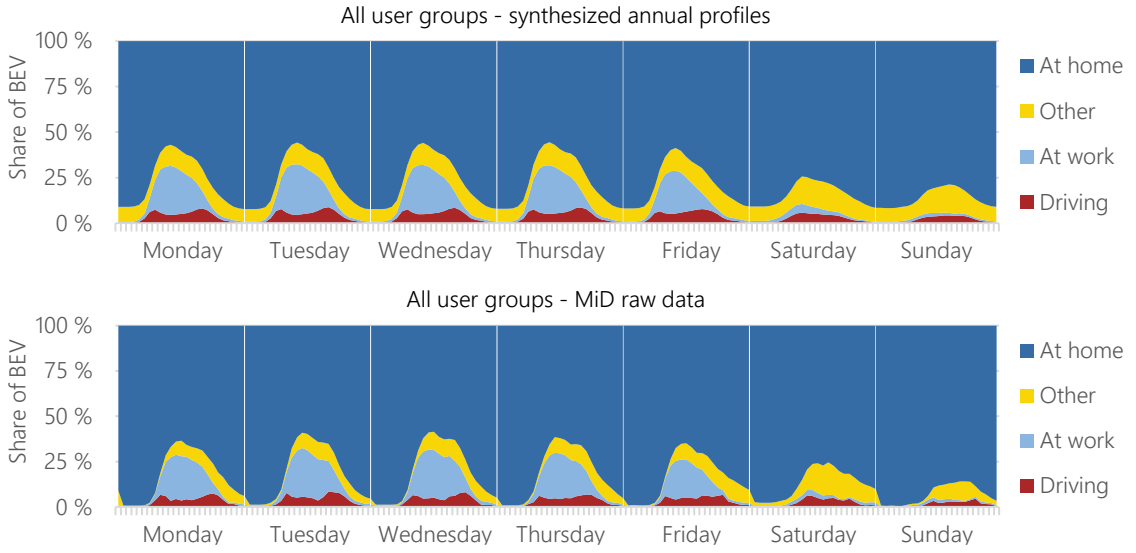

Figure 6-7: Average distribution of locations of the German fleet

The most significant difference between the synthesized annual profiles and the unprocessed original survey data can be identified in the transition from one day to the next. In case of the synthesized profiles a significant number of vehicles is not parked at home during the night. In case of the original data on the other hand, more vehicles are reported to end their day at locations "other" or "at work" than vehicles that start their trip at the corresponding location on the next day. Further analysis of these effects has shown that it is not an issue of the applied methodology, but a problem originating in the survey data itself. The official report of the survey also states that almost no cars are parked at other locations than at home [127]. The empirical analysis of three electric mobility studies in Germany's southwestern region by Schäuble et al. [86] on the other hand shows, that approximately 10 % of the vehicles are parked at unknown locations and 12 % are parked at work at the transition from one day to the next. Overall, the lack of available information prevents definitive validation of these relationships. However, it is assumed that the correlations are sufficiently valid overall, and that the procedure can be regarded as permissible. Besides these obvious differences, the progression of the shares of locations is very similar between the synthesized and original profiles.

At all times, at least 50 % of vehicles are parked at home. During the week, about 30 % of the vehicles are parked at work at noon. Due to the revised method for the calculation of commuting behavior and based on the information derived from the MOP data, some users also work on weekends. The ways to and from work lead to small peaks in trips in the morning and in the late afternoon. This is even more pronounced when looking at the mobility behavior of user group 2. Figure 6-8 shows the location of this group (full-time occupied, no children, frequent driver) in direct comparison to user group 9 (unemployed, no children, infrequent driver), a more extreme example at the other end of the spectrum.

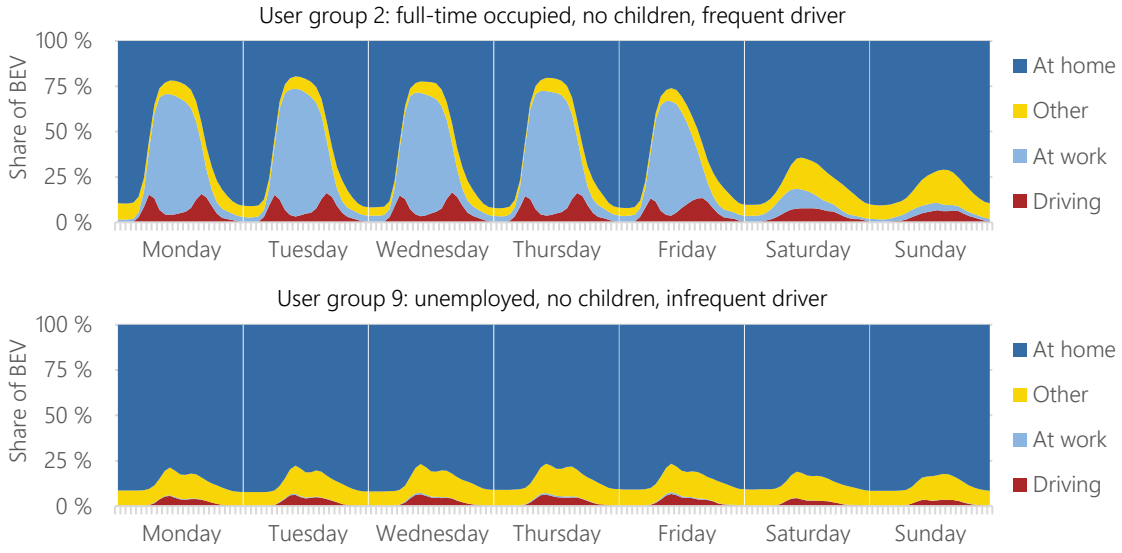

Figure 6-8: Average distribution of locations of user groups 2 and 9

Here, the difference in driving behavior is clearly pronounced. While only 25 % of the commuters leave their cars at home during the week, 60 % are parked at work. In addition, in that case, the driving peaks in the morning and evening are even more pronounced, starting a few hours earlier on Fridays. The unemployed, infrequent drivers, however, show a completely different driving behavior. Since no trips to work are considered, 75 % of the cars are always parked at home. Furthermore, behavior between weekdays and weekends does not differ substantially. These differences in parking times have a significant influence on the potential of charging strategies and are further assessed in the discussion of the potential of charging strategies in section 8.2.4.1. The mobility behavior of all user groups is presented in the appendix in section 12.3.

In a next step, the resulting annual driving distances are compared to the ones derived from the original survey data. In both surveys, annual mileage values given by the respondents are documented. However, these values are not suitable to be used as a reference since they represent the total annual mileage including multiday trips and long vacation trips. The report by [95] states that "40 percent of the total annual mileage of passenger cars is generated on routes of more than 50 kilometers and a good quarter on routes of more than 100 kilometers." MiD2017 participants, for example, reported an average annual mileage of 14,472 km, while multiplying the average daily distance derived from the survey data by 365 days only yields an annual short-distance mileage of 8,196 km. Therefore, a considerable share of the annual mileage must be categorized as long-distance trips. It is assumed, though, that those trips are not charged at home or at the workplace (where the potential of optimized charging is assessed in the context of this work) but during those trips at public charging stations. The charged electricity at those charging points is considered for the calculation of total emissions and costs, however. The methodology for the estimation of public charging behavior is described in section 7.3 For a validation of the annual mileage values of the synthesized profiles, this calculated annual mileage "short distance" is used, as presented in Figure 6-9.

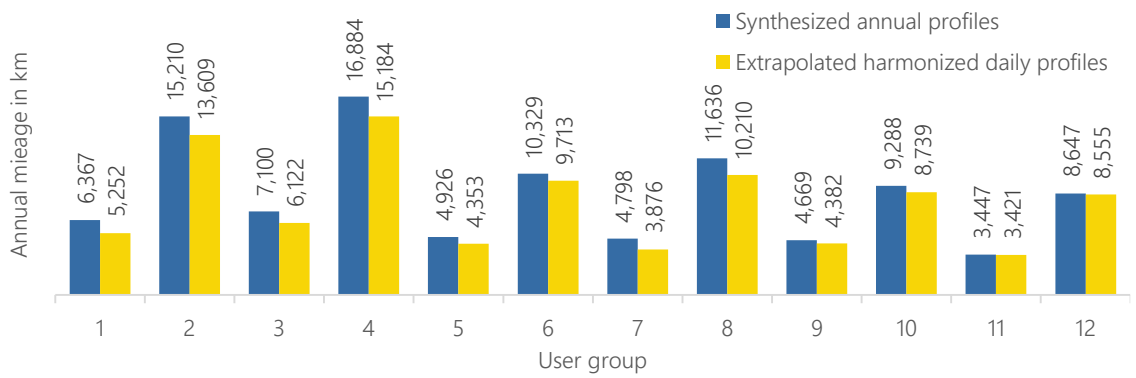

Figure 6-9: Annual mileage for the considered user groups

The average annual (short trip) mileage of the synthesized profiles is slightly higher than the extrapolated values of the harmonized daily profiles for all considered user groups. One explanation for this can be found in the concatenating process based on the weekly commuting behavior derived from the MOP survey. Survey data from the MOP shows that 41 % of all vehicles are not moved during the survey day, while this figure is 49 % for the MID. This leads to higher values in average daily driving distances of 24 km compared to 23 km in the MID. Using the weekly commuting behavior of the MOP as a concatenating criterion therefore leads to an overrepresentation of the MOP data in the model output and could explain the overall higher annual mileage. This can also be observed in the average annual mileage value of all vehicles regarding the shares of individual user groups on overall traffic. At 9,586 km, this value is higher than the average extrapolated value derived from uncoupled raw daily profiles (8,196 km).

With overall deviations being rather small, the resulting profiles are nevertheless considered sufficient for the evaluation of charging controls in the context of the present work and adequately represent the daily mobility behavior of German vehicle users.

7 Model for the Computation of Charging Strategies - eFLAME

The charging strategies assessed herein are modeled in the "electric Flexibility Assessment Modelling Environment" (eFLAME). In this chapter, an overview of the structure of the modeling environment is described in section 7.1, and the subsequent sections detail the steps from annual mobility profiles to the assessment of individual use cases. Section 7.5 presents a mathematical definition of the residential optimizer (ResOpt) model, which is used to calculate the optimized charging operations. In the context of this thesis unidirectional as well as bidirectional charging strategies are assessed. Unidirectional charging strategies only shift the charging operations while bidirectional charging control considers both charging and discharging of the vehicles. The last section discusses the identification of representative profiles to reduce overall computation time.

The modeling environment was mainly developed at the FFE within the project [128] and is used to assess the potential of various Vehicle to Home (V2H) and Vehicle to Grid (V2G) use cases. The MATLAB-based optimization framework ResOpt (described in section 7.5) is implemented in this thesis, with various adaptations allowing the assessment of the use cases and sensitivities under consideration.

7.1 Model structure of eFLAME

The eFLAME model consists of two basic parts. First, all relevant input data as well as the generated annual mobility profiles described in section 6.2 are stored in the PostgreSQL database FREM. The model for the computation of charging strategies itself is implemented in MATLAB. Figure 7-1 presents an overview of the current structure of the model and the corresponding sections where each module is described in more detail.

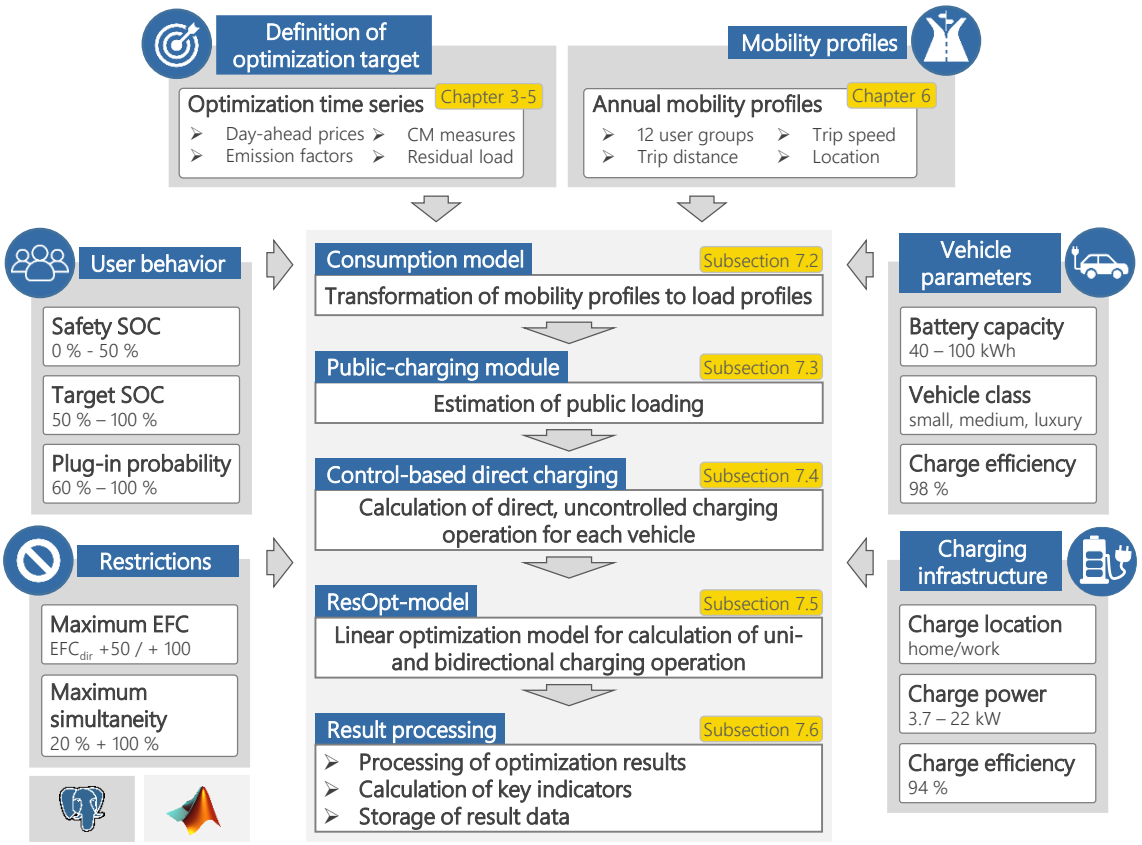

Figure 7-1: Model structure of eFLAME

The presented parameters, mobility profiles, and optimization time series are stored in the database in various topic-related tables. Further information on the selected solver (MATLAB or CPLEX), the optimization mode (linear or mixed-integer linear optimization, rolling horizon or perfect foresight, one vehicle at a time or all at the same time), simulation parameters (sample time, optimization time, etc.) can be defined in this structure as well.

An overview of those tables and the available variables is presented in the appendix (Figure 12-5). The core table of this structure is the scenario table *m_sim_scenario*. Here, individual simulation scenarios can be defined by combining IDs of all the relevant input data and therefore parameterizing the simulation run. When a scenario is defined in this way in the database, the appropriate IDs are retrieved from the scenario table in MATLAB, and the simulation run is parameterized using the information defined in the corresponding topic-related tables. In this way, parameters can be easily changed, sensitivities can be calculated, and scenarios can be simulated dynamically and reproducibly.

Generally, the model allows the simulation of all vehicles at the same time or loops over all considered vehicles. Due to the number of vehicles simulated, and to respect the influence of the charging decision of each vehicle on that of the next vehicle, the mode "loop-over-EV" was chosen here, as illustrated in Figure 7-2.

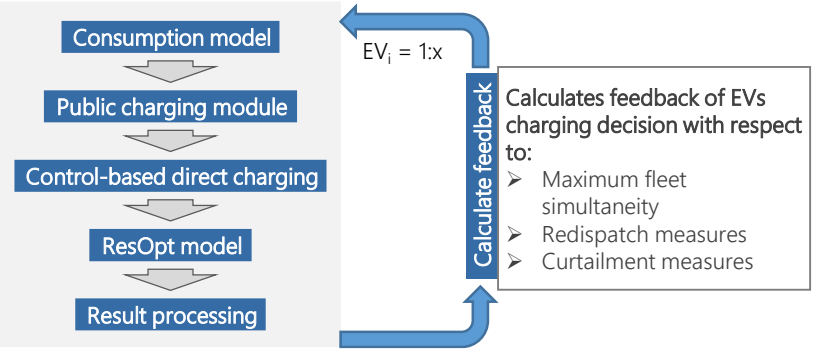

Figure 7-2: Structure of simulation mode "loop-over-EV"

After the simulation run of each vehicle, the feedback of the resulting electric load is calculated. For example, maximum values of charge simultaneity of the fleet can be considered here with respect to grid restrictions. Furthermore, when the influence of charge strategies on redispatch and curtailment measures is assessed, the coinciding reduction calculated here is weighted by the number of vehicles estimated in the coinciding region (see section 6.1). Table 7-1 presents an overview of the variables used in the model and in the descriptions in the following sections.

Table 7-1: Input parameters defining the optimization

	Parameter	Description	Unit
Mobility profiles	$Conn_t^{EV}$	Connection of EV at charge point at time interval t (0 - not present, 1 - present)	$\in \{0,1\}$
	Dep_t^{EV}	Departure or arrival of EV at charge point during time interval t	$\in \{-1,0,1\}$
	$E_t^{EV,cons.}$	Power consumption of EV while driving during time interval t	kWh
	$E_t^{EV,charge,pub.}$	Public charging of EV while driving during time interval t	kWh
	$E_t^{EV,buffer}$	Buffer value to satisfy state of charge (SOC)-safety constraint	kWh
Vehicle parameters	$E^{EV,bat.-cap.}$	Battery capacity of EV	kWh
	ev_{class}	Vehicle class (small, medium, luxury)	$\in \{1,2,3\}$
	$\eta^{EV,charge}$	Charging efficiency of the vehicle	%
	$\eta^{EV,discharge}$	Discharging efficiency of the vehicle	%
User behavior	$SOC^{EV,safety}$	Safety state of charge of EV, available for unexpected driving	%
	$SOC^{EV,dep.}$	Target state of charge of EV, should be available at departure	%
	μ_{SOC}	Median state of charge (SOC) value to derive SOC-dependent plug-in behavior	%
Charging infrastructure	$P^{IV,charge}$	Maximum charging power from wall box	kW
	$P^{IV,discharge}$	Maximum discharging power from wall box	kW
	$\eta^{IV,charge}$	Charging efficiency of the wall box inverter	%
	$\eta^{IV,discharge}$	Discharging efficiency of the wall box inverter	%
Simulation parameters	$SOC^{EV,init.}$	Initial SOC of EV	%
	$EFC^{EV,max}$	Maximum equivalent full cycles of EV in observation period	-
	$SIMU^{EV,max}$	Maximum simultaneity of EV	%
Prices	$p_t^{from\ grid}$	Price or incentive parameter per kWh from grid in time interval t	€/kWh
	$p_t^{to\ grid}$	Compensation or incentive parameter per kWh fed to grid in time interval t	€/kWh
	$p_t^{priority}$	Gradually increasing price curve incentivizing instant charging if no other incentive exists	€/kWh

The following section describes each of the modules mentioned in Figure 7-1.

7.2 Consumption model

In a first step, the trip information on traveled distance and speed is translated into electric consumption values. Most studies in the field of EV modeling only consider fixed consumption values (e.g., [100], [129]). However, Pasaoglu et al. [126] have shown that the power consumption not only varies with the vehicles speed but also has a significant dependence on the outdoor temperature. These relationships are also supported by the empirical study carried out by the NOW GmbH in [130]. Therefore, a consumption model for EVs was implemented and used in the context of this thesis, respecting both speed and temperature as input values. The model is based on measured values of the power consumption of EVs derived from [131] and the study [132] and was originally published and described in the projects [133] and [81].

The model calculates the energy consumption for three vehicle classes as a function of the average speed as well as the outdoor temperature. Energy consumption is comprised of auxiliary consumption, air conditioning, and drive consumption, all of which depend on outside temperature and speed. In [132], a wide range of measurements was conducted on test rigs to compare the consumption of EVs with conventional vehicles. A combination of the Artemis cycle and the new European driving cycle (NEDC) was assumed as the speed profile, the temperature was varied from -20°C to +30°C in 10°C increments, and the air-conditioning and auxiliary consumption of various vehicles was measured. Based on the assumptions made in [59] regarding drive consumption for the generic vehicle classes used, the average consumption for each phase of the driving cycle is calculated for each of the temperature levels considered. By means of a two-dimensional linear interpolation between the support points derived in this way, the consumption of each trip can be calculated using the values for speed and outdoor temperature. Figure 7-3 shows a heat map of the resulting consumption values $E_t^{EV,cons.}$ for an assumed medium class vehicle when values of temperature and speed are varied over the model's data range.

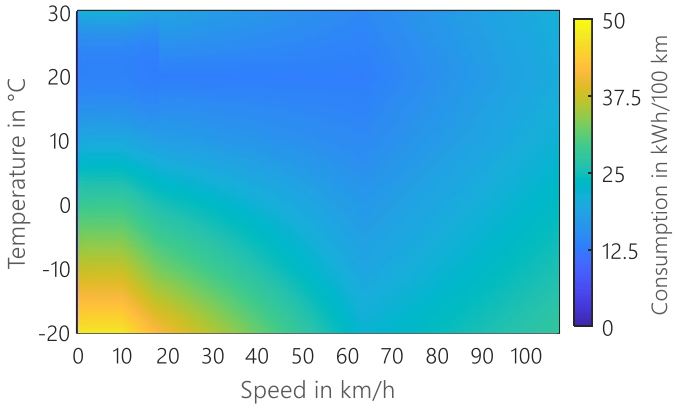

Figure 7-3: Electric consumption for a medium class vehicle as a function of outdoor temperature and speed

The clear influence of outdoor temperatures on the overall electricity consumption of the vehicles can be seen, reaching maximum values at the lowest considered temperature. This effect is stronger for lower speeds because electric consumption of the air conditioning is time dependent rather than speed dependent. This temperature dependency has a strong influence on the seasonal consumption values of EVs (see section 7.2) and is even more important when comparing consumption values in different countries (see section 8.2.5.1).

To validate those values, a simulation of all mobility profiles for each class was established for 2019. Furthermore, measured consumption values of current EVs were researched and are presented in

Table 12-1 in the appendix. The distribution of measured consumption values in comparison to the average model values are shown in Figure 7-4.

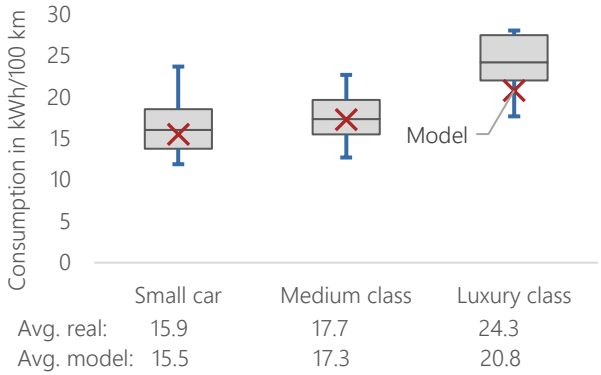

Figure 7-4: Comparison of real EV consumption values with model results

The measured values of the vehicles vary considerably within the defined classes. One explanation can be found in the vague nature of class definition, leading to a variety of different vehicles assigned to one class. Average values start at 15.9 kWh/100 km for small cars, 17.7 for medium class, and reach 24.3 kWh/ 100 km in the luxury class. These values are well met by the model results with a slight underestimation of the consumption of luxury-class vehicles.

7.3 Public charging module

As stated, the modeling approach for the creation of annual mobility profiles described in chapter 6 only considers intraday traffic, neglecting longer multiday trips. On average, only 9,586 of the 14,720 annually driven kilometers are captured that way. It is assumed that the remaining electricity demand for those longer trips is fulfilled by charging at public charging stations. Since no controlled charging is to be expected there, those charging operations are not relevant for the assessment of controlled charging. They are, however, relevant for the assessment of total annual emissions and costs. Since those depend on the points in time of these public charging operations, an estimation approach was developed based on the traffic census data of the Federal Highways Research Institute ("Bundesanstalt für Straßenwesen" [BASt]) [134]. The dataset includes census station data from 1,914 automatic census stations on highways and interstates.

The census data distinguishes between vehicle types and has an hourly resolution. It is assumed that long-distance public charging occurs primarily along these freeways and interstates. Therefore, the average temporal characteristic of traffic load of all Germany census stations over the course of a year is considered as a basis for the estimation of a public charging time series. The time series is normalized to one and scaled to the annual electricity demand from public charging derived from the remaining 5,134 kilometers mentioned above. This public charging time series is applied to each vehicle so that the fleet average annual mileage adds up to 14,700 kilometers. This is clearly a strong assumption, but it allows the evaluation of the potential of charging systems and at the same time reliable statements about the total electricity demand of the vehicles and the associated costs and emissions.

7.4 Control-based direct charging module

Since the direct charging of EVs is not to be considered an optimization problem, the underlying behavior is modeled with a control-based approach. For each of the vehicles under consideration, a charging scenario is parameterized using the relevant parameters on available charging infrastructure, technical parameters of the vehicle, user behavior, and further simulation boundary conditions. The mobility data containing information on the SOC of the battery, electric consumption of individual trips, and locations is hereby transformed to time series of charging processes.

In a last step, two more variables are calculated that are relevant for the optimization problem used in the module ResOpt to be solvable. The first is the variable $E_t^{EV,pub.charging}$, which is set when trips of the vehicle cannot be covered by the assumed capacity of the vehicle's battery. In that case, the assumption is made that the surplus energy needed is charged at a public charging station. The second variable in this module is $E_t^{EV,buffer}$, set when a vehicle arrives at home with a remaining battery capacity lower than the selected safety SOC $SOC^{EV,safety}$. For the optimization problem the be feasible, $E_t^{EV,buffer}$ is defined to fill that gap and to satisfy the associated constraint (see section 7.5.2).

Implementation of an SOC-dependent plug-in probability

For the assessment of charging strategies presented in the results (chapter 8), the basic assumption is made that vehicle users connect their vehicles every time they reach a location with a charging infrastructure. This is based on the assumption that users are incentivized, which is confirmed by user research in [135]. The resulting potential should therefore be regarded as a maximum estimate. Without proper incentives, users usually only connect their vehicles at a low to medium SOC though, as is shown in the evaluation of empirical data in [136]. Typical SOCs are reported to reach from 25 to 75 % according to the study. [137] estimates this value to be 60 % SOC.

To assess the influence of unincentivized user behavior on the potential of charging strategies, a probabilistic model is used to map the plug-in behavior as a function of the current SOC. Fischer et al. [138] followed a similar approach and used a logistic function to model the SOC-dependent charging decision. Hu et al. [139] used a cumulative prospect theory-based modeling framework to describe the charging behavior of EV drivers. They derived an almost normally distributed density of plug-in decisions with respect to the SOC at the start of charging events, with an average starting SOC level of 40.6 % at home. In the context of this thesis, the charging decision is estimated by an inverse cumulative distribution function as:

$$F(SOC, \mu, \sigma) = 1 - \frac{1}{\sigma\sqrt{2\pi}} \int_{-\infty}^{SOC} e^{-\frac{(t-\mu)^2}{2\sigma^2}} dt \quad (7\text{-}1)$$

The median μ is varied from an SOC at arrival of 50 to 90 %, whereas the standard deviation sigma is set to 0.1, resulting in rather smooth behavior of the plug-in probability curve. The resulting plug-in probabilities for those values are illustrated in Figure 7-5.

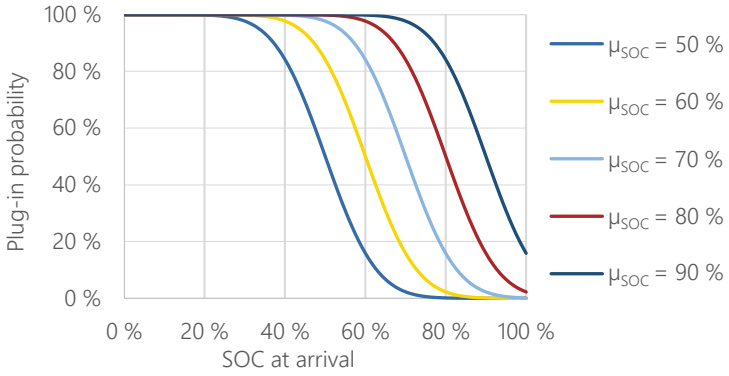

Figure 7-5: SOC-dependent plug-in probability

Based on this inverted cumulative distribution function, the plug-in behavior can be modeled in the control-based charging module. The time series of connections are adapted according to that plug-in behavior and then used for the modeling of optimized charge modes as well. That essentially means that a vehicle user who does not connect the vehicle in the direct charging mode also does not connect it in case of optimized charging. This function can be used to assess the influence of such user behavior on the potential of optimized charging.

7.5 Mathematical description of ResOpt model

The MATLAB-based optimization framework ResOpt was originally implemented by Englberger [140] in 2020 and used to assess the potential of self-consumption-optimized charging strategies, within the framework of distribution grid model GridSim[3] [141]. The same model was then extended by Morlock [142] with a mixed-integer optimization to account for and evaluate the influence of power-dependent charging efficiency. In cooperation with Schmidt-Achert [91], the model was adapted to include emission-optimized charging. The database framework was implemented with various adaptations described in this chapter to allow the assessment of the use cases and sensitivities under consideration. Furthermore, the CM-based charging strategy was implemented in the course of this thesis. In this section, the mathematical description of the model is summarized with a focus on the newly implemented features necessary for the assessment of the use cases at hand. The model itself also considers various other technical components such as the electricity generation from solar plants, heat pumps, and thermal and electrical storage devices. These, however, are not part of the charging strategies described here and are therefore excluded from the description in this chapter.

The model is implemented as a linear optimization problem in the form of a minimization problem, which can generally be described as follows:

$$\min\ c^T x \qquad (7\text{-}2)$$

$$\text{with} \quad Ax = b$$

$$Bx \leq d$$

where x is the decision variable vector, and c is the coefficient vector. The goal is to minimize the objective function (in our case, total emissions, costs, the amount of congestion management measures, or a combination of those) under consideration of a set of equalities ($Ax = b$) and inequalities ($Bx \leq d$), defined as constraints, so that

[3] GridSim - Power Grid and Energy System Model for Distribution Networks [141]f, www.ffe.de/gridsim

- A,b are the coefficient matrix and vector for equality constraints
- B,d are the coefficient matrix and vector for inequality constraints

The following sections describe the objective function as well as the decision variables and constraints relevant for the modeling of charging strategies in the use cases assessed.

7.5.1 Decision variables and input parameters

For the use case evaluations in this paper, no components other than the EV and charging infrastructure are considered. Accordingly, the number of decision variables is reduced to these two components. They are defined as follows for each time step $, t \in T$. Decision variables are distinguished from input parameters by a bold typeface.

Table 7-2: Definition of decision variables

Decision variable	Mathematical description	Unit
EV stored energy	$\mathbf{0} \leq \boldsymbol{E_t^{EV}} \leq E^{EV,bat.-cap.}, \forall t \in T$	kWh
EV charging power	$\mathbf{0} \leq \boldsymbol{P_t^{EV,charge}} \leq P^{IV,charge.}, \forall t \in T$	kW
EV discharging power	$\mathbf{0} \leq \boldsymbol{P_t^{EV,discharge}} \leq P^{IV,\mathrm{discharge.}}, \forall t \in T$	kW

All three decision variables are limited by the technical parameters of the EV and the charging infrastructure as an upper bound, as defined in Table 7-1.

7.5.2 Constraints

The optimization problem is restricted by a certain set of constraints resulting from the technical parameters and simulation restrictions. They are defined as follow:

Charging power

The charging and discharging power of the vehicles at a charging location is limited by the charging power of the associated wall box. The related constraint reads:

$$\boldsymbol{P_t^{EV,charge}} \leq Conn_t^{EV} \cdot P^{IV,charge}, \forall t \in T \quad (7\text{-}3)$$

$$\boldsymbol{P_t^{EV,discharge}} \leq Conn_t^{EV} \cdot P^{IV,discharge}, \forall t \in T \quad (7\text{-}4)$$

Energy conservation of EV

The energy stored in the EV in a time interval t consists of the following components:

- + energy stored in the prior time interval t-1
- + energy from charging process
- + energy from public charging
- - energy from discharging process
- - energy consumption of trips

The resulting constraint is defined as:

$$\boldsymbol{E_t^{EV}} = \boldsymbol{E_{t-1}^{EV}} + \boldsymbol{P_t^{EV,charge}} \cdot \eta^{EV,charge} \cdot \Delta t + E_t^{EV,pub.charge} - \boldsymbol{P_t^{EV,discharge}} \cdot \frac{\mathbf{1}}{\eta^{EV,discharge}} \cdot \Delta t - E_t^{EV,cons.}, \forall t \in \{2, \dots, N\} \quad (7\text{-}5)$$

For the first time step t=1, the state of the battery is defined by the parameter $SOC^{EV,init.}$ as:

$$\boldsymbol{E_t^{EV,initial}} = SOC^{EV,init.} \cdot E^{EV,bat.-cap.} \tag{7-6}$$

Safety SOC

The safety SOC, $SOC^{EV,safety}$, is a minimum threshold that should always be kept in the battery of the vehicle to allow for unplanned emergency trips. For the standard case, this threshold is set to 30 %. The constraint is defined as:

$$\boldsymbol{E_t^{EV}} + E_t^{EV,buffer} \geq SOC^{EV,safety} \cdot E^{EV,bat.-cap.} \cdot Conn_t^{EV}, \forall t \in T \tag{7-7}$$

Here, the parameter $E_t^{EV,buffer}$ calculated in the control-based direct charging module is expected to satisfy this constraint in all cases.

SOC at departure

Similar to the safety SOC, the variable $SOC^{EV,dep.}$ defines a minimum SOC that must be reached at the end of each charging operation. In the standard case, this value is set to 70 %. The constraint is defined as:

$$\boldsymbol{E_t^{EV}} + E_t^{EV,buffer} \geq SOC^{EV,dep.} \cdot E^{EV,bat.-cap.} \cdot Dep_t^{EV}, \forall t \in T \tag{7-8}$$

Limit maximum equivalent full cycles

Bidirectional charging often leads to a significant increase in battery use, represented by the equivalent full cycles (EFCs). To assess the influence of restrictions of battery use, in several simulations, this value is restricted using the EFC constraint defined as follows:

$$EFC^{EV,max} \leq \cdot \sum_{t \in T} (\boldsymbol{P_t^{EV,charge}} \cdot \eta^{EV,charge} \cdot \Delta t + E_t^{EV,pub.charge} + \boldsymbol{P_t^{EV,discharge}} \cdot \frac{\mathbf{1}}{\eta^{EV,discharge}} \Delta t) \cdot \frac{1}{E^{EV,bat.-cap.}} \tag{7-9}$$

The results of a restriction of EFC and its influence on emission reduction potential of the coinciding charging strategy are discussed in section 8.2.3.5.

7.5.3 Objective function

Based on those constraints and decision variables, the objective function is defined with the goal to minimize electricity costs. The price time series $p_t^{from\ grid}$ and $p_t^{to\ grid}$ are set according to the overall optimization target for each of the use cases. In the case of an emission reduction, for example, this "price" is represented by the EMF. Therefore, in that case, a cost reduction equals an emission reduction and is solved using the same objective function. Additionally, a charging priority incentive is defined as a time series of prices gradually increasing over the time horizon of the simulation. This incentive guarantees that, in case no clear incentive is set by the price during the charging operation, the vehicle is charged as soon as possible. The resulting objective function is defined as follows:

$$\min \sum_{t \in T} (p_t^{from\ grid} \cdot \boldsymbol{P_t^{EV,charge}} - p_t^{priority} \cdot \boldsymbol{P_t^{EV,charge}} - p_t^{to\ grid} \cdot \boldsymbol{P_t^{EV,discharge}}) \cdot \Delta t \tag{7-10}$$

This objective function for all time steps $t \in T$ is solved for each vehicle for the unidirectional and bidirectional charging operation assuming perfect foresight. Since generic price curves are used in some cases to incentivize a particular charging behavior, the results of this optimization process are then processed and evaluated in terms of charged emissions, operating costs, or reduction in CM measures.

7.6 Result processing and assessment of charging strategies

The model results for individual vehicles are then processed for further evaluation. For all simulations, resulting parameters are calculated considering both average values of the whole fleet as well as individual values for each vehicle. A summary of the most important simulation results is presented in Table 7-3.

Table 7-3: Resulting simulation parameters

Parameter	Description	Unit
$E^{EV,cons.}$	Annual consumption	kWh
$E^{EV,charge/discharge}$	Annual sum of charged electricity	kWh
$E^{EV,charge,pub.}$	Charged electricity public	kWh
$E^{EV,charge/discharge,home}$	Charged/discharged electricity at home/work	kWh
$E^{EV,losses,charge/discharge}$	Annual charging losses	kWh
mil_{EV}	Annual mileage	km
$cons_{EV}$	Average consumption	kWh/100 km
$simu_{charge/discharge}$	Charge/discharge simultaneity	% (only for whole fleet)
$simu_{discharge/discharge}$	Charging/discharging hours per day	hours
EFC_{EV}	EFC resulting from charging operation	

All use cases considered in this thesis are evaluated in terms of annual costs and emissions and, in case of the CM use case, in terms of a potential reduction of CM measures. In this context, certain assumptions must be made, which are briefly presented in the following.

7.6.1 Emission assessment

All use cases are assessed in terms of resulting emissions. As discussed in section 4.7, consumption-based mix-EMFs are considered for this purpose. This does neglect the feedback effects that the charging operations have on the energy system but is considered the best option at hand. For the use case of residual load smoothing, the system feedback was evaluated by means of an iterative simulation run with the energy system model ISAaR (see section 8.4.2). However, due to the very high simulative effort, this evaluation can only be considered as a sensitivity and cannot be performed for all use cases. For the general assessment of operational emissions, the time series of charging and discharging operations at home/work as well as public charging for each vehicle and charge mode is multiplied with that of the consumption-based EMFs as

$$EM_{EV} = \sum_{t \in T} (emf_t \cdot (\boldsymbol{P_t^{EV,charge}} \Delta t + E_t^{EV,charge,pub.} - \boldsymbol{P_t^{EV,discharge}} \Delta t) \quad (7\text{-}11)$$

From the perspective of the vehicle, discharging therefore leads to negative emission values, whereas charging results in positive values. In the case of the use cases of redispatch and curtailment, a different accounting method is used, as described in section 8.5.2.

7.6.2 Economic assessment

The use cases of emission-optimized, price-optimized, and smoothing of residual load are also assessed with respect to a possible revenue potential. The regulatory framework in Germany currently does not consider variable electricity tariffs for customers that represent the variability of wholesale electricity prices. There are, however, various research and pilot projects addressing local

flexibility markets and similar approaches [143]. For the assessment of revenue potentials, it is assumed that such a system would be applied, and vehicle owners could directly profit from the provision of their EV's flexibility.

Considering electricity price structure, certain assumptions must be made. In 2019, the wholesale electricity price (represented by the time series of day-ahead prices $p_{t,Da}$) only amounted to 23 % of the price that household customers pay ($p_{home} = 30.2\ ct/kWh$, [144]). For the assessment of revenues, it is assumed that that component can be influenced by the charging strategies. For the electric consumption of the vehicles, the remaining 77 %, consisting of taxes and levies p_{levies}, apply. Since the future development of these price components strongly depends on the regulatory framework and must at least be viewed with great caution, the same proportions are also applied for future electricity prices in this case. The amount of electricity charged and discharged during the bidirectional operation is assumed to be free of taxes and levies since such charging strategies are to be considered beneficiary for the overall energy system. This is viewed as a strong assumption since the current regulatory framework is far from such regulation, but the discussion about this has started, and it can be assumed that steps in that direction will be taken. For instance, Kern et al. [9] have discussed in detail the influence of additional charges on electricity on the revenue potential of EV and concluded that those charges are the "most decisive parameter for the potential revenues of bidirectionally chargeable EVs." (p. 23). Hence, a careful consideration of these coherences must be applied when evaluating these revenue potentials.

Since public charging is done at public charging infrastructures, different prices must be assumed here. [145] lists electricity prices at public charging stations for over 20 providers, amounting to an average of $p_{public} = 36\ ct/kWh$. That value is considered for all public charging operations in the evaluations conducted here.

Overall, annual costs are calculated as follows:

$$Cost_{EV} = \sum_{t \in T} ((p_{t,Da} + p_{levies}) \cdot (\boldsymbol{P_t^{EV,charge}} - \boldsymbol{P_t^{EV,discharge}})\Delta t + E_t^{EV,charge,pub.} \cdot p_{public}) \quad (7\text{-}12)$$

7.6.3 Assessment of congestion management reduction potential

Regarding the CM use cases, the primary goal is to reduce CM measures. To assess this reduction potential, the spatial distribution of EVs (see section 0) and the spatial assignment of CM measures described in section 5.5 are assumed. The number of vehicles in each Voronoi area is used to assess the influence of an optimized charging operation of the EV fleet on the CM measures in that region. The main assumption here is that the fleet of uncontrolled charging EVs is already part of the total electric load of the system. Therefore, when assessing the reduction potential, the delta between direct and optimized charging of all vehicles in the area must be considered. The reduction of CM measures by N vehicles in region r is calculated as follows:

$$CM_{new} = CM_{org} - \Delta CM$$

$$\Delta CM = \sum_{EV=1}^{N_r} \sum_{t \in T} (\boldsymbol{P_t^{EV,charge,dir}} - \boldsymbol{P_t^{EV,charge,opt}} - \boldsymbol{P_t^{EV,discharge,opt}})\Delta \boldsymbol{t} \quad (7\text{-}13)$$

7.7 Identification of representative profiles

The process for the synthesis of annual mobility profiles requires a certain number of profiles to be statistically viable and to adequately represent the average mobility behavior of German residents. However, a large number of simulated vehicles also leads to increasing computational effort. An initial scenario, for example, was defined for 10,000 profiles, resulting in a total simulation time of 14 hours. Since numerous simulation runs are necessary to evaluate the use cases under consideration and to assess sensitivities, this kind of computational effort is impracticable. Furthermore, even though this topic is not in the scope of this thesis, the created mobility profiles are to be integrated in the energy system model ISAaR for further analysis of the dynamic interactions between EVs and the energy system. Considering computation time and the integration of profiles into the system of equations of ISAaR, the number of profiles is the limiting parameter. The question is how many profiles are needed to still achieve sufficiently accurate results.

To reduce the number of profiles, two approaches were tested. The first is based on a randomly drawing of an increasing number of profiles (see section 7.7.1), and the second is based on the k-means clustering algorithm for the identification of representative profiles (see section 7.7.2). The evaluation criterion for the quality of the respective approach is the deviation of key indicators (e.g., resulting emissions, charging simultaneity, EFCs, etc.) from the reference simulation run with 10,000 profiles.

7.7.1 Random profile selection

The first approach, random profile selection, is based on the assumption that due to the stochastic nature of the mobility profiles, with increasing numbers of randomly drawn profiles, deviations from the original sample of 10,000 profiles become negligible. To eliminate the element of coincidentally drawing a "good" set of profiles, for each sample size, 10,000 drawings were undertaken. They were then assessed with respect to the abovementioned deviations of key indicators from those in the reference scenario of 10,000 profiles. In each case, the highest deviation in each of the 16 categories from the reference scenario was considered for the assessment of that sample size. It can therefore be assumed that the results are robust, and deviations represent the worst possible case. Figure 7-6 shows these values for samples of 25 to 950 randomly drawn profiles.

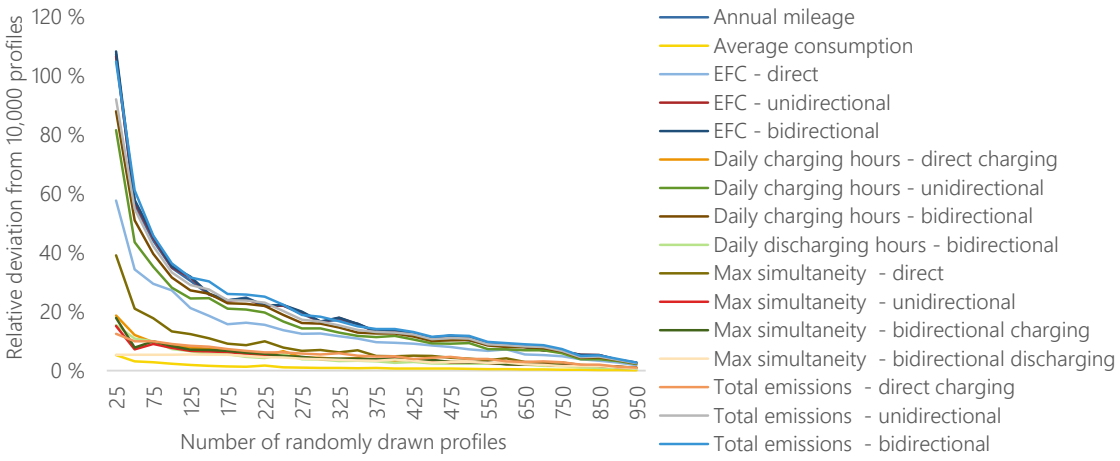

Figure 7-6: Relative deviation of 16 key indicators for simulation runs with increasing numbers of profiles from the reference simulation with 10,000 profiles

As expected, the deviations of all the indicators under consideration decrease with increasing sample sizes. Due to the nature of this worst-case assessment, however, deviations decrease slowly. Only

when reaching a sample size of 900+ profiles do deviations in all categories reach levels that are considered sufficient for that task at hand. For the largest sample of 950 profiles, all deviations are well below 3 %.

7.7.2 Cluster analysis with k-means

Especially for the integration of profiles into the system of equations of the energy system model ISAaR, the number of 950 individual profiles is not practical. A further reduction can only be achieved by a targeted selection of representative profiles. For that purpose, the clustering algorithm k-means is tested.

Cluster algorithms are generally used to divide input data into subgroups. The k-means algorithm basically tries to divide n d-dimensional observations into k clusters by reducing the Euclidean distance between each observation and the nearest mean. For the clustering, the Python-based module Scikit-learn was used [28] (https://scikit-learn.org). To apply k-means, the information contained in the profile time series (location, travel distance, speed) must first be translated into usable scalar features (defining a d-dimensional observation). Since the main objective of the integration of profiles in ISAaR is the assessment of bidirectional charging, it is assumed that the availability of vehicles at the charging locations is the most important feature defining the resulting load shifting potential. On the other hand, the distances traveled on the trips have an impact on the total electricity consumption and charging behavior in the case of direct charging and unidirectional optimization, but the impact in the case of bidirectional optimization is considered small. Therefore, each of the profiles is translated into average availability values of six hourly intervals (00:00–06:00, 06:00–12:00, 12:00–18:00, and 18:00–24:00) for each day of the week. For each of those features, a percentage value of 0–100 % is defined for each interval (100 % means that the vehicle is present at a charging location for all of the six hours, while 0 % means that the vehicle is not present at a charging location at all during that interval). In addition, two locations are considered here, resulting in a total of 56 features (four intervals per day, seven days per week, two charging locations).

This example already shows how important the selection of features is for the performance of cluster algorithms. The assumption made here focuses on a good representation of bidirectional charging, whereas the sole focus on availabilities may not be sufficient for the representation of direct and unidirectional charging. Based on these features, different approaches are tested with various cluster numbers, feature reduction using principal component analysis (PCA), and the consideration of annual mileages as an additional feature. Since cluster analysis was tested only as one of two ways to identify representative profiles and is not the focus of this thesis, it is not presented in detail. However, a corresponding publication of the exact methodology and results is planned.

The center of each of the resulting clusters is used as the representative profile, and the resulting weighting factors are calculated (i.e., how many of the profiles are represented by each representative). The resulting profiles are then used for the simulation of the same scenario as the reference case with 10,000 profiles. Key indicators such as annual mileage, EFCs, daily charging hours, the maximum charge simultaneity, and the resulting annual emissions are evaluated and compared to the values derived from the reference scenario. In total, 77 cluster scenarios were tested that way, and a total of 16 key indicators were compared. For all cluster scenarios and key indicators, the average deviation from the reference scenario was calculated. Table 7-4 shows the key features of the seven cluster scenarios with average deviation below 5 %.

Table 7-4: Key features of the seven best clusters identified

	Cl_1	Cl_2	Cl_3	Cl_4	Cl_5	Cl_6	Cl_7
# of clusters	15	20	25	12	16	60	100
Mileage as a feature	no	no	no	yes	no	no	no
PCA	yes	yes	yes	yes	no	yes	yes

In all cases, k-means was used for the clustering of profiles. The number of predefined clusters ranges from 12 to 100. In the case of Cl_4, the annual mileage of the profiles was considered as a feature; in all other cases, it was not. For all clusters except Cl_5, a PCA was performed prior to the clustering for the purpose of dimensionality reduction. Figure 7-7 shows the deviations of several of these indicators from those of the reference scenario for these seven cluster scenarios.

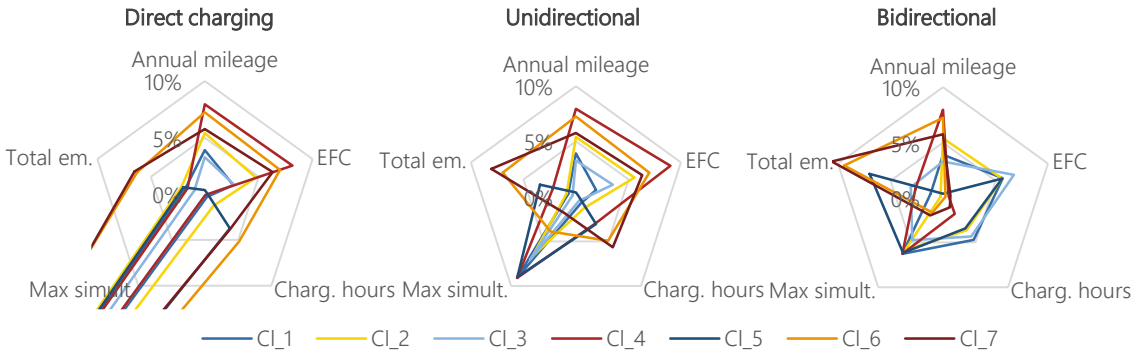

Figure 7-7: Deviation of key indicators of identified clusters from reference scenario

The results indicate that most of the deviations are below 10 % for all clusters under consideration. The only exception is the maximum charging simultaneity in direct charging. That makes sense since uncontrolled charging occurs very heterogeneously, and the average value over 10,000 profiles is considerably low compared to a smaller number of profiles. To further assess validity, the best overall cluster CL_3 is used for the simulation of a subset of 10 of the use case scenarios that are also simulated with 1,000 randomly drawn profiles. A description of the considered scenarios is presented in the appendix in Table 12-2. The resulting deviations of the key indicators of the cluster CL_3 compared to a simulation run with 1,000 profiles are displayed in Figure 7-8.

	Direct charging				Unidirectional				Bidirectional			
	EFC	Charg. hours	Max simult.	Total em.	EFC	Charg. hours	Max simult.	Total em.	EFC	Charg. hours	Max simult.	Total em.
Sc_1	20 %	12 %	226 %	15 %	20 %	18 %	5.5 %	19 %	8.0 %	5.1 %	5.0 %	0.3 %
Sc_2	20 %	5.1 %	258 %	14 %	19 %	16 %	5.9 %	18 %	9.2 %	6.1 %	5.0 %	7.5 %
Sc_3	15 %	15 %	210 %	16 %	15 %	23 %	5.6 %	20 %	1.7 %	1.5 %	4.9 %	1.8 %
Sc_4	15 %	6.5 %	264 %	15 %	14 %	21 %	5.9 %	19 %	3.2 %	3.0 %	4.9 %	4.0 %
Sc_5	31 %	10 %	233 %	22 %	31 %	18 %	5.6 %	36 %	8.0 %	4.8 %	5.0 %	1.1 %
Sc_6	18 %	12 %	216 %	15 %	17 %	20 %	5.7 %	20 %	2.8 %	1.9 %	4.9 %	0.6 %
Sc_7	17 %	4.6 %	284 %	14 %	17 %	19.0 %	5.8 %	19 %	5.0 %	4.2 %	4.9 %	5.9 %
Sc_8	14 %	14 %	198 %	14 %	13 %	20 %	5.4 %	18 %	1.2 %	0.8 %	4.9 %	1.7 %
Sc_9	17 %	13 %	214 %	16 %	17 %	22 %	5.6 %	20 %	1.7 %	1.5 %	4.9 %	0.9 %
Sc_10	18 %	12 %	216 %	15 %	17 %	20 %	5.8 %	20 %	13 %	10 %	4.0 %	7.4 %

Figure 7-8: Deviations of key indicators of cluster 3 from 10 scenarios assessed with runs with 1,000 randomly drawn profiles

Annual mileage is excluded from this evaluation since only one cluster is considered. The highest deviations can again be observed with respect to the values of maximum simultaneity in direct charging (as explained above). Deviations in the case of bidirectional charging are relatively low compared to direct and unidirectional charging. This is logical since the definition of features was primarily focused on applicability in bidirectional loading.

The results prove the general validity of this approach. The use of only 25 representative profiles overall shows a maximum deviation of 7.5 % with respect to the resulting total emissions of the vehicles in comparison to a scenario run with 1,000 profiles. Especially for the integration of bidirectionally charged EVs in the energy system model ISAaR, this can drastically decrease implementation effort and computational time. However, in the context of this thesis, bidirectional charging is not the only focus. Both operational emissions of EVs and the potential of unidirectionally optimized charging are assessed as well, in addition to the influence of charging operations on vehicle-specific parameters such as charging hours and EFCs. In those categories, deviations from the reference run of scenarios with 1,000 profiles are considerably higher. In comparison, the randomly drawn profiles (described in the prior subsection) demonstrate much lower deviations and consistency across indicators, especially with larger sample sizes. Since computational effort for a simulation with 1,000 profiles is deemed adequate, this approach has been chosen for the evaluations conducted in this thesis.

8 Results: Assessment of Charging Strategies

In this chapter, all four use cases are assessed with respect to resulting emissions, sensitivities, revenue potential, and the potential to reduce CM measures in the corresponding use cases. Since the emission assessment of charging strategies is the main focus of this thesis, all the fundamental coherences and the presentation of results are discussed most fully for emission-optimized charging in section 8.2. First, the results for the base configuration are presented for the years 2019, 2030, and 2040 regarding emission reduction and revenue potential. After that, an extensive sensitivity analysis is conducted to assess the influence of various parameters on potential emission reduction for unidirectional and bidirectional charging. Coherences and mechanisms of action are discussed in detail for each of the parameters under consideration, followed by a summary of the most important findings (section 8.2.6). Following the discussion of emission-optimized charging, results for the use cases cost reduction (section 8.3), smoothing of residual load (section 8.4), and reduction of CM measures (section 8.5) are evaluated. For the smoothing of residual load, an iterative simulation run of the ISAaR model was performed to discuss possible feedback effects of a future fleet on the energy system with respect to resulting electricity prices and the dispatch of power plants and storage units. Section 8.6 presents a comparison of the use cases regarding the revenue and emission reduction potential. Finally, the chapter closes with a discussion of the influence of the emission-optimized charging strategy on the LCA of EVs and a comparison to internal combustion engine vehicles (ICEVs).

Unless otherwise described, all simulations performed in this chapter are based on a base configuration of simulation parameters presented in Table 8-1.

Table 8-1: Base configuration of simulation parameters

	Parameter	Description	Value base configuration
	n_{EV}	Number of vehicles considered in the simulation	*1,000*
Vehicle parameters	$E^{EV,bat.-cap.}$	Battery capacity of EV	*60 kWh*
	ev_{class}	Vehicle class (small, medium, luxury)	*Medium class*
	$\eta^{EV,charge}$	Charging efficiency of the vehicle	*98 %*
	$\eta^{EV,discharge}$	Discharging efficiency of the vehicle	*98 %*
User behavior	$SOC^{EV,safety}$	Safety state of charge of EV, available for unexpected driving	*30 %*
	$SOC^{EV,dep.}$	Target state of charge of EV, should be available at departure	*70 %*
	μ_{SOC}	Median SOC value to derive SOC-dependent plug-in behavior	*Always connecting*
Charging infrastructure	$P^{IV,charge}$	Maximum charging power from wall box	*11 kW*
	$P^{IV,discharge}$	Maximum discharging power from wall box	*10 kW*
	$\eta^{IV,charge}$	Charging efficiency of the wall box-inverter	*94.5 %*
	$\eta^{IV,discharge}$	Discharging efficiency of the wall box-inverter	*98 %*
	$EFC^{EV,max}$	Maximum EFC of EV in observation period	*Unrestricted*
	$SIMU^{EV,max}$	Maximum simultaneity of EV	*Unrestricted*

This base configuration assumes a medium-class vehicle and technical parameters of vehicles and charging infrastructure that are to be considered state of the art. All parameters were discussed and approved by research partners from OEMs and charging station manufactures in the context of the project "Bidirectional Charging Management (BCM) - Intelligent interaction of electric vehicles, charging infrastructure and energy system" [128] . With regard to user behavior, the strongest assumption is that users are incentivized to plug in their vehicles every time they reach a charging station. The resulting potential of the assessed charging strategies must therefore be considered as a maximum estimate.

For each use case, various scenarios (combinations of varied parameters) are simulated. The results are presented either as boxplots or median values for all considered vehicles. As discussed in section 7.7, a number of 1,000 mobility profiles was identified to adequately represent the mobility behavior of the whole fleet. Therefore, all the following simulations are conducted for 1,000 profiles, either for the overall German fleet or individual user groups. The initial result representations in section 8.2 are discussed in more detail, assuming knowledge of the types of representations in the sections that follow.

8.1 Validation of uncontrolled charging behavior

Following the base configuration of simulations parameters in Table 8-1 the average hourly load from direct charging as well as the average daily energy consumption of all 1,000 vehicles is calculated as illustrated in Figure 8-1.

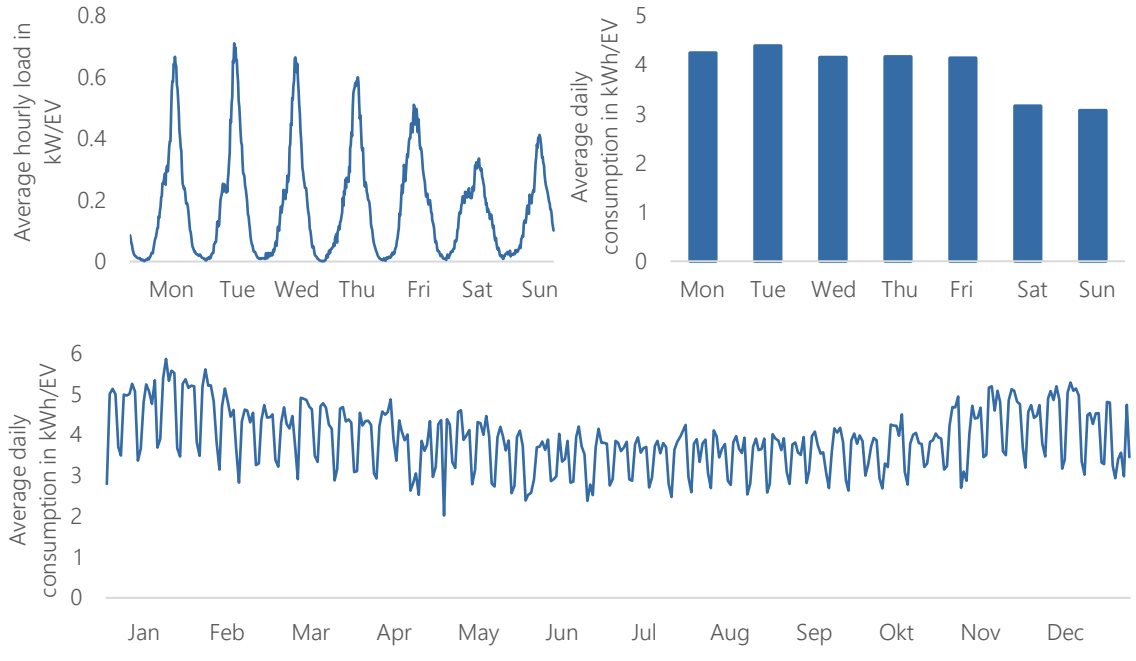

Figure 8-1: Average hourly load and average daily consumption of the simulated vehicles

Both evaluations are based on the average vehicle in Germany without consideration of any user groups. Furthermore the graphs only show the charging processes at home, public charging is not considered. First of all a clear peak in the evening hours during the week can be identified resulting from vehicles arriving at home. This peak starts earlier on Fridays, while on Saturdays the loads are more broadly distributed. Due to generally longer trips on Sundays, the evening peak exists here as well. The daily electricity demand on weekends is about 25 % lower than during the week. These values are perfectly matched by the data provided by Dodson et al. [146]. The empirical study carried

out by Element Energy Limited is based on a large data set of over 8.3 million charge events in Great Britain and covers the period from 2017 to 2018. The raw data was processed and aggregated to derive average load curves that compare well with the evaluations presented in Figure 8-1. The average hourly load curve shown in the upper left corner is also very similar to that provided by Dodson, but small differences do exist. The causes of these differences can be very diverse. For example, the results presented in Figure 8-1 only assume a relatively high charging power of 11 kW. The data in Dodson's field test, on the other hand, is based on a statistical distribution of charging powers between 3.7 and 11 kW. Furthermore the empirical data is based on observations in the United Kingdom whereas the model is based on German mobility surveys. Overall the course of the charging power both on a weekly level as well as on an annual level are similar to real charging data, so that a sufficient validity of the modeling approach is assumed.

Besides the illustration of weekly charging behavior an annual evaluation is carried out as well by Dodson, showing a similar pattern as the one presented on the bottom up Figure 8-1. The same temperature dependency can be identified leading to a clear seasonal behavior of the consumption values. The same temperature dependency and seasonal behavior of the resulting specific consumption values is also demonstrated by the empirical study carried out by the NOW GmbH in [130], proving the necessity of a consumption model that reflects this temperature influence.

8.2 Use case 1: Emission reduction

Figure 8-2 shows the results for the base case in 2019. Besides the resulting annual emissions presented in the boxplot, median values for key indicators of the scenario are presented in the table below. Such values are the specific resulting emission per km, EFCs, average charge or discharge simultaneity of the whole fleet, and other related values. In the following, the type of data presented in that table varies among evaluations and is specifically selected to support individual interpretations. Furthermore, this figure and all the similar ones following contain an information box at the bottom defining the scenario's key assumptions. The data illustrated in the boxplot represent the resulting annual GHG emissions for all 1,000 simulated vehicles. The boxplot displays the median value represented by a red line in the middle of the box, the first and third quartiles as the box's edges, and the minimum and maximum values, as well as the extreme outliers as blue circles. Since the number of extreme outliers is relatively small (<5 %), they are excluded from all the following boxplots for better readability.

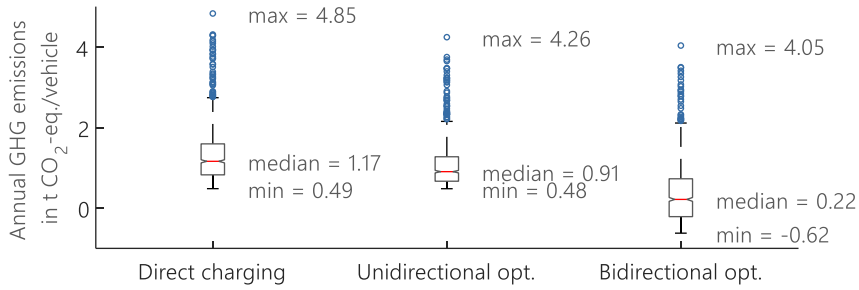

	Direct charging	Unidirectional opt.	Bidirectional opt.	
g CO_2-eq./km	84.9	68.2	16.2	
EFC	39.5	39.5	184.3	
Charge simultaneity	9 %	86.2 %	94 %	
Charged/discharged energy in MWh	1.56	1.56	10.1	7.3
Losses charging/ discharging in MWh	0.115	0.115	0.74	0.62

Vehicle type	Battery capacity	Charge power home / work	SOC departure	SOC safety	User group
Medium class	60 kWh	11 kW / -	90 %	30 %	all

Figure 8-2: Annual GHG emissions and key indicators for base scenario "Emission-optimized 2019"

The simulation of the base case in 2019 already shows the high emission reduction potential of an optimized charging operation. Specific emissions in g CO_2-eq./km can be reduced from 84.9 to 68.2 in the unidirectional case and to 16.2 in the bidirectional case. However, this emission reduction is accompanied by a significant increase in both EFCs and the overall simultaneity of charging operations. The first leads to a faster degradation of the vehicle's batteries due to electrochemical processes, known as cyclic aging. These coherences are discussed in more detail in section 8.2.3.5, where the sensitivity of a maximum EFC is presented. High values of charge simultaneity in a fleet of EV, on the other hand, lead to an increase in grid load, which may cause voltage band violations, especially in the distribution grid. Since no grid simulation is considered in this thesis, the influence of a restriction of maximum simultaneity on emission reduction potential of charging strategies is discussed in section 8.2.5.2.

Another aspect that must be considered is the amount of electricity that is charged and discharged to and from the battery over the course of the year as well as the associated losses. The simulation considers the efficiency of the wall box inverter during the conversion from alternating current (AC) to direct current (DC), as well as the efficiency of the charging process in the vehicle itself. Compared to direct charging, unrestricted bidirectional charging leads to an increase of charged electricity from 1.56 to 10.1 MWh and associated losses from 0.115 to 0.74 MWh per year. Those additional charging and discharging processes must be considered with respect to cyclic battery degradation as well as additional load on electric components.

It is assumed that one of the main influencing factors on the potential of charging strategies is the availability of the vehicles at the charging location. The longer a vehicle is connected to a charging station, the more flexibility is available to optimize charging operations, especially in the bidirectional case. To validate this assumption, the correlation of the availability (hours connected/hours of the year) of all 1,000 vehicles considered in the simulation with the resulting specific emissions in all three charging strategies are plotted in Figure 8-3.

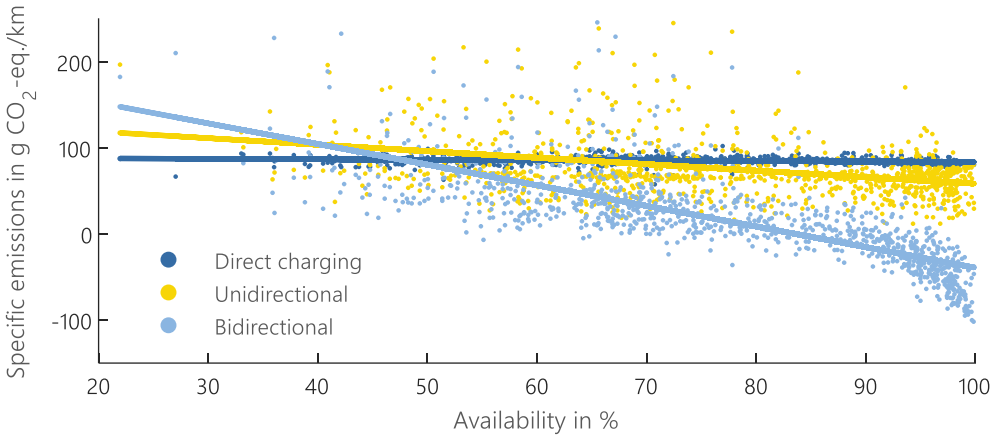

Figure 8-3: Correlation between resulting specific emissions and availability of vehicles at charge locations

For unidirectional and bidirectional charging, higher availabilities lead to a reduction in specific emissions, represented by a negative slope of the compensation line, while availability for direct charging shows no significant influence on the resulting emissions. High availabilities close to 100 % lead to disproportionately low specific emission values in the bidirectional case. The linear coherence can be explained by the availability itself. The longer a vehicle is available for unrestricted bidirectional optimization, the higher the possibility to shift loads and to minimize emissions. The more than linear drop in the curve at values close to 100 % can be explained by the calculation of specific emissions and low annual mileages. Vehicles with availability values as high as these tend to have low annual mileage values. Specific emissions are calculated by dividing total annual emissions by annual mileage. Low annual mileage means a small denominator and thus strongly negative specific emission values.

In a next step, the same simulation is applied to the two future years under consideration, 2030 and 2040. Figure 8-4 presents the results for those years in comparison to the historical year of 2019 as a boxplot. Again, key indicators relevant for interpretation are shown in the table below.

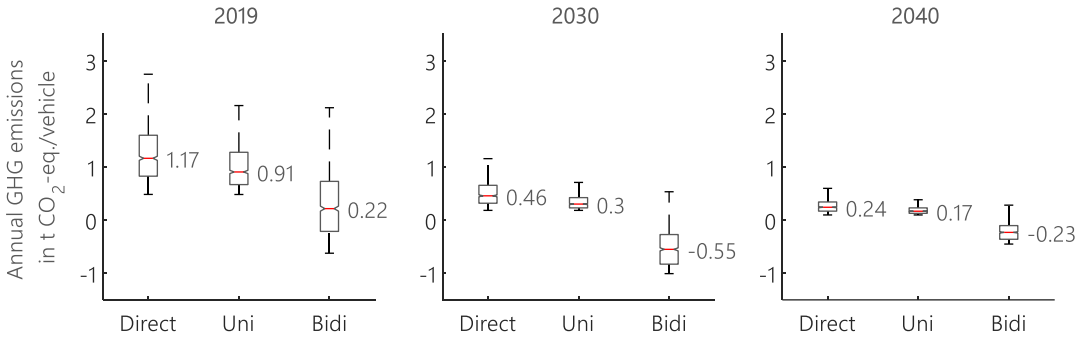

	2019			2030			2040		
	Direct	Uni	Bidi	Direct	Uni	Bidi	Direct	Uni	Bidi
g CO_2-eq./ km	84.9	68.2	14.3	33.9	23.9	-39.1	18.1	13.1	- 16.4
EFC	39.5	39.5	184.3	39.5	39.5	189.1	39.5	39.5	192.5
Rel. emission reduction by...	-	22.2 %	81.2 %	-	34.8 %	220 %	-	29.2 %	196 %

Vehicle type	Battery capacity	Charge power home / work	SOC departure	SOC safety	User group
Medium class	60 kWh	11 kW / -	90 %	30 %	all

Figure 8-4: Annual GHG emissions and key indicators for emission-optimized charging for base configuration in 2019, 2030, and 2040

Since specific emissions in electricity production have been declining over the years, so do the charged emissions in the direct charging operation from a median value of 1.17 t CO_2-eq. in 2019 to 460 kg in 2030 and 240 kg in 2040. This coincides with specific emissions per km of 84.9 in 2019, 33.9 in 2030, and 18.1 in 2040. A notable feature in the comparison of results is the fact that the interquartile range and the spread between minimum and maximum values decrease significantly in 2030 and 2040. Since the same mobility profiles are used, this can only be explained by the underlying time series of EMFs. As described in section 4.6.4, solar and wind generators increasingly dominating electricity production leads to longer periods of consecutive days with low EMF as well as low variations of EMF. In these periods, charging times do not play an important role in actual vehicle emissions, hence explaining their lower variability in annual values in future years. Furthermore, the emission reduction potential strongly depends on the underlying characteristic of the EMFs time series. Absolute and relative annual emission reductions per vehicle for both charging strategies are highest in 2030 (-34.8 % for unidirectional and -220 % for bidirectional charging). In 2030, both emission-intensive conventional generators and renewable generators contribute to electricity production, leading to the highest values for annual and daily standard deviations of EMFs (see Figure 4-6 and Figure 4-10). This reduction potential decreases slightly in 2040 since electricity generation is now mostly based on vRES, which reduces the statistical spread of EMFs.

8.2.1 Revenue assessment of emission-optimized charging

As discussed in section 4.6.4, overall improving correlation values between EMFs and wholesale electricity prices over time give an indication that an emission-optimized charging of EVs might gradually lead to an increase of potential revenues as well. To prove this assumption, resulting electricity costs of the emission-optimized charging were calculated for all three years, according to the methodology described in section 7.6.2. Figure 8-5 compares relative annual cost reductions with a potential emission reduction for unidirectional and bidirectional charging as well as Pearson's rank correlation coefficient.

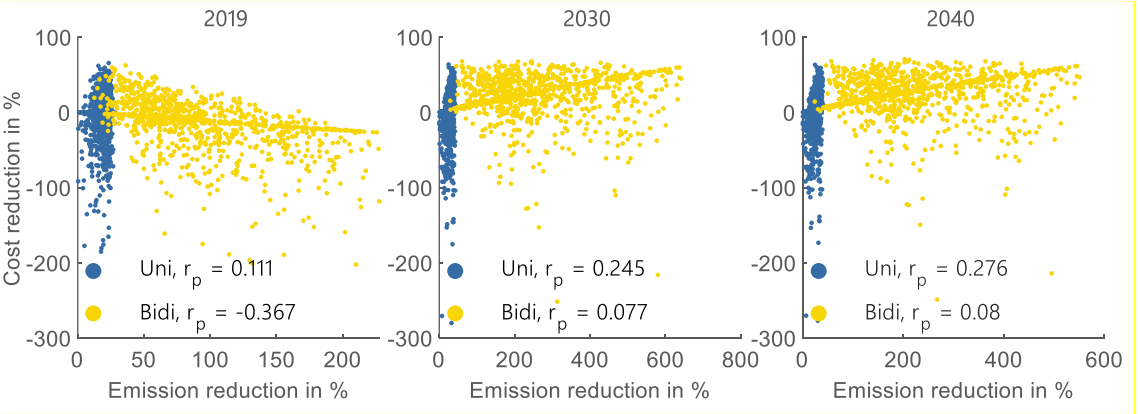

Figure 8-5: Annual revenues and emission reduction potential of emission-optimized charging for base configuration in 2019, 2030, and 2040

First, Pearson's correlation coefficient shows a weak to nonexistent correlation between relative emission and cost reduction values. The most dominant correlation can be observed in the bidirectional case in 2019 and has a negative sign. That confirms the assumption that due to the structure of the electricity market, power plants, and renewable generators, an emission reduction leads to an increase in costs in most cases. Correlation values for bidirectional charging in 2030 and 2040 are negligible but do, however, show a sign inversion, meaning that emission-optimized charging increasingly leads to a positive revenue as well.

In the unidirectional case, a positive, albeit small, correlation is also observed. Still, in all years, a relatively small range of possible emission reductions coincides with a large range of positive as well as negative cost reduction values, making the interpretation of r_p rather difficult. Overall, however, in 2019, an emission reduction coincides with increasing annual costs in 58.8 % of the cases. In 2030 and 2040, the figure is reduced to 31.8 % and 31.4 %, respectively.

In conclusion, the assumption made in section 4.6.4 can be confirmed, both in the unidirectional and bidirectional case. Figure 8-6 summarizes these findings in values for the median annual revenue and emission reduction potential of the first use case (emission-optimized charging).

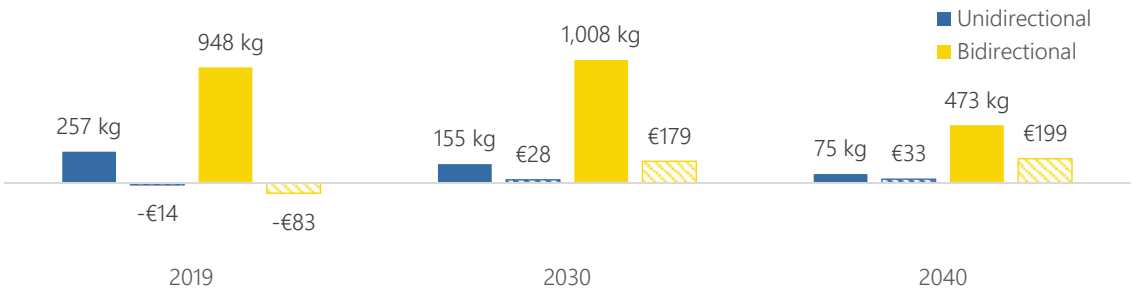

Figure 8-6: Median annual revenues and emission reduction potential in kg CO_2-eq. of emission-optimized charging for base configuration in 2019, 2030, and 2040

Where in the case of bidirectional charging in 2019, an emission reduction of 948 kg CO_2-eq. results in a negative revenue of €83, emission reductions in future years coincide with increasingly positive revenues. The same coherence can be observed for unidirectional charging.

Another aspect to be discussed at this point is the influence of such charging strategies on the market value of vRES generators. The market value of a specific generation type is calculated by multiplying its hourly generation with the wholesale price time series and dividing the result by the annual generation of this type. It therefore represents the expected revenue over the course of the year, compared to the average market price. Böing [147] has shown that increasing shares of vRES capacities result in decreasing market values of the same. High simultaneity of especially wind power basically leads to a self-cannibalization, reducing the wholesale price at times of high infeed. High vRES infeed also leads to low EMFs, which would be targeted by vehicles in the use case at hand. Shifting additional loads to times with low EMFs and high vRES infeed would therefore increase demand in the electricity market. Increasing demand results in higher prices and increasing market values of vRES. Therefore, such a charging strategy would not only reduce operational emissions but would also support refinancing of renewable generators on the wholesale electricity market. To assess these relationships further, iterative simulations with an energy system model would be needed.

8.2.2 Comparing mix and marginal emission factors as an optimization target

As discussed in section 4.7, mix EMFs are more suited as an optimization target since they better represent the current share of RES on total electricity production. For reasons of energy economic relevance and significance, as well as the resilience of the results, marginal EMF are neither deemed adequate for the accounting of operational emissions nor the assessment of charging strategies. To evaluate and discuss the effects of a consideration of marginal EMFs both as an optimization target and for the accounting of resulting emissions, corresponding simulations were performed for 2019 and 2030. Figure 8-7 shows resulting annual GHG emissions as well as key indicators for both EMF types and years.

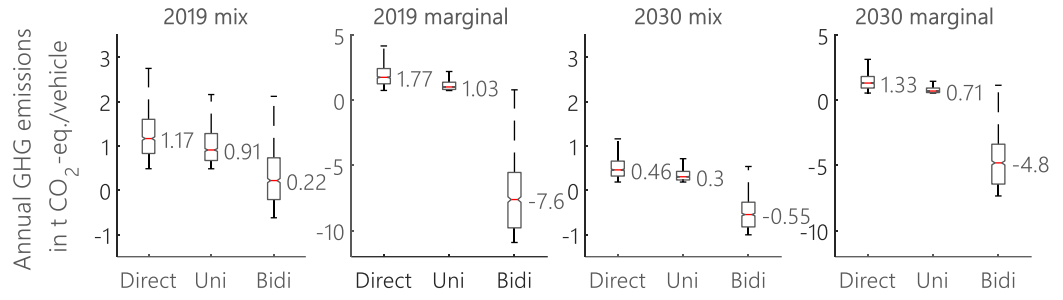

	2019 mix			2019 marginal			2030 mix			2030 marginal		
	Direct	Uni	Bidi	Direct	Uni	Bidi	Direct	Uni	Bidi	Direct	Uni	Bidi
g CO_2-eq./ km	84.9	68.6	14.3	128	81.4	-520	33.9	23.8	-39.1	97.8	58	-346
EFC	39.4	39.4	184	39.4	39.4	353	39.4	39.4	189	39.4	39.4	260

Simulation year	Vehicle type	Battery capacity	Charge power home / work	SOC departure	SOC safety
2019	Medium class	60 kWh	11 kW / -	90 %	30 %

Figure 8-7: Annual GHG emissions and key indicators for emission-optimized charging based on mix and marginal EMFs in 2019 and 2030

First, higher average values lead to higher annual and specific emissions when the accounting of operational emissions is based on marginal EMFs. In 2019, average specific emissions amount to 84.9 g CO_2-eq./km in the mix case, whereas accounting based on marginal EMFs leads to a value of 128 g CO_2-eq./km. Secondly, the high volatility of marginal EMFs (see Figure 4-11) leads to a much wider range of operational emissions in the case of direct charging. While the annual emissions spread over the range of values from 0.49 to 4.8 t CO_2-eq. when the mix method is considered, this range widens to 0.76 to 7.2 t CO_2-eq. in 2019. It should be noted that the same mobility profiles are considered for both simulations. This high volatility results in a wider range of emission spreads that can be used in the bidirectional case, leading to quite extreme emission reductions. Whereas the median annual emissions in the marginal case in 2019 amount to 1.77 t CO_2-eq., bidirectional charging reduces this value by 530 % to (negative) -7.61 t CO_2-eq. per year. However, this massive emissions reduction potential is also accompanied by a very significant increase in EFC, increasing from 39.4 in the unidirectional to 353 in the bidirectional case.

As discussed in theory in section 4.7, using marginal EMFs as an optimization target was dismissed since they do not reflect RES shares well. Furthermore, they cannot be considered a reliable indicator for the accounting of emissions of a larger fleet of vehicles. Their consideration in the present simulations supports rejection in practice as well. For those reasons, all the following emissions assessments and optimizations are based on consumption-based mix EMFs.

8.2.3 Influence of technical parameters

In the following sections, sensitivities are analyzed one factor at a time (OFAT), starting from the described base configuration of parameters. That means that only one factor is varied, while all others are fixed. That way, the relationship between each parameter and the output (here, the emission-reduction potential) can be described (e.g., whether the response is linear or nonlinear), and tipping points can be identified as described in Broeke et al. [148]. The approach does not, however, consider interrelations between input variables. For that purpose, more advanced methods like global sensitivity analysis or regression-based methods would have to be applied. Due to the complexity of the model at hand, and therefore the long computational time, such an approach was not considered.

8.2.3.1 Vehicle class

In a first step, the influence of three distinct vehicle classes is evaluated. Starting from the base case, a medium-class vehicle with 60 kWh of battery capacity, a small car with 40 kWh, and a luxury vehicle with 100 kWh are considered for the simulation. Since the consumption model described in section 7.2 distinguishes among the three vehicle classes, the associated electric consumption of each class is considered. Figure 8-8 shows the simulation results for 2019.

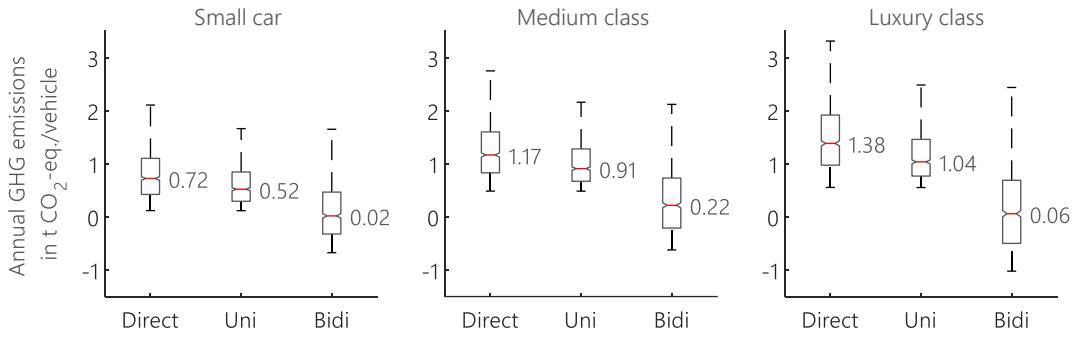

	Small car			Medium class			Luxury class		
Consumption in kWh/km		15.5			17.3			20.8	
g CO_2-eq./ km	77.5	56.4	2.36	84.9	68.6	14.3	103.4	80.1	4.7
EFC	36.7	36.7	194.1	39.5	39.5	184.4	27.6	27.6	142
Charged energy in MWh	1.32	1.32	7.47	1.56	1.56	10.1	1.98	1.98	13.5

Simulation year	Battery capacity	Charge power home / work	SOC departure	SOC safety	User group
2019	40-100 kWh	11 kW / -	90 %	30 %	all

Figure 8-8: Annual GHG emissions and key indicators for emission-optimized charging of three vehicle classes in 2019

In the case of direct charging, the influence of different consumption values appears most dominant. The median values of specific emissions per kilometer reach from 77.5 g CO_2-eq./km for small cars to 103.4 g CO_2-eq./km in case of luxury-class vehicles. Due to larger battery capacities, vehicles especially of the luxury class, however, have a much higher reduction potential in the bidirectional case, enabling lower annual emissions than mid-class vehicles, even though they have a higher consumption. EFC values are lower for higher vehicle classes, but this is only due to the higher battery capacity as the denominator in the calculation of this value. However, the higher battery capacity increases flexibility and the amount of electricity charged and discharged during the year, explaining the higher emission reduction potential. In the next step, the influence of battery capacity is isolated, considering only medium-class vehicles with battery capacities between 40 and 100 kWh.

8.2.3.2 Battery capacity

As described above, increasing battery capacities lead to a higher flexibility and therefore a higher potential for charge control strategies. Here, the sole influence of a variation of vehicles' battery capacity is analyzed. Figure 8-9 shows the distribution of battery capacities of EV models in 2019 and 2021.

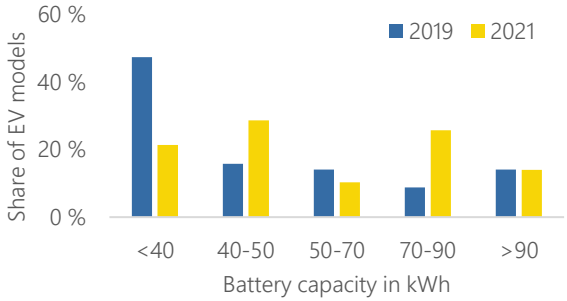

Figure 8-9: Battery capacities of current EV models [149]

In addition to the fact that the total number of available models doubled from 57 to 136 in two years, battery capacities tend to increase as well in the available models, with OEMs addressing the still-existing range anxiety of customers. For the sensitivity analysis, battery capacities were increased from 40 to 100 kWh, and the resulting emission reduction potential was evaluated for 2019, 2030, and 2040. Resulting emission reductions are shown in Figure 8-10.

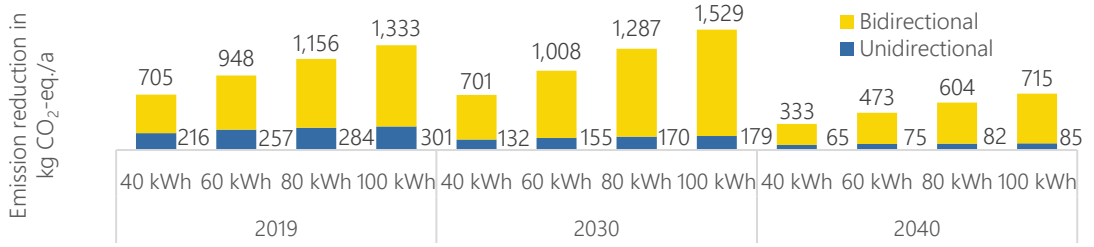

	2019				2030				2040			
Relative emission reduction uni. by...	19 %	22 %	24 %	26 %	29 %	34 %	37 %	39 %	27 %	31 %	33 %	35 %
Relative emission reduction bidi. by...	61 %	81 %	99 %	114 %	154 %	219 %	279 %	331 %	137 %	194 %	245 %	290 %
Increased charged energy bidi. by...	421 %	544 %	633 %	692 %	410 %	543 %	663 %	763 %	415 %	554 %	676 %	778 %

Vehicle type	Battery capacity	Charge power home/work	SOC departure	SOC safety	User group
Medium class	40-100 kWh	11 kW / -	90 %	30 %	all

Figure 8-10: Influence of battery capacity on remission reductions

In all years, battery capacity does not show a significant influence in the case of unidirectional charging. For bidirectional charging, however, increasing battery capacities lead to a strong increase in emission reductions, mainly explained by the additional amount of electricity that can be charged and discharged compared to the unidirectional case. In all the considered years, this amount remains more or less constant. Hence, the resulting emission reduction mainly depends on the underlying constitution of the energy system and the associated EMFs. In each of the years, a linear relationship between the battery capacity and the emission reduction potential can be observed with an increasing slope.

8.2.3.3 Charging infrastructure

Available flexibility, hence charged and discharged electricity, depends on the battery capacity of the vehicle, on the one hand, and on the assumed power of the wall box on the other. To assess its influence, standard charging and discharging powers of 3.7, 11, and 22 kW were considered as sensitivities. Figure 8-11 shows absolute emission reductions for both the uni- and bidirectional cases as well as the relative reduction in the bidirectional case.

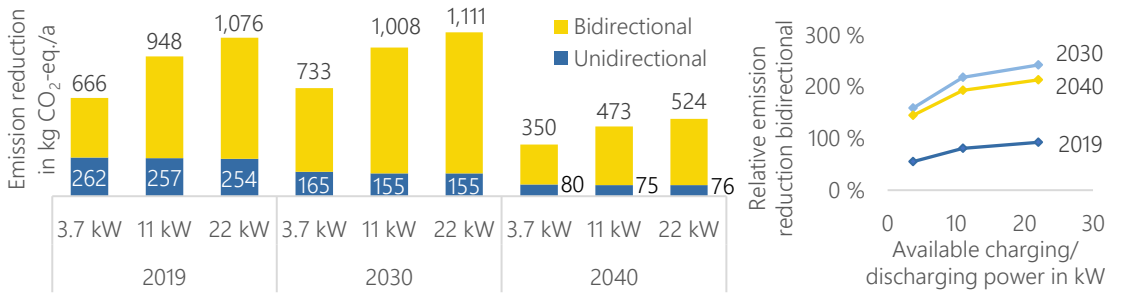

Vehicle type	Battery capacity	Charge power home/work	SOC departure	SOC safety	User group
Medium class	60 kWh	3.7-22 kW / -	90 %	30 %	all

Figure 8-11: Influence of available charging power at home on remission reductions

As with battery capacities, the charging power has almost no influence on the possible emission reductions in the unidirectional operation. With bidirectional charging, however, increasing charging power substantially increases the emission reduction potential as well. Since the charging duration directly depends on the charging power and takes about six times as long with 3.7 instead of 22 kW, the time left for optimized charging is limited. This is also notable in the resulting EFC. In the directional case in 2019, EFC values increase from 119 in the case of 3.7 kW to 209.2 in the case of 22 kW, meaning that more optimized charging and discharging can be used to reduce overall emissions.

In direct contrast to the influence of the battery capacity, the relationship between charging power and the emission reduction potential cannot be considered as linear. The slope, and therefore the additional emission reduction, between 3.7 and 11 kW is much higher than between 11 and 22 kW. The base case only considering a 60 kWh battery is the factor limiting flexibility in that case.

8.2.3.4 Influence of charging at work

In the base scenario, the configuration of only charging at home is considered. To assess the influence of additional charging (at 11 kW) at the workplace, corresponding simulations are conducted for the user group "full-time employed." All other technical and behavioral simulation parameters are kept constant. Figure 8-12 compares the annual emissions for the three charging strategies resulting from those two configurations.

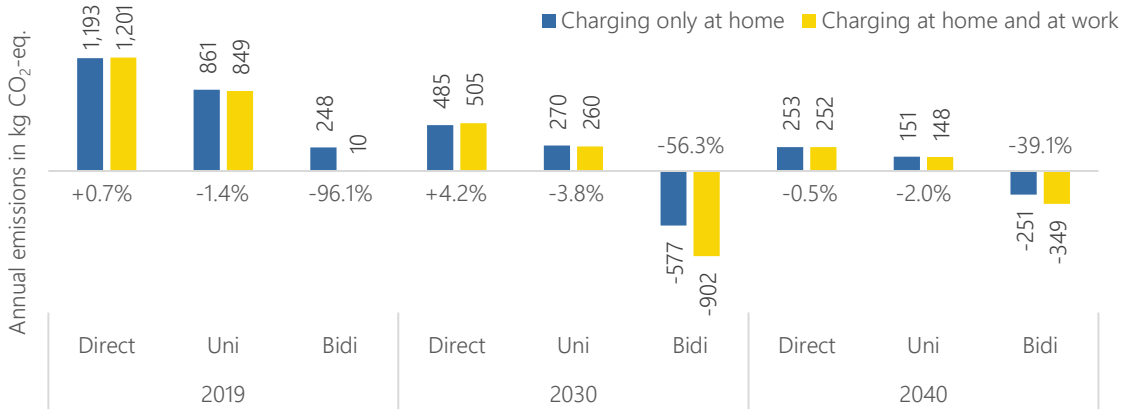

Vehicle type	Battery capacity	Charge power home/work	SOC departure	SOC safety	User group
Medium class	60 kWh	11 kW / -/11 kW	90 %	30 %	fulltime occupied

Figure 8-12: Annual emissions for charging only at home and charging at home and at work

In 2019 and 2030, emissions in direct charging actually increase when charging at work is considered. It should be noted that in the base configuration, vehicles are always connected and start the charging operation in the direct charging mode. As discussed in section 6.2.5, 50 % of all commuters reach their workplace before eight o'clock in the morning. In 2019 and 2030, EMFs are still relatively high during that time, whereas the increasing share of solar in combination with the decommissioning of coal-fired power plants in 2040 also leads to a decrease of EMFs in early-morning hours. With respect to the emission reduction potential by unidirectional and bidirectional charging, on the other hand, charging at work increases the amount of flexibility available for optimization of charging processes and therefore leads to an increase in emission reductions. Average availability of vehicles connected to a charging station increases from 72 % to 87 %. Furthermore, low emission periods due to solar infeed become available for the optimization, further increasing potential emission reductions. In 2030, this combination leads to an increase in emission reductions of an additional 56.3 % in the case of bidirectional charging. Figure 8-13 shows the average hourly charging and discharging power for all considered vehicles over the course of the day for 2030 for the scenarios "charging only at home" and "charging at home and at work."

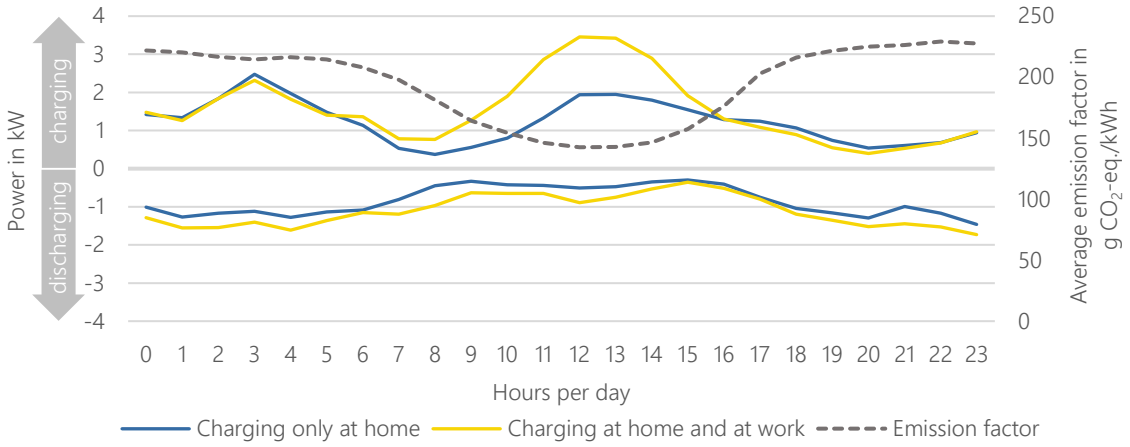

Figure 8-13: Average charging and discharging operation in kW/vehicle over the course of the average day in 2030

For the yellow curve, charging at work is considered; for the blue curve, it is not. Furthermore, the average course of the emission curve is shown in gray. Charging at work enables the vehicles to fully utilize the times of low EMFs during the day when they are parked at work. The additional electricity charged at work then tends to be discharged again at night, when EMFs are higher, which explains the significant increase in emission reduction potential.

In conclusion, enabling charging at work does not lead to significant improvements for direct or unidirectional charging, but due to higher availability values combined with low EMFs during the day, it does significantly increase the potential of bidirectional charging.

8.2.3.5 Influence of EFCs

All scenarios evaluated to this point show a significant increase in resulting EFCs in the bidirectional case, as shown in Table 8-2 for the reference scenario.

Table 8-2: Resulting EFCs in reference scenario (EMF-opt., 11 kW, 60 kWh)

	2019	2030	2040
Reference direct charging	39.5	39.5	39.5
Reference bidirectional	184.3	189.1	192.5
Increase by…	**x 4.7**	**x 4.8**	**x 4.9**

In direct comparison to direct charging, EFC values increase by 367 to 387 % in the considered years. Higher EFC puts additional stress on the battery's electrochemistry, resulting in faster cyclic aging. Aging processes of batteries can generally be subdivided in two types with fundamentally different mechanisms of action: calendric and cyclic aging. Calendric aging depends mostly on time, the state of charge of the battery, and the ambient temperature. Cyclic aging, on the contrary, refers to the loss of capacity due to degradation phenomena in the battery caused by the energy throughput and depends on various parameters such as cycle frequency, cycle depth, and charging and discharging currents [150]. Current battery degradation studies mostly focus on EFC-dependent degradation values of uncontrolled charged vehicles. When evaluating the acceptable number of EFCs, a degradation threshold must be defined, after which the battery has reached its end of life. Values for this end of life are not clearly defined and vary between 70 and 80 % ([151], [152], [153], [154]). Keil [155] has stated that the 1,000 EFCs until end of life can already be achieved under moderate outdoor temperatures. Considering the resulting annual EFC values as listed in Table 8-2, bidirectional charging could have a negative influence on battery life. However, it must be taken into account that values of 1,000 EFCs, mentioned in literature, result from normal driving and charging behavior, and as stated above, cyclic aging depends on various parameters such as cycle depth and charging/discharging currents. Especially while driving, currents easily exceed the assumed charging and discharging values of 3.7 to 22 kW. To reduce the influence of bidirectional charging on battery aging, a limitation of EFCs is considered in the simulations. In comparison to direct charging, a limit of 50/100 additional EFCs for bidirectional charging is defined. Figure 8-14 shows the influence of EFC restriction on bidirectional emission reductions.

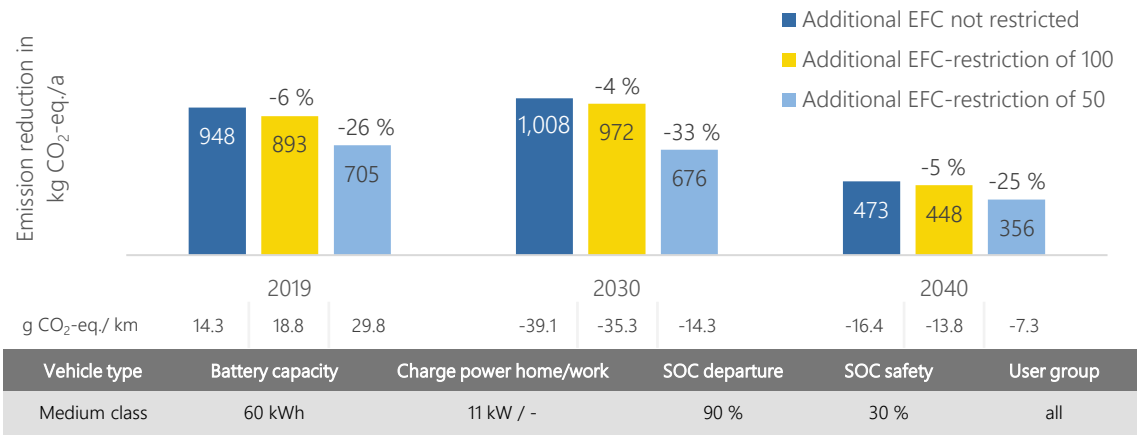

Figure 8-14: Influence of EFC restriction on bidirectional emission reductions

As expected, restricting the maximum number of EFCs limits flexibility and therefore diminishes possible emission reductions. In all considered years, a restriction of additional EFCs to 100 only affects emission reduction by 4 to 6 %, meaning that enough flexibility remains for the optimizer to significantly reduce emissions. Restricting the additional EFCs to 50 shows a more significant impact and limits the possible emission reduction by 25 to 33 % in the years considered.

8.2.4 Influence of user behavior

Besides technical parameters of the vehicle and the available charging infrastructure, the influence the behavior of vehicle users is also assessed. In addition to the obvious influence of the user's mobility behavior on arrival and departure times and energy consumption, two more charging parameters set by the user and a SOC-dependent plug-in probability are considered in this context. The influence of mobility behavior can be addressed by evaluating simulations for different user groups, as described in sections 6.2.4 and 6.2.5. Considering the two charging parameters, it is assumed that users are able to set a safety SOC and a target SOC via an app or a wall box interface that influences the charging behavior of the vehicle. The safety SOC defines a minimum allowed SOC during charging, and the target SOC defines a minimum value that must be reached at the scheduled departure time. The influence of both these parameters on a possible emission reduction for unidirectional and bidirectional charging is assessed in section 8.2.4.2. SOC-dependent plug-in behavior considers the fact that users might not connect the vehicle every time they reach a charging location but actually exhibit a plug-in behavior that depends on the SOC of the battery when arriving at a charging location.

8.2.4.1 User groups

First, the influence of user behavior with respect to the owner's behavior-homogeneous user group is assessed. Based on socioeconomic data derived from both mobility surveys, mobility profiles were subcategorized into 12 user groups considering information on occupation, use frequency of the vehicle, and children in the household. For the evaluation at hand, those 12 groups are summarized into four: full-time employed, unemployed, frequent driver, and nonfrequent driver. It should be noted that these definitions are not selective (e.g., a full-time employed user can be part of the frequent driver or nonfrequent driver group and vice versa). The resulting groups differ significantly in terms of annual mileage and the availability of vehicles at charging locations, as shown in Figure 8-15. For the evaluations, only charging at home is considered, and public charging (see section 7.3) is ignored, emphasizing the differences between groups.

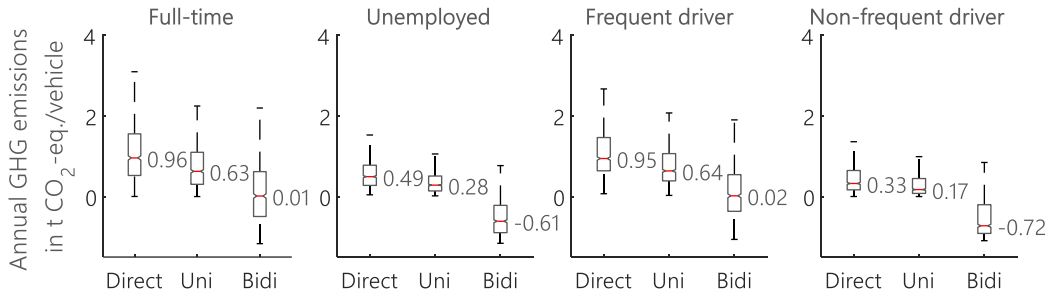

	Full-time			Unemployed			Frequent driver			Non-frequent driver		
Avg. availability	72.1 %			83.9 %			71 %			85.5 %		
Annual mileage „home" in km	12,530			6,653			12,790			5,413		
g CO_2-eq./ km	90.8	58.9	1.1	88.2	49.4	-88.5	89.6	59.5	1.4	89.4	48.4	-141.3

Simulation year	Vehicle type	Battery capacity	Charge power home / work	SOC departure	SOC safety
2019	Medium class	60 kWh	11 kW / -	90 %	30 %

Figure 8-15: Annual GHG emissions and key indicators for emission-optimized charging of four distinct user groups in 2019

Annual emissions in the direct charging case vary significantly due to the differences in annual mileage. Considering average emissions per km, however, only minor differences can be observed. The main difference among user group lies in the influence of optimized charging modes both for

the unidirectional and especially for the bidirectional case. Vehicles associated with the unemployed as well as the nonfrequent driver groups are parked much longer at charging locations and drive less. Hence, the optimization of charging strategies has more flexibility in choosing times with low emissions, reducing both annual and specific emissions per km. This correlation is most pronounced in the case of bidirectional charging, where both groups reach emission values below zero due to that effect. An EV mostly connected to the wall box basically acts as a storage unit and is able to fully use that flexibility, also represented by higher EFC values (+21 % full-time employed versus unemployed drivers, +11 % frequent versus nonfrequent drivers).

8.2.4.2 SOC departure and safety SOC

As mentioned above, another aspect of user behavior falls under the category of charging behavior. As described in section 7.5, the optimization of charging strategies provides the consideration of SOC limits, both target and safety SOC limits. The target SOC defines a minimum value that must at least be reached at scheduled departure. In the base case, that value is set to 70 % and represents an approximate range of 230 km (considering a battery capacity of 60 kWh). The safety SOC defines a lower limit during the charging operation that cannot be undercut. The idea is that owners can use the vehicle spontaneously at any time during the charging process and still have a certain battery capacity left for emergency trips. In the base case, this value is set to 30 %, allowing trips of about 100 km. Both SOC restrictions limit the available flexibility for optimized charging and are varied in the following ways to assess the influence on emission reduction potential. Figure 8-32 shows the resulting impairment of emission reductions for the years 2019, 2030, and 2040.

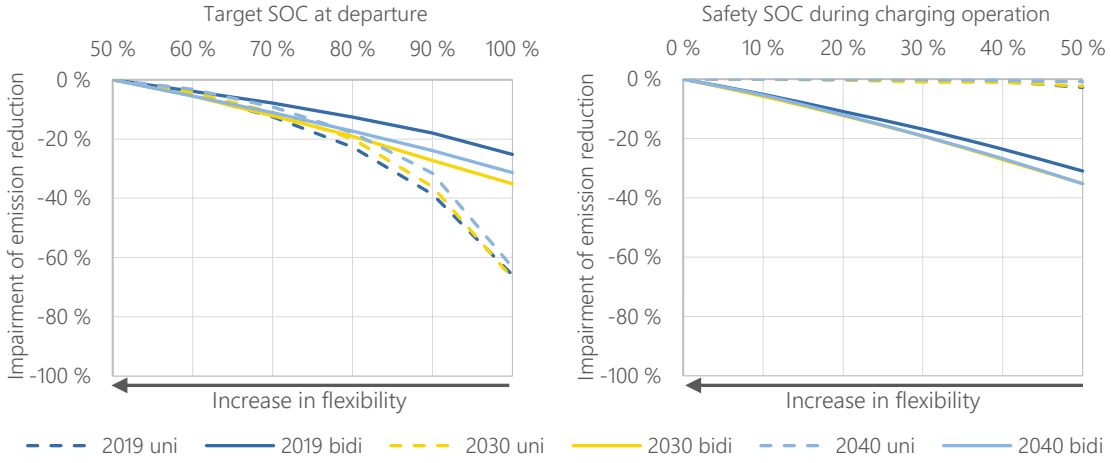

Vehicle type	Battery capacity	Charge power home/work	SOC departure	SOC safety	User group
Medium class	60 kWh	11 kW / -	50-100 %	0-50 %	all

Figure 8-16: Impairment of emission reduction potential due to target SOC (left) and safety SOC (right) in 2019, 2030, and 2040

First, the target SOC is gradually increased from 50 % to 100 %, consequently reducing available flexibility for the optimization, as shown on the left. The graph depicts the impairment of emission reductions compared to the minimal value of the target SOC of 50 %. In the considered range of values, the increase of the target SOC leads to an almost linear decrease in the possible emission reductions in the bidirectional case. Higher target SOC values limit the available time for optimized charging and therefore diminish emission reductions. In the unidirectional case, an increase of the target SOC results in an exponential decrease of possible emission reductions, even surpassing the ones in the bidirectional case. At a target SOC of 90 % or even 100 %, vehicles must charge almost

every time they are connected, while at lower values, they can skip charging for longer periods of time with high EMFs even if there are trips in between.

Moreover, in the case of unidirectional charging, only the absolute value of the EMFs determines the result of the optimization. Having to charge every time due to a high SOC departure value can therefore significantly increase overall emissions. In bidirectional charging, on the other hand, the spread of EMFs during charging and discharging is more decisive than the absolute level of EMFs. That means that an emission reduction can be achieved even when the absolute level of emission is high during the considered timeframe. Using spreads in EMFs works in times of both high and low EMFs, leaving only the reduced optimization timeframe as the decisive factor impairing the possible emission reduction.

In conclusion, EV users' decisions on the target SOC have a strong influence on the potential of optimized charging, especially for high target SOCs in the unidirectional case. Considering a target SOC value of 70 %, as defined in the base case of these simulations, only decreases the potential emission reduction by a maximum of 12 % and does not necessarily involve a loss of comfort. The same impairment can be demonstrated in the bidirectional case, which supports the choice of this value.

The mechanism of action in the case of the safety SOC is fundamentally different, however. Here, almost no influence on the resulting emissions can be seen with respect to unidirectional charging. Since, in the base case, EV users are assumed to connect their vehicle every time they reach a charging location, and they are charged regularly, SOC levels seldomly fall below the threshold defined by the safety SOC. Hence, little additional need for charging in unfavorable times arises by increasing that parameter. In the bidirectional case, setting this lower threshold basically reduces the usable capacity and thus the flexibility for optimization in a similar way as the target SOC. An almost linear coherence between the assumed safety SOC and the resulting impairment of emission reductions can be observed.

Consequently, from a user's perspective, setting a safety SOC in the unidirectional case does not influence the emission reduction at all. In the bidirectional case, a linear reduction can be observed, and the selected value depends on the user's sensitivity toward safety and a possible revenue/emission reduction potential.

8.2.4.3 SOC-dependent plug-in behavior

As the last parameter in the category of user behavior, the plug-in behavior of users is considered. In the base case of the simulations, it is assumed that users are incentivized and therefore connect their vehicles every time they reach a charging location to maximize the connection time and therefore revenues/emission reductions. As a sensitivity, SOC-dependent plug-in behavior is considered. As described in section 0, "normal," unincentivized charging behavior depends on the state of charge of the battery when the vehicle reaches a charging location. For the sensitivity analysis at hand, the charging probability is estimated by an inverse cumulative distribution, depending solely on the SOC of the battery at arrival, as described in section 0 and shown in Figure 8-17 on the left. The resulting impairment of possible emission reductions is shown on the right.

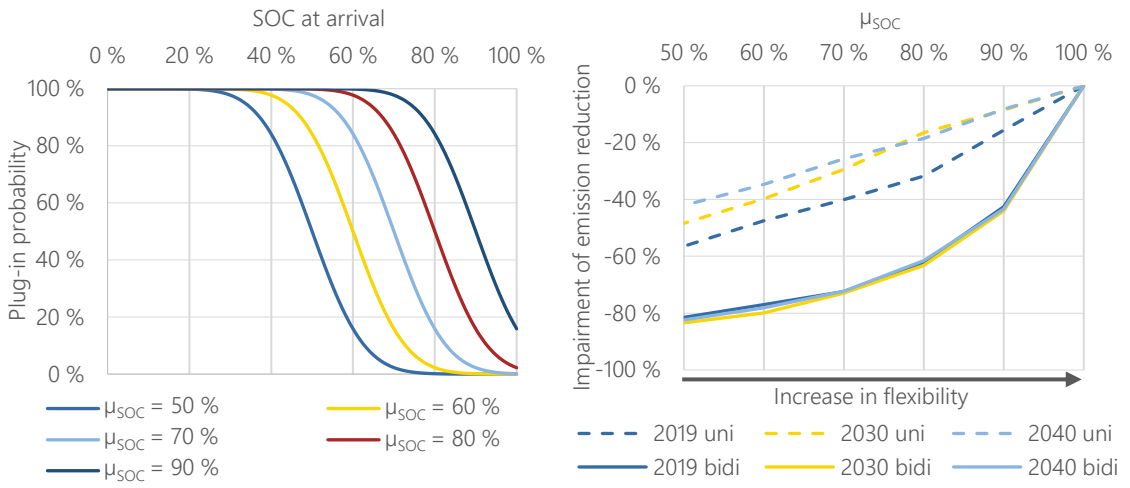

Vehicle type	Battery capacity	Charge power home/work	SOC departure	SOC safety	User group
Medium class	60 kWh	11 kW / -	70 %	30 %	all

Figure 8-17: Impairment of emission reduction potential due to SOC-dependent user plug-in behavior in 2019, 2030, and 2040

When a SOC-dependent charging behavior is assumed, coherences change fundamentally. The first and most obvious effect is that vehicles are connected less frequently, consequently reducing the timeframe for optimized charging. Users always connecting their vehicles whenever they reach a charging location leads to an average availability of 77 %. This value is reduced dramatically to 13.8 % in the most extreme case of a μ_{SOC} of 50 %. This explains, at least to some extent, the large impairment of potential emission reductions in the bidirectional case and follows the same mechanism of action as most of the other sensitivities assessed in this section that reduce the available timeframe for optimized charging. Less time at the charging station means less flexibility, which means higher impairment.

Another critical factor that comes into play here is the fact that the amount of energy that must be charged increases if the vehicles are not plugged in every time, they reach a charging station. When they do connect, more energy must be charged, and the remaining flexibility for optimized charging is much lower. For example, with unidirectional charging in 2019, the average SOC on arrival was 70.6 %, assuming "always connecting". In the most extreme case at a μ_{SOC} of 50 %, this SOC is reduced to only 28 %. That means that 2.5 times more electricity must be charged in that timeframe, significantly reducing the options for optimized charging.

Those two effects add up to a major impairment of emission reductions, especially in the bidirectional case. Even in the most SOC-sensitive case with a μ_{SOC} value of 90 %, emission reduction potential in the bidirectional case is decreased by 41 %. After that significant reduction for μ_{SOC} = 90 %, a further decrease of plug-in probability shows an almost perfect exponential decay.

For unidirectional charging, a more or less linear relationship between μ_{SOC} and the resulting impairment can be observed, with a steeper slope in 2019. The stronger effect in that year can be explained by the underlying energy system. Comparably low shares of RES in combination with large capacities of still-operational, emission-intensive coal-fired power plants define the overall structure of electricity generation and result in distinct patterns of EMFs. Windy and sunny phases lead to longer periods with low EMFs. When wind and solar yield is low, on the other hand, most of the electricity is still produced by coal-fired power plants, leading to longer phases of high EMFs. In future years, coal phaseout is (almost) completed, resulting in a lower spread between EMFs in times of high and low wind and solar yield (see section 4.6.4). Especially in the unidirectional case, if the

vehicle is not connected every time, the demand for charging larger amounts of electricity at inconvenient times increases, hence the greater impairment.

Consequently, plug-in behavior has one of the strongest effects on the potential of optimized charging strategies. To maximize emission reductions or revenue potentials, users should therefore be incentivized to plug in their vehicles as often as possible. Especially in the case of bidirectional charging, not connecting the vehicle every time drastically undermines the efficiency of the charging strategy.

8.2.5 Influence of the energy system

Since operational emissions directly depend on the electricity used for charging the vehicles, the underlying energy system must be considered one of the main influencing factors. Analysis conducted for future years in the German energy system support this assumption. To further assess these coherences, additional simulations were undertaken for a fleet of vehicles in 15 European countries, respecting their unique generation portfolio (section 8.2.5.1). Furthermore, simulations have shown that unrestricted, optimized charging leads to high simultaneities in charging processes. Assuming an increasing number of EVs in the system, these correlations might pose a challenge, especially considering the load in the distribution grid. To minimize grid load, the maximum simultaneity of charging processes can be restricted. The influence of such a restriction on possible emission reductions is assessed in section 8.2.5.2.

8.2.5.1 Underlying energy system

Increasing shares of RES in German electricity production in future years significantly influence both emissions of EVs in uncontrolled, direct charging operations as well as the potential of uni- and especially bidirectional charging in the case of an optimized charging operation.

However, electricity generation in European countries varies widely. For example, Polish electricity generation is dominated by coal-fired power plants, while 70.6 % of French electricity production in 2019 was provided by nuclear power plants [38]. From the sensitives discussed in this chapter, it is clear that both the overall emission intensity of the electricity generation and the statistical distribution of EMFs during the charging operation have an influence on resulting operational emissions and the emission reduction potential. In section 4.6.3, hourly EMFs were calculated and presented for 15 European countries. To assess the influence of the underlying energy system on operational emissions and the potential of charging strategies, the base case simulation was applied for all these countries. It must be noted that country-specific mobility behavior was not considered in this case. First, no coherent survey data are available for all these countries to synthesize corresponding annual mobility profiles. Furthermore, by using the same mobility profiles for all countries, we can isolate the influence of the underlying EMFs and compare the results across countries. The only difference in simulation parameters lies in the consideration of country-specific temperature curves. Figure 8-18 shows the resulting specific emission per km per country for uncontrolled charging in 2019 and compares these values with the emissions resulting from bidirectionally optimized charging. Values on the abscissa show the share of renewable energies on the total electricity generation in each country.

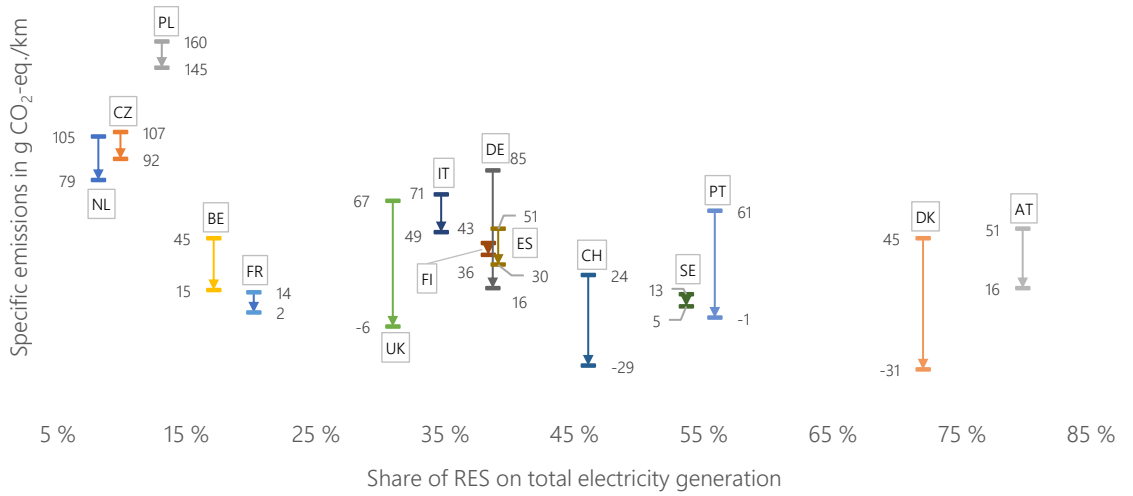

Figure 8-18: Specific emissions for direct (upper value) and bidirectional (lower value) charging in 15 European countries in 2019

To begin, some correlation between specific emissions resulting from uncontrolled charging and the share of RES can be observed. The higher the share of RES on total electricity production, the lower the resulting EV emissions. Exceptions do exist, however. France, for example, shows the second lowest value of operational specific emissions but only has a share of RES of 20 %. Non-RES generators in France are mainly nuclear with low GHG emissions; therefore, overall EV emissions are low as well.

Besides these operational emissions of EVs resulting from uncontrolled charging, the effect of bidirectional charging varies widely as well among countries. France, for example, has a very low reduction potential, whereas countries like the United Kingdom, Germany, Switzerland, Portugal, and Denmark show a very high potential. Shares of RES, however, do not sufficiently explain these results, ranging from 31 % in the case of the United Kingdom to 72 % in Denmark (r_p=0.293). To further analyze these coherences, absolute and relative emission reductions from bidirectional charging were compared to the share of volatile renewable energies (vRES) and the standard deviation of the hourly EMFs in each country, as presented in Figure 8-19.

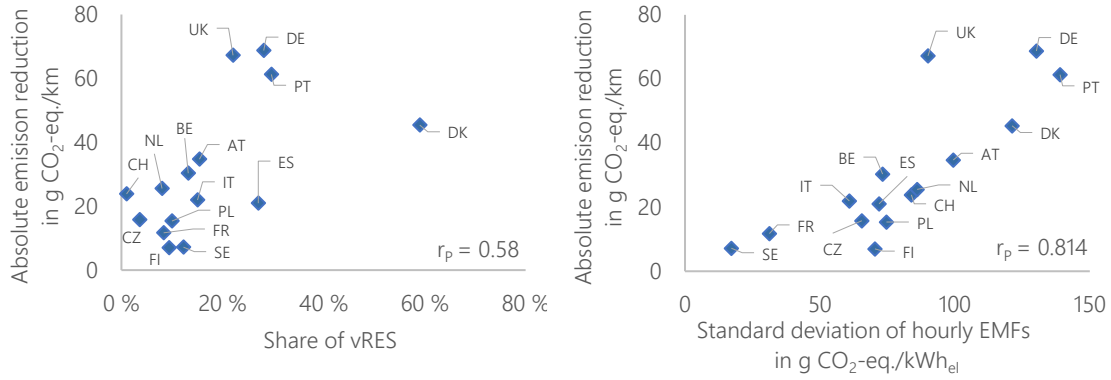

Figure 8-19: Correlation between absolute emission reductions and standard deviation of EMFs and between relative emission reduction and coefficient of variation

Both variables are better suited to explain the differences in absolute emission reduction potentials from bidirectional charging, shown in Figure 8-18. The higher the share of vRES on total emission reduction, the higher the potential of bidirectional charging is. Each of the energy systems under consideration has its own individual structure, some leaning more to fossil generators powered by

gas (such as Belgium) and others relying more on coal (Poland, Czech Republic) or nuclear generators (France) or having their own unique mix. All these factors play an important role when assessing the reduction potential of charging strategies.

When assessing emissions, these coherences can best be represented by calculating hourly EMFs. The higher their statistical distribution, the more spreads between these values can be used by the optimization to reduce overall emissions and the higher the potential, especially in direct charging. This coherence can be observed when considering the correlation between the standard deviation of EMFs and the potential emission reductions for bidirectional charging, as shown on the right in Figure 8-19.

8.2.5.2 Consideration of grid restrictions

As discussed in this chapter, unrestricted, optimized charging leads to high simultaneities in charging processes. Assuming an increasing number of EVs in the system, these simultaneities might pose a challenge, especially considering the load in the distribution grid. Nobis [92], for instance, conducted distribution grid simulations in selected grid areas to assess the influence that increasing numbers of EVs have on voltage quality. In case of uncontrolled charging, voltage quality decreased at an EV penetration of 40 %. However, charging simultaneity increases by a factor of 8-9 when comparing uncontrolled to optimized charging. It can therefore be assumed that unrestricted, optimized charging poses a much bigger challenge for grid stability. To fully assess the resulting load on the distribution network, simulations would need to be performed using an appropriate distribution network model. Such simulations can be performed with the FfE model GridSim; they are, however, not the focus of this thesis.

To still address these coherences properly and to minimize grid load, the maximum simultaneity of charging processes can be restricted in the eFLAME model. As described in section 7.1, the model iterates through all considered vehicles and performs the optimization individually for each one. After each iteration, charge decisions can be used to restrict the optimization space for the following vehicles. In the case of grid restrictions, a maximum charge simultaneity can be selected. When this maximum value is reached, the following vehicles are prevented from charging during these times. Overall, this leads to a smoothing of the resulting grid load and prevents load peaks. In the unrestricted case, all vehicles maximize their emission reduction by charging in times of low EMFs and discharging in times of high EMFs. Restricting the maximum simultaneity of the fleet also restricts the total reduction potential, as shown in Figure 8-20.

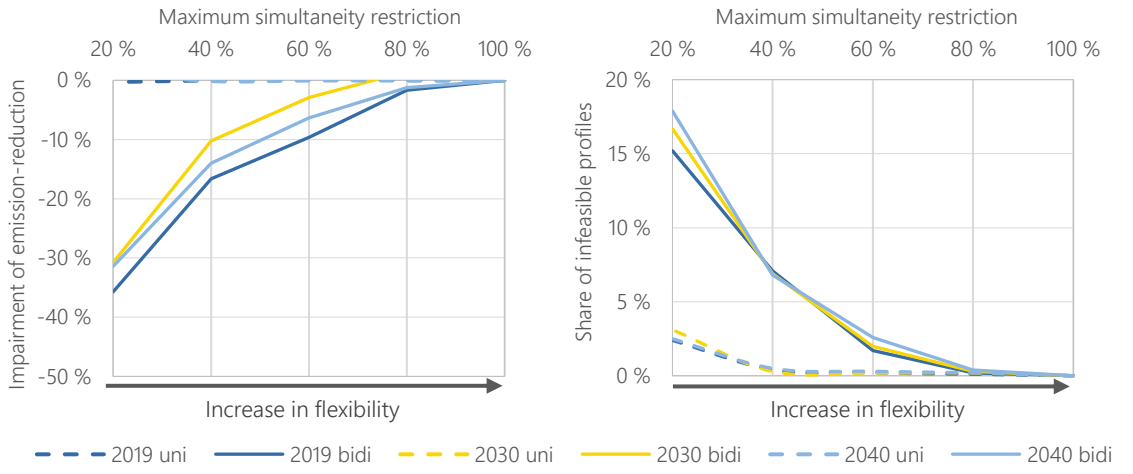

Vehicle type	Battery capacity	Charge power home/work	SOC departure	SOC safety	User group
Medium class	60 kWh	11 kW / -	70 %	30 %	all

Figure 8-20: Impairment of emission-reduction potential due to restrictions on maximum simultaneity in 2019, 2030, and 2040

Simulations show only negligible impairment in the unidirectional case. Since only small amounts of electricity are charged in the unidirectional mode, restricting simultaneity still leaves enough times with low EMFs. In the bidirectional case, much more electricity is charged and discharged. In that scenario, a restriction of the maximum simultaneity results in an exponential impairment of possible emission reductions, reaching up to 35 % when a maximum charging simultaneity of 20 % is considered. With regard to the additional load EVs pose, especially on the distribution grid level, such restrictions will most likely be adapted in the future regulatory framework. In a future energy system with large numbers of EVs, those restrictions must be considered. As [15] has shown, grid-serving charging of EVs can even relieve the load on the corresponding operating resources and reduce overall system costs. The intelligent combination of grid-serving and simultaneously cost- and emission-optimized charging should therefore be the subject of further research.

Figure 8-20 further shows the number of failed simulations, cases when constraints of the optimization problem lead to a mathematical infeasibility. At this point, the disadvantage of an iterative optimization looping over vehicles becomes apparent; the implementation iteratively sets charging constraints for the following vehicles, respecting the selected maximum charging simultaneity. Especially for low values of maximum simultaneity, this limits the periods where following vehicles are allowed to charge, resulting in infeasible problem definitions. The only way to solve this problem would be to consider an optimization of all vehicles at the same time. Due to computational limitations, however, this approach was not considered in the context of this thesis.

8.2.6 Summary of sensitivity analysis

As discussed in the beginning of this chapter, sensitivities were analyzed OFAT starting from the described base configuration of parameters. For all the parameters under consideration, the effect of their variation was assessed with respect to the influence on the potential emission reduction for unidirectional and bidirectional charging. Detailed interpretations of the corresponding correlations and the mechanisms of action are described in the corresponding section. It can generally be stated that limiting flexibility in any way results in a more or less linear reduction of potential emission reductions. In some cases, however, additional effects must be considered as well, increasing the influence of individual parameters. To present a compact overview of the magnitude of the influence for all parameters considered, they are summarized below. To assess all parameters together, the

variation of each one is compared to the resulting relative deviation of emission reductions from the base configuration. It is assumed that the results of this sensitivity analyses are valid for other use cases as well since the mechanisms of action are similar.

Figure 8-21 presents the results for both the unidirectional and bidirectional case in 2019. Coherences for 2030 and 2040 are considered similar, and deviations from that are explained in the corresponding section. Figure 12-6 in the appendix presents the same results for those future years. It must be noted that categorical parameters like the battery capacity and available charging power, where only these categories exist, are mixed here with numerical variables such as the assumed safety or departure SOC and the maximum charging simultaneity.

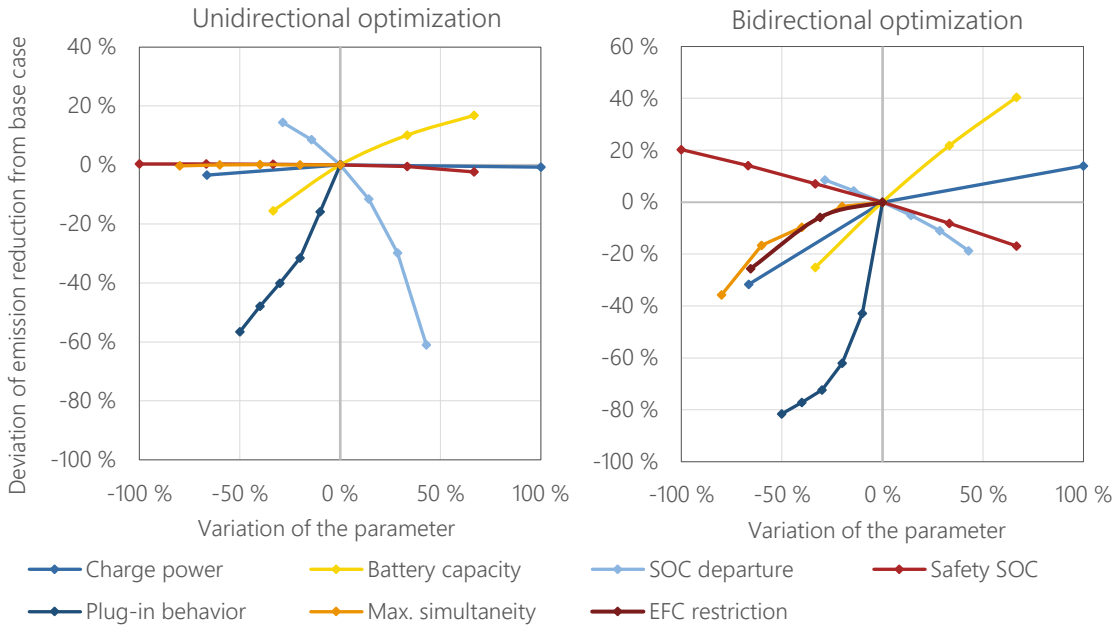

Figure 8-21: Overview of the considered sensitivities and the influence on annual emissions

In the unidirectional case, only three of the parameters have a significant influence on the resulting emission reduction, two of which are categorized as user behavioral parameters. High departure SOC set by the vehicle user forces the optimizer to charge almost every time the vehicle is connected. When no such restriction is set, vehicles can refrain from charging over longer periods of time even when trips are taken in between, allowing a more significant emission reduction. Similar coherences apply to the assumed plug-in behavior of vehicle users. The less often that users plug in the vehicle, the more energy must be charged during each of the remaining charging operations and the less flexibility remains for shifting of charge processes.

In conclusion, the most dominant influencing factors on the efficiency of unidirectional charging operation both depend on user behavior. To maximize efficiency, users should be incentivized to connect the vehicles as often as possible and consider setting the SOC departure as low as they are comfortable with.

In comparison to the potential of unidirectional charging, the effect of available flexibility in bidirectional charging is higher. In the first case, only small amounts of electricity must be charged in mostly longer periods of time. Often, only short trips are taken during the day; the vehicle arrives in the early afternoon and is connected during the night. Choosing the hours of low EMFs in unidirectional charging leads to an emission reduction. However, if that whole period can be used for the bidirectional charging operation, much higher emission reductions can be achieved.

On the other hand, if that time is restricted due to the various technical and behavioral parameters discussed in this chapter, the resulting relative impairment of the emission reduction from bidirectional charging is correspondingly higher as well. For that reason, a variation of battery capacities shows a much higher impact, represented by a larger slope of the yellow curve on the right. The amount of energy that can be charged and discharged in a fixed period of time, and therefore the usable flexibility, depends on the length of the time period and the power of the charging infrastructure. Therefore, compared to unidirectional charging, assumed charging power values also show a significant influence on potential emission reductions.

The influence of the selected departure SOC, in contrast, only shows a minor influence compared to the impairment in the unidirectional case. Further explanations on the underlying mechanisms of action are presented in section 8.2.4.2. Since the safety SOC, selected by the user, directly reduces the available battery capacity for the optimization, we see a linear correlation between that value and the resulting impairment on potential emission reductions. Restrictions on the maximum simultaneity negatively influence the potential emission reductions. However, it is a parameter defined by technical grid restrictions and will also be fixed in regulatory terms by the Federal Network Agency in the future. Again, as well as in the case of unidirectional charging, the most dominant factor is the plug-in behavior of the vehicle's users. Due to the discussed mechanisms of action, not connecting the vehicle as often as possible drastically impairs revenue or emission reduction potential.

As stated above, all these mechanisms of action and correlations do not depend on the optimization target but can be applied to all the other use cases universally. For this reason, no further sensitivity analyses are performed for the other use cases.

8.3 Use case 2: Cost reduction

For the second use case under consideration, the reduction of charging costs is the main focus. As discussed in section 7.6.2, the main assumption is that taxes and levies are only applied on electric consumption of the vehicle. The amount of electricity charged and discharged during the bidirectional operation is assumed to be free of taxes and levies since such charging strategies are to be considered beneficiary for the overall energy system. Kern et al. [9] have discussed in detail the influence of additional charges on electricity on the revenue potential of EVs and concluded that those charges are the "most decisive parameter for the potential revenues of bidirectionally chargeable EVs" (p. 23). Not considering taxes and levies for charged and discharged electricity in the bidirectional operation therefore must be considered a maximum estimation. Following the logic for economic assessment described in section 7.6.2, resulting annual costs are presented in Figure 8-22.

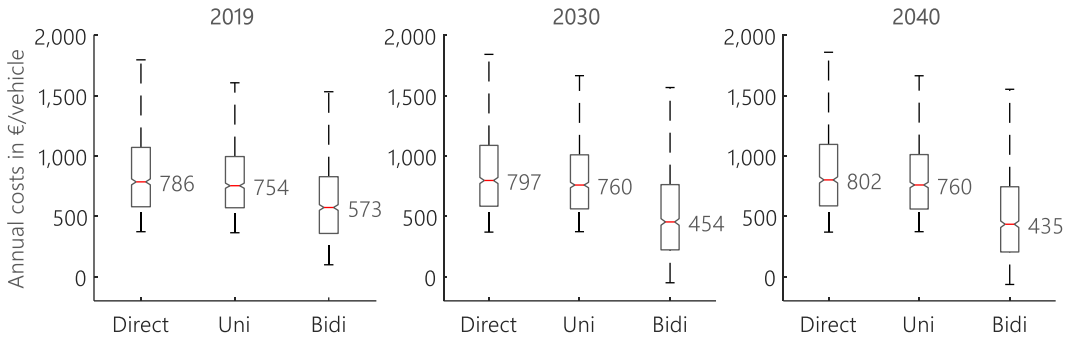

	2019			2030			2040		
	Direct	Uni	Bidi	Direct	Uni	Bidi	Direct	Uni	Bidi
EFC	39.5	39.5	308.4	39.5	39.5	277.6	39.5	39.5	219.6
Charge simultaneity	9 %	88.8 %	93.6 %	10.4 %	90.9 %	94.5 %	10.4 %	90.8 %	94.5 %

Vehicle type	Battery capacity	Charge power home / work	SOC departure	SOC safety	User group
Medium class	60 kWh	11 kW / -	90 %	30 %	all

Figure 8-22: Annual costs and key indicators for price-optimized charging for base configuration in 2019, 2030, and 2040

Due to increasing electricity prices over the course of the analyzed years, costs for direct charging slightly increase. However, the restructuring of the power sector leads to significant changes in the characteristics of the prices. Increasing RES shares lead to larger periods of low prices, while the phaseout of cheap coal and nuclear power plants and the increased need for flexibility result in higher peak prices. This price spread can be used both in unidirectional and bidirectional charging, resulting in an increasing cost reduction in 2030 and 2040. Since price spreads are the main driver for the potential of bidirectional charging, that cost reduction potential is especially pronounced in those years, leading to a reduction in annual costs by 43 % in 2030 and 45.8 % in 2040. The effects on resulting EFC values and charge simultaneity of the fleet are the same as those described for the use case emission reduction, both increasing substantially.

Emission assessment of price-optimized charging

The cost-optimized charging behavior is then assessed with respect to the resulting emissions. In Figure 8-23, the annual cost reductions for unidirectional and bidirectional charging are compared to the resulting emission reduction (or increase).

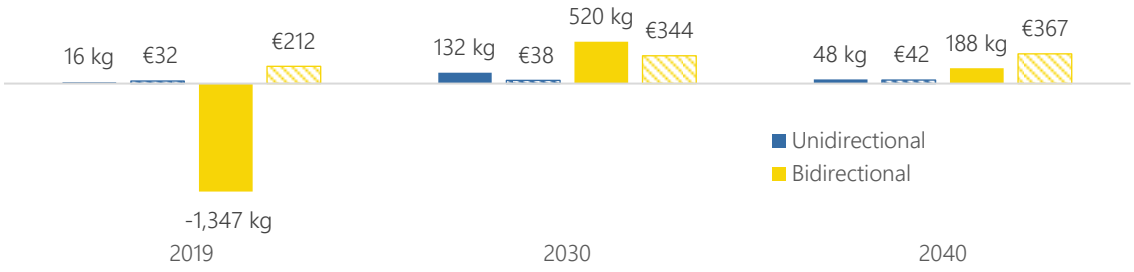

Figure 8-23: Median annual revenues and emission reduction potential in kg CO_2-eq. of price-optimized charging for base configuration in 2019, 2030, and 2040

As described in section 4.6.4, the correlation between EMFs and wholesale prices changes over the course of the selected years. In 2019, the merit order dilemma of emissions, (see section 4.5) still prevails. Cheap but emission-intensive lignite and hard coal-fired power plants continue to dominate the generation of electricity to a large extent, resulting in hours of low prices but high EMFs. Charging in those times of low prices therefore increases operational emissions. This coherence is resolved

with the phaseout of those power plants, resulting in an improved correlation between electricity prices and EMFs. The described relationships have a significant impact on the resulting emission reduction potential and revenues of EVs. In 2019, an annual cost reduction of €212 results in quite extreme additional emissions of 1,347 kg CO_2-eq. In contrast, in 2030 and 2040, potential revenues of €344 and €367, respectively, also lead to a reduction of emissions by 520 and 188 kg per year, respectively. The same is not true, however, in the unidirectional case. Here, an annual cost reduction of €32 in 2019 is also accompanied by an emission reduction of 16 kg. Most charging processes are simply shifted from the afternoon to early morning hours. In those specific cases low load values are often accompanied by low EMFs. In contrast to that bidirectional charging leads to a steady charging and discharging amplifying the effect of the merit order dilemma and resulting in additional emissions. Those correlations must be considered when implementing a price-optimized charging strategy, especially in current years.

8.4 Use case 3: Smoothing of residual load

As discussed in section 4.6.4, consumption-based EMFs only represent the share of RES in the system to a certain extent. Especially in future years, when periods of time with negative residual load increase, considering the residual load as an optimization target provides a better representation of the share of RES on total electricity production. Therefore, the smoothing of residual load is considered as a third charging strategy by shifting charging operations to times of negative residual loads and discharging operations to times of high residual loads. Even though such a strategy might not lead to the same emission reduction for individual vehicles, benefits for the overall energy system are high. To assess the actual feedback effect of such charging behavior on the energy system, an iterative run of the energy system model ISAaR was performed and is presented in section 8.4.2.

The corresponding charging strategy was first implemented and simulated in the eFLAME model for the base configuration and the years 2019, 2030, and 2040. Resulting emissions are then assessed by the associated time series of consumption-based EMFs and presented in Figure 8-24.

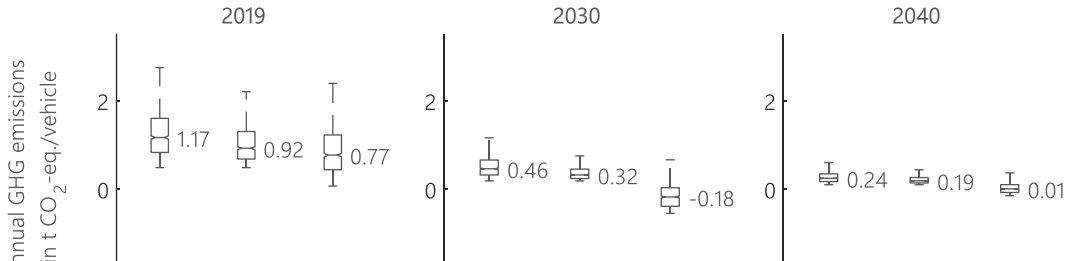

	2019 Direct	2019 Uni	2019 Bidi	2030 Direct	2030 Uni	2030 Bidi	2040 Direct	2040 Uni	2040 Bidi
g CO_2-eq./ km	84.9	69.7	54.7	33.9	24.9	- 12.6	18.1	14.3	0.3
EFC	39.5	39.5	286	39.5	39.5	255	39.5	39.5	252

Vehicle type	Battery capacity	Charge power home / work	SOC departure	SOC safety	User group
Medium class	60 kWh	11 kW / -	90 %	30 %	all

Figure 8-24: Annual GHG emissions and key indicators for residual-load-optimized charging for base configuration in 2019, 2030, and 2040

Since consumption-based EMFs have a high correlation with the residual load (see section 4.6.4.4), the resulting annual emissions are expected to be quite similar. Comparing results for emission-optimized charging in Figure 8-4 with those at hand supports that assumption. Using EMFs as an

optimization target leads to slightly better results from the perspective of the vehicles, but overall quality and assertions prove to be comparable. It must be noted, though, that those results consider the base configuration with unrestricted charging of vehicles. Furthermore, no dynamic system feedback can be evaluated since simulations are based on but independent from the energy system model. To address that shortcoming and assess the actual system feedback on the energy system of such optimized charging, resulting loads from charging and discharging are used for an iterative simulation run of the energy system model. Findings are discussed in section 8.4.2.

8.4.1 Revenue assessment of residual-load-optimized charging

Finally, the resulting charge operations in the use case of smoothing of residual load are assessed with respect to potential revenues for vehicle users. This potential is evaluated for unidirectional and bidirectional charging and compared to the resulting emission reductions. Figure 8-25 shows this comparison for all three years under consideration.

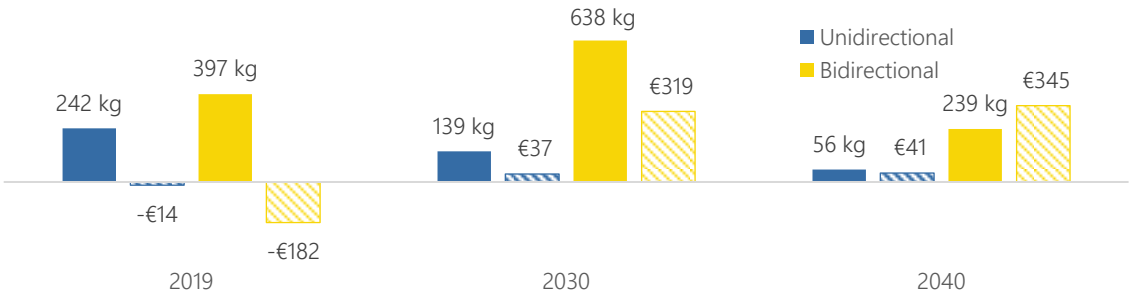

Figure 8-25: Median annual revenues and emission reduction potential in kg CO_2-eq. of residual-load-optimized charging for base configuration in 2019, 2030, and 2040

In 2019, the same correlation can be demonstrated that was already present in emission-optimized charging. Due to the merit order dilemma of emissions (see section 4.5), a reduction in emissions (242 kg CO_2-eq. in the case of unidirectional, 397 kg CO_2-eq. in the case of bidirectional charging) leads to negative revenues (-€14 in unidirectional and -€182 in bidirectional charging). That is also true for an optimization aiming at a smoothing of residual load. Due to cheap and emission-intensive lignite power plants still in operation, periods of low residual loads (and low emissions) do not necessarily coincide with low wholesale prices, resulting in a decrease in revenues. This relationship dissipates in the future years of 2030 and 2040. Similar to emission-optimized charging, residual-load-optimized charging here leads to both emission reduction and positive revenues.

8.4.2 Assessment of system feedback

Especially with increasing numbers of EVs, the feedback effects that charging strategies have on the energy system must be considered. To address this topic, an iterative analysis is conducted with the energy system model ISAaR. Due to the large computational effort of a simulation run with the energy system model, this evaluation is only considered for one of the use cases in this thesis. Since the residual load best represents the share of RES in the system, the related charging strategy of smoothing of residual load is determined most beneficial for the integration of those volatile generators. Therefore, the resulting load curves for the number of EVs expected in each year are used for three distinct simulations runs for the future years of 2030 and 2040. With regard to the assumptions about the future development of the energy system, the same basic scenario was used that underlies all other evaluations in this thesis (see section 3.3).

As discussed in the course of this chapter, the unrestricted optimization of the entire fleet of vehicles with base configuration of simulation parameters results in high charging simultaneities, which lead to a significant additional load on the grid infrastructure, especially at the distribution grid level. To limit this load, a restriction of 50 % charging simultaneity is considered for the simulation run (see section 8.2.5.2). All other simulation parameters correspond to the base configuration. Figure 8-26 illustrates the influence of a unidirectionally and bidirectionally optimized fleet on the residual load over the course of an average day in 2030. Again, 2.69 million EVs are considered for this assessment.

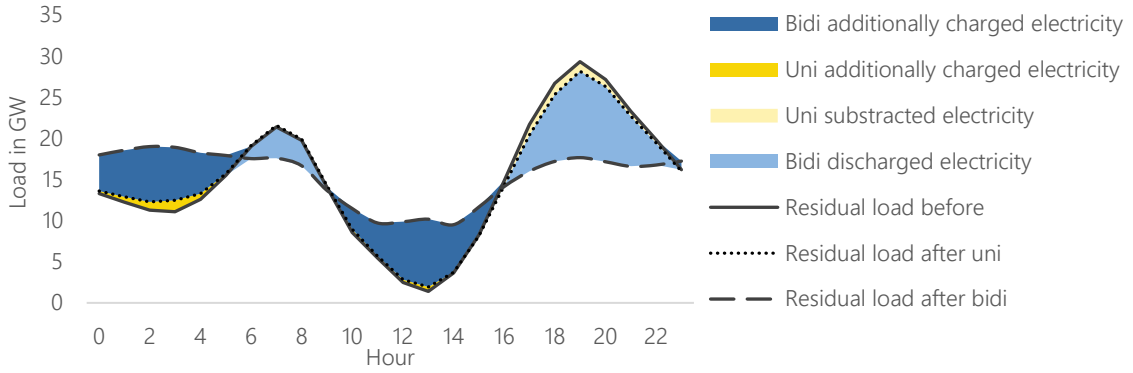

Figure 8-26: Average residual load before and after consideration of a unidirectionally and bidirectionally charged fleet of EVs in 2030 (max simultaneity = 50 %)

The shifting of charge processes in the unidirectional operation from periods with high residual load values to those with lower values leads to a slightly smoother course of the curve. Bidirectional charging, however, increases that effect significantly. As discussed throughout this chapter, bidirectional charging (as well as unidirectional charging) not only leads to higher values of charging simultaneity but also increases the total electricity demand of vehicles due to losses in the charging and discharging process. Considering a fleet of 2.69 million EVs in 2030 or 4.7 million in 2040, the effect on overall electricity demand can be considered significant, as illustrated in Table 8-3.

Table 8-3: Charged and discharged energy, losses, and resulting net electricity demand in 2030 and 2040 for residual-load-optimized charging

		Direct charging/ unidirectional optimization	Bidirectional optimization	Unit
EV level	Charged energy	2,652	13,755	kWh
	Losses charging	119.7	1016.4	kWh
	Discharged energy	-	9,499	kWh
	Losses discharging	-	812.6	kWh
System level	Net electricity demand @2.69 million EVs (2030)	7.13	11.45	TWh
	Net electricity demand @5.7 million EVs (2040)	15.12	24.26	TWh

Where losses might seem relatively small on the EV level, they add up to an additional electricity demand of 4.31 TWh in 2030 and 9.14 TWh in 2040 when the whole fleet is considered. This increased demand must be met by an expansion of new electricity generators or an increase of conventional production. In the following section, the system feedback of a fleet with uni- and bidirectionally optimized EVs is compared to a reference case where only direct charging is considered.

8.4.2.1 Effect on electricity generation

Regarding the electricity sector, feedback effects can be divided into two categories: the expansion of generators, represented by the installed capacities, and the actual dispatch of those generators as well as storage units. Generally, energy system models like ISAaR aim at the reduction of overall system costs. Therefore, especially with regard to the resulting (negative or positive) expansion of renewable generators, the underlying cost assumptions are vital for the interpretation of results. ISAaR considers four types of renewable generators that can be used for the provision of renewable electricity: wind on- and offshore as well as offsite and rooftop solar generators. Based on capital expenditures (CAPEX) and operational expenditures (OPEX) data summarized in [156], levelized costs of electricity (LCOE) are derived for all four, as presented in Table 8-4.

Table 8-4: Assumed LCOE for vRES generators

	Wind onshore	Wind offshore	Offsite solar	Rooftop solar
LCOE in €/MWh	33	35	23	59

To minimize system costs, generators will be expanded and dispatched according to these underlying costs as well as with regard to their individual temporal generation characteristics. The better this characteristic matches the time characteristic of the electrical load, the more efficient the operation of the overall system (less storage required, less curtailment). These relationships must be taken into account when interpreting the following results. Findings are discussed based on the simulation results for 2030. Results for 2040 can be found in the appendix in Figure 12-7.

Unidirectional optimization

First, the influence of a unidirectionally optimized charging of vehicles is discussed. Unidirectional charging operations do not result in additional electricity demand but simply shift charging operations to times with lower residual load values. As illustrated in Figure 8-26, this charging strategy reduces the electric load in the evening hours and shifts charging to the early-morning hours and, although less pronounced, to the midday hours. To assess the influence on the energy system, the differences of expansion and dispatch of generators as well as the use of storage units between the direct charging simulation run and the unidirectional charging simulation run are evaluated, as illustrated in Figure 8-27.

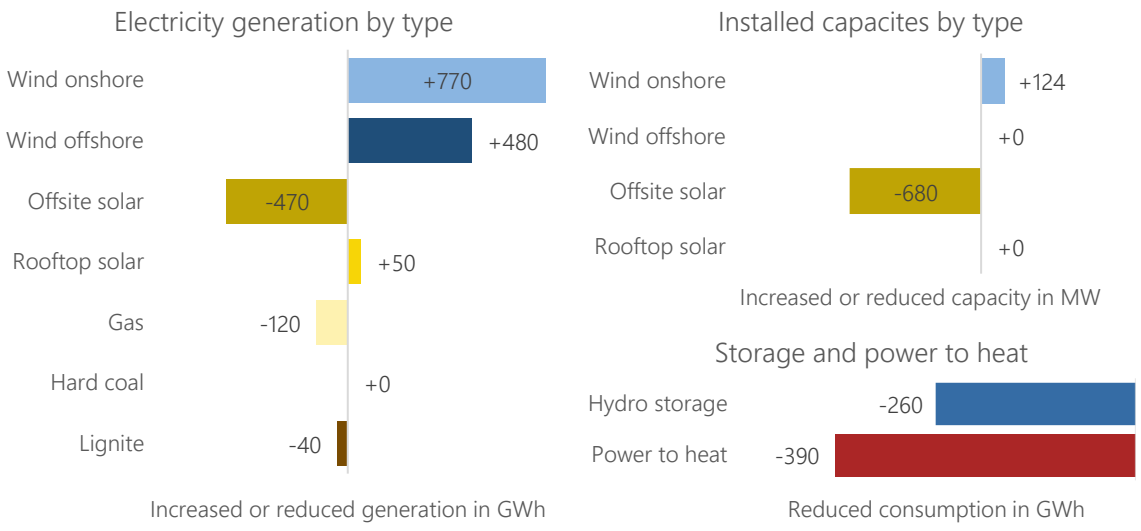

Figure 8-27: Influence of unidirectional charging operation on the electricity sector in 2030

To begin, due to the rather small number of EVs considered in 2030, the impact on the electricity sector is minimal. In relation to total electricity generation (or consumption), the deviations shown above are in the low single-digit percentage range. For example, the maximum relative change is only 1.7 % in the case of reduced consumption of the water reservoirs. The increase of 770 GWh of wind onshore generation only amounts to 0.4 % in relative terms. However, the basic relationships and system effects can be demonstrated even at these small values. Starting with the influence on electricity generation, the shift from periods of high residual loads to periods of lower values leads to a decrease of fossil electricity production as well as offsite solar power. In the case of conventional generators, installed capacities do not change, but the generation from existing ones is reduced. In the case of offsite solar, however, coherences are not as apparent. Shifting charging processes to early-morning hours creates an additional electricity demand that is mainly provided by an expansion of wind onshore turbines since no solar generation is possible during that period. The resulting additional electricity generation from wind turbines reduces the need for solar generators during the day. Corresponding capacities are expanded less and thus also reduce the total generation from solar plants.

The most expansive vRES types, wind offshore and rooftop solar, are not expanded at all, but the shifting of charging processes reduces the market-related downregulation (periods where vRES infeed cannot be fully used) of those generators and therefore increases overall production. The targeted smoothing of the residual load also leads to a reduction of electricity stored in hydro storage plants and used for power to heat applications. As flexible consumers, both usually follow a price-dependent charging/consumption behavior. The more loads are shifted to periods of low residual loads (usually accompanied by low prices), the less often those units are needed to store or use electricity.

Bidirectional optimization

In the next step, the influence of a bidirectional optimization is assessed. As mentioned, and in contrast to unidirectional charging, bidirectional charging increases overall electricity demand of the EV fleet due to charging and discharging losses (+4.31 TWh in 2030 and +9.14 TWh in 2040). Furthermore, as illustrated in Table 8-3 and Figure 8-26, the amount of energy displaced is much higher in bidirectional charging, leading to a more significant reduction of residual loads. Similarly, the system feedback effects are more pronounced, as presented in Figure 8-28.

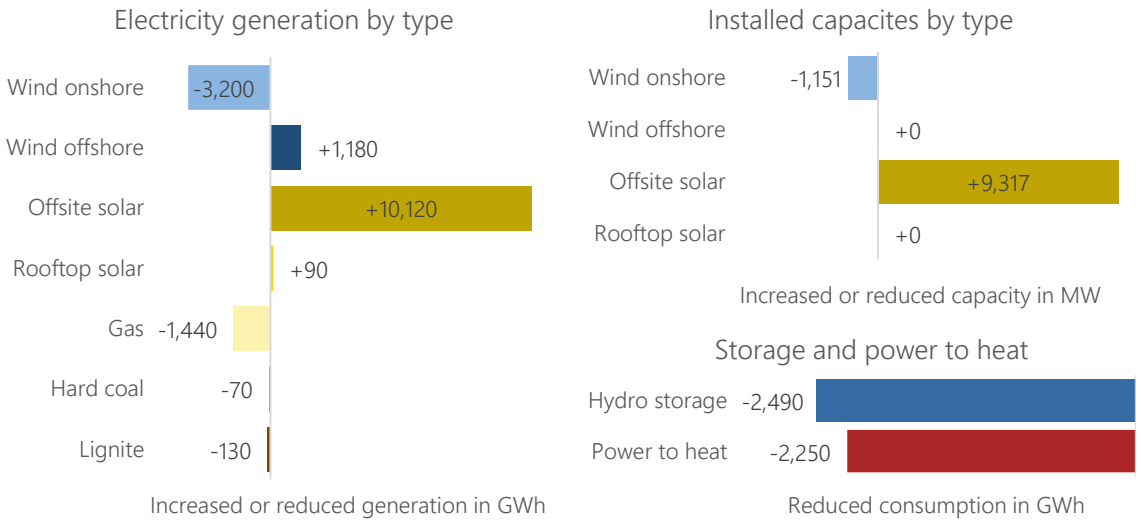

Figure 8-28: Influence of bidirectional charging operation on the electricity sector in 2030

Where relative changes in the case of unidirectional were in the low single-digit percentage range, bidirectional charging has a much greater influence. One of the most pronounced effects is the increase of offsite solar generation by 16.5 %, resulting from an increase in installed capacity of 15.4 %. The effect on energy consumption of hydro storage facilities is also decreased significantly by 15.7 %. As illustrated in Figure 8-26, large amounts of electricity can be shifted from periods of high residual loads in the evening to periods of low residual loads during the day. That additional demand for electricity during the day can now largely be fulfilled by additional offsite solar capacities. This additional electricity demand in times of low residual loads also enables a better integration of otherwise curtailed electricity from vRES and reduces the overall curtailment by 23.5 % from 9.86 TWh to 7.54 TWh. Since that additional electricity can now be shifted to times of higher residual loads, less wind and conventional power is needed in those periods. Because offsite solar is the cheapest vRES, that shift from wind to offsite solar alone would reduce overall system costs. As with unidirectional charging, the consideration of bidirectional charging also leads to a significant reduction of electricity used to power hydro-pumped power plants (-15.7 %) and power to heat applications (-5.1 %).

8.4.2.2 Influence on wholesale prices

As mentioned, shifting loads from periods of higher residual load to periods of lower values leads to a change in wholesale prices, as illustrated in Figure 8-29.

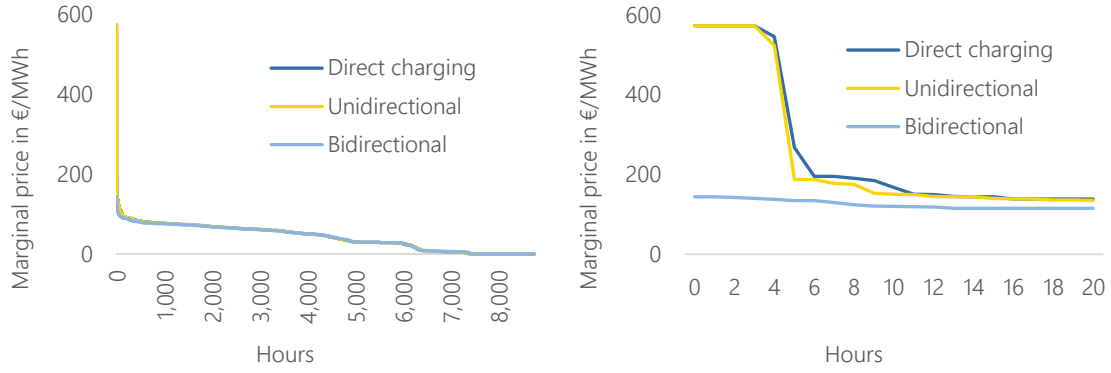

Figure 8-29: Annual duration curve of marginal prices resulting from the three charging strategies in 2030

Due to low numbers of EVs, the effect on the overall price structure is considered rather small. Average values decrease slightly but are negligible. However, bidirectional charging has an especially significant influence on peak prices. High prices result from high demand in combination with low supply. Such a period is usually also characterized by high values of residual loads and therefore prioritized by EVs that can discharge during those times. The discharging reduces the demand for electricity and therefore lowers peak prices significantly. (The influence on resulting wholesale prices in 2040 can be found in the appendix in Figure 12-8.)

8.4.2.3 Conclusion on system feedback

The simulations show that an optimization of EV charging strategies aiming at the smoothing of the residual load curve leads to a better integration of vRES and a decrease of emission-intensive conventional generators and use of hydro storage and power to heat applications. Due to the overall small number of EVs considered in 2030, a simple shift of charging processes in the unidirectional case leads only to a rather small effect. In bidirectional charging, however, more energy can be shifted, leading to a more significant system feedback. Especially the discharging in high-residual

load periods in the evening and charging during solar-dominated low residual load periods during the day leads to a significant increase of usable solar power. Since offsite solar is considered the cheapest vRES, large additional capacities are installed, displacing more expensive wind onshore generators, and decreasing overall system costs. The discharging of vehicles also reduces peak prices significantly, but the overall effect on wholesale prices is small.

Here, the limitations of the iterative simulation approach used in this context must be discussed. For the simulations, it is assumed that EVs optimize their charging strategies based on the fixed residual load curve, originating from a prior simulation run. The then-altered electric load of those vehicles is used for the next simulation run of the energy system model. That way, the optimization of EVs is considered as preexisting, and all other components of the energy system are expanded and dispatched based on that new electric load.

In reality, though, the decision if EVs are considered or other flexibility providers are used is based on the dynamic interactions and decisions of all market participants. Hence, to fully assess the resulting market behavior of all components at the same time, EVs and all other components would have to be mapped in the energy system model and simulated following such an integrated approach. To gain further insights into the behavior of individual actors and map their dynamic interactions, an agent-based modeling approach could be considered (e.g., Dallinger [98]). The goal at this point, however, is the assessment of feedback effects on charging strategies. For that specific research question, the described iterative approach is deemed adequate.

8.5 Use case 4: Reduction of CM measures

As the fourth and last use case under analysis, possible reductions of CM measures are discussed in this section. As outlined in section 5.5, the underlying assumption for the assessment performed in this section is that all vehicles in the vicinity of the high-voltage grid nodes, as represented by the Voronoi areas, can be used to reduce CM measures. It is also assumed that the grid congestion leading to curtailment or redispatch occurs mostly on the high-voltage level (as stated in [78]) and that electricity can still be transported in the medium-voltage and distribution grid of each Voronoi region. Given the assumed distribution of EVs in 2019 and 2030, described in section 6.1, the reduction potential of CM measures by the given fleet is evaluated. Furthermore, the influence of such charging strategies on operational emissions of the vehicles is discussed.

8.5.1 Curtailment

In case of curtailment, two charging strategies are defined, aiming at the reduction of the otherwise curtailed electricity. First, the reduction of those measures is considered as the only target. In that case, when no curtailment occurs, vehicles simply charge whenever they reach a location where they can be charged. In the second case, a combined charging strategy is assumed. Here, the primary target is the reduction of emissions, based on the time series of EMFs. Since otherwise curtailed renewable electricity can be considered as free of emissions, the time series of EMFs in these times is set to zero. That way, vehicles are incentivized to shift their charging operation to times of curtailment measures and otherwise follow the emission-optimized charging strategy. Results for both strategies are presented in the following subsections.

8.5.1.1 Optimization target: reduction of curtailment

Figure 8-30 illustrates the reduction potential for the case where only curtailment is considered for each Voronoi region for the year 2019. The coloring represents the amount of curtailed energy before

the simulation, whereas the values featured in each area represent the possible reduction in percent as calculated by equation (7-13). The number of vehicles present in each region is estimated based on the methodology described in section 6.1 and presented in Figure 8-30 on the right.

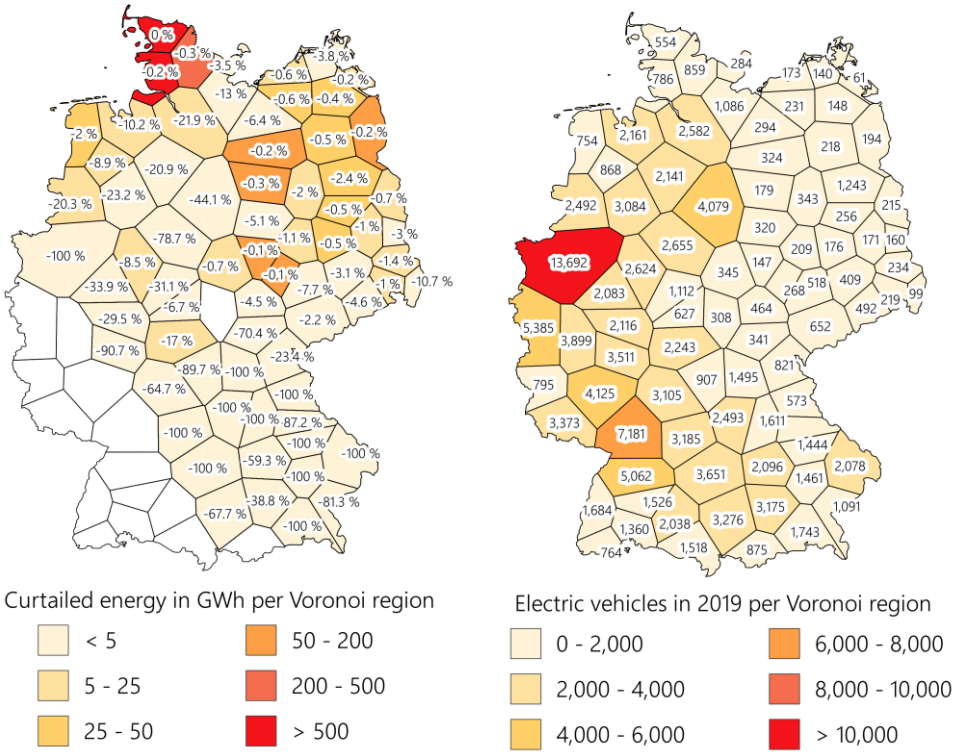

Figure 8-30: Reduction of curtailed energy by Voronoi region (left) and estimated number of EVs (right) [unidirectional charging]

First, since only 136,600 EVs are registered in 2019, the actual number of vehicles per Voronoi region that can be used to reduce curtailment measures is rather small. Secondly, the distribution of vehicle density and curtailment measures does not match well since the majority of (mostly affected) wind farms are localized in the less densely populated areas of northern Germany. In high-density populated areas like the Ruhr region, with higher numbers of EVs, little to no generation is subject to curtailment (R^2 = 0.0095). For those reasons, the overall reduction of curtailment measures in the unidirectional case only amounts to 0.58 % or 20.3 GWh. However, in some regions with high EV density and small numbers of curtailment measures, especially in the south and west of Germany, up to 100 % of the electricity otherwise curtailed can be used for charging when unidirectional charging optimization is considered. Table 8-5 presents the specific data for the top five regions with the highest values in curtailment reduction. Results for all regions with considerable curtailment measures are presented in Table 12-3 in the appendix.

Table 8-5: Top five regions by absolute reduction of curtailment

Voronoi ID	Number of EVs	Annual curtailment in GWh	Hours of curtailment	Reduction of curtailment in GWh	Relative reduction	Charged curtailed energy per EV in kWh
32	2,582	6.8	1,115	1.5	21.9 %	580
20	2,161	12.2	417	1.3	10.2 %	577
3	2,492	5.8	570	1.2	20.3 %	475
76	1,243	45.4	1,584	1.1	2.4 %	872
22	2,243	6.3	619	1.1	17.0 %	473

In Voronoi region 32, located at the border between Lower Saxony and Schleswig-Holstein in the north of Germany, the highest absolute values of reductions can be observed. Neither the number of EVs nor the annual amount of curtailment measures can be characterized as high, but the combination of both leads to a significant reduction of 21.9 % (1.5 GWh). In contrast, region 20, which ranks second with regard to absolute reduction values, records about twice the amount of annual curtailment in less than half the time. The absolute reduction potential in each region depends on the quantity of curtailed energy and the number of vehicles but also on the temporal characteristics of curtailment measures. Further region-specific analysis beyond the scope of this research would be needed to fully characterize those correlations.

Despite the still rather small influence on overall curtailment measures, the effect on the vehicle level, especially in regions with high amounts of curtailed energy, can be very significant. Figure 8-31 presents the average share of energy charged from curtailment measures for unidirectional charging and the 20 regions with the highest shares.

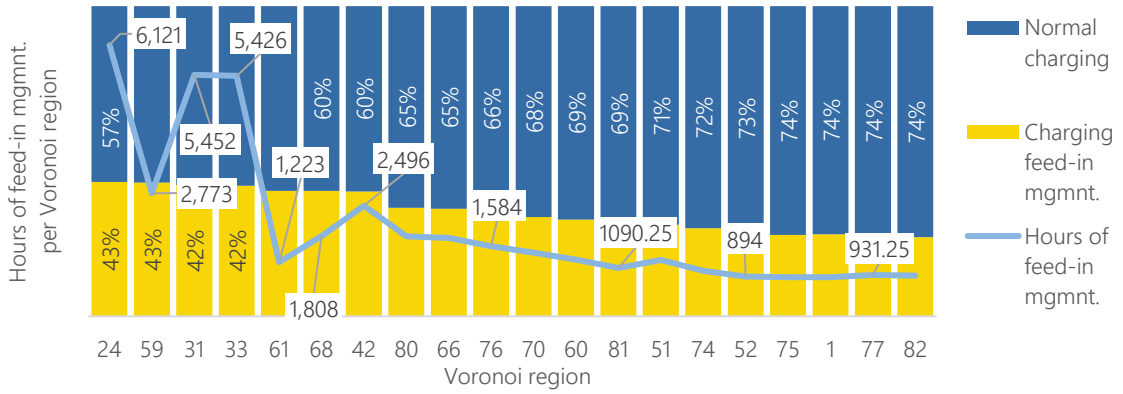

Figure 8-31: Hours of curtailment per Voronoi region and share of charged energy from curtailment measures (unidirectional charging)

Curtailment has become a normal part of system operations, especially in regions with high wind shares, leading to a maximum of 6,121 hours of curtailment measures in Voronoi region 24. On average, 43 % of the annual consumption of EVs in that region could be charged by vehicles using otherwise curtailed electricity. This number remains relatively high even in regions with fewer curtailment hours per year. On average, over all regions where curtailment measures occurred, otherwise curtailed energy was used to cover 15.1 % (393 kWh) of the vehicles' annual energy consumption.

8.5.1.2 Optimization target: reduction of curtailment and emission-optimized charging

In a next step, emission-optimized charging is implemented as a secondary optimization target. Results show that in the bidirectional case, when emission optimization is considered as well, even higher reductions of curtailment measures can be achieved. When bidirectional charging is utilized, EVs can provide more flexibility, which can be used for the reduction of curtailment measures. Speaking practically, EVs are able to discharge before a measure occurs, and as a result, can therefore charge more electricity when it does. By considering a bidirectional charging operation, the aforementioned 0.58 % reduction can be increased to 1.65 % or 57.2 GWh. The amount of otherwise curtailed energy charged per vehicle can be increased to 1,366 kWh per year. Table 8-6 shows the influence of bidirectional charging on the charged curtailed energy per EV for the top five regions with respect to the amount of energy charged in the unidirectional case.

Table 8-6: Charged energy from curtailment measures for unidirectional and bidirectional charging for top five regions in Figure 8-31

			Charged curtailed energy per EV in kWh		
Voronoi ID	**Number of EVs**	**Annual curtailment in GWh**	**Unidirectional charging**	**Bidirectional charging**	**Relative increase**
24	786	577	1,120	4,623	+313 %
31	554	1,598	1,095	5,754	+425 %
33	859	314	1,091	5,466	+401 %
59	324	195	1,115	7,453	+568 %
61	179	58	1,045	5,723	+448 %

The consideration of bidirectional charging leads to an increase of charged energy, which would have otherwise been curtailed, of up to 568 %. Since these amounts can be considered emission-free, the impact of such charging strategies on vehicles' operational emissions is evaluated next.

8.5.1.3 Emission assessment of curtailment-optimized charging

First, the effect on total emissions of the vehicles is assessed and compared to the charging strategy solely optimized on EMFs. In a second step, a combination of both charging strategies is considered. Since in most regions, curtailment still occurs only sporadically, "normal" emission-optimized charging is assumed in those times. Figure 8-32 shows the resulting annual emissions for all three cases and charging modes.

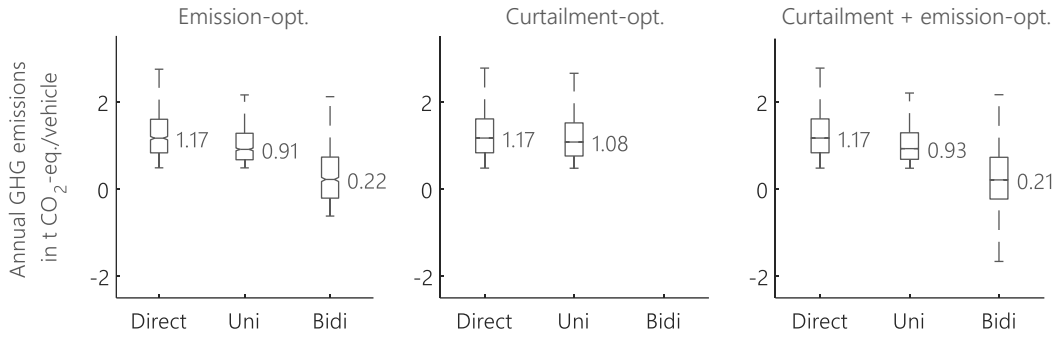

	Emission-opt.			Curtailment-opt.			Curtailment + emission-opt.		
	Direct	Uni	Bidi	Direct	Uni	Bidi	Direct	Uni	Bidi
g CO_2-eq./ km	84.9	68.6	14.3	84.9	78	-	84.9	68.8	6.7
Charged energy "curtailment" in kWh	-	-	-	-	394	-	-	394	1,366

Simulation year	Battery capacity	Charge power home / work	SOC departure	SOC safety	User group
2019	60 kWh	11 kW / -	90 %	30 %	all

Figure 8-32: Emission assessment of curtailment-based charging strategies

In the first case, only the reduction of curtailment measures was considered as an optimization goal. Since curtailed energy can only be reduced by shifting charging operations into those periods, only unidirectional charging was analyzed here. Overall, an emission reduction of 17.9 % can be achieved compared to 22.2 % in the case of emission-optimized charging. Curtailment measures constitute routine system operation in some regions, but in most, they are still the exception. This is also represented by the overall relatively low share of curtailment electricity used by the vehicles for charging. Whereas in several regions, this share adds up to 43 % of the charged energy (see Figure 8-31), the average vehicle in all considered regions can only utilize 15.9 %. However, since this electricity is considered emission-free, these relatively small values result in a comparatively significant reduction in overall emissions. These emission reductions depend strongly on the region where the EVs are located. Depending on the number of vehicles, the temporal characteristics, and the absolute amount of feed-in management measures, very different values of specific emissions can be achieved. Figure 8-33 shows the resulting emissions for direct charging as well as the unidirectional optimization aiming at the reduction of curtailment measures. Here, only the curtailment-optimized charging is presented without considering the additional EMF optimization to highlight the region-specific differences.

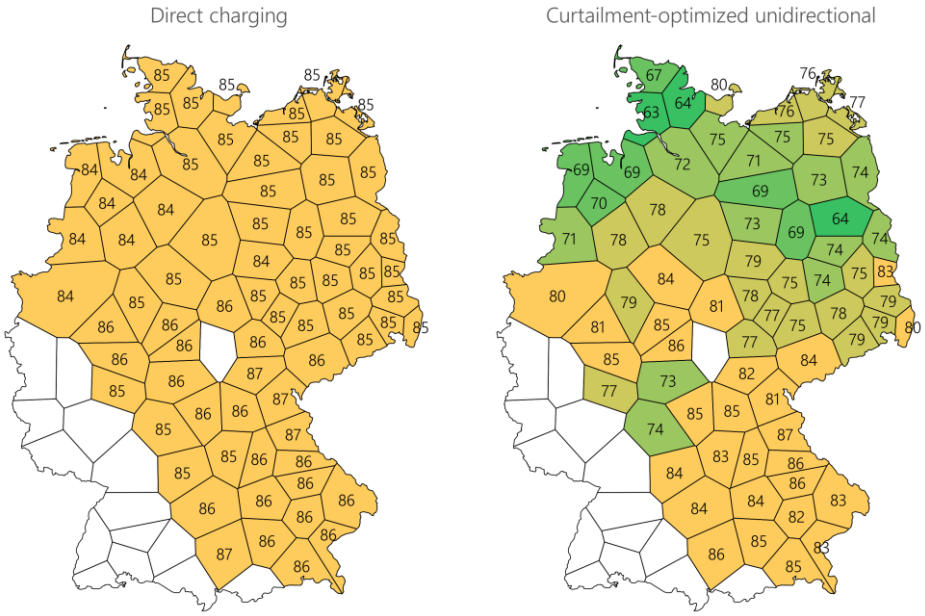

Figure 8-33: Specific emissions in g CO_2-eq./km per region for direct charging as well as curtailment-optimized unidirectional optimization in 2019

The region-specific differences of specific emissions in the direct charging mode are a result of the temperature-dependent electric consumption of EVs described in section 7.2. In the case of unidirectional optimization, shown on the right, significant differences can be observed with regard to resulting emissions. Regions with high amounts of curtailed energy and low numbers of EVs generally show the most significant reductions of EV's operational emissions. The combination of region-specific temporal characteristics as well as the absolute amount of curtailment measures and the respective number of vehicles makes overarching conclusions very difficult. Those evaluations are outside the scope of this thesis but should be the subject of further investigation.

Those values even increase when a combined optimization, aiming at the reduction of curtailment measures and overall emissions, is considered. The availability of emission-free electricity enables emission reductions that even undercut those of normal emission-optimized charging. In bidirectional charging, this effect is further pronounced since, as discussed, vehicles can discharge before curtailment occurs to then utilize those periods fully for charging. This results in a 247 % increase of the average amount of otherwise curtailed charged electricity. Increasing the use of that emission-free electricity leads to a further reduction of mean annual emissions in the bidirectional case by 81 %, resulting in average emissions per km of 6.7 g CO_2-eq..

8.5.1.4 Conclusion on curtailment charging

The small number of vehicles considered for 2019 leads to an overall minimal reduction potential of curtailment measures. The reduction only amounts to 0.58 % in the unidirectional case and 1.65 % when bidirectional charging is considered. However, in some regions with larger numbers of vehicles and small amounts of curtailed electricity, up to 100 % of those measures could have been avoided if EV charging operations would have been optimized accordingly. The potential reduction depends on both the number of vehicles and the absolute amount of curtailed energy as well as their temporal characteristics. Due to the large number of variables and dependencies, a more in-depth assessment would allow more sophisticated insights into those relationships. Nevertheless, since the focus of this thesis is more on the emission assessment and comparison of all four charging strategies, we refrain from further analysis at this point.

The effects on a vehicle level, on the other hand, can still be significant. The usable amount depends on the type of charging (unidirectional/bidirectional), optimization target (sole reduction of curtailment measures or the combination with emission-optimized charging), and region, with its individual number of vehicles and curtailment measure characteristics. In unidirectional curtailment-optimized charging, up to 43 % (1,120 kWh) of the annually charged energy can be used from otherwise curtailed energy. Considering bidirectional charging, this value can increase to 7,453 kWh (or 57 % of the totally charged energy). Since this electricity is regarded as emission-free, using it for the charging of vehicles significantly reduces their operational emissions. Especially in the bidirectional case, when emission reduction is considered as a secondary optimization target, the lowest values of operational emissions in the assessments for 2019 can be achieved. That combination should therefore be strongly considered by policymakers and system operators since it benefits both the overall energy system and EV emissions.

To assess the cost reduction potential, individual curtailment measures would have to be monetarily quantified. However, this approach would involve large uncertainties and is beyond the scope of this research.

8.5.2 Redispatch

Besides the curtailment measures of RES, grid congestion is currently primarily addressed by the redispatch of conventional power plants. The corresponding use case aims at the reduction of those measures through a bidirectionally charging operation. This essentially means that upregulation of power plants during positive redispatch is replaced by discharging EVs, and downregulation of power plants during negative redispatch is prevented by vehicles shifting their charging operations to these times. It should be noted that in direct contrast to the reduction of curtailment measures, this reduction of redispatch measures does not necessarily reduce overall system or vehicle emissions but aims at the reduction of system costs resulting from redispatch measures.

Simulations are conducted for the year 2019 in all Voronoi areas where redispatch measures occur. Since redispatch is bidirectional, and both directions should be addressed, only bidirectional charging is considered here. As with curtailment evaluations, two cases are analyzed in this case: one with the reduction of redispatch as the only optimization target and another with the combination of redispatch and emission optimization. Both are presented in the following sections.

8.5.2.1 Optimization target: reduction of positive and negative redispatch

Figure 8-34 shows the results for each Voronoi region for the first case for 2019. The coloring represents the number of redispatch measures before the simulation, whereas the values featured in each area represent the possible reduction in percent. The same distribution of vehicles is assumed as in the curtailment evaluations (see Figure 8-30 on the right).

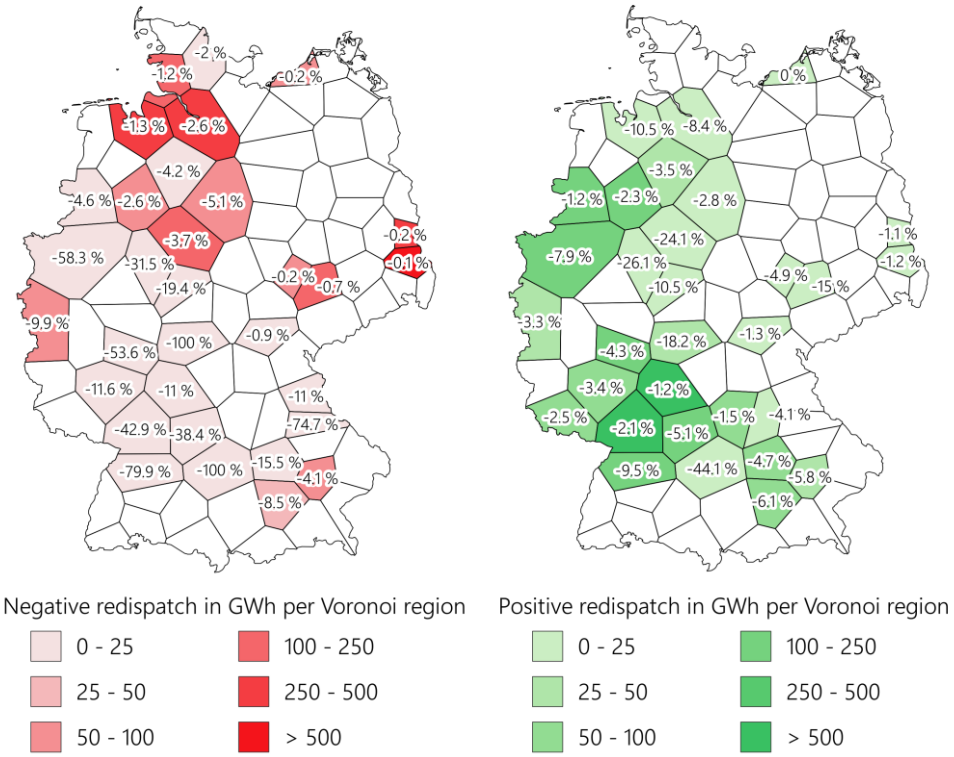

Figure 8-34: Reduction of negative (left) and positive (right) redispatch in 2019

In the case of negative redispatch, similar geographical correlations apply as for curtailment. The distribution of vehicle density and locations of negative redispatch measures do not match well, resulting mostly in minor reductions (R^2 = 0.0749). Considering all regions, negative redispatch could therefore only be reduced by 1.8 % or 53.4 GWh. As shown in Figure 8-34, this relative decline varies significantly among regions. Similar to the results of curtailment, in regions with a small number of redispatch measures and a larger number of vehicles, even a 100 % reduction is possible. Table 8-7 presents the specific data for the top five regions with the highest values in negative redispatch reduction. Results for all regions are presented in Table 12-4 and Table 12-5 in the appendix.

Table 8-7: Top five regions by absolute negative redispatch reduction

Voronoi ID	Number of EVs	Annual negative redispatch in GWh	Hours of redispatch	Reduction of redispatch in GWh	Relative reduction	Charged redispatch energy per EV in kWh
32	2,582	308	1,540	8.1	2.6 %	3,124
9	13,692	12.4	50.0	7.2	58.3 %	527
30	2,655	187	990	7.0	3.7 %	2,626
2	5,385	59	253	5.9	9.9 %	1,089
20	2,161	414	1,348	5.4	1.3 %	2,480

With regard to the reduction potential in each region, the quantity of redispatched energy, the number of vehicles, and the temporal characteristics of redispatch measures are the defining factors. Region 32 in the north of Germany, for example, shows the highest absolute reduction of all regions, even though the number of vehicles (2,582) is relatively low (the average across all regions results in 2,674). However, the region has one of the highest levels of negative redispatch (308.3 GWh in 1,540 h of the year) and ranks fourth in this regard. The relative reduction of 2.6 % is therefore considerably low, whereas the amount of energy charged per vehicle to reduce redispatch (3,124.4 kWh) ranks third in all the considered regions. Region 9, on the other hand, is a good example with opposing correlations. Here, the largest number of vehicles per region meets a

relatively low amount of negative annual redispatch measures in only 50 hours of the year. The combination of both leads to a significant reduction both in relative (58.3 %) and absolute terms (7.2 GWh).

With respect to positive redispatch and in contrast to negative redispatch, the locations of occurrences coincide better with the distribution of vehicles (R^2 = 0.2141). While power plants in the north are mostly downregulated due to high wind yields, others near major load centers in the west and south of Germany tend to need to be upregulated to compensate for those shortfalls. In those regions, higher densities of EVs are assumed due to higher population density. Whereas negative redispatch could only be reduced by 1.8 %, positive redispatch can therefore be reduced by at least 3.6 % on average or 106.6 GWh in total. As with respect to negative redispatch and shown in Figure 8-34, this relative decline varies significantly among regions. To provide a better understanding of the coherences in those regions, Table 8-8 presents the specific data for the top five regions with the highest values in positive redispatch reduction. Results for all regions are presented in Table 12-5 in the appendix.

Table 8-8: Top five regions by absolute positive redispatch reduction

Voronoi ID	Number of EVs	Annual positive redispatch in GWh	Hours of redispatch	Reduction of redispatch in GWh	Relative reduction	Discharged redispatch energy per EV in kWh
15	7,181	888	2,241	19.0	2.1 %	2,651
9	13,692	212	678	16.8	7.9 %	1,224
13	5,062	132	1,878	12.4	9.5 %	2,456
14	3,511	188	2,660	8.1	4.3 %	2,309
34	3,185	153	1,756	7.8	5.1 %	2,460

As mentioned, the regions with high values of annual positive redispatch measures better match those with high EV numbers, resulting in higher absolute reductions. All of the top five regions are assumed to have above-average number of EVs and an above-average amount of positive redispatch measures. Voronoi region 15 combines both values best with the highest value of annual positive redispatch measures and the second-highest number of assumed EVs. This combination leads to a total reduction of 19 GWh (or 2.1 %) and, in addition, the highest value of energy discharged to reduce positive redispatch per vehicle.

8.5.2.2 Optimization target: reduction of redispatch and emission-optimized charging

Additionally in the case of redispatch, emission-optimized charging is implemented as a secondary optimization target. As with the sole optimization to reduce redispatch measures described before, only bidirectional charging is considered in this case. To incentivize charging and discharging during times of negative and positive redispatch measures in the case of emission-optimized charging as well, the time series of EMFs is adapted accordingly. When negative redispatch measures occur in the region, the EMF is set to zero, incentivizing charging operations. In the case of positive redispatch measures, the EMF time series is set to its maximum value, incentivizing discharging operations. It should be noted that the charging strategy is not implemented as a fixed constraint of the optimization problem, leaving a certain amount of flexibility.

In the case of the sole optimization of curtailment reduction, only unidirectional charging was considered. The additional analysis of bidirectional charging in the combined optimization (curtailment reduction and emission-optimized charging) led to an increase of potential curtailment reductions since bidirectionally charged EVs can provide more flexibility. In the case of redispatch,

however, bidirectional charging was already considered in the first case (sole reduction of redispatch measures). The additional consideration of EMFs as a secondary optimization target therefore does not increase flexibility. Indeed, results show that it actually diminishes the overall reduction of redispatch measures slightly. Table 8-9 presents the relative reduction of negative and positive redispatch for both cases.

Table 8-9: Comparison of relative redispatch reduction in top five regions for only redispatch versus redispatch and emission optimization

Negative redispatch			Positive redispatch		
Voronoi ID	**Relative reduction only redispatch**	**Relative reduction redispatch + EMF-opt.**	**Voronoi ID**	**Relative reduction only redispatch**	**Relative reduction redispatch + EMF-opt.**
32	2.6 %	2.6 %	15	2.1 %	2.1 %
9	58.3 %	44.0 %	9	7.9 %	7.3 %
30	3.7 %	3.7 %	13	9.5 %	7.6 %
2	9.9 %	9.9 %	14	4.3 %	4.0 %
20	1.3 %	1.3 %	34	5.1 %	4.0 %

Accounting for an additional optimization on EMFs decreases the potential redispatch reduction in most of the regions. Overall, the reduction of negative redispatch measures is slightly impaired from 53.46 to 51.54 GWh (or 1.88 to 1.81 %), while the reduction of positive redispatch measures is decreased from 106.6 to 93.48 GWh (or 3.55 to 3.11 %). A simple consideration of redispatch reduction as the sole optimization target allows the optimizer to better utilize EVs' flexibility for that single purpose.

8.5.2.3 Emission assessment of redispatch-optimized charging

Both charging strategies are then assessed with respect to the resulting emissions of the vehicles. In direct contrast to curtailment-optimized charging, charging otherwise redispatched electricity cannot be accounted for with zero emissions. Instead, the actual emissions of the power plants undertaking the redispatch measures must be taken into account. For that purpose, the time series of redispatch emissions described in section 5.4 is considered in each region. EVs that reduce negative redispatch by shifting their charging operations to these periods are therefore offset against the emission of the power plant(s) whose downregulation was prevented. EVs that reduce positive redispatch by shifting their discharging operations to the related periods are (negatively) offset against the emission of the power plant(s) whose upregulation was prevented. Figure 8-35 compares the resulting emissions for both redispatch-based bidirectional charging strategies with the results of emission-optimized charging.

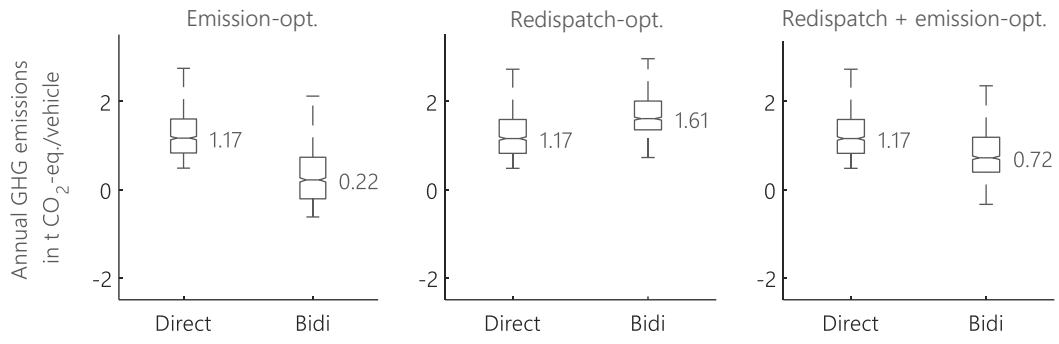

g CO_2-eq./ km	84.9	14.3	84.9	93.2	84.9	32.1
Charged energy "redispatch" in kWh	-	-	-	902	-	897
Discharged energy "redispatch" in kWh	-	-	-	763	-	659

Simulation year	Battery capacity	-	SOC departure	SOC safety	User group
2019	60 kWh	11 kW / -	90 %	30 %	all

Figure 8-35: Emission assessment of redispatch-based charging strategies

In 2019, the redispatch of power plants led to a net reduction of emissions by 531 Mt CO_2 because, overall, more high-emission lignite power plants were regulated down, and lower-emission hard coal- and gas-fired power plants were regulated up. EVs used for the reduction of those measures essentially charge lignite-based electricity and discharge in times of lower-emission hard coal- or gas-based electricity. Overall, such a bidirectional charging strategy leads to an increase in operational emissions by 37.6 %, as illustrated in the boxplot in the middle. Hence, the goal of reducing costly redispatch measures collides with that of reducing operational emissions of the vehicles. As with the curtailment-optimized charging strategy these results strongly depend on region where EVs are located. Figure 8-36 shows the resulting specific emissions for direct charging as well as the bidirectional optimization aiming at the reduction of both positive and negative measures. Again, only the results for redispatch-optimized charging are presented without considering the additional EMF optimization to highlight the region-specific differences.

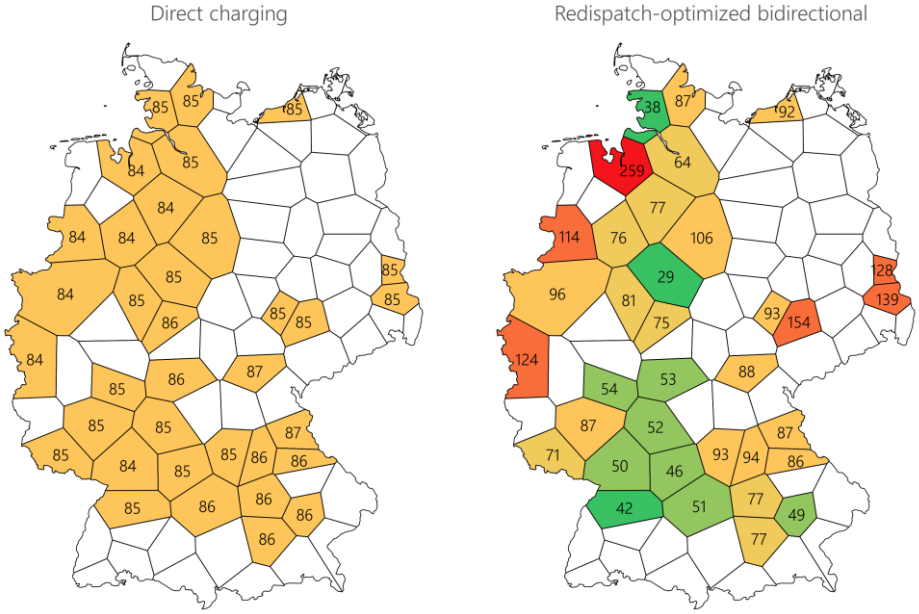

Figure 8-36: Specific emissions in g CO_2-eq./km per region for direct charging as well as redispatch-optimized bidirectional optimization

Again, the region-specific differences of specific emissions in the direct charging mode (on the left) are a result of the temperature-dependent electric consumption of EVs described in section 7.2. The resulting emissions from bidirectional optimization vary considerably, ranging from a 66 % reduction in emissions from 85 to 29 g CO_2-eq./km to a tripling from 84 to 259 g CO_2-eq./km. These significant differences can be explained by the way emissions are accounted for, when redispatch is reduced. In positive and negative redispatch, the specific emissions of the power plant affected by the redispatch measure are fully attributed to the EVs. When positive redispatch, i.e., increasing the generation of power plants, is reduced by a shifting of discharging processes, the emission accounting leads to a substantial reduction of EVs' operational emissions. On the other hand, if negative redispatch, i.e., shutting down power plants, is prevented by shifting charging operations, operational emissions of EVs are significantly increased. Since in some regions both negative and positive redispatch occurs and all other complex coherences apply as with curtailment (number of vehicles, amount, and temporal characteristics of redispatch measures), overarching conclusions are even more difficult here and not within the scope of this thesis. A very promising evaluation would lie in focusing exclusively on positive redispatch measures, where both the potential reduction of redispatch costs as well as the positive effect of EV's operational emissions could be achieved.

When a combination of redispatch-oriented charging with emission optimization is considered, however, those increases in emissions can be limited. It must be noted, though, that in this case, the marginal and mix emissions accounting approaches are basically combined. In times of redispatch measures, the marginal emissions of redispatched power plants are used for the accounting of both the charging and discharging processes. Since mostly lignite and hard coal-fired power plants are affected (83 % in the case of negative and 76.5 % in the case of positive redispatch), these emissions are usually much higher than the time series of consumption-based mix EMFs used for the accounting of emission in times when no redispatch measures occur. Overall, the consideration of EMFs as a secondary optimization target leads to average annual emissions of 720 kg CO_2-eq.. The consideration of that combination enables both the reduction of redispatch measures as well as an overall reduction of EV operational emissions.

8.5.2.4 Conclusion on redispatch charging

As with curtailment-optimized charging, the small number of vehicles limits the effects of redispatch-optimized charging on a systemwide level. When redispatch reduction is considered as the only optimization target, negative redispatch can be reduced by 1.8 % and positive by 3.6 %. Again, as with curtailment-optimized charging, those values vary widely among regions, depending on the number of EVs and the total number and temporal characteristics of redispatch measures. Positive redispatch measures usually occur near load centers in the west and south of Germany, where power plants tend to need to be regulated up to compensate for the downregulation of power plants in the north of Germany. In most of those regions, larger numbers of vehicles are assumed since those areas are usually more densely populated. Discharging those vehicles in times of positive redispatch results in a relative reduction of up to 44 % in Voronoi region 35 in southern Germany, underscoring the fundamental potential of such charging control.

In contrast to curtailed energy, however, charging otherwise redispatched electricity results in overall higher operational emissions. For that reason, a combined redispatch- and emission-optimized charging strategy was assessed. The additional consideration of EMFs as an optimization target decreases the potential redispatch reduction slightly but leads to significantly lower operational emissions of EVs. At this point, no further strategies were considered. However, a more detailed analysis of these relationships should be performed in the future. To optimize system benefits and

increase the reduction of EVs' operational emissions, for example, the sole reduction of positive redispatch combined with an emission-optimized charging could prove promising.

With respect to the quantification of monetary effects, similar constraints apply as for curtailment-optimized charging. Under the current regulatory framework, small electric consumers such as EVs are not used to provide redispatch, and no corresponding compensation models exist. The evaluation of possible revenue potential is subject to strong uncertainties and is therefore not undertaken within the scope of this work.

8.6 Comparison of use cases and discussion of results

The resulting emissions as well as the associated revenue potential of four distinct use cases are presented in sections 8.2 ("Emission reduction"), 8.3 ("Cost reduction"), 8.4 ("Smoothing of residual load"), and 8.5 ("Reduction of congestion management"). For the main use case of emission reduction, different sensitivities regarding technical parameters, user behavior, and the underlying energy system were evaluated and are discussed in sections 8.2.3 to 8.2.6.. It is assumed that the influence of the studied parameters is also transferable to the other use cases. For the smoothing of residual load use case, an iterative simulation run was performed with the ISAaR power system model to assess the system feedback effects of such a charging behavior. Results are discussed in section 8.4.2. All those scenarios are based on the base configuration of simulation parameters presented in the beginning of this chapter in Table 8-1, without restrictions on maximum EFCs or charging simultaneity and should therefore be considered a maximum estimation.

Especially in the bidirectional case, the lack of restrictions leads to a significant increase of EFCs in all use cases, which can have an influence on battery aging processes (see section 8.2.3.5 for a more comprehensive discussion of that topic). Since no restrictions regarding the maximum charging simultaneity were considered either, both unidirectional and bidirectional charging processes lead to charging simultaneities of 90 to 98 % in all use cases. Such values result in a significant additional load on the distribution networks and will therefore most likely be limited by appropriate regulation, especially with increasing penetration of EVs (see section 8.2.5.2 for a further discussion of this topic). Considering these assumptions of the base configuration, resulting specific emissions and annual costs for 2019 are shown in Figure 8-37. The results for 2030 and 2040 are presented in Figure 12.8 in the appendix.

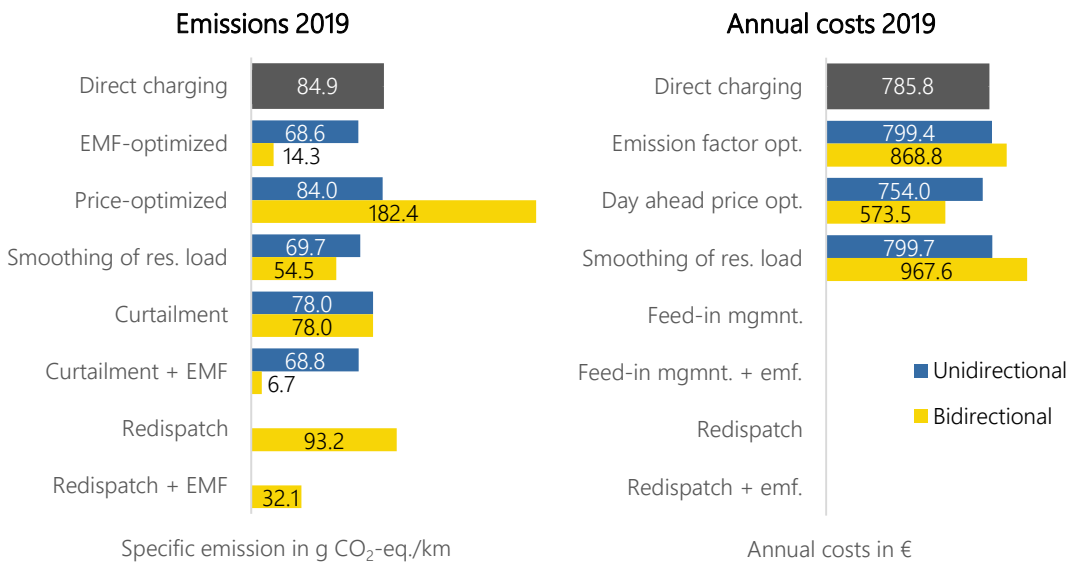

Figure 8-37: Comparison of resulting emissions and annual costs for 2019

In the first column of each side, the resulting specific emissions and annual costs from direct charging are presented as a reference. Since no costs are assessed for the CM use cases, no corresponding values are shown on the right. Furthermore, in the case of redispatch, only bidirectional charging was considered.

Regarding potential emission reduction, the bidirectional charge strategies of EMF optimization and curtailment and EMF yield the best results. The use of otherwise curtailed energy in combination with the optimization of charge processes based on the specific EMFs leads to the lowest values of specific emissions. In addition, both of these charging strategies add value to the overall system by mitigating CM measures and therefore reducing operation costs.

As discussed in section 4.5, the current structure of the electricity market in Germany results in a negative correlation of potential revenues and emission reductions, especially in the bidirectional case. Therefore, the price-optimized use case leads to an increase in emissions, whereas the emission-optimized use case leads to an increase in operational cost. As discussed in the respective chapters (see sections 8.2.1 and 0), this negative correlation will dissipate in future years. Accordingly, price-optimized charging will then also lead to emission savings and vice versa. Since the EMFs show a relatively high correlation with the residual load, the resulting emissions and costs follow the same relationships. Both unidirectional and bidirectional charging leads to reduced emissions but increasing costs.

As a general remark, it must be stated again at this point that all those evaluations must be considered as static with respect to the feedback effects such charge controls might have on the energy system. Especially with increasing numbers of EVs on Germany's streets, these effects can be significant. To address these feedback effects, an iterative simulation run with the energy system model ISAaR was conducted based on the electric load time series of EVs resulting from residual-load-optimized charging. The evaluations show that electricity production from conventional generators is reduced and, depending on the charging operation (unidirectional or bidirectional), can be replaced by additional capacities of wind or solar generators. Furthermore, the utilization of hydro-pumped power plants and power-to-heat applications, as well as peak prices, is reduced.

8.7 Influence on the vehicles' LCA and comparison to ICEVs

In Fattler and Regett [157], the influence of intelligent charging strategies on the environmental impact of EVs was discussed within the context of an LCA of those vehicles. A unidirectional price-optimized and emission-optimized charging was considered to derive operational emissions and to assess the influence of such charging strategies on the environmental payback period compared to a conventional ICEV. This payback period describes the time after which lower operational emissions of the EV in the operating phase overcompensate for the larger carbon footprint during the production of the vehicle. The evaluations were conducted for a compact-class EV with a battery capacity of 35.8 kWh in comparison to an equivalent diesel and gasoline ICEV. However, the overview of current EV models shows that only 21 % of all models have batteries with capacities lower than 40 kWh (Figure 8-9). To account for this development, the same evaluations were performed again for an EV corresponding to the baseline configuration used in this work. In addition, the energy system boundary conditions are adjusted to reflect the same trends that underlie all other assessments conducted herein. To assess the impact of the evaluated charging strategies, the resulting emissions of the emission-based unidirectional and bidirectional optimization were considered.

With regard to emissions in the production phase of the vehicles, it is assumed that production is based in Germany. The coauthor Regett in [157] has shown in [158] that the carbon footprint of the vehicle's battery strongly depends on the state of the art of the production process and the location of the manufacturing plant with its underlying electricity mix. For a state-of-the-art industrial plant, she calculated energy-related GHG emissions of 106 kg CO_2-eq. per kWh battery capacity produced, of which electricity demand in battery manufacturing constitutes the largest share with about 40 %. This value was adapted considering the average consumption-based EMF of the German electricity generation in 2020 of 472 g CO_2-eq./kWh_{el}, increasing that value to 110 kg CO_2-eq. per kWh battery capacity. For a production in Germany in 2030, the average consumption-based EMF of 204.8 g CO_2-eq./kWh_{el} (Table 4-4) is considered, resulting in 83.1 kg CO_2-eq. per kWh battery capacity. The climate impact of the other components and the ICEV is derived from [159]. With regard to the operating phase of the vehicles, the following assumptions are made.

Table 8-10: Operational parameters of the considered vehicles

	Diesel ICEV	Gasoline ICEV	EV (60 kWh)	Source
Consumption	5.0 l/100 km	5.8 l/100 km	17.3 kWh/100 km	[160]
Lifetime		10 years		[161]
Annual mileage		13,257 km		[162]

The fuel consumption of the ICEV is translated to GHG emissions with regard to combustion-related emissions from [163] and upstream emissions for fuel supply from [164]. With regard to operational emissions of the EV, results for 2019, 2030, and 2040 for direct and emission-optimized charging presented in section 8.2 are considered. Based on those assumptions, the original evaluation conducted in [157] for an EV consistent with the base configuration presented in Table 8-1 is reevaluated for 10 years of operation between 2020 and 2030 and 2030 and 2040. It is assumed that the difference in operational emissions between the main historical year employed in this thesis (2019) and the starting year (2020) is negligible. The resulting production and operational emissions over the assumed lifetime of 10 years for an EV, according to the configuration in [157] and this work's baseline configuration, is illustrated in Figure 8-38.

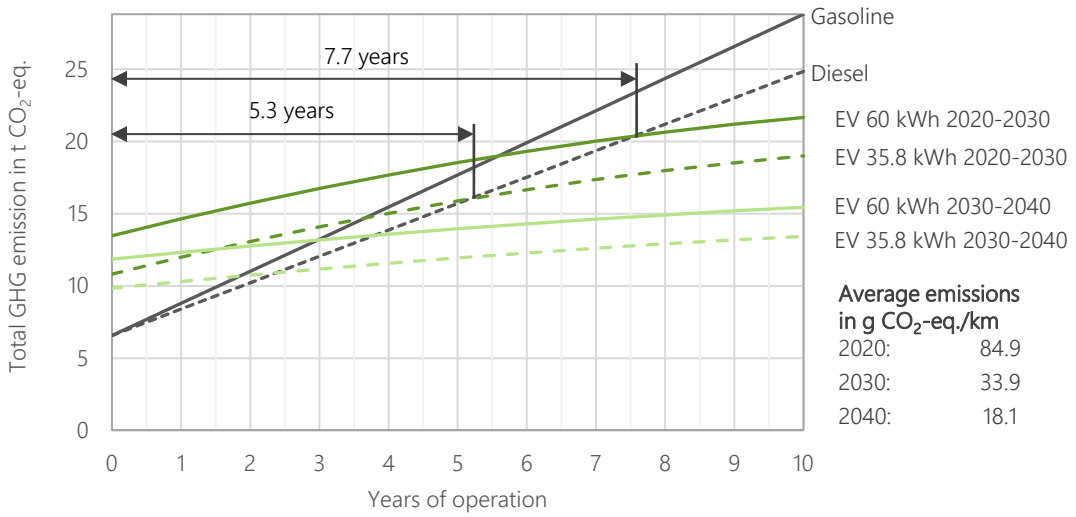

Figure 8-38: Comparison of the total climate impact of ICEVs and EVs according to the configuration in [157] and this work's baseline configuration

The illustration shows the climate impact of the production and the operating phase of each vehicle. For the operational emissions of the EVs, the reduction of emissions due to the restructuring of the electricity production over the course of their lifetime is analyzed. Here, a linear reduction among the years 2020, 2030, and 2040 is imputed. The intersection of the curves of the EVs with those of the ICEVs corresponds to the ecological payback period, after which the larger carbon footprint during the production phase of an EV is offset by the lower emissions during the operation phase. The consideration of a battery capacity of 60 instead of 38 kWh increases the footprint during the production phase and leads to a longer payback period. Considering a period of operation between 2020 and 2030, the payback period compared to the diesel ICEV is increased from 5.3 to 7.7 years. In case of the gasoline ICEV, the payback period is increased from 3.8 to 5.5 years. It should be noted that the same annual mileage, lifetime, and utilization of all vehicles are assumed, while possible advantages due to a larger range of ICEVs and the EVs with 60 kWh of battery capacity are not considered. If the further decarbonization of electricity generation in Germany is assumed for an operating period between 2030 and 2040, the advantages of EVs become even more apparent. Comparing both EVs with the diesel ICEV in that period, these values drop to 3.9 and 2.4 years, respectively. In case of the gasoline ICEV the values drop to 3.0 and 1.9 years.

In all cases, a direct charging of EVs is assumed. To assess the influence of an optimized charging operation, the same evaluation is conducted based on the operational emissions resulting from the emission-optimized charging strategy described in section 8.2. For that assessment, only the larger EV with 60 kWh is considered in alignment with the base configuration of simulation parameters presented in Table 8-1. The evaluation is performed for the periods between 2020 and 2030, as illustrated in Figure 8-39, and 2030 and 2040.

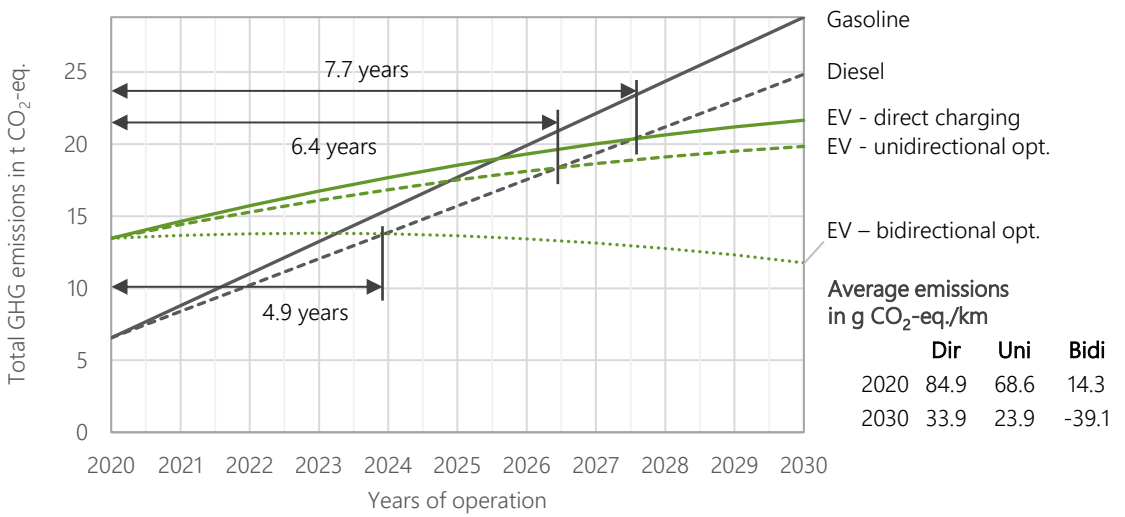

Figure 8-39: Comparison of the total climate impact of ICEVs and EVs considering emission-optimized charging between 2020 and 2030

The unidirectional optimization of charging processes leads to a relative reduction in specific operational emissions of the EV by 19.2 % in 2020 and 29.5 % in 2030. For the years in between, a linear reduction is considered. This reduction leads to a reduced payback period in comparison to the diesel ICEV of 6.4 instead of 7.7 years in the case of direct charging. As discussed in section 8.2, bidirectional charging can even lead to negative emissions. Those result in a negative slope of emissions during the operating phase of the vehicle, further reducing the payback period to 4.9 years. The decarbonization of the power sector leads to even lower payback periods when an operating time between 2030 and 2040 is considered as illustrated in Figure 8-40.

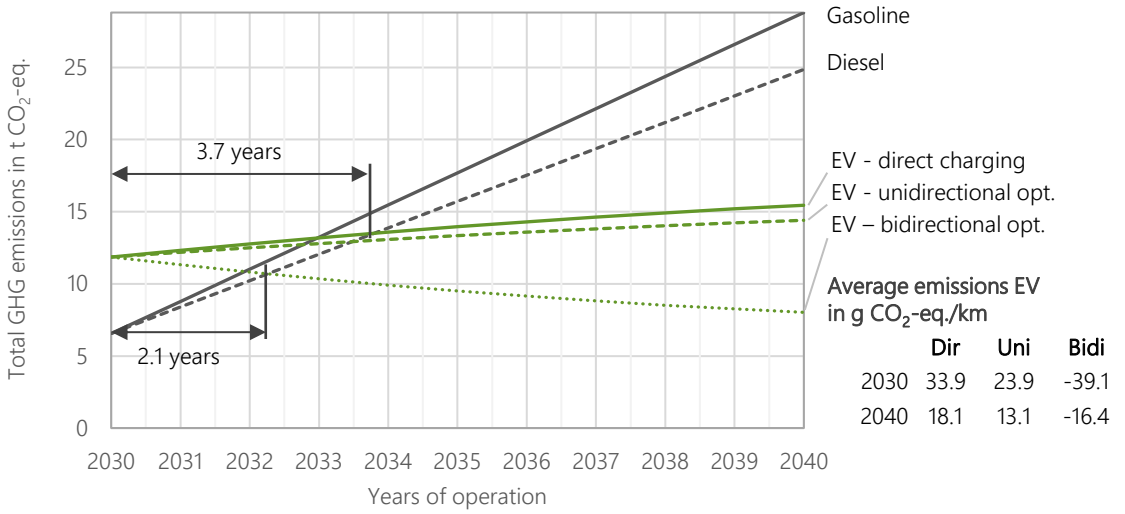

Figure 8-40: Comparison of the total climate impact of ICEVs and EVs considering emission-optimized charging between 2030 and 2040

Even considering a relatively high battery capacity of 60 kWh, payback periods only amount to 3.7 years when compared to the diesel ICEV and 2.9 years for the gasoline ICEV. In case of bidirectional charging these values can be reduced to 2.1 and 2 years respectively.

Conclusion on impact on LCA

The evaluations performed in this chapter build on the analyses in Fattler and Regett [157] and account for the increasing demand for EVs with higher battery capacities. Higher battery capacities result in a larger impact in the production phase of the vehicle and increase the ecologic payback period compared to a diesel ICEV by 31 % to 7.7 years when an operation time between 2020 and 2030 is considered. The decarbonization of the energy system and resulting lower values of operational emissions reduce that value significantly to 3.7 years for an operating time between 2030 and 2040. Further reductions are possible when optimized charging is considered. Using the potential emission reductions of the emission-optimized use case leads to a reduction in payback periods to 6.4 years in the unidirectional case and, due to potentially negative operational emissions, to 4.9 years in the bidirectional case for an operating time between 2020 and 2030. Potential reductions are even higher when the operating period between 2030 and 2040 is considered.

However, negative emissions must be viewed with caution since no dynamic system feedback effects are considered, and mix EMFs are employed for the evaluation. The assessment of the system feedback effects in section 8.4.2 supports the assertion that the charge optimization of EVs not only has positive effects on the operational emissions of the vehicles themselves but can also be regarded as beneficial for the operation of the energy system as well.

9 Conclusion and Outlook

The main objective of this thesis was the assessment of electric vehicle (EV) charging strategies with respect to resulting costs and emissions. The focus was on those strategies that have a particularly high potential for reducing emissions or improving the integration of variable renewable energy sources (vRES). To that end, four distinct charging strategies aimed at the reduction of emissions and costs, the smoothing of residual load, and a decrease in congestion management (CM) measures were identified. Operational emissions as well as operating costs of EVs depend strongly on the nature of the underlying energy system. To do justice to this relationship, the historical and future (assumed) developments of German electricity generation were first presented in detail. They lay the foundation for the assessment of those charging strategies, of which the first three were evaluated both for the historical year 2019 as well as the future years 2030 and 2040. The last one, aiming at the reduction of CM measures, was only conducted for 2019.

For the assessment of EVs' operational emissions, time-resolved emission factors (EMFs) were calculated, representing the electricity generation in each hour. Three distinct methods were taken into account: generation-based and consumption-based EMFs (following the attributional approach) and marginal EMFs (following the consequential approach). All three were evaluated in terms of their temporal characteristics and correlations with relevant variables in the power system. Based on these assessments, their applicability for the accounting of EVs' operational emissions, as well as the consideration as an optimization target for the charging strategies, was discussed.

Besides the boundary conditions set by the underlying energy system, the charged emissions and the potential of charging strategies strongly depend on the mobility behavior of vehicle users. To adequately address this correlation, a methodology was developed for the calculation of annual mobility profiles. A consumption model for EVs was implemented to translate those mobility profiles into vehicle-specific time series of electric consumption. The linear optimization model eFLAME was adapted to allow the economic and ecological assessment of the use cases and sensitivities under consideration. Various sensitivities were analyzed with respect to technical parameters, user behavior, and the influence and constraints imposed by the power system. Finally, the influence of the resulting operational emissions on the lifecycle assessment (LCA) of the vehicles and the environmental payback period, in comparison to conventional ICEVs, was analyzed. Overall, based on the developed methodology and generated results, the following core statements could be identified and are discussed with respect to recommendations for further research.

The choice of accounting methods for the calculation of EMFs has a significant influence on results and must be considered carefully with regard to the research question.

In the context of this thesis, three distinct accounting methods were applied for the accounting of hourly EMFs. Generation-based and consumption-based EMFs follow the attributional approach, accounting for the mix of all generators providing electricity, whereas marginal EMFs follow the consequential approach and are derived from the marginal power plant at the given hour. Consumption-based EMFs take into account the reality of an integrated European energy market with the associated exchange of electricity across national borders. If the data needed for the calculation is available, the consumption-based approach should always be preferred over the generation-based approach since at least in some countries, the difference can be significant. The decision between the attributional and consequential approach depends strongly on the research question to be answered—in this case, how charging operations of EVs should be optimized to

reduce operational emissions and maximize system benefits. Therefore, maximizing the utilization of vRES' volatile infeed is one of the main objectives. Since the mix method better represents those coherences, the resulting mix-EMF are used as an optimization target for the vehicles.

Regarding the accounting of EVs' operational emissions as well as the evaluated charging strategies in the context of this thesis, both are considered to be an integral part of the overall state of the energy system. The use of mix EMFs as a basis for emissions accounting is therefore deemed plausible. When the causal relationship between marginal load changes and their environmental impacts are assessed, however, marginal EMFs or consecutive energy system model simulations should be employed.

Emission-optimized charging leads to significant reductions of operational emissions and, in the case of bidirectional charging in future years, even reaches negative values.

When unidirectional charging is considered, shifting the charging processes to times of lower EMFs results in a significant reduction of EVs' operational emissions. Charging electricity in times of low emissions and discharging in times of high emissions results in net negative emissions for that bidirectional charging process. In 2030 and 2040, the structure of the power sector results in high temporal dispersion of and at the same time overall low average EMFs. This combination leads to negative median values of EVs' operational emissions in case of bidirectional charging. Overall negative values of operational emissions essentially means that the benefits arising from the bidirectional optimization compensate for the emissions resulting from drive consumption. Bidirectionally charged vehicles in this case serve as storage and contribute an integral part of an overall more efficient system. The combination of a further decarbonization of the power sector in future years and emission-optimized charging of EVs furthermore leads to a significant reduction of the ecologic payback period when lifecycle emissions of those vehicles are compared to conventional internal combustion vehicles.

Under the current constitution of the power sector, price-optimized charging leads to increasing emissions, and emission-optimized charging results in higher operational costs. The phaseout of cheap but emission-intensive lignite and hard coal-fired power plants resolves this negative correlation.

Currently, cheap but emission-intensive lignite and hard coal-fired power plants still dominate the generation of electricity to a large extent, resulting in hours of low prices but high EMFs. Charging in those times therefore increases overall operational emissions, especially when bidirectional charging is considered. The opposite is true when a cost-optimized charging strategy is implemented. Those interrelationships must be considered when planning appropriate charging strategies. However, the phaseout of these low-cost, high-emission power plants will break this link in the coming years, allowing green and low-cost charging strategies to be reconciled.

Unrestricted optimization of charging processes can lead to a significant additional load on both the grid infrastructure and the vehicles themselves and must be addressed accordingly.

The basic configuration of the simulation parameters does not take into account restrictions on the maximum simultaneity of charging operations within the fleet, nor on the number of equivalent full cycles (EFC) at the vehicle level. From the perspective of a potential charging strategy provider or EV user, this maximizes the potential of the charging strategy. However, as the number of EVs increases, the resulting high simultaneity of charging processes can have a significant impact on grid operations and will most likely have to be addressed in the future through appropriate regulatory action. Restricting the maximum simultaneity does not show a significant impairment of potential emission reductions in the unidirectional case but does reduce them by up to 35 % in the bidirectional case.

Research has shown that grid-serving charging strategies of EVs on the other hand can even relieve the grid load and reduce overall system costs. The intelligent combination of grid-friendly and simultaneously user-oriented charging strategies should therefore be the subject of further research.

Besides the additional grid load, an unrestricted optimization of charging processes leads to a significant increase of EFCs. Higher EFCs put additional stress on the battery's electrochemistry, resulting in faster cyclic aging. This accelerated aging can have a significant impact on customer acceptance regarding such charging strategies. However, the detailed modeling of those relationships was not in the scope of this thesis. To fully assess the influence of optimized charging on the aging processes of the battery as well as power electronics of the vehicle, an integrated approach with a battery aging model would be needed and should be subject to further research.

With regard to the potential of charging strategies, user behavior is the most significant influencing factor.

The decisive factor for the potential of all considered charging strategies, especially when bidirectional charging is considered, is the available flexibility. This flexibility depends on technical parameters like the battery capacity and the availability of charging infrastructure but is most strongly influenced by the vehicle's user. First, the mobility behavior of users significantly influences the availability for optimized charging and thus the reduction potential of such charging strategies. Furthermore, it is assumed that when the vehicle is plugged in, the user can specify a minimum state of charge (SOC), which must be met at all times, and a target SOC, which defines the minimum level that the battery must reach at the end of the charging process. Both constraints limit the available flexibility and thus the potential of the respective charging strategy. An even more decisive factor for the potential of charging strategies is the plug-in behavior of the vehicle user. Here, even a small decrease in plug-in frequency leads to a significant reduction of the potential.

Incentivizing vehicle users to be able to utilize the flexibility potential of EVs as fully as possible should therefore be the focus of both social sciences and OEMs or charging service providers. As research has shown, monetary incentives may not be adequately supportive. Moreover, the resulting revenues, especially considering the impact of taxes and duties, will not be sufficient to encourage appropriate user behavior. The focus should therefore be on nonmonetary incentives such as gamification or similar approaches.

Due to the small number of EVs in 2019, potential reductions of congestion management (CM) measures are relatively small. The reduction of curtailment measures combined with emission-optimized charging, however, leads to lowest overall operational emissions.

The simulations have shown that even in the best case of bidirectional charging, the potential reduction of CM measures is rather small, mainly due to the low number of EVs registered in 2019. However, the effect in some regions, as well as at the vehicle level, can be significant. In some regions with larger numbers of vehicles and small amounts of CM measures, up to 100 % of those measures could have been avoided if EV charging operations would have been optimized accordingly. Since otherwise curtailed renewable energies can be considered emission-free, the combination of emission-optimized and curtailment-optimized charging leads to the lowest overall operational emissions. In contrast to curtailed energy, however, charging otherwise redispatched electricity from conventional power plants results in overall higher operational emissions.

The combination of region-specific temporal characteristics of CM measures and the respective number of vehicles makes overarching conclusions very difficult. Generally it can be assumed, that the reduction potential will increase with rising numbers of vehicles. An assessment of such charging behavior in a future year with more EVs could thus prove interesting and should be the focus of

further research. Furthermore, the large number of region-specific influencing factors necessitates further evaluations to clearly identify interrelationships and derive appropriate recommendations for action. To optimize system benefits and decrease EVs' operational emissions, for example, the sole reduction of positive redispatch combined with an emission-optimized charging could prove promising. Besides the need for more detailed analysis, the regulatory framework for such charging strategies must still be defined. Especially the coordination between grid operators and charging service providers presents a challenge that must be addressed accordingly.

The evaluations of system feedback effects have shown that the optimization of vehicles charging processes on the smoothing of residual load results in a better integration of vRES and a reduced dispatch of conventional power plant and storage units.

All use cases were implemented primarily from the perspective of the vehicle owner or the provider of smart charging strategies. Benefits for the overall system could be assumed in some cases but were not the primary target of the strategies. To assess those feedback effects, iterative simulation runs were carried out with the energy system model ISAaR based on the charging strategy aiming at the smoothing of residual load. The results show a better integration of vRES and a decrease of emission-intensive conventional generators and use of hydro storage and power to heat applications. Due to the small number of vehicles assumed in the context of these evaluations the overall effect is rather small, especially in the unidirectional case. In case of bidirectional charging more energy can be shifted, and the overall impact is more pronounced. In addition, a significant reduction in peak prices has been demonstrated with bidirectional charging. Due to the high simulative effort, these evaluations were only carried out for the use case aiming at the smoothing of residual load but should be conducted for the other use cases as well to understand the resulting system feedback effects. Furthermore the effects were only described with regard to the dispatch and expansion of generation units and the impact on electricity prices. To fully assess system effects, more comprehensive evaluations, aiming at overall system costs and emissions, and the dynamic interactions between multiple suppliers of flexibility, should be subject to further research.

Overall, smart charging of EVs can significantly reduce operational emissions and make an important contribution toward a decarbonized energy system. The evaluations carried out in this thesis focus on the EV's or marketer's perspective and provide valuable insights into the most important influencing factors on the potential of those charging strategies. They show that an optimized charging of EVs can bring economic and environmental benefits to vehicle owners, especially in the coming years, while also contributing to a more efficient overall energy system. The developed modeling environment can be used to evaluate further combinations and specifications of charging strategies to accompany the integration of a growing number of EVs into the energy system of the future. In this context, the impact of those charging strategies on grid infrastructure and vehicle components should be regarded as crucial. In the interest of a cost-efficient and sustainable design of the energy system, an integrated approach should be pursued that respects the requirements of all stakeholders and the dynamic interactions of its individual components.

10 Bibliography

[1] *Klimaschutzplan 2050 (Entwurf) - Klimaschutzpolitische Grundsätze und Ziele der Bundesregierung*. Berlin, Germany: Bundesministerium für Umwelt, Naturschutz, Bau und Reaktorsicherheit (BMUB), 2016.

[2] *Emissionsquellen*. Dessau-Roßlau, Germany: Umweltbundesamt (UBA), 2016.

[3] Conrad, Jochen et al.: *Nur im Stromsektor kommt der Anteil regenerativer Energien voran*. In: https://www.ffe.de/publikationen/pressemeldungen/795. (Accessed on 2018-07-30); (Archived by WebCite® at http://www.webcitation.org/71IS0LGal); Munich, Germany: Research Center for Energy Economics e.V. (FfE), 2018.

[4] *Treibhausgasemissionen sinken 2020 um 8,7 Prozent*. In: https://www.bmu.de/pressemitteilung/treibhausgasemissionen-sinken-2020-um-87-prozent/. (Accessed on 2021-03-20); Berlin, Germany: Bundesministerium für Umwelt, Naturschutz und nukleare Sicherheit, 2021.

[5] Gebert, Philipp et al.: *Klimapfade für Deutschland*. Munich, Germany: The Boston Consulting Group (BCG), prognos, 2018.

[6] *Klimaschutzprogramm 2030 der Bundesregierung zur Umsetzung des Klimaschutzplans 2050*. Berlin, Germany: Bundesregierung, 2020.

[7] *Monitoringbericht 2017*. Bonn, Germany: Bundesnetzagentur für Elektrizität, Gas, Telekommunikation, Post und Eisenbahnen (BNetzA), 2017.

[8] Ried, Sabrina: *Gesteuertes Laden von Elektrofahrzeugen in Verteilnetzen mit hoher Einspeisung erneuerbarer Energien*. Dissertation. Published by Karlsruhe Institute for Technology (KIT), exam approved by Fichter, Wolf: Karlsruhe, Germany, 2021.

[9] Kern, Timo et al.: *Integrating Bidirectionally Chargeable Electric Vehicles into the Electricity Markets*. Basel, Switzerland: Energies 2020, 13(21), 5812, 2020.

[10] Wulff, Niklas et al.: *Comparing Power-System and User-Oriented Battery Electric Vehicle Charging Representation and Its Implications on Energy System Modeling*. Stuttgart, Germany: Department of Energy Systems Analysis, Institute of Engineering Thermodynamics, German Aerospace Center, 2020.

[11] Gaete-Morales, Carlos et al.: *An open tool for creating battery-electric vehicle time series fromempirical data:emobpy*. Berlin, Germany: German Institute for Economic Research (DIW Berlin), 2020.

[12] Xu, Lei et al.: *Greenhouse gas emissions of electric vehicles in Europe considering different charging strategies*. In: Transportation Research Part D: Transport and Environment Volume 87, October 2020. Karlsruhe, Germany: Karlsruhe Institut für Technologie (KIT), 2020.

[13] Wietschel, Martin et al.: *Die aktuelle Treibhausgasemissionsbilanz von Elektrofahrzeugen in Deutschland* - Working Paper Sustainability and Innovation No. S 02/2019. Karlsruhe, Germany: Fraunhofer-Institut für System- und Innovationsforschung ISI, 2019.

[14] IRENA: *Innovation Outlook: Smart charging for electric vehicles*. Abu Dhabi, United Arab Emirates: International Renewable Energy Agency, 2019.

[15] Navigant, Kompetenzzentrum Elektromobilität und RE-xpertise: *Verteilnetzausbau für die Energiewende - Elektromobilität im Fokus*: Study commissioned by Agora Verkehrswende, Agora Energiewende und The Regulatory Assistance Project (RAP), 2019.

[16] *Klimabilanz von Elektroautos - Einflussfaktoren und Verbesserungspotenzial*. Heidelberg, Germany: Agora Verkehrswende, 2019.

[17] Schill, Wolf-Peter: *Power System Impacts of Electric Vehicles in Germany: Charging with Coal or Renewables?* - Discussion Papers. Berlin, Germany: German Institute for Economic Research (DIW Berlin), 2018.

[18] Zhao, Yang; Noori, Mehdi; Tatari, Omer: *Boosting the adoption and the reliability of renewable energy sources: Mitigating the large-scale wind power intermittency through vehicle to grid technology* in: Energy. Amsterdam, Netherlands: Elsevier Science, 2017.

[19] Jochem, Patrick et al.: *Assessing CO_2 emissions of electric vehicles in Germany in 2030*. In: Transportation Research Part A 78 (2015). Karlsruhe, Germany: Karlsruhe Institut für Technologie (KIT), 2015.

[20] The FfE Regionalized Energy System Model (FREM) in: https://www.ffe.de/frem. Munich, Germany: Research Center for Energy Economics e.V. (FfE), 2014

[21] Integrated simulation model for unit dispatch and expansion with regionalization (ISAaR) in: https://www.ffe.de/isaar. Munich, Germany: Research Center for Energy Economics e.V. (FfE), 2016

[22] Fiedler, Claudia; Pellinger Christoph: *Laufendes Projekt: Verbundprojekt eXtremOS – Wert von Flexibilität im Kontext der europäischen Strommarktkopplung bei extremen technologischen, regulatorischen und gesellschaftlichen Entwicklungen*. In: www.ffe.de/extremos. (Accessed on 2018-05-28); (Archived by WebCite® at http://www.webcitation.org/6zkjLAHjs); Munich, Germany: Research Center for Energy Economics e.V. (FfE), 2018.

[23] Bundesministerium Energie: *Energiedaten: Gesamtausgabe*. In: https://www.bmwi.de/Redaktion/DE/Artikel/Energie/energiedaten-gesamtausgabe.html. (Accessed on 2020-07-20); Berlin, Germany: Bundesministerium für Wirtschaft und Energie, 2020.

[24] *Auswertungstabellen zur Energiebilanz Deutschland*; Berlin, Germany: AG Energiebilanzen e.V., 2020.

[25] *Electrical production profiles from CHP in the public sector and in the industry in Germany*. Munich, Germany: Forschungsgesellschaft für Energiewirtschaft mbH, 2015.

[26] Kern, Timo et al.: *Development of new power and heat profiles for CHP-Types*. Munich, Germany: Forschungsgesellschaft für Energiewirtschaft mbH, 2018.

[27] *AGFW - Hauptbericht 2019*. Frankfurt am Main, Germany: AGFW, Der Energieeffizienzverband für Wärme, Kälte und KWK e.V., 2020.

[28] Pedregosa, Fabian et al.: *Scikit-learn: Machine Learning in Python*. In: Journal of Machine Learning Research 12 (2011) 2825-2830. Palaiseau, France: Parietal, INRIA Saclay, 2011.

[29] Fiedler, Claudia et al.: *Modelling transformation pathways for EU27+3 final energy demand using temporally and spatially resolved sector models*. Munich, Germany: Research Center for Energy Economics e.V. (FfE), 2020.

[30] Böing, F., & Regett, A. (2019). *Hourly CO_2 Emission Factors and Marginal Costs of Energy Carriers in Future Multi-Energy Systems*. Energies, 12(12), 2260. Basel, Switzerland: MDPI AG, 2019.

[31] Fattler, Steffen; Conrad, Jochen; Regett, Anika et al.: *Dynamis Hauptbericht - Dynamis - Dynamische und intersektorale Maßnahmenbewertung zur kosteneffizienten Dekarbonisierung des Energiesystems* - Online: https://www.ffe.de/dynamis. Munich, Germany: Research Center for Energy Economics e.V. (FfE), 2019. DOI: 10.34805/ffe-144-19

[32] Johnson, Jeremiah X. et al.: *Comparative Assessment of Models and Methods To Calculate Grid Electricity Emissions*. 2350 Hayward Street, Ann Arbor, Michigan 48109, United States, 2350 Hayward Street, Ann Arbor, Michigan 48109, United States, 440 Church Street, Ann Arbor, Michigan 48109, USA: Center for Sustainable Systems, School of Natural Resources & Environment, University of Michigan, 2016.

[33] Regett, Anika: *Development of Instruments for a Circular Energy Economy - Potential of the Circular Economy to Reduce the Critical Resource Demand and Climate Impact of Electric Vehicle Batteries*. Dissertation. Published by Technische Universität München - Lehrstuhl für Energiewirtschaft und Anwendungstechnik, exam approved by Wagner, Ulrich und Schebek, Liselotte: Munich, Germany, 2020.

[34] Tranberg, Bo et al.: *Real-Time Carbon Accounting Method for the European Electricity Markets*. Aarhus, Denmark: Aarhus University, 2018.

[35] Marmiroli, Benedetta et al.: *Electricity Generation in LCA of Electric Vehicles: A Review.* Milano, Italy: Politecnico de Milano, 2018.

[36] *The ecoinvent Database, Version 3.6*: www.ecoinvent.org; Zürich, Switzerland: ecoinvent, 2019.

[37] Icha, Petra et al.: *Entwicklung der spezifischen Kohlendioxid-Emissionen des deutschen Strommix in den Jahren 1990-2019*. In: Climate Change 13/2020. Dessau-Roßlau, Germany: Umweltbundesamt, 2020.

[38] *Transparency Plattform*. In: https://transparency.entsoe.eu. (Accessed on 2019-05-08); Brussels, Belgium: ENTSO-E, 2019.

[39] *Transparenzdaten - [Online] ftp-Server*: infoproducts.eex.com, continuous update since 2014: www.infoproducts.eex.com; Leipzig, Germany: European Energy Exchange, 2021.

[40] Wulff, Fiete: *Kraftwerksliste*. In: https://www.bundesnetzagentur.de/DE/Sachgebiete/ElektrizitaetundGas/Unternehmen_Institutionen/Versorgungssicherheit/Erzeugungskapazitaeten/Kraftwerksliste/kraftwerksliste-node.html. (Accessed on 2020-03-25); Bonn, Germany: Bundesnetzagentur, 2020.

[41] *Electricity Production Data from Transparency Platform*. In: https://transparency.entsoe.eu/. (Accessed on 2019-01-24); Brussels, Belgium: European Network of Transmission System Operators for Electricity (ENTSO-E), 2019.

[42] Hirth, Lion et al.: *The ENTSO-E Transparency Platform – A review of Europe's most ambitious electricity data platform*. Berlin, Germany: Hertie School of Governance, 2018.

[43] Beer, Michael; Wagner, Ulrich: *Ganzheitliche Bilanzierung von KWK* in: 5. Internationale Energiewirtschaftstagung (IEWT) vom 14.02 bis 16.02.2007. Vienna, Austria: TU Wien, Institut für Elektrische Anlagen und Energiewirtschaft, 2007.

[44] Wiesemeyer, Karin; Schwentzek, Marco; Corradini, Roger; Mauch, Wolfgang: *Allokationsmethoden für spezifische CO_2-Emissionen von Strom und Wärme aus KWK-Anlagen* in: Energiewirtschaftliche Tagesfragen 60. Jg. (2010) Heft 9. Essen, Germany: etv Energieverlag GmbH, 2010.

[45] Tereshchenko, Tymofii et al.: *Uncertainty of the allocation factors of heat and electricity production of combined cycle power plant*. Trondheim, Norway: Norwegian University of Science and Technology (NTNU), Department of Energy and Process Engineering, 2014.

[46] Hertle, Hans et al.: *Die Nutzung von Exergieströmen in kommunalen Strom-Wärme-Systemen zur Erreichung der CO_2- Neutralität von Kommunen bis zum Jahr 2050*. Heidelberg, Germany: ifeu-Institut für Energie- und Umweltforschung Heidelberg GmbH, 2014.

[47] Arbeitsgemeinschaft Energiebilanzen e.V. (AGEB): *Vorwort zu den Energiebilanzen für die Bundesrepublik Deutschland*. Berlin, Germany: Arbeitsgemeinschaft Energiebilanzen e.V. (AGEB), 2010.

[48] Konstantin, Panos: *Praxisbuch Energiewirtschaft - Energieumwandlung, -transport und -beschaffung*, Übertragungsnetzausbau und Kernenergieausstieg 4. Auflage. Berlin, Germany: VDI Verlag GmbH, 2017.

[49] Juisto, Scott: *The differences that methods make: Cross-border power flows and accounting for carbon emissions from electricity use*. Worcester, USA: Worcester Polytechnic Institute, 2006.

[50] Li, Baowei et al.: *Carbon Flow Tracing Method for Assessment of Demand Side Carbon Emissions Obligation*. Beijing, China: Tsinghua University, 2013.

[51] Zhang, Zengkai et al.: *From production-based to consumption-based regional carbon inventories: Insight from spatial production fragmentation*. Tianjin, China: Tianjin University, 2017.

[52] *Why and when?* In: https://consequential-lca.org/clca/why-and-when/. (Accessed on 2021-03); Aalborg, Denmark: 2.-0 LCA consultants, 2021.

[53] *Consequential-LCA (2020). Forecasting and time horizon*. In: https://consequential-lca.org/clca/marginal-suppliers/forecasting-time-horizon/. (Accessed on 2021-03); Aalborg, Denmark: 2.-0 LCA consultants, 2020.

[54] Regett, Anika et al.: *Emission Assessment of Electricity: Mix vs. Marginal Power Plant Method.* In: 2018 15th International Conference on the European Energy Market (EEM). Piscataway, USA: IEEE, 2018.

[55] *Kraftwerksliste der Bundesnetzagentur* - Version: 01.04.2020: https://www.bundesnetzagentur.de/DE/Sachgebiete/ElektrizitaetundGas/Unternehmen_Institutionen/Versorgungssicherheit/Erzeugungskapazitaeten/Kraftwerksliste/kraftwerksliste-node.html. (Accessed on 2020-10-12); Bonn, Germany: Bundesnetzagentur, 2020.

[56] *WEPP Database (Europe)*. Washington, DC, USA: Platts, 2018.

[57] *Kraftwerke in Deutschland (ab 100 Megawatt elektrischer Leistung)*: https://www.umweltbundesamt.de/dokument/datenbank-kraftwerke-in-deutschland. (Accessed on 2020-03-28); Dessau-Roßlau, Germany: Umweltbundesamt, 2018.

[58] Ellersdorfer, Ingo; Hundt, Matthias; Sun, Ninghong; Voß, Alfred: *Preisbildungsanalyse des deutschen Elektrizitätsmarktes*. Stuttgart, Germany: Institut für Energiewirtschaft und Rationelle Energieanwendung (IER), Universität Stuttgart, 2008.

[59] Pellinger, Christoph; Schmid, Tobias; et al.: *Merit Order der Energiespeicherung im Jahr 2030 - Hauptbericht*. Munich, Germany: Research Center for Energy Economics e.V. (FfE), 2016.

[60] Böing, F. et al.: *Das Merit-Order-Dilemma der Emissionen - Eine Diskussionsgrundlage zur klimapolitischen Debatte*. Munich, Germany: Research Center for Energy Economics e.V. (FfE) e.V., 2019.

[61] *EU-Kommission: Überarbeitung für Phase 4 (2021–2030)*. In: https://ec.europa.eu/clima/policies/ets/revision_de. (Accessed on 2018-12-17); (Archived by WebCite® at http://www.webcitation.org/74jWNcPOp); Brussels, Belgium: European Commission, 2018.

[62] Ostermann, Adrian et al.: *Analysen zum EU-ETS und Bewertung von CO_2-Verminderungsmaßnahmen*. In: 11. Internationale Energiewirtschaftstagung an der TU Wien; Vienna, Austria: TU Wien, 2019.

[63] *Energiebilanz der Bundesrepublik Deutschland 2018*: https://ag-energiebilanzen.de/index.php?article_id=29&fileName=bilanz18d.xls. (Accessed on 2020-06-18); Berlin, Germany: AG Energiebilanzen e.V. (AGEB), 2020 (revised: 2020).

[64] *Estonia 2019 Review. ENERGY POLICIES OF IEA COUNTRIES*. Paris, France: International Energy Agency, 2019.

[66] *Gesetz für den Ausbau erneuerbarer Energien (Erneuerbare-Energien-Gesetz - EEG 2017) § 78 Stromkennzeichnung entsprechend der EEG-Umlage (EEG §78)*. Issued on 2014-07-21, Version from 2017-07-17; Berlin, Germany: Bundesministerium für Wirtschaft und Energie, 2017.

[68] *Gesetz über die Elektrizitäts- und Gasversorgung (Energiewirtschaftsgesetz - EnWG) § 13 Systemverantwortung der Betreiber von Übertragungsnetzen (EnWG)*. Issued on 2005-07-07, Version from 2019-05-13; Berlin, Germany: Bundesministerium der Justiz und für Verbraucherschutz, 2019.

[69] *Gesetz für den Ausbau erneuerbarer Energien (Erneuerbare-Energien-Gesetz - EEG 2017)*. Berlin, Germany: Bundesregierung Deutschland, 2017.

[70] *Das Erneuerbare-Energien-Gesetz*. In: https://www.erneuerbare-energien.de/EE/Redaktion/DE/Dossier/eeg.html?cms_docId=401880. (Accessed on 2019-11-05); Berlin, Germany: Bundesministerium für Wirtschaft und Energie (BMWi), 2019.

[71] *Monitoringbericht 2019*. Bonn, Germany: Bundesnetzagentur für Elektrizität, Gas, Telekommunikation, Post und Eisenbahn, 2020.

[72] *Quartalsbericht Netz- und Systemsicherheit - Viertes Quartal 2019*. Bonn, Germany: Bundesnetzagentur für Elektrizität, Gas, Telekommunikation, Post und Eisenbahnen, 2019.

[73] *Entwurf eines Gesetzes zur Beschleunigung des Energieleitungsausbaus*. Issued on 2020-10-01, Version from 2018-12-11; Berlin, Germany: Bundesministerium für Wirtschaft und Energie, 2018.

[74] *Redispatch 2.0 - Mindestfaktor-Festlegung Konsultation*. In: https://www.bundesnetzagentur.de/DE/Sachgebiete/ElektrizitaetundGas/Unternehmen_Institutionen/Versorgungssicherheit/Engpassmanagement/Redispatch/redispatch-node.html. (Accessed on 2020-11-24); Bonn, Germany: Bundesnetzagentur (BNetzA), 2020.

[75] *Netztransparenz.de - Informationsplattform der deutschen Übertragungsnetzbetreiber* in: http://www.netztransparenz.de/de/index.htm. (Accessed on 2020-11-18); Berlin, Dortmund, Bayreuth, Stuttgart; Germany: 50Hertz Transmission GmbH, Amprion GmbH, TransnetBW GmbH, TenneT TSO GmbH, 2014.

[76] Fattler, Steffen et al.: *Einspeisemanagement - Auf der Suche nach den Ursachen*. In: ET - Energiewirtschaftliche Tagesfragen 11/2017. Essen, Germany: etv Energieverlag, 2017.

[77] Simon, Köppl et al.: *Congestion management and its interdependency with the energy system in Germany - an empirical analysis*. In: 19th International Workshop on Large-Scale Integration of Wind Power into Power Systems as well as on Transmission Networks for Offshore Wind Plants; Munich, Germany: Research Center for Energy Economics e. V (FfE)., 2020.

[78] *Quartalsbericht Netz- und Systemsicherheit - Gesamtes Jahr 2019*. Bonn, Germany: Bundesnetzagentur für Elektrizität, Gas, Telekommunikation, Post und Eisenbahnen, 2019.

[79] Corder, Gregory W. et al.: *Nonparametric Statistics for Non-Statisticians*. New Jersey: John Wiley & Sons, Incorporated, 2011.

[80] Fattler, Steffen et al.: *Potenzialanalyse zur Ladesteuerung von Elektrofahrzeugen im Engpassmanagement*. Munich, Germany: Research Center for Energy Economics e.V. (FfE), published at 11. Internationalen Energiewirtschaftstagung in Wien, Austria, 2019.

[81] Köppl, Simon; Samweber, Florian; Bruckmeier, Andreas; Böing, Felix; Hinterstocker, Michael; Kleinertz, Britta; Konetschny, Claudia; Müller, Mathias; Schmid, Tobias; Zeiselmair, Andreas: *Projekt MONA 2030: Grundlage für die Bewertung von Netzoptimierenden Maßnahmen - Teilbericht Basisdaten*. Munich, Germany: Research Center for Energy Economics e.V. (FfE), 2017.

[82] *OpenStreetMap und Mitwirkende: Elemente in OSM. OpenStreetMap Wiki, 2017*. URL: http://wiki.openstreetmap.org/wiki/DE:Elemente (accessed on 18.04.2017). (Archived by WebCite® at http://www.webcitation.org/6poMjpscl).OpenStreetMap Wiki, 2017.

[83] Wiegmans, Bart: *Improving the Topology of an Electric Network Model Based On Open Data*. Groningen, Netherlands: University of Groningen, 2016.

[84] Medjroubi, W.; Matke, C.: *SciGRID Open Source Transmission Network Model - USER GUIDE V 0.2*. Oldenburg, Germany: SciGRID, 2015.

[85] Aurenhammer, Franz: *Voronoi Diagrams - A Survey of a Fundamental Geometric Data Structure*. In: ACM Computing Surveys, Vol. 23, No. 3. New York, USA: Association for Computing Machinery (ACM), 1991.

[86] Schäuble, Johannes et al.: *Generating electric vehicle load profiles from empirical data of three EV fleets in Southwest Germany*. Karlsruhe, Germany: Karlsruhe Institut für Technologie (KIT), 2017.

[90] Gerossier, Alexis et al.: *Modeling and Forecasting Electric Vehicle Consumption Profiles*. In: 11th Mediterranean Conference on Power Generation, Transmission, Distribution and Energy Conversion (MEDPOWER 2018); Dubrovnik, Croatia: MINES ParisTech, PERSEE-Center for Processes, Renewable Energies and Energy Systems, PSL University, 2018.

[91] Schmidt-Achert, Tapio: *Statistical Modelling of German Traffic Behavior for the Evaluation of Charging Strategies of Electric Vehicles* . Master Thesis. Published by Technische Universität München, supervised by Mauch, Wolfgang: Munich, Germany, 2020.

[92] Nobis, Philipp: *Entwicklung und Anwendung eines Modells zur Analyse der Netzstabilität in Wohngebieten mit Elektrofahrzeugen, Hausspeichersystemen und PV-Anlagen*. Dissertation. Munich, Germany: Technische Universität München - Fakultät für Elektrotechnik und Informationstechnik, 2016.

[93] Mauch, Wolfgang Prof. Dr.-Ing.; Nobis, Philipp Dipl.-Ing.; Pellinger, Christoph Dipl.-Phys.; Staudacher, Thomas Dipl.-Phys.; Hener, Heinrich; Knodt, Janina; Koppelt, Kristoffer; Schwerd, Stephan; Pfrogner, Magnus; Münst, Christopher; Wimmer, Patrick: *eFlott - Wissenschaftliche Analysen zur Elektromobilität*. Munich, Germany: Research Center for Energy Economics e.V. (FfE), 2011.

[94] Follmer, Robert; Gruschwitz, Dana; Jesske, Birgit; Quandt, Sylvia; Lenz, Barbara; Nobis, Claudia; Köhler, Katja; Mehlin, Markus: *Mobilität in Deutschland 2008 - Struktur – Aufkommen – Emissionen – Trends*. Bonn, Germany: infas Institut für angewandte Sozialwissenschaft GmbH, 2010.

[95] *Mobilität in Deutschland 2017 - Datensatz*; Bonn, Germany: infas Institut für angewandte Sozialwissenschaft GmbH, 2019.

[96] *Deutsches Mobilitätspanel (MOP) - Längsschnittstudie zum Mobilitätsverhalten der Bevölkerung*. Karlsruhe, Germany: Institut für Verkehrswesen, Karlsruhe Institut für Technologie (KIT), 2019.

[97] Wermuth, Manfred: *Kraftfahrzeugverkehr in Deutschland 2010 (KiD 2010) - Schlussbericht*. Braunschweig, Germany: Verkehrsforschung und Infrastrukturplanung GmbH, 2012.

[98] Dallinger, David: *Plug-in electric vehicles integrating fluctuating renewable electricity* - Dissertation. Kassel, Germany: Universität Kassel, Fachbereich Elektrotechnik, 2012.

[99] Heinz, Daniel: *Erstellung und Auswertung repräsentativer Mobilitäts- und Ladeprofile für Elektrofahrzeuge in Deutschland*. Bachelor Thesis. Published by Karlsruher Institut für Technologie - Institut für Industriebetriebslehre und Industrielle Produktion (IIP), betreut durch Ried, Dipl.-Wi.-Ing. Sabrina: Karlsruhe, Germany, 2018.

[100] Harbrecht, Alexander et al.: *Behavior-oriented Modeling of Electric Vehicle Load Profiles: A Stochastic Simulation Model Considering Different Household Characteristics, Charging Decisions and Locations*. In: Working Paper Series in Production and Energy 29. Karlsruhe, Germany: Karlsruher Institut für Technologie, 2018.

[101] Pareschi, Giacomo et al.: *Are travel surveys a good basis for EV models? Validation of simulated charging profiles against empirical data*. In: Applied Energy 275/220. Zürich, Switzerland: ETH, 2020.

[102] Dinkel, Felix: *Entwicklung eines integrierten Generators für Lastgänge und Mobilitätsprofile privater Haushalte unter Verwendung von Markow-Ketten*. Master Thesis. Published by Technische Universität München, supervised by the Research Center for Energy Economics e. V.: Munich, Germany, 2019.

[103] Köppl, Simon Dipl.-Ing.; Samweber, Florian Dipl.-Ing.: *Das Projekt MONA 2030 - Das zeigt der Vergleich der Netzoptimierenden Maßnahmen in: MONA Ergebnisveranstaltung*. Munich, Germany: Research Center for Energy Economics e.V. (FfE), 2017.

[104] Fattler, Steffen; Böing, Felix; Pellinger, Christoph: *Ladesteuerung von Elektrofahrzeugen und deren Einfluss auf betriebsbedingte Emissionen* in: IEWT 2017 - 10. Internationale Energiewirtschaftstagung Wien, Austria. TU Wien 2017.

[105] Follmer, Robert; et al.: *Mobilität in Deutschland 2008 - Datensatz auf DVD*. Clearingstelle für Verkehr. Bonn, Germany: infas Institut für angewandte Sozialwissenschaft, 2010.

[106] Fattler, Steffen et al.: *Charge optimization of privately and commercially used electric vehicles and its influence on operational emissions*. Munich, Germany: Research Center for Energy Economics, 2018.

[107] Ebner, Michael et al.: *Kurzstudie Elektromobilität - Modellierung für die Szenarienentwicklung des Netzentwicklungsplans*. Munich, Germany: Research Center for Energy Economics e.V. (FfE), 2019.

[108] *Förderung von elektrisch betriebenen Fahrzeugen - Merkblatt für Anträge nach der Richtlinie zur Förderung des Absatzes von elektrisch betriebenen Fahrzeugen (Umweltbonus) vom 26.02.2018 (gilt für alle ab dem 03.03.2018 gestellten Anträge)*. Eschborn, Germany: Bundesamt für Wirtschaft und Ausfuhrkontrolle, 2018.

[109] *Regulation (EC) No 443/2009 of the European Parliament and of the Council of 23 April 2009, setting emission performance standards for new passenger cars as part of the community's integrated approach to reduce CO_2 emissions from light-duty vehicles*. Issued on 2009-04-23, Version from 2018-05-17; Brussels, Belgium: European Union, 2018.

[110] *Jahresbilanz des Fahrzeugbestandes am 1. Januar 2020*. In: https://www.kba.de/DE/Statistik/Fahrzeuge/Bestand/b_jahresbilanz.html. (Accessed on 2020-04-01); Flensburg, Germany: Kraftfahrtbundesamt, 2020.

[111] Schlesinger, Michael; Lindenberger, Dietmar; Lutz, Christian: *Entwicklung der Energiemärkte - Energiereferenzprognose - Projekt Nr. 57/12 - Studie im Auftrag des Bundesministeriums für Wirtschaft und Technologie*. Berlin, Germany: Bundesministerium für Wirtschaft und Technologie (BMWi), 2014.

[112] Adolf, Jörg Dr.; Rommerskirchen, Stefan Dr.: *Shell PKW-Szenarien bis 2040 - Fakten, Trends und Perspektiven für Auto-Mobilität*. Hamburg, Germany: Shell Deutschland Oil GmbH, 2014.

[113] Zimmer, Wiebke Dr.; Blanck, Ruth; Bergmann, Thomas; Mottschall, Moritz: *Renewbility III - Optionen einer Dekarbonisierung des Verkehrssektors*. Berlin, Germany: Öko-Institut e. V., 2016.

[114] Knörr, Wolfgang; Heidt, Christoph; Gores, Sabine; Bergk, Fabian: "*Aktualisierung "Daten- und Rechenmodell: Energieverbrauch und Schadstoffemissionen des motorisierten Verkehrs in Deutschland 1960-2035" (TREMOD) für die Emissionsberichterstattung 2016 (Berichtsperiode 1990-2014) - Endbericht*. Heidelberg, Germany: Ifeu - Institut für Energie- und Umweltforschung Heidelberg GmbH, 2016.

[115] *dena-Leitstudie Integrierte Energiewende - Zwischenfazit Impulse und Erkenntnisse aus dem Studienprozess*. Berlin, Germany: Deutsche Energie-Agentur GmbH (dena), 2017.

[116] Nationale Plattform Elektromobilität (NPE): *Fortschrittsbericht 2018 – Markthochlaufphase*. Berlin, Germany: Gemeinsame Geschäftsstelle Elektromobilität der Bundesregierung (GGEMO), 2018.

[117] *Netzentwicklungsplan Strom 2030 (Version 2019), zweiter Entwurf*. Berlin, Dortmund, Bayreuth, Stuttgart, Germany: 50Hertz Transmission GmbH, Amprion GmbH, TenneT TSO GmbH, TransnetBW GmbH, 2019.

[118] Prognos et al.: *Klimaneutrales Deutschland - In drei Schritten zu null Treibhausgasen bis 2050 über ein Zwischenziel von -65 % im Jahr 2030 als Teil des EU-Green-Deals*. Berlin, Germany: Agora Energiewende, 2020.

[119] *Eckpunkte für das Klimaschutzprogramm 2030*. Berlin, Germany: Fassung nach Klimakabinett, Bundesregierung, 2019.

[120] Dossow, Patrick et al.: *Application-based energy and emission balances for Europe - eXtremOS final report*. Munich, Germany: Research Center for Energy Economics e. V. (FfE), 2020.

[121] *TYNDP 2018 Scenario Report*. Brussels, Belgium: ENTSO-E AISBL, 2018.

[122] *OpenStreetMap (OSM) - Die freie Wiki-Weltkarte. Veröffentlicht unter der freien CC-BY-SA-Lizenz durch OpenStreetMap und Mitwirkende*. http://www.openstreetmap.org/, 2010.

[123] *Regionaldatenbank Deutschland*: https://www.regionalstatistik.de/genesis/online/; Wiesbaden, Germany: Statistische Ämter des Bundes und der Länder, 2017.

[124] *Marktstammdatenregister - Öffentliche Marktakteursübersicht*: https://www.marktstammdatenregister.de/MaStR/Akteur/Marktakteur/Index. (Accessed on 2020-11-22); Bonn, Germany: Bundesnetzagentur, 2020.

[125] *Ergebnisse ohne Grenzen: der Zensus-Atlas in: www.zensus2011.de*. (Accessed on 23.11.2015); Wiesbaden, Germany: Statistische Ämter des Bundes und der Länder, 2015.

[126] Pasaoglu, Guzay et al.: *Projections for Electric Vehicle Load Profiles in Europe Based on Travel Survey Data*. Luxemburg: European Commission - Joint Research Centre, 2013.

[127] BMVI: *Mobilität in Deutschland - MiD Ergebnisbericht*. In: https://www.bmvi.de/SharedDocs/DE/Artikel/G/mobilitaet-in-deutschland.html. (Accessed on 2020-04-01); Bonn, Germany: Bundesministerium für Verkehr und digitale Infrastruktur, 2017.

[128] *Bidirektionales Lademanagement (BDL) - Intelligentes Zusammenspiel von Elektrofahrzeugen, Ladeinfrastruktur und Energiesystem*. In: https://www.ffe.de/themen-und-methoden/mobilitaet/932-bidirektionales-lademanagement-bdl-intelligentes-zusammenspiel-von-elektrofahrzeugen-ladeinfrastruktur-und-energiesystem. (Accessed on 2021-01-29); Munich, Germany: Research Center for Energy Economics e.V. (FfE), 2021.

[130] Held, Michael et al.: *Abschlussbericht: Bewertung der Praxistauglichkeit und Umweltwirkungen von Elektrofahrzeugen*. Berlin, Germany: Bundesministerium für Verkehr und digitale Infrastruktur (BMVI), 2016.

[131] Huss, Arno; Maas, Heiko; Hass, Heinz: *JEC WELL-TO-WHEELS ANALYSIS*. Ispra, Italy: European Commission, Joint Research Centre, Institute for Energy and Transport, 2013.

[132] *Batterieelektrische Fahrzeuge in der Praxis*. Vienna, Austria: Österreichischer Verein für Kraftfahrzeugtechnik (ÖVK), 2012

[133] Pellinger, Christoph; Schmid, Tobias; et al.: *Merit-Order der Energiespeicherung im Jahr 2030 - Entwicklung und Darstellung kostenoptimierter Speicherinfrastrukturen in Form von Merit Order Kurven* in: http://www.ffe.de/die-themen/speicher-und-netze/414. Munich, Germany: Research Center for Energy Economics e.V. (FfE), 2012.

[134] *Datensatz zu Automatischen Zählstellen auf Autobahnen und Bundesstraßen* – Accessed data from: https://www.bast.de/BASt_2017/DE/Verkehrstechnik/Fachthemen/v2-verkehrszaehlung/zaehl_node.html. (Accessed on 2020-07-18); Bergisch Gladbach, Germany: Bundesanstalt für Verkehrswesen, 2018.

[135] Westerburg, Michael et al.: *Herausforderungen und Ergebnisse im BMUB Förderprojekt „Gesteuertes Laden V3.0" (Challenges and results in the BMUB research project 'Controlled Charging V3.0')*. In: Grid Integration of Electric Mobility; Wiesbaden, Germany: Springer Vieweg, 2016.

[136] Quirós-Tortós, Jairo et al.: *A statistical analysis of EV charging behavior in the UK*. Montevideo, Uruguay: IEEE, 2015.

[138] Fischer, David et al.: *Electric vehicles' impact on residential electric local profiles - A stochastic modelling approach considering socio-economic, behavioural and spatial factors*. Amsterdam, Netherlands: Fraunhofer Institute for Solar Energy Systems, 2019.

[139] Hu, Liang et al.: *Modeling Charging Behavior of Battery Electric Vehicle Drivers: A Cumulative Prospect Theory Based Approach*. Iowa, USA: Iowa State University, 2019.

[140] Englberger, Sabine: *Optimized Prosumer Households with Bidirectional Electric Vehicles: a Techno-Economic Analysis of Self-Consumption, Battery Utilization, and Distribution Grid Effects*. Master Thesis. Published by Technische Universität Müchen (TUM), supervised by Prof. Dr.-Ing Wagner, Ulrich; Prof. Dr.-Ing Mauch, Wolfgang; Müller, Mathias: Munich, Germany, 2020.

[141] FfE-Grid-Simulation Model GridSIM in: https://www.ffe.de/gridsim. Munich, Germany: Research Center for Energy Economics e.V. (FfE), 2016

[142] Morlock, Elena Sophie: *Entwicklung eines techno-ökonomischen Bewertungsmodells für Vehicle-to-Home-Systeme - Analyse der Erlöspotenziale von bidirektionalen Elektrofahrzeugen durch Eigenverbrauchserhöhung sowie durch tarifoptimiertes Laden und Entladen anhand eines Optimierungsmodells in MATLAB*. Master Thesis. Published by Technische Universität Berlin, supervised by Forschungsgesellschaft für Energiewirtschaft mbH. Berlin, Germany, 2020.

[143] *C/sells – Großflächiges Schaufenster im Solarbogen Süddeutschlands* in: www.ffe.de/csells. Munich, Germany: Research Center for Energy Economics e.V. (FfE), 2017.

[144] Schwencke, Tilman et al.: *BDEW-Strompreisanalyse Januar 2019 - Haushalte und Industrie*. Berlin, Germany: BDEW Bundesverband der Energie- und Wasserwirtschaft e.V., 2019.

[145] *Ladestationen für Elektroautos: Das kostet der Strom*. In: https://www.adac.de/rund-ums-fahrzeug/elektromobilitaet/laden/elektroauto-ladesaeulen-strompreise/. (Accessed on 2021-02-25); Munich, Germany: ADAC, 2021.

[146] Dodson, Tristan et al.: *Electric Vehicle Charging Behaviour Study*. Cambridge, United Kingdom: Element Energy Limited, 2019.

[147] Felix, Böing: *Cross-sector assessment of CO_2 abatement measures and their impact on the transmission grid*. Dissertation. Published by the TU München, supervised by: Wagner, Ulrich: Munich, Germany, 2020.

[148] ten Broeke, Guus et al.: *Which Sensitivity Analysis Method Should I Use for My Agent-Based Model?* Wageningen, Netherlands: Wageningen University, 2016.

[149] *GreenGear.de - Liste der Elektroautos im Jahr 2021*: https://www.greengear.de/vergleich-uebersicht-elektroautos-eautos; Karlsruhe, Germany: GreenGear.de, 2021 (Abruf: 03/2021).

[150] Danzer, Michael et al.: *Aging of lithium-ion batteries for electric vehicles*. Ulm, Germany: Zentrum für Sonnenenergie- und Wasserstoff-Forschung Baden-Württemberg, 2015.

[151] Neubauer, Jeremy; Pesaran, Ahmad: *The ability of battery second use strategies to impact plug-in electric vehicle prices and serve utility energy storage applications* in: Journal of Power Sources, 196, S.10351 - 10358. Golden, Colorado, USA: National Renewable Energy Laboratory, 2011.

[152] Wood, Eric; Alexander, Marcus; Bradley, Thomas H.: *Investigation of battery end-of-life conditions for plug-in hybrid electric vehicles in*: Journal of Power Sources, Bd. 196. Amsterdam, Netherlands: Elsevier Ltd, 2011.

[153] Faria, R. et al.: *Primary and secondary use of electric mobility batteries from a life cycle perspective* in: Journal of Power Sources 262 (2014) 169. Oxford, United Kingdom: Elsevier, 2014.

[154] Heymans, Catherine; Walker, SeanB.; Young, Steven B.; Fowler, Michael: *Economic analysis of second use electric vehicle batteries for residential energy storage and load-levelling* in: Energy Policy 71(2014) 22-30. Waterloo, USA: University of Waterloo, 2014.

[155] Keil, Peter: *Aging of Lithium-Ion Batteries in Electric Vehicles*. Dissertation. Published by TU München, exam approved by Jossen, Andreas und Kowal, Julia: Munich, Germany, 2017.

[156] Fattler, Steffen, Conrad, Jochen, Regett, Anika et al.: *Dynamis Datenanhang - Dynamis - Dynamische und intersektorale Maßnahmenbewertung zur kosteneffizienten Dekarbonisierung des Energiesystems* - Online: https://www.ffe.de/dynamis. Munich, Germany: Research Center for Energy Economics e.V. (FfE), 2019. DOI: 10.34805/ffe-146-19

[157] Fattler, Steffen; Regett, Anika: *Environmental Impact of Electric Vehicles: Influence of Intelligent Charging Strategies*. In: Grid Integration of Electric Mobility 2019; Munich, Germany: Research Center for Energy Economics e. V. (FfE), 2019.

[158] Regett, Anika et al.: *Environmental Impact of Electric Vehicles: Potential of the Circular Economy?*. In: Der Antrieb von morgen 2019 (p. 121-140). Wiesbaden, Germany: Springer Vieweg, 2019.

[159] Hawkins, Troy et al.: *Comparative environmental life cycle assessment of conventional and electric vehicles - supporting information*. In: Journal of Industrial Ecology 17(1), 53-64. Hoboken: Wiley, USA, 2013.

[160] *ADAC Ecotest*. In: www.adac.de/infotestrat/tests/eco-test. (Accessed on 2019-08-28); Munich, Germany: ADAC e.V., 2019.

[161] Thielmann, Axel et al.: *Energiespeicher-Roadmap (Update 2017) - Hochenergie-Batterien 2030+ und Perspektiven zukünftiger Batterietechnologien*. Karlsruhe, Germany: Fraunhofer-Institut für System- und Innovationsforschung ISI, 2017.

[162] *Kurzbericht - Verkehr in Kilometern, Jahr 2017*. Flensburg, Germany: Kraftfahrt-Bundesamt, 2018.

[163] *Submission under the United Nations Framework Convention on Climate Change and the Kyoto Protocol 2016 - National Inventory Report for the German Greenhouse Gas Inventory 1990 - 2014*. Dessau-Roßlau, Germany: UBA - Umweltbundesamt, 2016.

[164] *The ecoinvent Database, Version 3.5*: www.ecoinvent.org; Zürich, Switzerland: ecoinvent, 2018.

[165] Wieler, Jochen: *Aktuelle Elektroautos im Test: So hoch ist der Stromverbrauch*. In: https://www.adac.de/rund-ums-fahrzeug/tests/elektromobilitaet/stromverbrauch-elektroautos-adac-test/. (Accessed on 2020-07-18); Munich, Germany: Allgemeiner Deutscher Automobil-Club e.V. (ADAC), 2020.

[166] *fueleconomy*. In: https://www.fueleconomy.gov/. (Accessed on 2021-01-05); USA: U.S. Department of Energy, 2021.

[167] *German magazine compares real-world electric-car ranges, efficiencies in cold weather*. In: https://www.greencarreports.com/news/1114660_german-magazine-compares-real-world-electric-car-ranges-efficiencies-in-cold-weather. (Accessed on 2021-01-01); El Segundo, California, USA: Green Car Reports, 2021.

[168] *Real life EV test - which one went furthest with highest efficiency?* In: https://drivetribe.com/p/real-life-ev-test-which-one-went-Fa5yDo9dTkysjS24C7wBTw?iid=T691a0N5TlqETnmHuJgFkw (Accessed on 2021-01); London, United Kingdom: Drivetribe, 2021.

[169] *Elektroautos im Vergleich*. In: https://www.elektroauto-news.net/wiki/elektroauto-vergleich. (Accessed on 2021-01); Neckargemünd, Germany: Elektroauto-News.net, 2021.

11 Publications of the Author

Simon Köppl, Adrian Ostermann, Steffen Fattler: "*Congestion management and its interdependency with the energy system in Germany - an empirical analysis*". In: 19th International Workshop on Large-Scale Integration of Wind Power into Power Systems as well as on Transmission Networks for Offshore Wind Plants. Munich, Germany, 2020.

Steffen Fattler and Anika Regett. "*Environmental Impact of Electric Vehicles: Influence of Intelligent Charging Strategies*". In: Grid Integration of Electric Mobility - 4. Internationale ATZ-Fachtagung. Mannheim, Germany, 2019.

Adrian Ostermann and Steffen Fattler: „*Analysen zum EU-ETS und Bewertung von CO_2-Verminderungsmaßnahmen*". In: 11. Internationale Energiewirtschaftstagung an der TU Wien. Vienna, Austria, 2019.

Steffen Fattler; Jochen Conrad; Anika Regett et al.: „*Dynamis Hauptbericht - Dynamis - Dynamische und intersektorale Maßnahmenbewertung zur kosteneffizienten Dekarbonisierung des Energiesystems*" - Online: https://www.ffe.de/dynamis. Munich, Germany, 2019. DOI: 10.34805/ffe-144-19

Britta Kleinertz, Andrej Guminski, Anika Regett, Alois Kessler, Demir Gamze, Jochen Conrad, Steffen Fattler, Simon Pichlmaier, Elsa Rouyrre and Serafin von Roon. "*Kosteneffizienz von fossilen und erneuerbaren Gasen zur CO_2-Verminderung im Energiesystem*". In: Zeitschrift für Energiewirtschaft 43 pp. 51–68, 2019.

Jochen Conrad; Anika Regett; Steffen Fattler; Fabian Jetter: „*Von statischen CO_2-Verminderungskosten zur dynamischen Bewertung von Klimaschutzmaßnahmen*". In: Energiewirtschaftliche Tagesfragen – Zeitschrift für Energiewirtschaft, Recht, Technik und Umwelt Ausgabe 10. Berlin, Germany, 2019.

Felix Böing, Anika Regett; Constanze Kranner, Christoph Pellinger, Steffen Fattler, Jochen Conrad: „*Das Merit-Order-Dilemma der Emissionen - Eine Diskussionsgrundlage zur klimapolitischen Debatte*". Munich, Germany, 2019.

Steffen Fattler, Adrian Ostermann, Michael Hinterstocker: "*Potenzialanalyse zur Ladesteuerung von Elektrofahrzeugen im Engpassmanagement*". In: 11. Internationale Energiewirtschaftstagung (IEWT). Vienna, Austria, 2019.

Jochen Conrad, Steffen Fattler, Anika Regett: „*Bewertung der dynamischen Systemeffekte von CO_2-Verminderungsmaßnahmen – Erläuterung des vierstufigen Bewertungsansatzes in dem Projekt Dynamis*". In: Netzwerktreffen Energie Systemanalyse. Berlin, Germany, 2018.

Anika Regett, Felix Böing, Jochen Conrad, Steffen Fattler, Constanze Kranner: "*Emission Assessment of Electricity: Mix vs. Marginal Power Plant Method*". In: European Energy Markets-Conference 2018. Łódź, Poland, 2018

Steffen Fattler, Simon Pichlmaier: „*Charge optimization of privately and commercially used electric vehicles and its influence on operational emissions*". In: 41th IAEE International Conference (International Association for Energy Economics). Groningen, Netherlands, 2018

Simon Pichlmaier, Steffen Fattler, Caspar Bayer: "*Modelling the Transport Sector in the Context of a Dynamic Energy System*". In: 41th IAEE International Conference (International Association for Energy Economics). Groningen, Netherlands, 2018

Steffen Fattler, Simon Pichlmaier, Thomas Estermann und Adrian Ostermann: "*Einspeisemanagement – Auf der Suche nach den Ursachen*". et - Energiewirtschaftliche Tagesfragen (2017) Heft 11

Steffen Fattler, Christoph Pellinger, Felix Böing: „*Ladesteuerung von Elektrofahrzeugen und deren Einfluss auf betriebsbedingte Emissionen*". In: 10. Internationale Energiewirtschaftstagung (IEWT). Vienna, Austria, 2017. Awarded with „Best Paper Award"

Ulrich Wagner, Wolfgang Mauch, Michael Dronia, Thomas Estermann, Sebastian Fischhaber, Steffen Fattler, Felix Böing: „*Faktencheck zur Elektromobilität und Marktprämie*" in: et - Energiewirtschaftliche Tagesfragen (2016) Heft 9

Florian Samweber, Steffen Fattler, Simon Köppl: "*Grid optimization employing electric vehicles in a cross-system comparison*" in: 1. Internationale ATZ-Konferenz Netzintegration der Elektromobilität. Wiesbaden, Germany, 2016.

Thomas Estermann, Florian Samweber, Steffen Fattler: „*Mehrwert des Smart Meter-Rollouts für die Implementierung von Netzoptimierenden Maßnahmen*". In: VDE Kongress Internet of Things. Mannheim, Germany, 2016

Steffen Fattler and Christoph: „*Auswertungen und Analysen zur International Grid Control Cooperation*". In: 9. Internationale Energiewirtschaftstagung (IEWT). Vienna, Austria, 2015.

Steffen Fattler and Christoph Pellinger: "*Influence of the time discrete trade of electricity on the demand for secondary control reserve*". In: ENERDAY 2015. Dresden, Germany, 2015

Christoph Pellinger and Steffen Fattler: „*Möglichkeiten und Grenzen des europäischen Verbundsystems - Eine empirische Analyse für den deutschen Kraftwerkspark - Basisjahr 2013*" in: VDI-Wissensforum Leittechnik in Kraftwerken. Nürnberg, Germany, 2014

12 Appendix

12.1 Completeness of ENTSO-E data

	Load					Generation by type					CBPF export					CBPF import				
	2015	2016	2017	2018	2019	2015	2016	2017	2018	2019	2015	2016	2017	2018	2019	2015	2016	2017	2018	2019
AL	62 %	12 %	0 %	0 %	0 %	0 %	0 %	0 %	0 %	0 %	98 %	100 %	100 %	100 %	80 %	97 %	100 %	100 %	100 %	80 %
AT	100 %	100 %	100 %	100 %	100 %	100 %	100 %	100 %	100 %	100 %	100 %	100 %	100 %	100 %	100 %	100 %	100 %	100 %	100 %	100 %
BA	0 %	0 %	84 %	99 %	100 %	0 %	0 %	81 %	87 %	100 %	98 %	100 %	100 %	100 %	100 %	98 %	100 %	100 %	100 %	100 %
BE	100 %	100 %	100 %	100 %	100 %	75 %	100 %	96 %	100 %	96 %	100 %	100 %	74 %	77 %	100 %	100 %	100 %	74 %	77 %	100 %
BG	100 %	100 %	100 %	100 %	100 %	100 %	100 %	74 %	100 %	100 %	83 %	100 %	99 %	98 %	95 %	90 %	80 %	99 %	98 %	95 %
CH	100 %	100 %	100 %	100 %	100 %	70 %	99 %	100 %	100 %	100 %	98 %	100 %	100 %	100 %	100 %	97 %	100 %	100 %	100 %	100 %
CY	0 %	28 %	100 %	98 %	85 %	44 %	100 %	100 %	98 %	85 %	0 %	0 %	0 %	0 %	0 %	0 %	0 %	0 %	0 %	0 %
CZ	100 %	99 %	100 %	100 %	100 %	100 %	100 %	100 %	100 %	100 %	100 %	100 %	100 %	100 %	100 %	100 %	100 %	100 %	100 %	100 %
DE	100 %	100 %	100 %	100 %	100 %	94 %	93 %	86 %	94 %	100 %	99 %	100 %	95 %	100 %	100 %	99 %	100 %	95 %	100 %	100 %
DK	100 %	100 %	100 %	100 %	100 %	100 %	100 %	100 %	100 %	100 %	100 %	100 %	100 %	100 %	83 %	100 %	100 %	100 %	100 %	83 %
EE	100 %	100 %	100 %	98 %	100 %	100 %	100 %	100 %	98 %	100 %	99 %	99 %	100 %	92 %	100 %	99 %	99 %	100 %	92 %	100 %
ES	100 %	100 %	100 %	100 %	100 %	100 %	100 %	100 %	100 %	100 %	100 %	100 %	100 %	100 %	100 %	100 %	100 %	100 %	100 %	100 %
FI	100 %	100 %	100 %	100 %	100 %	100 %	100 %	100 %	100 %	100 %	100 %	100 %	100 %	99 %	100 %	100 %	100 %	100 %	99 %	100 %
FR	100 %	100 %	100 %	100 %	100 %	100 %	100 %	100 %	100 %	100 %	100 %	99 %	100 %	100 %	100 %	100 %	99 %	100 %	100 %	100 %
GB	99 %	99 %	100 %	100 %	99 %	99 %	99 %	93 %	100 %	99 %	100 %	98 %	100 %	76 %	100 %	100 %	98 %	100 %	76 %	100 %
GR	100 %	99 %	100 %	100 %	100 %	99 %	99 %	100 %	100 %	100 %	98 %	99 %	100 %	100 %	100 %	100 %	99 %	100 %	100 %	100 %
HR	100 %	100 %	100 %	100 %	100 %	0 %	0 %	0 %	0 %	0 %	100 %	100 %	100 %	100 %	100 %	100 %	100 %	100 %	100 %	100 %
HU	100 %	100 %	100 %	100 %	100 %	100 %	100 %	100 %	100 %	94 %	100 %	100 %	100 %	100 %	100 %	100 %	100 %	100 %	100 %	100 %
IE	99 %	99 %	100 %	100 %	100 %	100 %	100 %	100 %	100 %	100 %	100 %	100 %	100 %	98 %	100 %	100 %	100 %	100 %	98 %	100 %
IT	100 %	100 %	100 %	100 %	100 %	3 %	100 %	100 %	100 %	99 %	93 %	100 %	100 %	100 %	86 %	93 %	100 %	100 %	100 %	86 %
LT	99 %	100 %	99 %	99 %	100 %	97 %	93 %	99 %	100 %	100 %	76 %	94 %	99 %	100 %	100 %	76 %	94 %	99 %	100 %	100 %
LU	100 %	100 %	100 %	100 %	100 %	0 %	0 %	0 %	0 %	0 %	0 %	0 %	37 %	100 %	100 %	0 %	0 %	37 %	100 %	100 %
LV	100 %	100 %	100 %	100 %	100 %	83 %	100 %	100 %	100 %	100 %	99 %	97 %	99 %	93 %	100 %	99 %	97 %	99 %	93 %	100 %
MD	0 %	0 %	0 %	0 %	0 %	0 %	0 %	0 %	0 %	0 %	0 %	0 %	24 %	99 %	95 %	0 %	0 %	24 %	99 %	95 %
ME	99 %	100 %	100 %	100 %	100 %	98 %	100 %	40 %	79 %	100 %	99 %	100 %	100 %	100 %	60 %	99 %	100 %	100 %	100 %	60 %
MK	91 %	91 %	86 %	97 %	92 %	0 %	54 %	84 %	95 %	89 %	98 %	66 %	99 %	98 %	96 %	89 %	99 %	99 %	98 %	96 %
NL	100 %	100 %	100 %	100 %	100 %	92 %	93 %	74 %	92 %	100 %	100 %	100 %	100 %	100 %	86 %	100 %	100 %	100 %	100 %	86 %
NO	100 %	100 %	100 %	100 %	99 %	100 %	100 %	99 %	100 %	100 %	100 %	100 %	100 %	100 %	100 %	100 %	100 %	100 %	100 %	100 %
PL	100 %	100 %	100 %	100 %	100 %	95 %	100 %	100 %	100 %	100 %	83 %	100 %	98 %	100 %	100 %	85 %	100 %	100 %	100 %	100 %
PT	100 %	100 %	100 %	100 %	100 %	100 %	100 %	100 %	100 %	100 %	100 %	100 %	100 %	100 %	100 %	100 %	100 %	100 %	100 %	100 %
RO	99 %	100 %	100 %	100 %	100 %	99 %	100 %	100 %	100 %	100 %	94 %	100 %	97 %	100 %	100 %	91 %	100 %	97 %	100 %	100 %
RS	91 %	100 %	100 %	100 %	100 %	0 %	2 %	100 %	100 %	100 %	97 %	100 %	100 %	100 %	100 %	98 %	100 %	100 %	100 %	100 %
SE	99 %	100 %	100 %	100 %	100 %	98 %	100 %	100 %	100 %	100 %	100 %	99 %	100 %	100 %	100 %	100 %	99 %	100 %	100 %	100 %
SI	100 %	100 %	100 %	100 %	100 %	100 %	100 %	100 %	100 %	100 %	100 %	100 %	100 %	100 %	100 %	100 %	100 %	100 %	100 %	100 %
SK	100 %	100 %	100 %	100 %	100 %	96 %	100 %	99 %	99 %	100 %	100 %	100 %	98 %	100 %	100 %	100 %	100 %	99 %	100 %	100 %
UA	0 %	0 %	25 %	99 %	95 %	0 %	0 %	0 %	0 %	0 %	97 %	100 %	65 %	99 %	98 %	92 %	100 %	63 %	99 %	98 %

excluded due to data quality/considered for evaluation

Figure 12-1: Completeness of data provided by ENTSO-E Transparency Platform and discussed in section 4.1.2. This evaluation forms the basis for the selection of countries that can be considered for the calculation of the historical consumption-based EMFs described in section 4.4

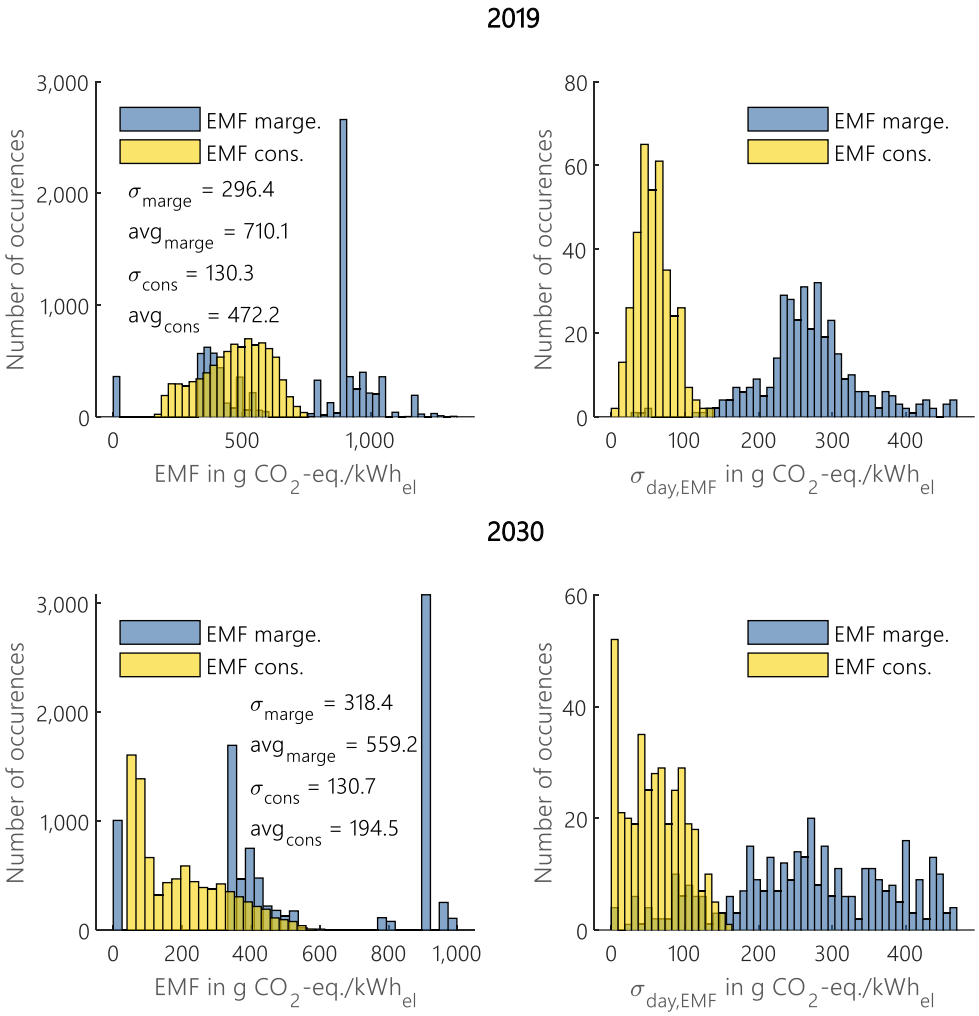

Figure 12-2: Histogram of marginal and consumption-based EMFs (left) and their daily Standard deviation (right) for the years 2019 and 2030. Discussion of these results for the year 2019 can be found in section 4.6.4.1.

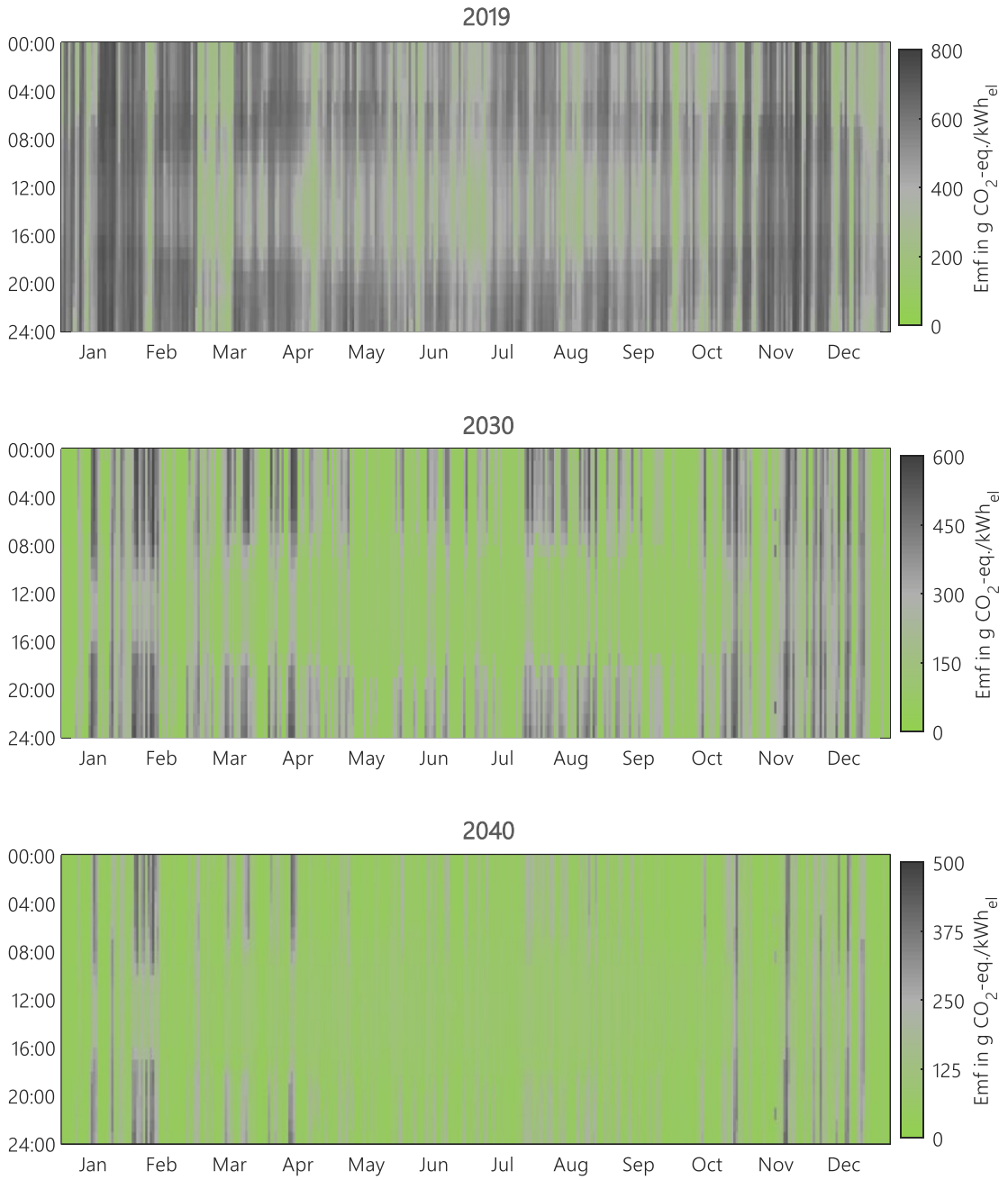

Figure 12-3: Heat map of consumption-based EMFs in 2019 (top), 2030 (middle) and 2040 (bottom) (see section 4.4)

12.3 Mobility behavior of behavior-homogeneous user groups

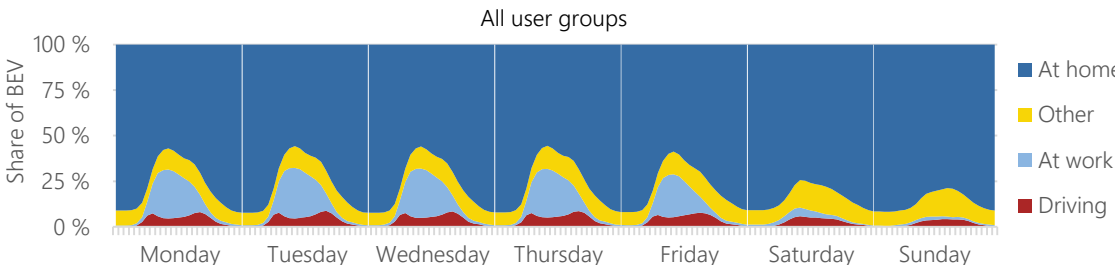

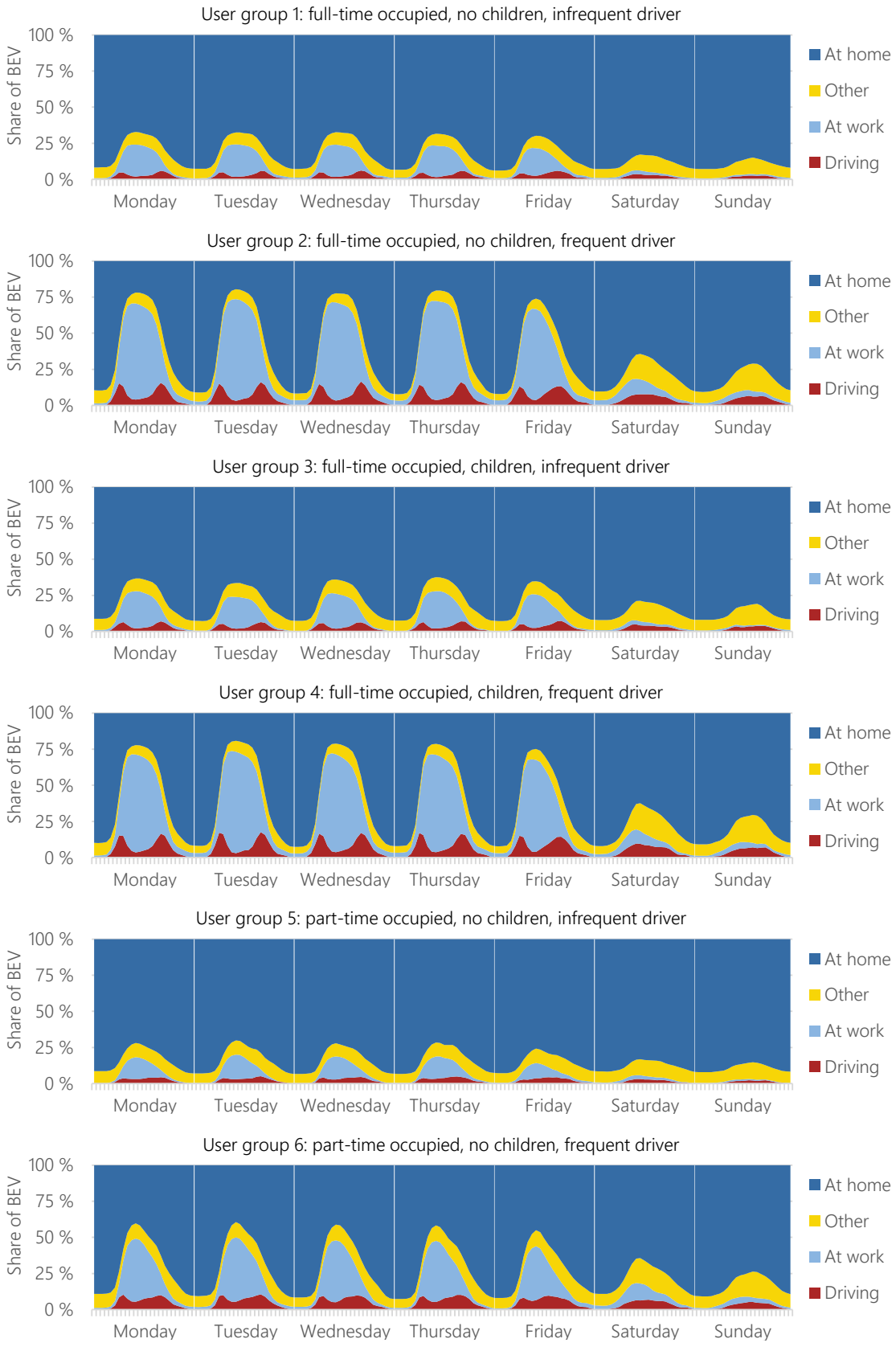
User group 1: full-time occupied, no children, infrequent driver
User group 2: full-time occupied, no children, frequent driver
User group 3: full-time occupied, children, infrequent driver
User group 4: full-time occupied, children, frequent driver
User group 5: part-time occupied, no children, infrequent driver
User group 6: part-time occupied, no children, frequent driver
Share of BEV
100 %
75 %
50 %
25 %
0 %
Monday
Tuesday
Wednesday
Thursday
Friday
Saturday
Sunday
At home
Other
At work
Driving

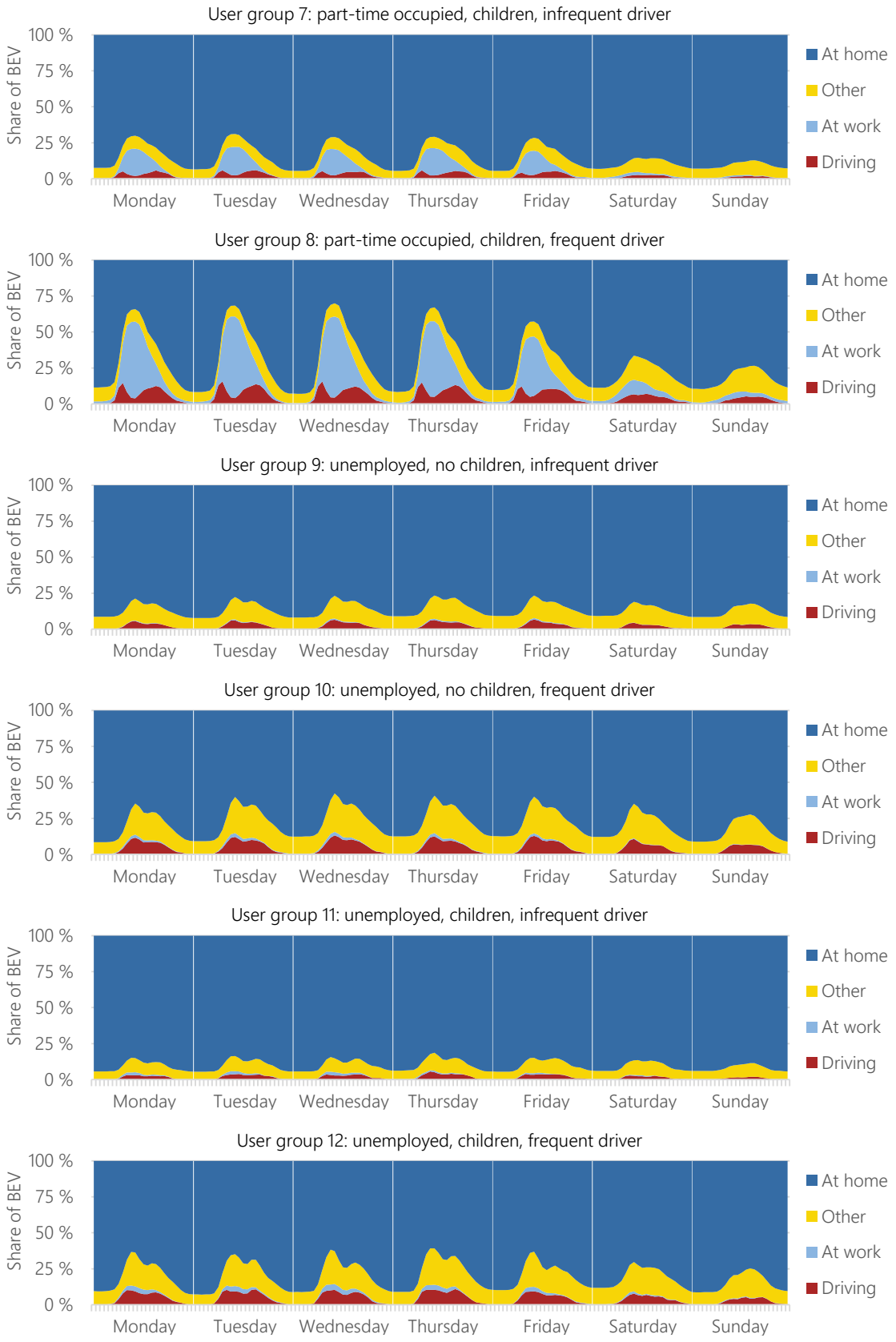

Figure 12-4: Average distribution of locations of user groups (see section 6.2.4)

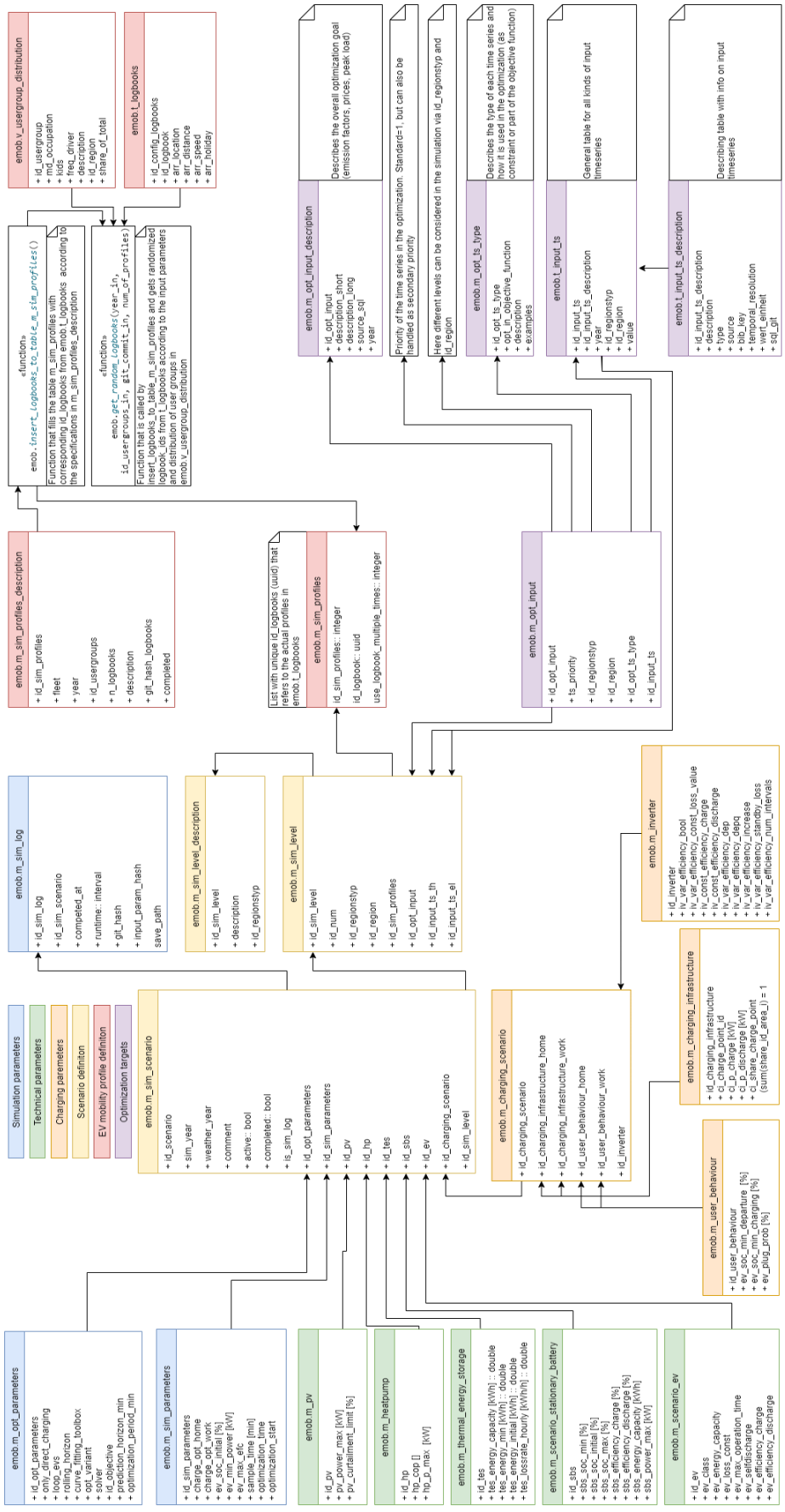

Figure 12-5: Database structure of the model eFLAME (see chapter 6)

Table 12-1: Electric consumption of current EV models in kWh/100 km

		Source:	ADAC [165]	U.S. Department of Energy [166]	Autobild Test [167]	Drivetribe Test [168]	Elektroauto news [169]
Small car	Microcars	Seat Mii Electric Plus	17.3				
		Renault Fluence Z.E.					14.0
		Smart Forfour EQ passion	18.4				15.4
		Chevrolet Spark		17.4			
		Volkswagen e-up! (18.7 kwh)			23.7		
		e.Go Life 20					11.9
		e.Go Life 40					12.1
		e.Go Life 60					12.5
		Smart EQ ForTwo Cabrio (60 kW)					14.5
		Smart ForTwo (17.6 kwh)			21.0	15.1	
		Honda Fit		18.0			
	Small car	BMW i3 (22 kWh)					12.9
		BMW i3 (33 kWh)					12.7
		BMW i3 (120 Ah)	17.9	18.6			
		Peugeot iOn					12.6
		Kia e-Soul EV Play					14.3
		Kia Soul (30 kwh)			18.0		
		Kia e-Soul (64 kWh) Spirit	18.8	19.2			14.6
		Renault Zoe Intens (52 kWh)	19.0				
		Renault Zoe Intens (41 kWh)	20.3		16.8	13.7	
		Hyundai Kona Elektro (150 kWh)					14.3
		Hyundai Kona Elektro (100 kWh)					14.3
		Hyundai Kona Elektro (64 kWh)	19.5	16.7		13.0	
Medium class	Compact class	VW e-Golf	17.3	17.4	17.2		12.7
		Peugeot iOn					18.0
		Chevrolet Bolt		17.4			
	Lower medium class	Hyundai Ioniq Elektro Style	16.3	15.5	14.6		
		Renaul Fluence Z.E.					14.0
		Kia e-Niro Spirit (64 kWh)	18.1	18.6			
		Opel Ampera-e First Edition	19.7		22.0		16.0
		Nissan Leaf 3.Zero e +					
		Nissan Leaf					20.6
		Nissan Leaf (30 kWh)					15.0
		Nissan Leaf Acenta (40 kWh)	22.1	18.6		18.9	
		Nissan Leaf e+ Tekna (62 kWh)	22.7	19.8			
	Medium class	Tesla Model 3 Standard Range+	19.5	14.9			14.1
		Tesla Model 3 Long Range AWD	20.9	15.5			
Luxury class	Luxury class	Tesla Model X 100D	24.0	21.7			
		Tesla Model S				19.5	
		Tesla Model S 70					20.5
		Tesla Model S P90D					23.3
		Tesla Model S 70 D					28.0
		Tesla Model S90D					17.7
		Porsche Taycan Turbo S			24.5		
		Porsche Taycan Turbo			23.0		
	SUV	Jaguar i-Pace EV400 S AWD	27.6	27.3		23.9	
		Mercedes EQC 400 AMG Line	27.6				
		Audi e-tron 55 quattro	25.8	26.7			

Table 12-2: Scenario definition of scenarios for cluster assessment described in section 7.7.2

Scenario ID	Description
Sc_1	Emission-optimized, Germany 2030: 11 kW and 40 kWh, charging only at home
Sc_2	Emission-optimized, Germany 2030: 22 kW and 40 kWh, charging only at home
Sc_3	Emission-optimized, Germany 2030: 11 kW and 100 kWh, charging only at home
Sc_4	Emission-optimized, Germany 2030: 22 kW and 100 kWh, charging only at home
Sc_5	Emission-optimized, Germany 2030: 11 kW, small car 40 kWh, charging only at home
Sc_6	Emission-optimized, Germany 2030: 11 kW, medium class 60 kWh, charging only at home
Sc_7	Emission-optimized, Germany 2030: 22 kW, medium class 60 kWh, charging only at home
Sc_8	Emission-optimized, Germany 2030: 3.7 kW, medium class 60 kWh, charging only at home
Sc_9	Emission-optimized, Germany 2030: 11 kW, luxury class 100 kWh, charging only at home
Sc_10	Emission-optimized, Germany 2030: 11 kW, medium class 80 kWh, charging only at home
Sc_11	Emission-optimized, Germany 2030: 11 kW, medium class 60 kWh, charging only at home, EFC_{max} = 100

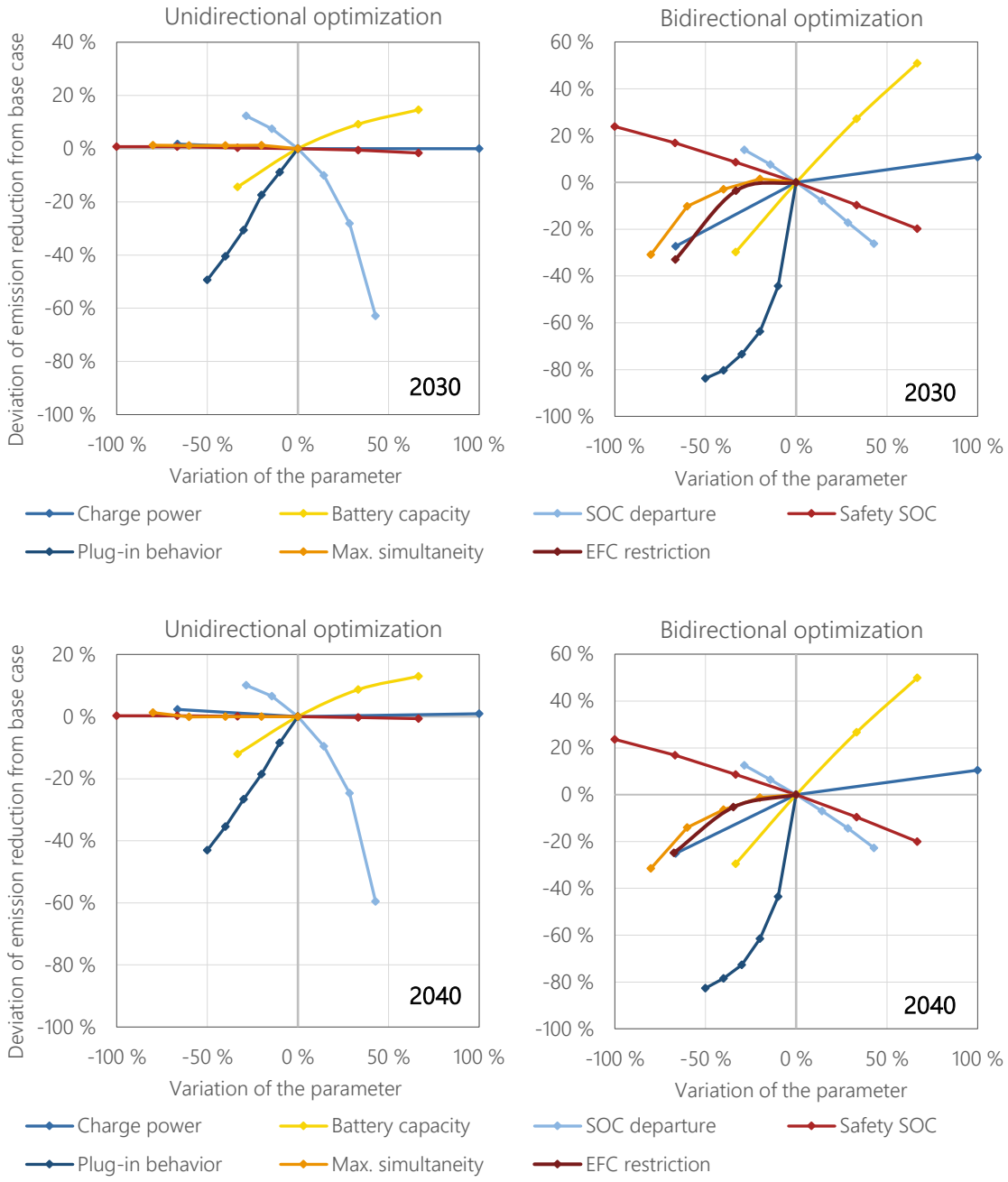

Figure 12-6: Overview of the considered sensitivities in the sensitivity analyses carried out in section 8.2 and their influence on annual emissions for the years 2030 and 2040, for detailed discussion of the underlying coherences, see section 8.2.6

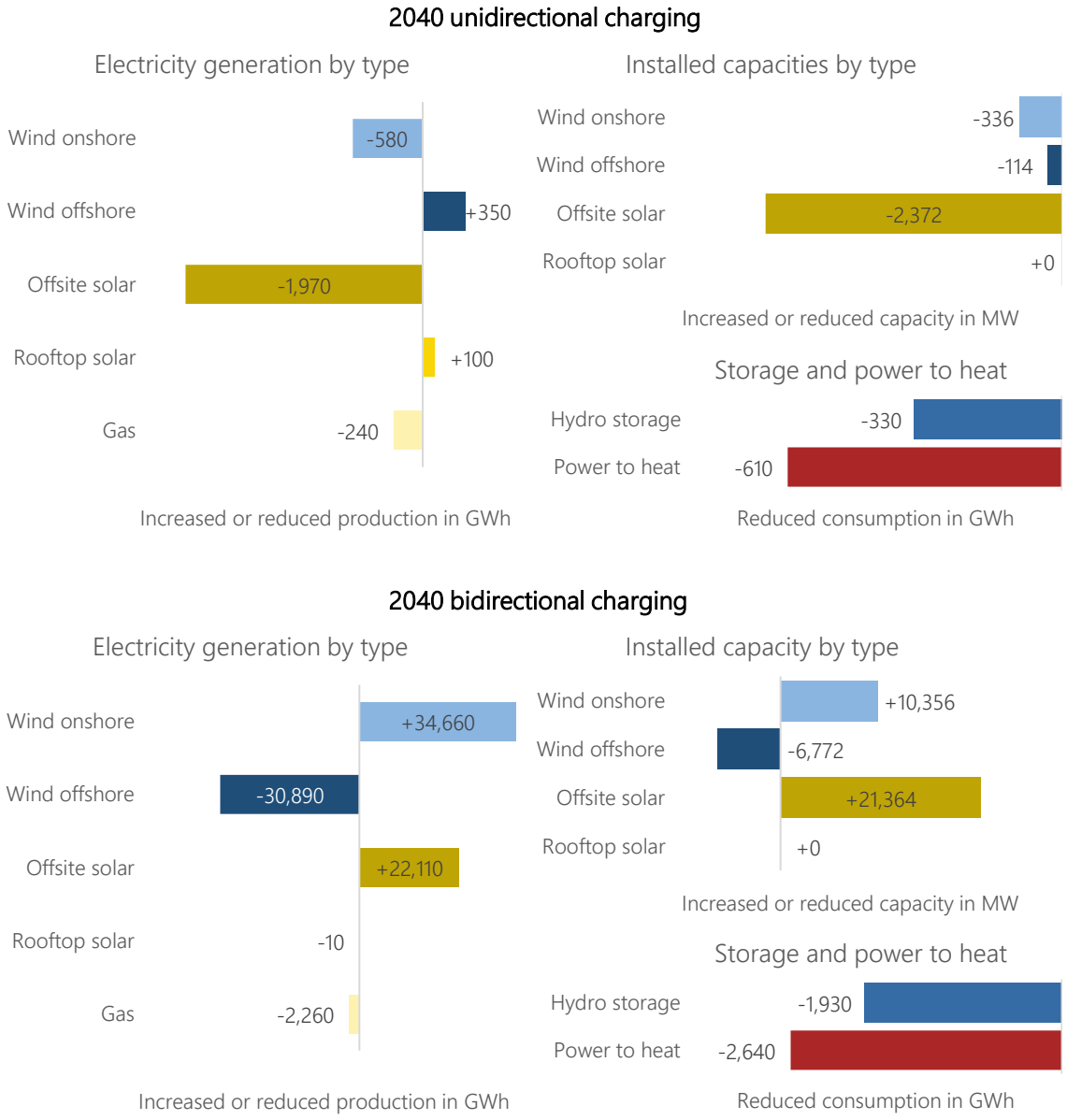

Figure 12-7: System effects of uni- and bidirectional charging optimized on "smoothing of residual load" for the year 2040. For interpretation of underlying coherences, see section 8.4.2.1

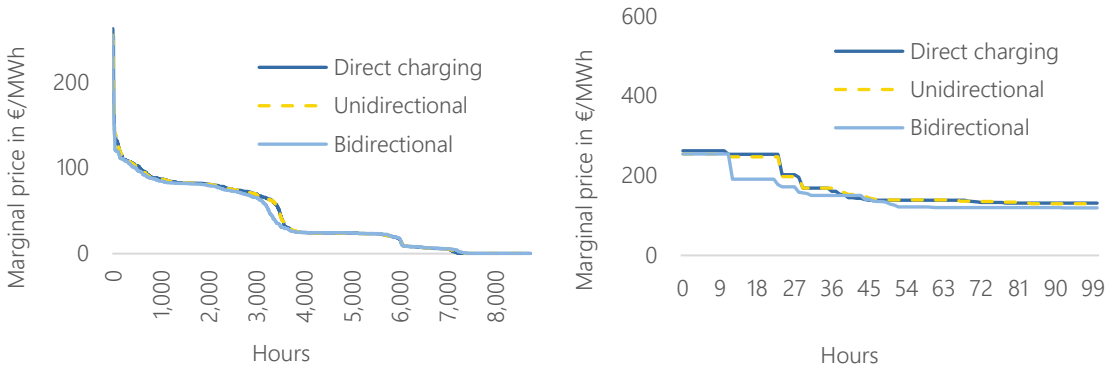

Figure 12-8: Annual duration curve of marginal prices resulting from the three charging strategies in 2040. Evaluations describe the system feedback on the three charging strategies as described in section 8.4.2

12.7 Curtailment and redispatch reductions by Voronoi region

Table 12-3: List of potential curtailment reductions by Voronoi region resulting from bidirectional optimization of EV in 2019. See section 8.5.1 for detailed discussion of results

Voronoi ID	Number of EV	Annual curtailment in GWh	Hours of curtailment	Reduction of curtailment in MWh	Relative reduction	Charged curtailed energy per EV in kWh
32	2,582	6.8	1,115	1,496.7	21.9 %	579.7
20	2,161	12.2	417	1,247.4	10.2 %	577.2
3	2,492	5.8	570	1,184.8	20.3 %	475.4
76	1,243	45.4	1,584	1,083.7	2.4 %	871.8
22	2,243	6.3	619	1,061.9	17.0 %	473.4
39	4,079	2.3	145	991.5	44.1 %	243.1
23	3,105	1.5	451	954.3	64.7 %	307.4
33	859	314.2	5,426	936.9	0.3 %	1,090.7
24	786	576.8	6,121	880.5	0.2 %	1,120.2
14	3,511	0.9	248	795.6	90.7 %	226.6
31	554	1597.9	5,452	606.9	0.0 %	1,095.5
21	2,624	6.4	180	547.0	8.5 %	208.5
11	3,084	2.3	95	532.5	23.2 %	172.7
1	754	25.0	881	511.9	2.0 %	678.9
19	868	5.4	718	477.6	8.9 %	550.2
45	1,086	3.4	558	441.7	13.0 %	406.7
25	2,141	2.0	92	415.6	20.9 %	194.1
10	2,083	1.1	152	364.9	33.9 %	175.2
59	324	194.9	2,773	361.3	0.2 %	1,115.1
68	343	17.6	1,808	358.1	2.0 %	1,044.0
42	294	4.8	2,496	306.1	6.4 %	1,041.2
56	518	3.0	616	232.8	7.7 %	449.4
48	464	4.6	554	208.6	4.5 %	449.6
66	218	40.7	1,768	196.4	0.5 %	900.9
61	179	58.4	1,223	187.0	0.3 %	1,044.7
60	231	32.7	1,276	186.9	0.6 %	809.1
58	821	0.8	111	180.9	23.4 %	220.3
80	194	91.2	1,802	176.2	0.2 %	908.2
77	256	31.6	931	170.6	0.5 %	666.4
81	215	23.5	1,090	169.8	0.7 %	789.8
79	492	3.4	166	158.0	4.64 %	321.1
78	409	4.8	170	146.6	3.1 %	358.4
9	13,692	0.1	0	141.8	100.0 %	10.4
62	209	12.5	812	136.0	1.1 %	650.7
46	3,175	0.3	21	135.8	38.8 %	42.8
74	176	25.4	1,029	129.0	0.5 %	733.0

Table 12-4: Full list of potential reductions of negative redispatch by Voronoi region resulting from bidirectional optimization of EV in 2019. See section 8.5.2 for a detailed discussion of results.

Voronoi ID	Number of EV	Annual negative redispatch in GWh	Hours of redispatch	Reduction of redispatch in MWh	Relative reduction	Charged redispatch energy per EV in kWh
32	2,582	308.3	1,540	8,067	2.6 %	3,124.4
9	13,692	12.4	50	7,217	58.3 %	527.1
30	2,655	186.5	990	6,974	3.7 %	2,626.6
2	5,385	59.4	253	5,868	9.9 %	1,089.8
20	2,161	414.0	1,348	5,360	1.3 %	2,480.5
39	4,079	78.6	402	3,994	5.1 %	979.1
46	3,175	27.9	218	2,359	8.5 %	743.0
63	1,461	51.1	420	2,092	4.1 %	1,432.0
24	786	160.3	1,216	1,936	1.2 %	2,463.2
56	518	203.3	1,053	1,485	0.7 %	2,866.2
11	3,084	52.5	163	1,372	2.6 %	444.9
84	234	758.4	1,978	1,123	0.1 %	4,800.0
54	2,096	6.5	174	1,008	15.5 %	481.2
25	2,141	22.5	162	948	4.2 %	442.7
86	160	354.1	1,952	772	0.2 %	4,823.1
15	7,181	1.8	12	770	42.9 %	107.2
21	2,624	1.5	15	461	31.5 %	175.6
3	2,492	8.1	31	375	4.6 %	150.5
27	1,112	1.8	15	353	19.4 %	317.4
13	5,062	0.2	3	189	80.0 %	37.4
34	3,185	0.4	5	165	38.4 %	51.8
64	268	57.8	244	140	0.2 %	522.4
52	173	70.5	297	111	0.2 %	643.9
14	3,511	0.1	3	72	53.6 %	20.5
33	859	3.2	31	64	2.0 %	73.9
7	4,125	0.5	5	57	11.6 %	13.9
23	3,105	0.3	3	35	11.0 %	11.2
55	341	2.9	10	26	0.9 %	76.2
35	3,651	0.0	0	25	100.0 %	6.9
67	847	0.0	2	16	74.7 %	18.7

Table 12-5: Full list of potential reductions of positive redispatch by Voronoi region resulting from bidirectional optimization of EV in 2019. See section 8.5.2 for a detailed discussion of results.

Voronoi ID	Number of EV	Annual negative redispatch in GWh	Hours of redispatch	Reduction of redispatch in MWh	Relative reduction	Charged redispatch energy per EV in kWh
15	7,181	887.9	2,241	19,041	2.1 %	2,651.6
9	13,692	212.4	678	16,758	7.9 %	1,224.0
13	5,062	131.5	1,878	12,433	9.5 %	2,456.2
14	3,511	188.2	2,660	8,107	4.3 %	2,309.1
34	3,185	152.5	1,756	7,837	5.1 %	2,460.4
23	3,105	567.6	2,636	6,915	1.2 %	2,227.0
35	3,651	14.2	820	6,243	44.1 %	1,709.9
22	2,243	26.5	2,212	4,835	18.2 %	2,155.6
46	3,175	73.7	935	4,468	6.1 %	1,407.2
54	2,096	74.8	1,122	3,538	4.7 %	1,687.8
11	3,084	106.2	758	2,396	2.3 %	776.8
7	4,125	67.9	282	2,318	3.4 %	561.9
3	2,492	182.6	552	2,242	1.2 %	899.6
6	3,373	88.1	337	2,212	2.5 %	655.9
63	1,461	28.0	889	1,626	5.8 %	1,112.7
25	2,141	45.4	735	1,579	3.5 %	737.5
2	5,385	40.6	146	1,324	3.3 %	245.9
43	2,493	66.0	268	1,003	1.5 %	402.4
53	1,611	15.6	267	647	4.1 %	401.8
30	2,655	1.8	25	441	24.1 %	166.2
39	4,079	13.4	53	380	2.8 %	93.2
21	2,624	0.4	5	99	26.1 %	37.5
32	2,582	0.7	3	59	8.4 %	22.8
27	1,112	0.5	5	49	10.5 %	44.1
20	2,161	0.2	3	26	10.5 %	11.8
55	341	1.8	13	24	1.3 %	71.6
56	518	0.1	4	15	15.0 %	28.7
84	234	0.7	4	8	1.2 %	35.5
64	268	0.2	3	8	4.9 %	29.7
86	160	0.7	6	8	1.1 %	47.0
52	173	12.2	61	5	0.04 %	27.7

12.8 Summary of optimized charging in 2030 and 2040

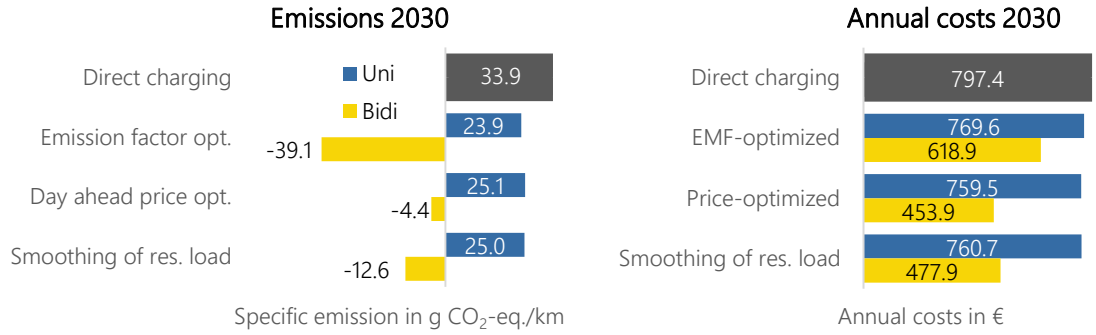

Figure 12-9: Comparison of resulting specific emissions and annual costs of the three use cases "Emission reduction", "Cost reduction" and "Smoothing of residual load" in 2030. A discussion of results for 2019 is provided in section 8.6

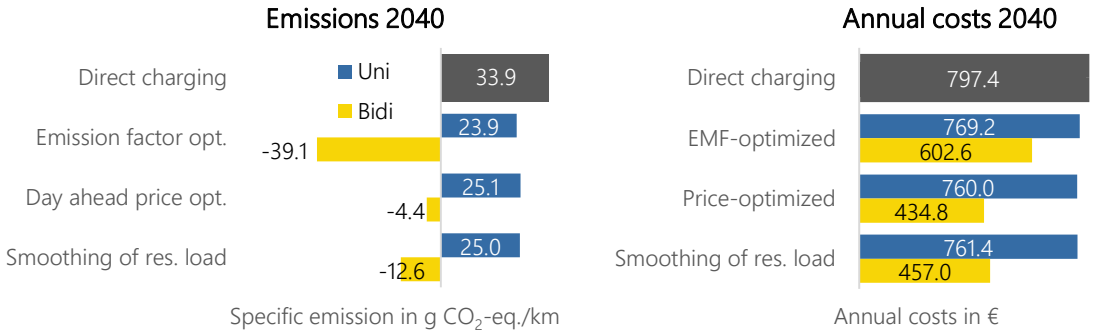

Figure 12-10: Comparison of resulting specific emissions and annual costs of the three use cases "Emission reduction", "Cost reduction" and "Smoothing of residual load" in 2040. A discussion of results for 2019 is provided in section 8.6